

# Conceptual Design of the Spillway into the Energy Storage Lake of Delta21

Part of a new approach to improve the  
flood protection in the Southwest Delta  
of the Netherlands

D. H. Donkers



# Conceptual Design of the Spillway into the Energy Storage Lake of Delta21

Part of a new approach to improve the flood  
protection in the Southwest Delta of the  
Netherlands

by

**D. H. Donkers**

to obtain the degree of Master of Science  
at the Delft University of Technology,

Student number: 4374673  
Project duration: October 16, 2020 – September 20, 2021  
Thesis committee: Dr. ing. M. Z. Voorendt, TU Delft, supervisor, chairman  
Dr. D. Wüthrich, TU Delft  
Dr. ir. B. Hofland, TU Delft  
Ir. B. Belfroid, Ballast Nedam

An electronic version of this thesis is available at <http://repository.tudelft.nl/>.

# Abstract

In the upcoming decades, the Netherlands is going to face challenges regarding the protection against flooding. The reason for this is the expected rapid change in climate around the world. These changes are also affecting the Netherlands. As a result of the changing climate, the sea levels rise and the peak river discharges increase. These changes lead to higher water levels in the Dutch rivers. To deal with this increase, the current flood defence system has to be improved. Although expensive, the most commonly used method to improve the flood defence system is to increase the retaining heights of existing dikes. A new method to improve the flood defence system in the Southwest Delta of the Netherlands is the Delta21 concept. Besides the improvement of the flood defence system, it will also improve the nature of the Haringvliet basin and the balance on the energy market.

The focus of the Delta21 concept is on the Southwest Delta, the region around Rotterdam and the Haringvliet. One of the biggest problems around this area is situated near Dordrecht. Close to Dordrecht, multiple places are not protected by existing flood defence structures and this area is therefore vulnerable to flooding events. The idea is to create a lake, the Energy Storage Lake, next to Maasvlakte II in the North Sea. During high discharge conditions in the rivers of the Southwest Delta, the Rhine and the Meuse, the lake can be used to store excess river water. From the Energy Storage Lake, the water can be pumped into the sea. In combination with a closed storm surge barrier next to the Energy Storage Lake, the water level in the rivers upstream of the lake can be lowered. To achieve the lowering of the water levels in the upstream rivers, a spillway is required to let the water flow into the Energy Storage Lake.

This thesis aims to come up with a conceptual design for the spillway discharging the water from the Tidal Lake towards the Energy Storage Lake. This design must fulfil the functional and structural requirements, must be affordable, constructible and must fit within the ideology of Delta21. To achieve this, the hydraulic engineering design method is used. The first step in this method is to analyse the problem, in which climate change plays a vital role.

In the second step, the basis of design is elaborated. This includes the boundary conditions of the design and the requirements that need to be fulfilled. The main requirements for the spillway are the discharge capacity of  $20\,000\text{ m}^3/\text{s}$  and that the water level near Dordrecht may not exceed  $\text{NAP} + 2.5\text{ m}$ .

In the third step, the location of the spillway is first decided upon. The location is chosen based on the results of a sieve analysis. For this sieve analysis, multiple criteria are used to eliminate unfavourable locations. After this, four different concepts are generated that differ in, among other things, the type of flow and the way the structure is part of the surrounding flood defence structures. The different concepts are concept Siphon, concept Underflow, concept Caisson and concept Ogee.

The fourth step is the verification of the concepts. This step is divided into two parts. In the first part, the hydraulic design and a part of the structural design are verified. This part is used to obtain the main dimensions of the concepts. The second part of the verification focuses on the second part of the structural design, the strength verification and the design of the scour protection. This part is performed after the selection of the best scoring concept. The hydraulic design and the first part of the structural design are focused on respectively the functional requirements and the stability requirements. The main functional requirement is the previously mentioned required discharge capacity of  $20\,000\text{ m}^3/\text{s}$ . After the first part of the verification, one of the concepts, concept Ogee, is rejected due to stability issues and large flow velocity at the end of the spillway.

Before the second part of the verification, an evaluation and selection process has been performed. This is the fifth step of the hydraulic engineering design cycle. In this step, a multi-criteria analysis is carried out to compare the concepts which are still deemed feasible. For this analysis, multiple criteria are used, for instance the ease of maintenance of the structure. The multi-criteria analysis is combined with a cost esti-

mation of the concepts. These costs are determined based on information retrieved from the Tender Infra Projects section of Ballast Nedam. By combining the results of the two, a final concept is chosen. The most optimal concept is the concept Caisson. This concept can be seen in Figure 1 and Figure 2.

After the selection of the final concept, the last part of the verification is realised. In this part, the strength verification is performed and the scour protection is designed. In the strength verification, the thickness of – and the reinforcement in – the concrete elements of the caisson are obtained by using the requirements obtained from Eurocode 2. Afterwards, the scour protection at both sides of the spillway is designed. Only local scour problems are considered in the design of the scour protection and it has to be considered that the obtained design is a preliminary design. No modelling of the flow is done and therefore the obtained design shows a preliminary design of what a possible protection could look like.

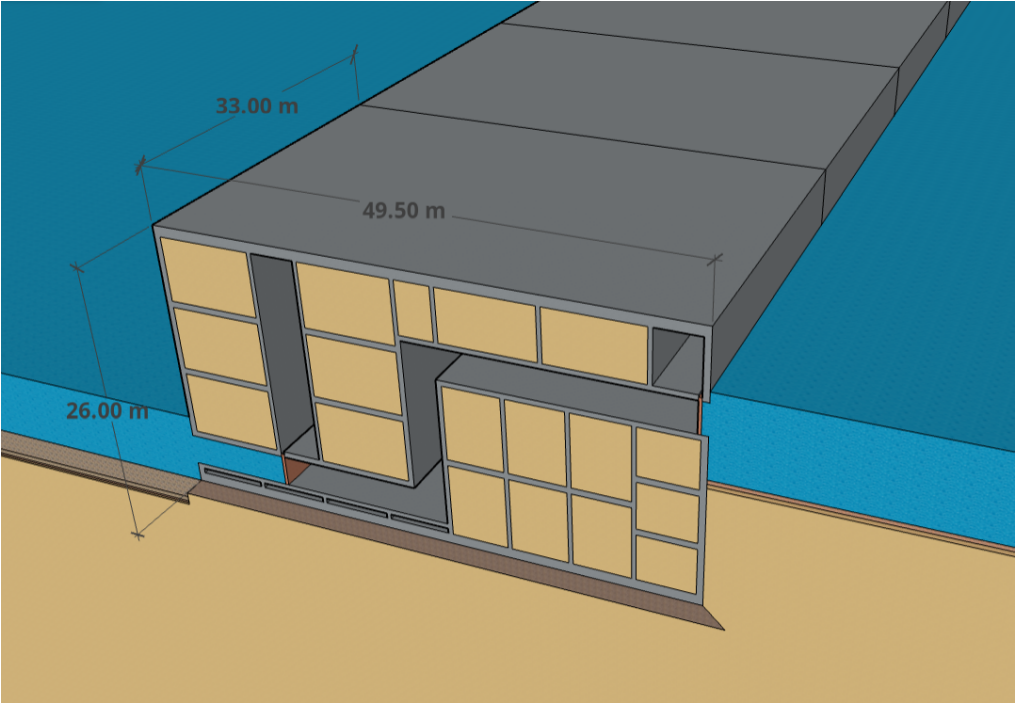


Figure 1: 3D View of the concept Caisson

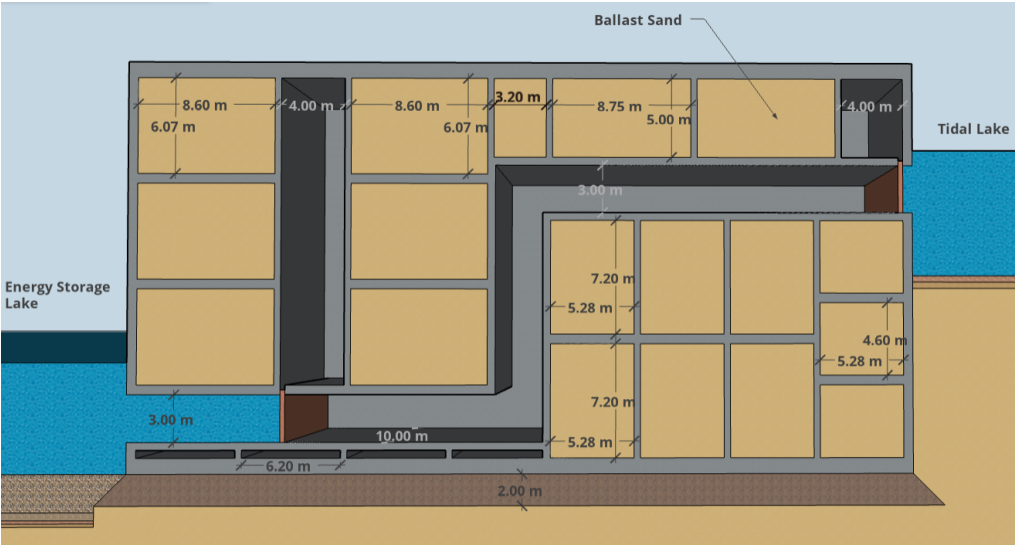


Figure 2: Front view of the concept Caisson

# Preface

This thesis has been written to obtain my MSc degree in Hydraulic Engineering at the TU Delft. First, I want to thank the chairman of my committee, Mark Voorendt. Without his help at the start of my thesis, I would never have been in contact with the initiators of Delta21, Huub Lavooij and Leen Berke, and getting to know the ideas of Delta21. During my thesis, I was very happy with all the feedback I got after each meeting. It helped me a lot in improving my thesis report during my graduation period. I want to thank the other members of my committee as well for their time, knowledge and input during our meetings.

Next, I want to thank Huub Lavooij and Leen Berke for making me part of the Delta21 team and bringing me in contact with Ballast Nedam. During my graduation period, it was great to have some meetings with you to talk about my design and the development of the Delta21 project. I hope this conceptual design can help you with the further developments of this challenging project. Looking at the current situation in the Netherlands, it is good that these kinds of projects are present to improve the flood protection.

During my graduation period I was part of the Infra Projects department of Ballast Nedam. Although I have not been at the office that much due to the COVID-19 measurements, I had a great time there and I learned a lot. From Ballast Nedam team I want to give a special thanks to Bas Belfroid for being my supervisor during my period at Ballast Nedam. Your guidance during my thesis was very helpful and very much appreciated. Besides Bas Belfroid, I want to thank the other members of the Ballast Nedam team for letting me feel part of the team.

Besides all the people that were part of my graduation period, I also want to thank my friends and family for being there for me and helping me when necessary. I want to give special thanks to Dieuwke van den Oudenrijn, Abe Feenstra and Jesse Dijkstra for their help at the end of the graduation period.

*D. H. Donkers  
Delft, September 2021*

# Contents

- Abstract . . . . . i
- Preface . . . . . iii
- 1 Introduction . . . . . 1
  - 1.1 Thesis Motivation . . . . . 1
  - 1.2 Methodology and Report Outline . . . . . 2
- 2 Problem Analysis . . . . . 4
  - 2.1 Dutch Flood Defence System . . . . . 4
  - 2.2 Climate Change . . . . . 5
    - 2.2.1 Global Change . . . . . 5
    - 2.2.2 Scenarios for the Netherlands . . . . . 6
    - 2.2.3 Sea Level Rise at the Dutch Coast . . . . . 6
    - 2.2.4 River Discharges . . . . . 7
    - 2.2.5 Uncertainties . . . . . 8
  - 2.3 The Delta21 Concept . . . . . 8
    - 2.3.1 Level of Safety . . . . . 8
    - 2.3.2 The Idea . . . . . 9
    - 2.3.3 Purposes of Delta21 . . . . . 10
    - 2.3.4 Discharge of Excess River Water by the Energy Storage Lake . . . . . 12
  - 2.4 Process and Function analysis . . . . . 12
    - 2.4.1 Process Analysis of the Delta21 System. . . . . 12
    - 2.4.2 Function Analyses . . . . . 13
  - 2.5 Stakeholder Analysis . . . . . 14
    - 2.5.1 Stakeholder Inventory . . . . . 14
    - 2.5.2 Stakeholder Involvement . . . . . 14
  - 2.6 Problem Statement . . . . . 15
- 3 Basis of Design . . . . . 16
  - 3.1 The Design Objective . . . . . 16
  - 3.2 Scope . . . . . 16
  - 3.3 Requirements . . . . . 16
    - 3.3.1 Functional Requirements . . . . . 16
    - 3.3.2 Structural Requirements . . . . . 17
  - 3.4 Location Criteria . . . . . 17
  - 3.5 Evaluation Criteria . . . . . 17
  - 3.6 Legal Boundary Conditions . . . . . 18
    - 3.6.1 Laws and Regulations . . . . . 18
    - 3.6.2 Reliability . . . . . 18
  - 3.7 Natural Boundary Conditions. . . . . 19
    - 3.7.1 Geo-technical Conditions . . . . . 19
    - 3.7.2 Meteorological Conditions. . . . . 20
    - 3.7.3 Water Levels . . . . . 21
    - 3.7.4 Wave Conditions. . . . . 22
    - 3.7.5 Wind Set-up and Set-down. . . . . 23
    - 3.7.6 River Discharge . . . . . 24
    - 3.7.7 Overview. . . . . 25

4	Location Selection	26
5	Generation of Concepts	29
5.1	Spillway Characteristics	29
5.1.1	Type of Flow	29
5.1.2	Type of Inlet	30
5.1.3	Type of Outlet	30
5.1.4	Type of Cross Section	30
5.2	The Concepts	31
5.2.1	Concept Siphon	31
5.2.2	Concept Underflow	32
5.2.3	Concept Caisson	32
5.2.4	Concept Ogee	33
6	Verification of Concepts	34
6.1	Safety Approach	34
6.2	Verification Checks	35
6.2.1	Piping	36
6.2.2	Sliding Resistance	37
6.2.3	Rotational Stability	37
6.2.4	Bearing Capacity	37
6.2.5	Draught of the Caisson	38
6.2.6	Floating Stability	38
6.3	Concept Siphon	39
6.3.1	Dimensions and Number of Pipes	39
6.3.2	Dimensions Inlet and Outlet	41
6.4	Concept Underflow	51
6.4.1	Dimensions and Number of Pipes	51
6.4.2	Dimensions Inlet and Outlet	52
6.5	Concept Caisson	53
6.5.1	Dimensions and Number of Conduits	53
6.5.2	Retaining height of the Caisson	55
6.5.3	Width and Length of the Caisson	55
6.6	Concept Ogee	61
6.6.1	Dimension and Number of Openings	61
6.6.2	Shape of crest	63
6.6.3	Stability of the Structure	64
6.7	Conclusion of the Verification	65
7	Evaluation and Selection	66
7.1	The Multi-Criteria Analysis	66
7.1.1	The Criteria	66
7.1.2	The Weighting Factors	67
7.1.3	The Scores of the Concepts	67
7.2	The Cost Estimation	68
7.3	Selection	68
8	Strength Verification and Scour Protection	69
8.1	Strength Verification	69
8.1.1	Classification of the Structure and Material Properties	69
8.1.2	Strength Verification Checks	70
8.1.3	Initial Lay-out	72
8.1.4	Verification of Initial-Layout	73
8.1.5	Improved Lay-out	73
8.1.6	Verification of the Improved Lay-Out	74

---

8.2 Scour Protection . . . . .	75
8.2.1 Determination of the Governing Situation for the Scour Protection . . . . .	75
8.2.2 Design of the Scour Protection. . . . .	77
8.2.3 Potential Adjustments of the Scour Protection . . . . .	80
9 Discussion, Conceptual Design and Recommendations . . . . .	81
9.1 Discussion . . . . .	81
9.2 Conceptual Design of the Spillway . . . . .	83
9.3 Recommendations . . . . .	85
Appendices . . . . .	86
A Stakeholders . . . . .	87
B Geotechnical Soil Profile . . . . .	91
C Wind Calculations . . . . .	100
D Wave Calculations . . . . .	103
E Discharge Calculations . . . . .	107
F Stability Concept Siphon . . . . .	120
G Retaining Height . . . . .	149
H Stability Concept Caisson . . . . .	151
I Dimensions of the concept Ogee . . . . .	170
J Stability Concept Ogee . . . . .	173
K Multi-Criteria Analysis . . . . .	176
L Cost Evaluation . . . . .	180
M Strength Verification of Concept Caisson . . . . .	186
N Verification of the Scour Protection . . . . .	216
References . . . . .	228



# 1

## Introduction

### 1.1. Thesis Motivation

In the upcoming decades, the Netherlands will be facing challenges regarding the protection against flooding. The climate is changing around the world and this is also affecting the Netherlands. The average global temperature is increasing which leads to glaciers melting more rapidly, the total volume of water increasing due to thermal expansion, and more intense precipitation events. These changes lead to sea level rise and increased peak discharges in rivers. Hence, improvements to the current flooding protection are necessary to face these challenges (Attema et al., 2014).

The Netherlands is a low-lying country which means that most of the Netherlands is below sea level. This leads to the Netherlands being highly dependent on a well-functioning flood defence system. Without this system, the Netherlands would not exist. This flood defence system includes dikes, dams, dunes and barriers. Although the flood defence system is functioning appropriately at the moment, the sea level rise and increase in peak discharges will have a significant impact on the current system. In coastal areas, sea level rise will lead to higher water levels during storm conditions. For instance, this leads to more frequent closure of the Europoort barrier. More inland, the flood defence system must retain higher water levels during peak conditions due to the increased peak discharges. If no measures are taken to improve the flood defence system, the level of safety in The Netherlands will decrease and will be below the required level of safety (Het Hoogwaterbeschermingsprogramma, 2019).

Traditionally, the most common way to improve the Dutch flood defence system is by increasing the retaining height of the dikes. However, due to the high number of dikes, this is an expensive mitigation. An alternative solution to counter the increasing water levels and improve the flood protection is the Delta21 concept.

The Delta21 concept aims to decrease the water level in the river branches located in the Southwest Delta of the Netherlands during extreme discharge conditions. To accomplish this, the water level at the river mouth of the Southwest Delta, the Haringvliet, should consistently be kept low. By keeping this part of the river system at a low level, the upstream water levels will decrease as well. Due to this, the flood protection in the Southwest Delta can be kept at an acceptable level without raising the dikes. In addition, the Delta21 concept aims to decrease the number of closures of the Europoort barrier. A decreased water level upstream of the Haringvliet affects the area of Rotterdam as well. Therefore, the Europoort barrier will be closed less frequent. The location of the Delta21 concept can be found in Figure 1.1.

In order to achieve the goals of Delta21, a lake needs to be constructed in the North Sea next to Maasvlakte II. This lake is referred to as the Energy Storage Lake. During situations of high discharge in the Rhine and Meuse, excess river water can flow from the Haringvliet into this lake by using the spillway. By doing this, the water level in the Haringvliet can be controlled. After the water enters the lake, a pumping station will discharge the water into the sea. In between the lake and the island of Goeree-Overflakkee, a storm surge barrier will be constructed. During conditions leading to high discharge in combination with storm surge from the sea,



**Figure 1.1:** Overview of Southwest Delta

this barrier will be closed and the sea has no longer any influence on the water level in the Haringvliet. If the barrier is closed, the water from the Haringvliet can only flow into the sea by using the combination of the spillway and pumping station (Lavooij and Berke, 2018c). A lay-out of the Delta21 concept can be found in Figure 1.2. Besides the aim of Delta21 to increase the flood protection in the Southwest Delta, the project also aims to improve the ecology around the Haringvliet and contribute to the energy transition. A more detailed description regarding the influence of this project on the ecology and its contribution to the energy transition can be found in Section 2.3. This thesis focuses on the design of one of the components of the Delta21 concept: the spillway from the Haringvliet to the energy storage lake.

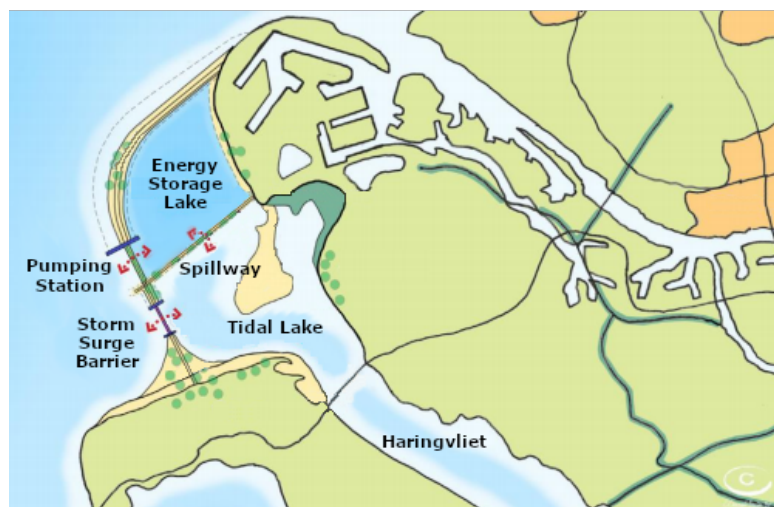


**Figure 1.2:** Layout of the Delta21 Concept

## 1.2. Methodology and Report Outline

In this thesis, a conceptual design of the spillway of the Delta21 concept is presented. The hydraulic engineering design method is used to achieve this design. The description of this design method is based on the design method of Roozenburg and Eekels (1995). Their method is mostly used for product designs but the steps that are taken are similar to the design of hydraulic structures. The hydraulic engineering design method consists of the following design phases: problem analysis, design definition, development of concepts, verification of

concepts, evaluation of alternatives, integration and validation. The schematization of these phases can be seen in Figure 1.3. This schematization is also called the engineering design cycle.

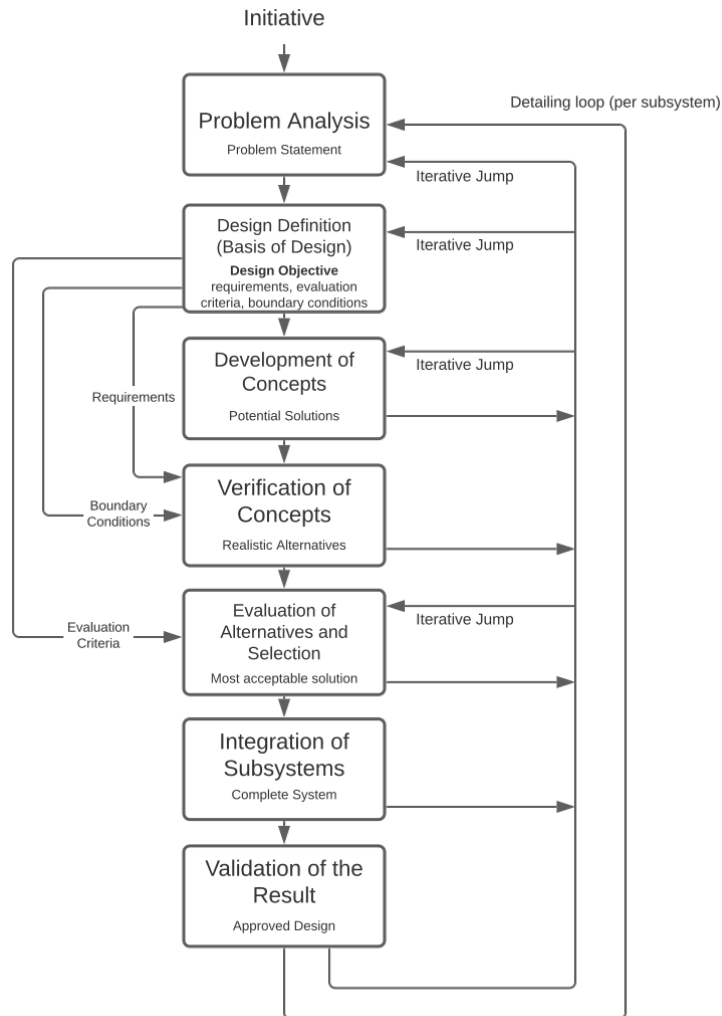


**Figure 1.3:** Engineering Design Cycle (Voorendt and Molenaar, 2020a)

The engineering design cycle presented in Figure 1.3 is used throughout this research. The approach applied starts with the problem analysis, which is carried out in Chapter 2 of this research. Then, the basis of the design is drawn up in Chapter 3. Lastly, three design loops are formed in which the design cycle can be distinguished.

1. Location Selection, Chapter 4
2. Hydraulic Design and Stability, Chapter 5, 6 and 7
3. Strength Verification and Scour Protection, Chapter 8

Important to note is that the design method uses an iterative approach to find solutions. This means that the design cycle is carried out multiple times in entirety. To improve the quality of the evaluation process in Chapter 7, the structural design is divided into two parts. The stability part is performed in combination with the hydraulic design and the strength verification and scour protection is only performed for the best concept, in Chapter 8. In Chapter 9 the final design is shown, the design process is discussed and the recommendations for further development are given.

# 2

## Problem Analysis

In this chapter the first phase of the engineering design cycle is described: the problem analysis phase. The aim of this stage is to explore the problem. This is accomplished by looking at the background of the problem, describing the possible solution and creating an inventory of the stakeholders.

### 2.1. Dutch Flood Defence System

Without the existing flood defence system, the Netherlands would be vulnerable to flood events. A well-known example is the North Sea flood of 1953, known as the 'Watersnoodramp van 1953'. A heavy storm came from the northwest and reached the Netherlands on the 31st of January. In combination with spring tide, an extreme storm surge occurred which resulted in an excessive sea level rise. The high sea level combined with the high waves caused more overtopping than the dikes had been designed for. This extreme overtopping led to sliding of the inner slopes of many dike sections. This failure mechanism was the main cause of dike breaches (Rijkswaterstaat, 1961). In multiple locations around Zeeland, South-Holland and North-Brabant these breaches occurred. An extensive area of The Netherlands was flooded which resulted in many casualties and much damage.

After this disaster, the Dutch government appointed the Delta Commission. This commission came up with the Delta Programme which had the main purpose to increase the safety against flooding. The Delta Programme included the construction of multiple dams and storm surge barriers, known as the Delta Works (Rijkswaterstaat, 2020a). Most of these structures are located near the coast of Zeeland but some of them can be found more upstream. The first structure was completed in 1958 and the last structure was completed in 1997. The last structure, the Maeslantkering, was not part of the original delta plan but was required to ensure a sufficient level of safety. In Figure 2.1, the location of the structures can be found. By building multiple dams around the coast of Zeeland, the total length of the coast was shortened. This has decreased the probability of flooding in the region of Zeeland.

The Delta Works are not the only Dutch flood defences. The current primary flood defence system of The Netherlands consists of a large number of dikes, dunes, dams and barriers all around the country. The defence structure that has been used the most are the dikes, which can be found throughout the Netherlands. These dikes can be found along the rivers but also near the coast. In total, there



**Figure 2.1:** Location of the Delta Works (Stichting Deltawerken Online, 2004)

is 3 500 kilometres of primary flood defences in the Netherlands and 14 000 kilometres of regional flood defences. The difference between these two is that the primary flood defence system protects The Netherlands against the water from the sea and the big rivers. The regional flood defences protect the Netherlands from the smaller rivers and other small waters. All the Dutch defence structures need to live up to the Dutch safety standards. Since 2017, new safety standards are in use which look at the probability of failure of a structure, rather than the probability of exceedance of the design load for that structure (Slootjes and van der Most, 2016).

An important criterion that has influence on the probability of failure of a flood defence structure is the water level that has to be retained. If the water level increases, the probability of failure will increase too. An increase of the water levels is expected in the Netherlands due to the ongoing climate change. This increase will lead to bigger probabilities of failure if no measures are taken to improve the current structures. Therefore, it is of the utmost importance to consider the impact of climate change when designing a new structure or improving the current structures.

## 2.2. Climate Change

### 2.2.1. Global Change

The climate is continuously changing around the world. The mean global temperature is fluctuating over longer periods of time. One of the reasons for this are the Milankovitch cycles. These cycles consist of the change in shape of the Earth's orbit, the tilting of the Earth's axis with respect to its orbital plane and the fact that the Earth is wobbling upon its axis. The duration of these cycles is long, between 26 000 up to 100 000 years per cycle. Each of these cycles influences the climate on Earth on the long term (Buis, 2020). However, this change is happening faster due to the increase in greenhouse gasses in the atmosphere (Core Writing Team et al., 2014). The significant increase of greenhouse gasses can be related to human activities. The emissions from industry, vehicles, energy production and agriculture are constantly growing. The greenhouse gasses are responsible for trapping heat in the atmosphere. The increase of greenhouse gasses in the atmosphere lead to more heat being trapped and a rise in mean global temperature (Kweku et al., 2018). This temperature increase influences the volume of water in the oceans, melting of the glaciers and ice sheets in Greenland and the Antarctic and the precipitation. The current warming trend cannot be stopped but the rate of change can be slowed down (NASA, 2020). It is important that the rate of change is slowed down because the impact of climate change can be excessive. From a hydraulic perspective, there are multiple relevant effects of climate change. The most important effect is the global sea level rise but the increase in river discharge and change in wave climate may not be underestimated.

The global sea level is influenced by the higher temperature on earth in multiple ways. In the polar areas, an increase in temperature results in increased melting of glaciers and ice sheets. Since the density of water is greater than the density of ice, the water will expand if it goes from ice to water. This leads to an increase in the volume of water in the oceans, raising the sea level. Locally a rise of the sea level can occur due to the gravitational attraction of the water to the ice sheets. If the ice sheets melt, the water level close to the ice sheets is decreasing but far away from the ice sheet an increase can occur (Bosboom, 2015). Another cause for the sea level rise due to the increasing temperature is the expansion of water. For water above 4°C, a normal positive thermal expansion can be seen. This means that at higher temperatures, the expansion of water is bigger and leads to an increase in sea level.

The change in river discharge is mainly caused by the change in precipitation, earlier melting of ice and reduced snow storage. For seasonal rivers which depend on the snowfall, this can lead to higher winter discharge and lower summer discharge (Döll and Schmied, 2012).

The influence of climate change on the wave climate is different around the world according to Mori et al. (2010). For the mean waves, climate change can lead to an increase in wave height in the middle latitudes and the Antarctic ocean but it can also lead to a decrease at the equator. At the Dutch coast, the change in wave climate is expected to be low (de Winter et al., 2012).

### 2.2.2. Scenarios for the Netherlands

The Intergovernmental Panel on Climate Change (IPCC) is doing research on climate change and the global effects of it. The results that follow from these investigations are translated to the effects at the Dutch coast by the KNMI, the Dutch national weather forecasting service. In 2006 and in 2014, reports have been published about the climate change effects in The Netherlands. Van den Hurk et al. (2006) focused mainly on the effects on the climate in 2050 and Attema et al. (2014) focused on the effects on the climate in 2100. Both Van den Hurk and Attema are researchers of the KNMI.

In the report by Van den Hurk et al. (2006) a distinction had been made between four scenarios for 2050 and 2100. These scenarios are depending on the global temperature rise and the change in air circulation patterns. Two of them consider a rise in temperature of 1°C by 2050 and 2°C by 2100 and the other two take a rise of 2°C by 2050 and 4°C by 2100. The influence of the change of the air circulation pattern distinguishes the two global temperature rise scenarios into a total of 4 scenarios. The influence of the change of the air circulation pattern can either be high or low.

In the report by Attema et al. (2014), the scenarios are also depending on the global temperature rise and the change in air circulation patterns. But Attema et al. (2014) took a different time period in consideration compared to Van den Hurk et al. (2006). In the report of Attema et al. (2014), two of the scenarios consider a rise in temperature of 1°C and 1.5°C by 2050 and 2085 and two other scenarios take a rise of 2°C and 3.5°C by 2050 and 2085. The distinction due to the air circulation pattern is the same as in Van den Hurk et al. (2006).

### 2.2.3. Sea Level Rise at the Dutch Coast

For the design of a flood defence structure near the coast, it is important to consider the sea level rise. Attema (2014) and Van den Hurk (2006) predicted the sea level rise at the Dutch coast with the use of different models. The main distinction between the two models is the choice of reference period. Van den Hurk et al. (2006) used the period 1975-2005 as reference period. According to Van den Hurk et al. (2006), the expected sea level rise by 2050 is 0.15-0.35 m compared to the reference period. This is 0.15-0.25 m for the low temperature rise scenarios and 0.2-0.35 m in the high temperature rise. By 2100 the sea level is expected to be risen by 0.35-0.6 m with a low rise in temperature and 0.4-0.85 m with high temperature rise. The maximum expected sea level rise of 0.85 m by 2100 is corrected to 0.95 m after the publication of the 2014 report.

In the research by Attema et al. (2014) the reference period of 1981-2010 was taken. In this reference period the sea level was at NAP +0.03 m. According to the report, a sea level rise of 0.1-0.4 meter is expected by 2050. This is 0.1-0.3 m in the low temperature rise estimate and 0.2-0.4 meter in the high temperature rise. By 2085 the sea level will rise 0.25-0.6 m with a low rise in temperature and 0.45-0.8 m with high temperature rise. In 2100 a maximum sea level rise of 1 m will occur according to the KNMI models. In the research it is concluded that the influence of the change in air circulation pattern on the sea level rise can be neglected. In the reference period the sea level rise was equal to 2 mm per year. In the most severe scenario, the sea level rise per year is expected to be 10.5 mm by 2085. The increase in sea level rise per year can be linked to the higher increase in global temperature and therefore a more rapid melting of the glaciers. Within the two reports, the differences are small and both show an increase of approximately 1 meter in sea level at the end of the century.

According to Deltares (2018) a more rapid rise in sea level is expected in the upcoming period. The reason behind the change in expected sea level rise is a new view on the breaking down and melting of the land ice of Antarctica. In the study of Attema et al. (2014) these new insights have not been taken into consideration. With the new information Deltares modelled two new scenarios. One with a temperature rise of 2°C and low emissions by 2100 and one with a temperature rise of 4°C and high emissions by 2100. These scenarios are the same as the scenarios given by the IPCC. These scenarios lead to a higher expected sea level rise by 2100 than in KNMI'14 scenarios. With the new information a sea level rise from 0,3 m up to 2 m is expected for the scenario in which the temperature rise is 2°C. For the scenario with 4°C temperature rise, a sea level rise is predicted of 0.8 m up to 3 m. The new scenarios can be found in Figure 2.2. These scenarios are characterised as RCP4.5 and RCP8.5 in which RCP stands for Representative Concentration Pathway. These corresponds with respectively the low temperature rise prediction and the high temperature prediction. The RCP scenarios are not fully corresponding with the KNMI scenarios and therefore some caution needs to be taken while

comparing them.

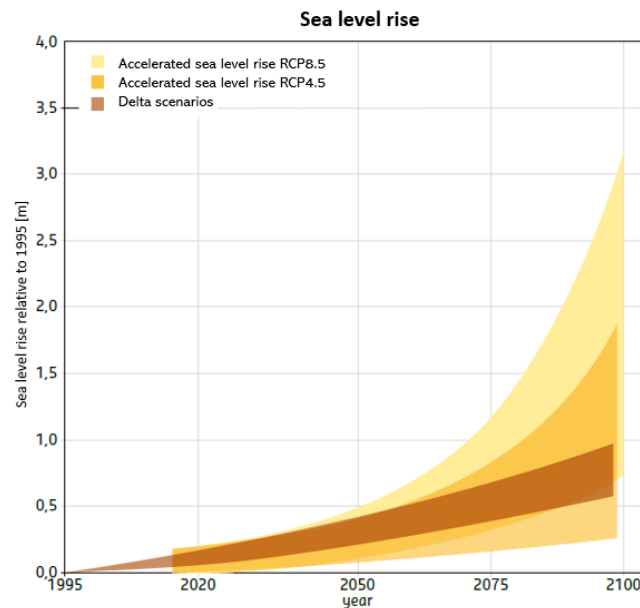


Figure 2.2: Prediction of the sea level rise (Deltares, 2018)

#### 2.2.4. River Discharges

The second relevant effect of climate change from a hydraulic perspective is the change in the river discharges in the Netherlands. The most relevant rivers to consider are the Rhine and the Meuse.

Buishand and Lenderink (2004) published in the name of the KNMI the expectations for the Rhine river. In the winter period an increase of mean discharge at Lobith is expected of 20-30 % by 2100. This is due to the increase of precipitation in this period, early melting of ice and reduced snow storage. In the summer period the discharge will decrease 30-40 %, due to less snow melting in the Alps and less precipitation during this period. The winter period is already the most extreme period with the highest discharges. So, with an increase in that period the maximum occurring discharge will increase as well. A later study by Klijn et al. (2015b) also showed an increase in Rhine discharge for the future. For the development of the discharge, predictions were made for 2050 and 2085. In 2015, a probability of 1:1250 years corresponds to a discharge of 17 000 m<sup>3</sup>/s, by 2050 this will correspond to 19 000 or 20 000 m<sup>3</sup>/s and by 2085 to 19 000 to 22 000 m<sup>3</sup>/s.

The discharge at Lobith is influenced by the conditions upstream. The maximum occurring discharge is depending on the flood protection measures in Germany. In 2020, their flood defence structures are designed for discharges up to 16 000 m<sup>3</sup>/s. If this design discharge is exceeded, flood events will occur upstream of Lobith. Therefore, the Ministry of Infrastructure and Water Management of the Netherlands advises to take a discharge of 16 000 m<sup>3</sup>/s as governing discharge. According to Klijn et al. (2015a), the maximum discharge at Lobith will increase to 17 000 - 18 000 m<sup>3</sup>/s by 2100. In The Deltaprogram of 2015, it is advised to consider a governing discharge at Lobith of 18 000 m<sup>3</sup>/s. This value is also advised by Demon (2005). The governing discharges of the Rhine can be found in Table 2.1

The other relevant river, the Meuse, has a lower discharge than the Rhine. The expected developments for the Rhine are also expected for the Meuse according to Klijn et al. (2015b). The winter discharge will increase and the summer discharge will decrease. The difference with the Rhine river is the degree of change. By 2050 the expected increase of the discharge is 20% and by 2085 this will be 25%. In the summer period, the discharges remains constant or decreases depending on the climate scenario. In 2015 the probability of oc-

currence of 1:1250 years corresponded with 3 900 m<sup>3</sup>/s and this can increase to 4 450 m<sup>3</sup>/s by 2050 and 4 750 m<sup>3</sup>/s by 2100 for the least favourable scenario. According to Demon (2005) the normative discharge by 2100 is expected to be 4 600 m<sup>3</sup>/s, as presented in Table 2.1.

	2000	2100
Rhine by Lobith	16 000 m <sup>3</sup> /s	18 000 m <sup>3</sup> /s
Meuse by Borgharen	3 900 m <sup>3</sup> /s	4 600 m <sup>3</sup> /s

**Table 2.1:** Governing river discharges

### 2.2.5. Uncertainties

Predicting sea level rise or changes in mean global temperature are subject to uncertainties. These uncertainties need to be taken into consideration when the prediction outcomes are used for the design of flood defence systems. In Figure 2.2, the uncertainties in the expected sea level rise are clearly visible. By 2100, the predicted sea level varies between 1 and 3 m for the RCP 8.5 case. These uncertainties cause more difficulties in the design phase of a structure. Besides the uncertainties within the models, there are also uncertainties regarding the models. There is currently a debate about the validation of the models used for the predictions. According to Christy (2016), the models used for predicting the global temperature are not validated and lead to more negative projections than shown by the measured data. Other scientists like Gavin Schmidt, CEO of NASA Goddard Institute for Space Studies, have a different view and use the same data that is used as input by Christy to present small deviations from measured data compared to the model data (Nuccitelli, 2016). Due to the complexity of climate change and the predictions of it, there will always be a debate on the validity of the predictions.

## 2.3. The Delta21 Concept

### 2.3.1. Level of Safety

The introduction has presented several risks related to the level of safety of the Dutch flood defence system, specifically for the Southwest Delta. The rising sea level and increasing discharge of the rivers in the Netherlands are two phenomena that result in this decrease in the level of safety. Due to sea level rise, the primary flood defences will have to retain higher water levels during normal and storm conditions respectively. As a result of the rising sea levels, the water level in the rivers that flow towards the sea will increase as well. This relates to the fact that upstream water levels are affected by the water level at the seaside of the river. The current defence structures are designed for a given probability of flooding. If the occurrence of high water in the rivers increases, it becomes more likely that the probability of flooding that the system is designed for, will be exceeded as well. This leads to structures not meeting their reliability requirement. To ensure an acceptable probability of flooding at the Southwest Delta in case of sea level rise, the Europoort barrier must be closed more frequently to overcome high water levels in the upstream areas. A more frequent closure of these storm surge barriers is not desirable regarding the accessibility of the port of Rotterdam. The increase of the river discharge is accompanied by an increase of the water levels in those rivers. This increase will lead to a bigger probability of flooding of the defence structures along the river.

Traditionally, the most common solution to improve the flood protection is to increase the dike height and strength. This improvement cost approximately 10 million euros per kilometre of dike (Het Hoogwaterbeschermingsprogramma, 2019). This is an expensive measure due to the spatial configuration of dikes, which run alongside the whole river branch and over this entire length the improvements must be executed for them to be effective. In the Water Authority of Hollandse Delta alone, more than 364 km of dike can be found. An alternative for raising the dikes to improve the flood protection in the Southwest Delta is the Delta21 concept. This concept has as main goal to increase the flood protection in the Southwest Delta area. In Figure 2.3, an overview of the Southwest Delta is given including the suggested project side of Delta21.

Another problem that occurs more frequently due to the increase in water levels is the increase of probability of high water at Dordrecht. A part of Dordrecht is situated between the Oude Maas (a distributary of the



Rhine) and the flood defence structures. If the water level near Dordrecht exceeds NAP +2.5 m, problems regarding flooding will occur. One of the aims of the Delta21 concept is to increase the level of safety in this specific location.



Figure 2.3: Overview of Southwest Delta

### 2.3.2. The Idea

The idea of Delta21 is that during extreme conditions, the water level in the Haringvliet is kept low. A low water level in the Haringvliet results in lower water levels in the rivers upstream. If the water levels upstream are lowered during extreme conditions, raising the dikes is not necessary anymore. To achieve a lower water level in the Haringvliet, excess water has to be removed from the river system. This can be accomplished by constructing a lake in which the excess river water can flow. The lake will be constructed in the North Sea next to Maasvlakte II. The lake is referred to as the Energy Storage Lake and the suggested location of this lake is presented in Figure 2.4. The presented lay-out is still subject to changes since Delta 21 project is in the conceptual phase. From the lake, the water can be pumped into the sea. To let the water flow into the lake a spillway needs to be constructed and to let the water flow back into the sea a pumping station is needed. The design criterion for the pumping station is to have a discharge capacity of 10 000 m<sup>3</sup>/s. For the spillway, the design discharge criterion is set to 20 000 m<sup>3</sup>/s. These criteria are based on the predicted river discharge in the upcoming decades (Lavooij and Berke, 2018c).



Figure 2.4: Overview of Delta21 (Lavooij and Berke, 2020)

To decrease the water level in the Haringvliet, a new storm surge barrier has to be constructed between the Energy Storage Lake and the island of Goeree-Overflakkee. During storm conditions at sea, it will be possible to close off the Haringvliet basin by using the storm surge barrier. The water level upstream of the barrier will rise because the water cannot flow into the sea. By using the spillway of the Delta21 concept, water at the inland side of the barrier will be able to flow out of the river system. Consequently, the water level at the inland

side of the barrier can be controlled. With the construction of the barrier, a part of the North Sea is changed into a lake during closed conditions. This lake is referred to as the Tidal Lake and can be seen in Figure 2.4. More information regarding the impact of the Delta21 concept on the water levels can be found in Section 2.3.3. More information on how the system works can be found in Section 2.4.1.

The construction of the storm surge barrier means that the Haringvliet sluices lose their water retaining function as primary flood defence. Subsequently, the configuration in which the sluices are partly opened can be replaced by the configuration in which the sluices are completely opened. With the closure of the Haringvliet in 1970, the environment upstream of the sluices changed. The additional aim of the Delta21 concept is to restore this environment. Only during conditions with a low river discharge the Haringvliet sluices will be closed to overcome salt intrusion far upstream.

The Delta21 concept is also aiming on covering the shortages and surplus on the electricity market and to generate sustainable energy. Shortages and surpluses of electricity can occur due to the variability in supply and demand on the electricity market. For instance, due to cloudy weather the effective energy harvesting of solar energy is temporarily reduced. To prevent these shortages on the market, the pumping station of Delta21 can be used to let water flow into the Energy Storage Lake from sea. The pumps are then used as turbines which generate electricity. During a surplus on the market, water can be pumped out of the Energy Storage Lake which requires electricity. A more detailed description of the use of Delta21 for energy can be found in Section 2.3.3.

### **2.3.3. Purposes of Delta21**

#### **2.3.3.1. Flood Protection**

The main purpose of the Delta21 plan is to improve the flood protection in the Southwest Delta. The plan aims to improve the flood protection in two different conditions. Firstly, a condition in which there is a high discharge in the rivers without storm surge at sea. In Figure 2.5 a schematization of this condition is presented. When high river discharge is expected, the new storm surge barrier will be closed during high water. The spillway will be opened to let water out of the river system and into the Energy Storage Lake. The water level in the Tidal Lake can be controlled and will be lowered in this configuration. Consequently, the water levels upstream will decrease. The water of the Haringvliet is originated from the Rhine and the Meuse. However, not all the water is leaving the system by the Haringvliet. Part of the water is leaving the system at Hoek van Holland by using the Nieuwe Waterweg. By keeping the water level at the Haringvliet low, the discharge distribution between the Haringvliet and the Nieuwe Waterweg will change. More water will flow into the Haringvliet basin and less will flow into the Nieuwe Waterweg. This all to establish a balance in the water levels at the bifurcation of the rivers. This results in lower water levels in vulnerable areas like Dordrecht. Dordrecht is one of the cities that is very vulnerable to flooding due to the low defence structures in that area. The water that leaves the system by using the spillway can then be pumped into the North Sea by using the pumping station.

In the second condition, high discharges occur in combination with storm surge at sea. A storm surge at sea causes an increase in sea level which results in an increase of the water levels in the rivers. Combining this storm surge at sea with high river discharges will have an accumulated effect on the water level increase. During storm surge situations, the storm surge barrier of the Delta21 plan will be closed. This helps in counteracting the impact of the storm surge on the water level. To ensure the water level upstream does not increase as a result of the closed barrier, the spillway towards the Energy Storage Lake will be opened. Now, the same happens as in the condition without the storm surge, the water level at the Tidal Lake will decrease. As a result of this the water levels upstream will decrease as well.

Besides the improvement of the flood protection during the conditions with high discharge, Delta21 aims to decrease the frequency of closure of the Europoort barrier in the future. Due to the expected sea level rise, the frequency of closure will increase if no measures are taken. For navigational purpose, it is not desirable to let the barrier close more often. The use of the Energy Storage Lake to improve the flood protection in the Southwest Delta can lead to a lower frequency of closure of the Europoort barrier. This can be accomplished by extracting water from the Haringvliet which affects the water levels at the bifurcation upstream.

This can lead to lower water levels in the Nieuwe Waterweg and therefore a lower frequency of closure for the Europoort barrier.

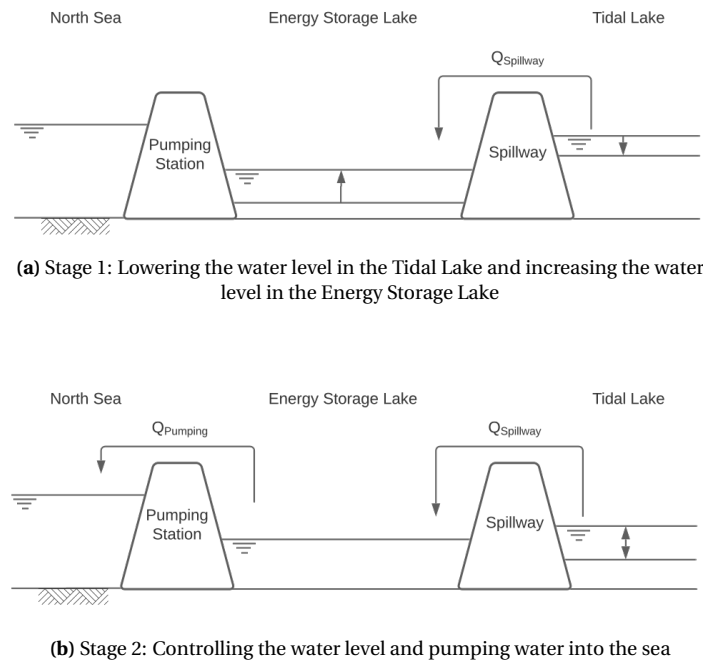


**Figure 2.5:** Schematization of Delta21 for the Flood Protection

### 2.3.3.2. Energy Transition

The goal of the National Climate Agreement (2019) is to have net zero carbon emissions from energy generation. This means a change from fossil fuels, which have high CO<sub>2</sub> emissions, to sustainable energy which have limited CO<sub>2</sub> emission. This change is also referred to as the energy transition. Many solutions providing renewable energy are weather-dependent. Because of this dependence and the weather conditions in The Netherlands, surpluses and shortages occur on the electricity market. A surplus means that the supply of energy is more than the demand. This can occur in situations with sunny and windy weather. When it is cloudy and there is no wind, the demand is greater than the supply. This is a situation with shortages of electricity on the market. The second purpose of the Delta21 concept is to generate a better balance in the electricity market. If there is a surplus, water can be pumped into the sea, using electricity, and if there is an electricity shortage, water can flow into the lake, generating electricity (Lavooij and Berke, 2018a). In Figure 2.6, a schematization is presented for the use of Delta21 for the energy transition. Besides this, the Energy Storage Lake can also be used to increase the percentage of sustainable energy by placing solar panels on the water surface or wind turbines around the lake.

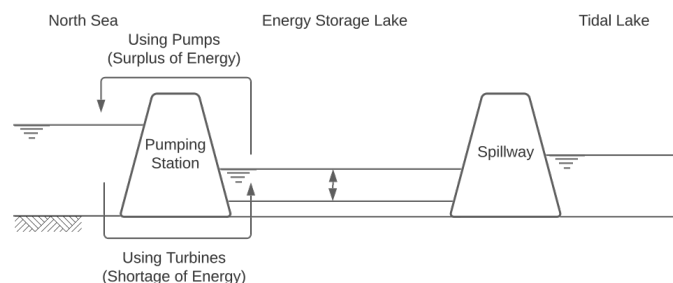


**Figure 2.6:** Schematization of Delta21 for Energy

### 2.3.3.3. Nature Restoration

The third purpose of Delta21 is to restore the nature in the Haringvliet basin. After the Haringvliet sluices were built, the initial idea was that only water could flow into the sea and not into the basin. Consequently, the upstream water became fresh, the water quality decreased, the ecological system changed and the diversity of fish decreased (Ministerie van Infrastructuur en Milieu, 2015). Several years later, it was decided that the sluices should be opened more. This to bring back salt water into the basin and make room for a greater diversity of fish. When realising the Delta21 concept, the Haringvliet sluices can be fully opened. By fully opening the sluices, the biodiversity in the region will increase even more. More fish like salmon and trout can easily enter the river basin and new vegetation can grow next to the water (Lavooij and Berke, 2018b). In Wijsman et al. (2018) the effects of different ways of using the Haringvliet sluices were investigated. Two scenarios that were used in this research are very similar to the situation of Delta21. This is the situation in which the Haringvliet sluices are used as storm surge barrier, which means an open system during normal conditions without considering sea level rise and the scenario in which sea level rise is considered. Other scenarios that were investigated were the current situation with a small opening of the sluices (Kierbesluit) and a situation in which part of the tide would have influence in the basin. The conclusion of this research is that for the improvement of the nature, the situation in which sea level rise is not considered and the sluices are fully opened is most optimal. But, even with including the sea level rise, fully opening the sluices result in a more optimal situation compared to the current situation.

### 2.3.4. Discharge of Excess River Water by the Energy Storage Lake

To let river water flow into the lake, a spillway between the Tidal Lake and the Energy Storage Lake needs to be created. Otherwise, the excess water of the Rhine and Meuse cannot flow into the lake and from there on be pumped into the sea when the storm surge barrier is closed. For the inflow structure, multiple solutions can be thought of but not all are equally effective. During storm conditions the inflow structure should have a maximum capacity of 20 000 m<sup>3</sup>/s. The pumping station has a maximum capacity of 10 000 m<sup>3</sup>/s. The Energy Storage Lake has a total volume capacity of 400 000 000 m<sup>3</sup>. This capacity is based on the minimum and maximum water level of the Energy Storage Lake. With a pumping capacity of 10 000 m<sup>3</sup>/s it takes around 11 hours to empty the Energy Storage Lake. The inflow discharge will only reach the 20 000 m<sup>3</sup>/s during extreme conditions. Over time, the discharge will decrease because the water level difference stimulating this flow will decrease. Therefore, it is difficult to tell the duration of the filling process. This depends on the type of inlet structure and the water levels.

## 2.4. Process and Function analysis

In this section the process and function analyses are described. First, the process analysis is performed and after that the process analyses can be found. These analyses give an insight in the desired use and behaviour of the structure (Voorendt and Molenaar, 2020a).

### 2.4.1. Process Analysis of the Delta21 System

In the process analyses an overview of all the stages that occur during different scenarios for the Delta21 system can be seen, Figure 2.7 (Lavooij and Berke, 2018c). Three different scenarios can be distinguished in Figure 2.7. In the first scenario an increase in river discharge occurs, in the second scenario a storm surge at sea is present and the third scenario is a combination of the two. All scenarios are depending on the water level at Dordrecht. If this water level reaches NAP +2.5 m, the spillway should be opened and the pumping station needs to be activated. The boundary conditions for these scenarios are given in *Delta21 en Waterveiligheid* (Lavooij and Berke, 2018c).

During normal conditions, the spillway is closed and only the pumping station is active. The way the pumping station is functioning during normal conditions can be divided into two different scenarios. In the first scenario the pumping station is pumping water out of the Energy Storage Lake. This requires electricity and will be performed during a surplus on the electricity market. In the second scenario there is a shortage on the market. In this scenario the pumping station is used as turbine station to generate electricity by letting water

flow into the Energy Storage Lake. By flowing into the lake, the water is passing the turbine which generates electricity.

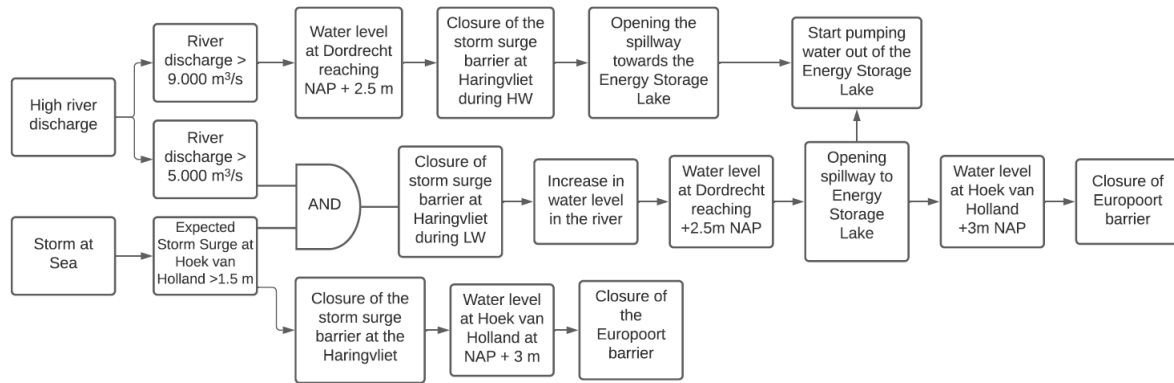


Figure 2.7: Process of Delta21 system

### 2.4.2. Function Analyses

The functions of the system can be divided in three different types: principal, preserving and additional functions. The principal function is the main reason to create the structure. A preserving function is a function that has the aim to remove or reduce the negative effects caused by the structure and an additional function is a function that is not originated from the principal function of the structure (Voorendt and Molenaar, 2020a). For the Delta21 concept the following functions can be distinguished.

Principal function:

- Protecting the hinterland from flooding

Preserving function:

- Enable ships to navigate to sea or into the Haringvliet
- Ensure the river discharge into the sea
- Reduce the saltwater intrusion in the Haringvliet
- Restoration of the ecology behind Haringvliet sluices

Additional function:

- Extending the length of the shore for recreation
- Generating sustainable energy

The goals of Delta21 can be found in the functions of the concept. The main goal is to increase the flood protection of The Netherlands, mainly the Southwest Delta, which makes it also the principal function of the system. The other two goals, nature restoration and energy transition, are preserving or additional functions.

Looking with more detail at the spillway between the Haringvliet and the Energy Storage Lake, the following functions can be distinguished.

Principal function:

- Enable water flow from the Haringvliet into the Energy Storage Lake

Preserving function:

- Protecting the hinterland from flooding

As mentioned above, three different types of functions can be distinguished but for this structure only two types are relevant. There are no additional functions for this structure.

## 2.5. Stakeholder Analysis

Each stakeholder at a project has its own interests and ideas about the project. It is important to identify the stakeholders and get to know their interests. The interest of the stakeholders are converted into requirements and evaluation criteria in Chapter 3. The stakeholders are divided into three groups: key stakeholders, primary stakeholders and secondary stakeholders.

- **Key Stakeholders**

Key stakeholders are the most important stakeholders, without them the project will not even start. They have the power to enforce laws or regulations that are necessary to successfully realise the project or for it to be terminated. A key stakeholder can also be a primary or secondary stakeholder.

- **Primary Stakeholder**

Primary stakeholders are stakeholders that are directly influenced by the project.

- **Secondary Stakeholders**

Secondary stakeholders are indirectly influenced by the project.

### 2.5.1. Stakeholder Inventory

The stakeholders are identified by using the information provided by their website. The power of the stakeholder depends on the extent to which the stakeholder has influence on the way the project develops. For example, a ministry can enforce laws and due to this, their power is very high. On the other side, citizens have no means to enforce anything so their power is low. In this stakeholder analyse there has not been any contact with the stakeholders themselves. In this section the key stakeholders are elaborated and in Appendix A the primary and secondary stakeholders are discussed.

#### Ministry of Infrastructure and Water Management

The Ministry of Infrastructure and Water Management is a key stakeholder in this project. They are responsible for the legislation and rules for water safety in the Netherlands. One of their aims is to keep The Netherlands safe against flooding by decreasing the probability of flooding (Government of The Netherlands, 2020b). Delta21 has a positive contribution for the ministry because it increases the water safety in the area. The power of the ministry is very high because they are the policy makers. Their aim is to keep The Netherlands as safe as possible against flooding and therefore their interest is also very high.

#### Rijkswaterstaat

Rijkswaterstaat is the client of the project. Rijkswaterstaat is one of the government agencies of the Ministry of Infrastructure and Water Management. On the website of Rijkswaterstaat their mission is stated as: 'Working together on a safe, liveable and accessible Netherlands. That is Rijkswaterstaat.' (Rijkswaterstaat, 2020b). In which safe stands for the safety against the water. They are responsible for the construction and the maintenance of the Dutch flood defence structures. Therefore they have a lot of power within the project. For Rijkswaterstaat, flood protection is just as important as for the Ministry of Infrastructure and Water Management. The project has a positive effect on the flood protection and therefore the interest in this project is very high.

### 2.5.2. Stakeholder Involvement

Each stakeholder needs to be involved in another way. The way of involvement depends on the power and the interest of the stakeholder. In Figure 2.8, the estimated power and interest can be found of each stakeholder. The key stakeholders should be involved in the project from the start. With decreasing power and interest, the involvement decreases as well. It is important to identify the requirements and wishes of the key stakeholders, because these are the most important requirements and wishes for the design. For the group of stakeholders that are on the low side of power and interest, delivery of information is critical. It is important to keep those stakeholders informed during the project. The same applies for the stakeholders with more interest but less power. Keep them informed and involve them once in a while. The wishes and interest of the stakeholders with less power should be considered and implemented in the design if possible but not at all costs.

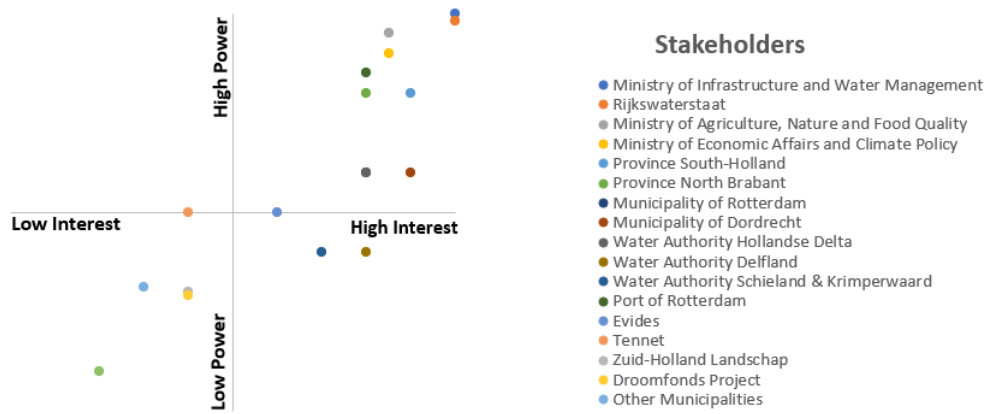


Figure 2.8: Stakeholder Classification Matrix

## 2.6. Problem Statement

Based on the exploration of the problem in the previous sections, the following problem statement can be formulated:

It is not yet known in sufficient detail, how to let the excess river water flow in a controlled manner into the Energy Storage Lake. This should be done in such a way that during situations with a closed barrier and high discharge, the water level in Dordrecht does not exceed NAP + 2.5 m.

# 3

## Basis of Design

In this chapter, the second design phase is described: the basis of design. In this phase, the design objective is stated, the scope of the thesis is determined, the requirements for the design are given, evaluation criteria are shown, and the boundary conditions are listed.

### 3.1. The Design Objective

The design objective of this thesis is to come up with a conceptual design of the inflow point for the excess river water between the Tidal Lake and the Energy Storage Lake. The conceptual design is found by developing multiple concepts and choosing the best functioning concept. This design should fulfil all the functional and structural requirements and should be affordable, constructible and should fit within the ideology of Delta21.

### 3.2. Scope

This thesis focuses on the conceptual design of the spillway itself. The integration of the spillway and the other components of the Delta21 concept are outside of the scope. In the verification of the design, the hydraulics, stability and strength are used to establish a feasible design. The design of the spillway includes a preliminary design of the required scour protection in both the Tidal Lake as the Energy Storage Lake. In the design of the scour protection, the focus is on the local scour problems.

### 3.3. Requirements

The required performance of the spillway is given in the design requirements. These requirements follow from the interest of the stakeholders and the required operation to function as a flood defence structure. The requirements of a design can be divided into functional requirements and structural requirements. The conceptual design must fulfil both these requirements.

#### 3.3.1. Functional Requirements

- The required discharge capacity is 20 000 m<sup>3</sup>/s during storm conditions
- The water level at the Tidal Lake does not exceed NAP +2 m, otherwise flood event will occur in Dordrecht
- The spillway can be closed
- The discharge is controllable
- The spillway is part of the primary defence system
- The spillway prevents fish to enter the Energy Storage Lake



- The lifespan of the structure must be at least 100 years

### 3.3.2. Structural Requirements

- The structure is maintainable
- The structure is constructible
- The structure is overall stable
- The structural elements have sufficient strength

## 3.4. Location Criteria

Before the development of the concepts, the possible locations for the spillway within the dune trajectory that separates the Tidal Lake and the Energy Storage Lake. This is part of the third phase in the engineering design cycle. For the selection of the final location, the following criteria are used:

- **The morphological influence**

As a consequence of the discharge requirement of 20 000 m<sup>3</sup>/s for the spillway, high flow velocities near the structure are expected. These high flow velocities can have a big influence on the morphodynamics in the area. For the optimal location, it is important that the morphodynamics near the structure have less influence on other structures near the spillway.

- **Influences on other structures**

Besides the morphological influence, the spillway can also influence structures nearby. For example, the discharge of the spillway can lead to high forces on other structures. This is not desirable because it can lead to larger strength requirements for the structures nearby. A larger load due to the outflow of the water can therefore lead to higher costs of surrounding structures, for instance the pumping station or the dunes.

- **Ease of construction**

During the construction stage, there must be enough space available. For example, transport of construction elements needs to be possible, and during the placement of the scour protection sufficient space needs to be available.

## 3.5. Evaluation Criteria

In the evaluation process of the different concepts, Chapter 7, multiple evaluation criteria are used in the multi-criteria analysis.

- **Ease of operation:**

Each concept differs regarding the necessary steps that need to be taken during the operations of the spillway. If more steps have to be taken, the system can be considered more complex and receives a lower rating for the ease of operation. For example, a higher number of gates leads to a more extensive system but is still relatively less complex than a system that requires a pumping system. The ease of operation criterion is derived from the interest of Rijkswaterstaat, which will be in the lead of the operation of the spillway.

- **Ease of construction:**

The ease of construction depends on the design of the construction. Bigger structures are more difficult to transport and to place on the final location. Accessibility of the construction site will be taken into consideration within this evaluation criterion. The ease of construction is important for the main contractor and the government stakeholders. This influences the amount of work and their planning.

- **Serviceability and possibility of inspection:**

The maintenance of a structure is very important but sometimes overlooked during the design stage. This can lead to high costs during the operation stage. For this reason, the structure must be easy to maintain. To compare the concept on the serviceability and possibility of inspections, the accessibility of the structure is also taken into account. Besides this, the ease of replacement of components of the

spillway is considered. Again, the serviceability and possibility of inspection is derived from the interest of Rijkswaterstaat because they are responsible for the inspection and maintainability.

- **Integration in the environment:**

For the integration in the environment, the implementation of the structure in the surroundings is taken into consideration. This criterion is relevant for the environmental stakeholders, for instance the Zuid Hollands Landschap. The structure can be part of the environment, which results in a higher score for this specific criterion, or a stand-alone structure that is not integrated into its surroundings, which results in a lower score. In areas in which nature is important, the integration of the structure into its environment is desired.

- **Sustainability:**

The idea of Delta21 is to restore the nature of the Haringvliet basin. This criterion is again important for the environmental stakeholders. It is important that the design will have a positive influence on the ecology. A design that uses large volumes of concrete is not sustainable and has a large carbon footprint. This will be considered in this criterion, which regards the sustainability of the spillway concept design. Besides the carbon footprint, the reuse of materials is taken into consideration.

## 3.6. Legal Boundary Conditions

### 3.6.1. Laws and Regulations

The legal boundary conditions are the constraints of the project by regulations and laws. For the Delta21 concept there are multiple important and relevant laws and regulations. The relevant laws and regulations are presented below by their English name and Dutch name:

• Water Act	Waterwet
• Nature Conservancy Act	Wet Natuurbescherming
• Environmental Management Act	Wet Milieubeheer
• Spatial Planning Act	Wet Ruimtelijke Ordening
• Environmental Permitting (General Provisions) Act	Wet Algemene Bepalingen Omgevingsrecht
• Dutch Building Decree 2012	Bouwbesluit 2012 <sup>1</sup>
• Environmental Structures Decree	Besluit Bouwwerken Leefomgeving <sup>2</sup>

For the design of the spillway, the Water Act is the most relevant regulation. This act is a combination of multiple older water regulations and is active since 2009. The water act consists of regulations and laws for the usage and management of the water systems in The Netherlands. Another important guideline is *Leidraad Kunstwerken*. In this guideline, a lot of information about loads and load combinations on defence structures can be found. The Eurocodes are also used for the design of the spillway.

### 3.6.2. Reliability

For the construction of flood defence structures, there are two relevant reliability requirements to consider: The reliability regarding the water retaining function of the flood defence structure and the reliability regarding the loads, load combinations and the individual structural parts. The first one is described in the Water Act and the second one is described in the Dutch Building Decree 2012 (Jongejan and Steenbergen, 2015). In the past, the spillway would be a c-type barrier. C-type barriers are either situated behind a primary flood defence or play a role in the flood protection if other defence structures fail. However, in distinguishing the type of barriers, the c-type barrier is not used anymore and therefore the spillway can either be seen as a primary or secondary defence structure. Although the spillway is not retaining water during extreme conditions, the importance of the spillway is significant in this regard. The spillway affects a vast majority of the primary flood defence structures in the Southwest Delta. Therefore, the spillway can be considered as a

<sup>1</sup>The Dutch Building Decree will expire in 2022

<sup>2</sup>The Environmental Structures Decree is the successor of the Dutch Building Decree 2012

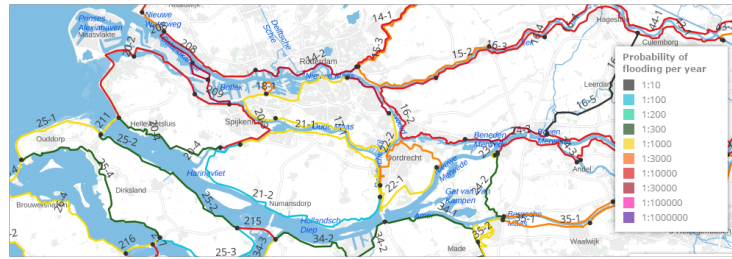


**Figure 3.1:** Primary flood defence standards of the Southwest Delta

primary defence structure. In the Water Act, the safety standards for the primary flood defences are stated. Since 2017 these standards are defined as the probability of flooding of a certain section of the flood defence. This probability of flooding depends on the probability of failure of the section during different hydraulic loads and the impact of the flooding on the area. For the Southwest Delta, the probabilities of flooding per year can be found in Figure 3.1. For the design of the spillway of Delta21, the old safety standards are used. This results in a safety standard of 1:1000 years for the spillway, the same standard as for the Haringvliet sluices (211 in Figure 3.1). For the reliability requirements regarding the loads, load combinations and the individual construction parts the Dutch Building Decree 2012 refers to the Eurocode NEN-EN 1990.

### 3.7. Natural Boundary Conditions

#### 3.7.1. Geo-technical Conditions

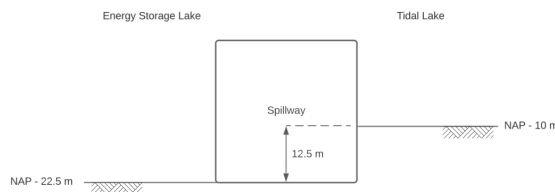


**Figure 3.2:** Bed levels around the Spillway

The bed level of the Tidal Lake is at approximately NAP -10 m near the location of the spillway and NAP - 8 m near the start of the dunes. The Energy Storage Lake will be excavated to a depth of NAP -22.5 m (Lavooij and Berke, 2019). In Figure 3.2, the bed levels can be seen. The current seabed level is equal to the bed level of the Tidal Lake. The soil conditions below the bed are determined with the use of multiple cone penetration test (CPT) results. These CPTs are retrieved from the database of the Dinoloket (2020). In Appendix B the results of the three most relevant CPTs can be found. The relevance of the test depends on the depth of the test and the location of the test. By comparing the results of the three relevant tests, the conclusion can be made that the soil mostly consists of sandy layers with small clay layers in between. Because the results from the investigations are very similar, one of the investigations, CPT S36H00033-00, is taken as governing for the design of the spillway. The soil profile that corresponds to this governing result can be found in Figure 3.3.

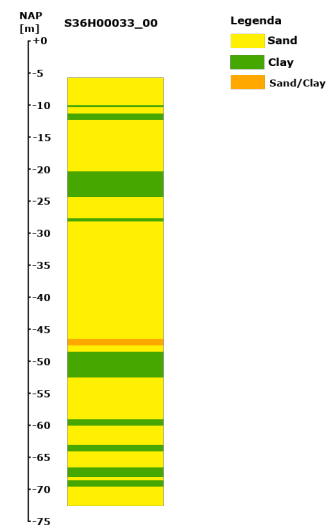


**Figure 3.3:** The governing soil profile

The relevant depths are the depth of the Energy Storage Lake relative to NAP and the depth of the Tidal Lake relative to NAP. By excavating the Energy Storage Lake, the clay layer between NAP -20 m and NAP -25 m will be removed and afterwards a new sand layer will be placed between NAP -22.5 m and NAP -25 m. This results in a large sand layer between the bottom of the Energy Storage Lake at NAP -22.5 m and NAP -47 m. The bed level of the Tidal Lake is at NAP -10 m. Below this, a clay layer is present. The representative values of the soil parameters can be found in Table 3.1.

Name	Admixture	Consistency	$\gamma$ [kN/m <sup>3</sup> ]	$\gamma_{sat}$ [kN/m <sup>3</sup> ]	$q_c$ [MPa]	$C'_p$	$C''_p$	$C_c/(1+e_0)$ [-]	$C_\alpha$ [-]	$C_{sw}/(1+e_0)$ [-]	$E_{100}$ [MPa]	$\phi$ [Degree]	$c'$ [kPa]	$C_u$ [kPa]
Sand	Clean	Mediocre	18	20	15	600	$\infty$	0.0038	0	0.0013	45	32.5	0	-
Sand	Clay	-	19	21	8	300	$\infty$	0.0015	0	0.0005	20	35	0	-
Clay	Clean	Mediocre	17	17	1	15	160	0.1533	0.0061	0.0511	2	17.5	5	50

**Table 3.1:** Representative values of the soil properties, retrieved from NEN-EN1997 NB:2019 Table 2.b

### 3.7.2. Meteorological Conditions

The wind direction and velocity is influencing the wind-set up and the wave height near the spillway. Figure 3.4 shows the direction from which the wind originated near the location of the spillway from 1970 to 2020. This data is retrieved from the KNMI database (2020). It can be seen that the wind originating from the Southwest has the highest frequency of occurrence. This direction is parallel to the dike trajectory in which the spillway will be constructed.

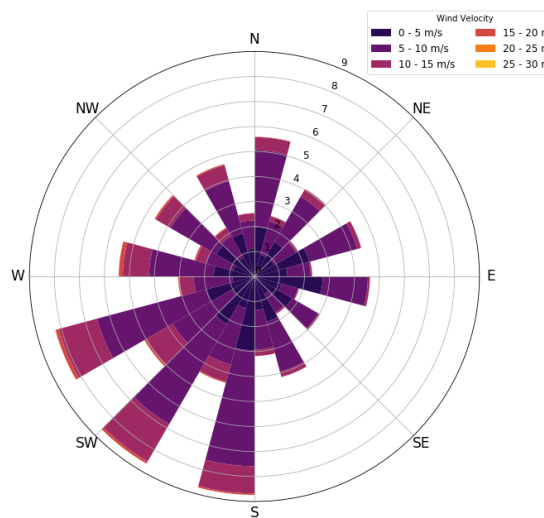
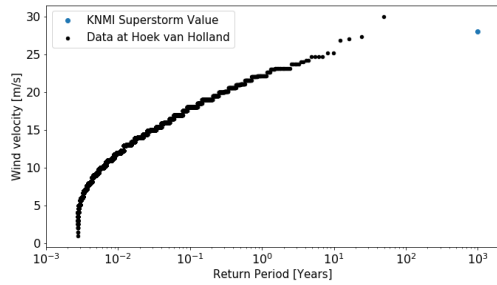
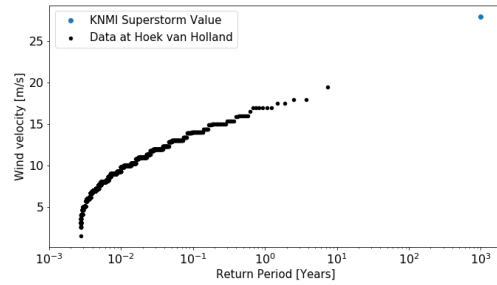


**Figure 3.4:** Wind direction at Hoek van Holland

In Figure 3.4, it can be seen that the wind velocity is rarely exceeding the 20 m/s. The return period of the wind velocity can be seen in Figure 3.5a. The probability of flooding of the spillway is 1:1000 and therefore a return period of 1000 years is taken for the wind velocity. According to the KNMI (2020), this corresponds to a wind velocity of 170 km/h. This velocity is considered at 2 km height and takes into consideration climate change. For design calculations, the wind velocity at 10 m height is required. Therefore a conversion is carried out to retrieve the wind velocity at a height of 10 m. This conversion can be seen in Appendix C and leads to a design wind velocity of 28 m/s. Comparing this value to the return periods in Figure 3.5a, it can be concluded that this is in line with the expectations from the measured data from all wind directions. It has to be taken into account that perpendicular wind conditions are the most critical. However, the higher wind velocities do not originate from the perpendicular directions. The use of a design velocity of 28 m/s leads to a conservative value for wind set-up and wave height. In Figure 3.5b, it can be seen that the design velocity is not completely in line with the measured data.



(a) Return period of the wind velocity (All Directions)



(b) Return period of the wind velocity (Perpendicular to Spillway)

### 3.7.3. Water Levels

The spillway will be situated between the Energy Storage Lake and the Tidal Lake. Therefore the only relevant water levels regarding the design of the spillway are the water levels in those lakes. The water level of the Energy Storage lake is only affected by the components of the Delta21 concept. The difference in inflow by the spillway and outflow by the pumping station determines the water level in this lake. For the Tidal Lake, the water level is depending on several factors, for instance the storm surge barrier but also the inflow from the Rhine and the Meuse.

#### 3.7.3.1. Energy Storage Lake

The pumping station requires a minimum water depth of 5 m to function properly (Lavooij and Berke, 2018c). This corresponds to a minimum water level at NAP -17.5 m. For pumping efficiency purposes, the maximum allowable water level in the lake should not exceed NAP -5 m. This results in a maximum variation of 12.5 m in the Energy Storage Lake. During normal conditions, the water level in the Energy Storage Lake will vary over time to generate and use energy to establish a more balanced electricity market. In extreme conditions, the Energy Storage Lake is at the lowest possible level. With a volume of 400 million m<sup>3</sup> and a pump capacity of 10 000 m<sup>3</sup>/s it takes between 11 and 12 hours to fully empty the Energy Storage Lake. At Lobith, an increase in discharge and water level is predicted approximately three days before the event. For a storm surge event, this is predicted approximately 24 hours before the event (Kwadijk, 2004). This means that there is sufficient time to empty the Energy Storage Lake before the event occurs.

#### 3.7.3.2. Tidal Lake

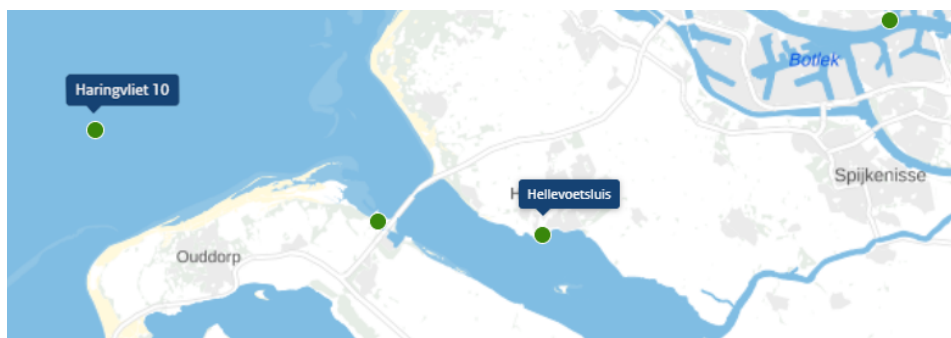


Figure 3.6: Location of the measurement stations

During normal conditions the storm surge barrier is open and the water level in the Tidal Lake is solely dependent on the sea level. This means that in an open situation, the water level of the Tidal Lake is influenced by the tide. The general tide characteristics for the North Sea near the Delta21 location can be seen in Table 3.2. These characteristics are retrieved from measurement station Haringvliet 10, see Figure 3.6. The expected general characteristics by 2100 can also be seen in Table 3.2. For these characteristics, a sea level rise of 1 m is

taken as the expected rise. This corresponds to the maximum expectation of the KNMI provided in the 2014 climate scenarios. The same expectation for the sea level rise is used for the construction of the sluices of IJmuiden and Terneuzen by Rijkswaterstaat (van Waveren, 2018). It is assumed that the construction of the storm surge barrier does not influence the tide.

Time Period	Reference	Mean Sea Level (MSL)	Mean Tide		Spring Tide		Neap Tide	
			High Water	Low Water	High Water	Low Water	High Water	Low Water
2020	NAP [m]	+0	+1.24	-0.86	+1.45	-0.92	+0.93	-0.77
2100	NAP [m]	+1	+2.24	+0.14	+2.45	+0.08	+1.93	+0.23

**Table 3.2:** General tide characteristics Haringvliet 10 (Dillingh, 2013)

During extreme conditions, the storm surge barrier will be closed. The water level in the Tidal Lake is then depending on the incoming discharge by the Rhine and the Meuse and the outflow through the spillway. With the operation of the spillway, the water level in the Tidal Lake can be controlled. If a storm is expected with a storm surge of 1.5m at Hoek van Holland, the new barrier will be closed. This leads to a maximum water level in the Tidal Lake of NAP +1.5m. If the storm surge results in even higher sea levels, the Maeslantkering will be closed as well. If this closure fails, it can lead to higher water levels in the Tidal Lake. This situation will lead to a maximum water level of NAP +2 m in the Tidal Lake. With these maximum levels, the water level at Dordrecht is expected to stay below NAP +2.5 m (Lavooij and Berke, 2018c). It can be expected that by 2100, the storm surge barrier needs to be closed more frequently due to sea level rise.

The governing minimum water level in the Tidal Lake is dependent on the operation of the spillway. Depending on the discharge of the spillway and the inflow from the Rhine and the Meuse, the water level in the Tidal Lake can either rise or drop. Most of the time, the discharge from the spillway will exceed the discharge from the Meuse and Rhine combined. Therefore the water level in the Tidal Lake will drop. The rate at which the water from the Tidal lake is discharged through the spillway will decrease when the water level in the Tidal Lake decreases. The reason for this is the decrease in head level difference between the Tidal Lake and the Energy Storage Lake. The minimum water level in the Tidal Lake is NAP - 2 m. In normal conditions, this level will not be reached because the minimum water level due to the tide is higher. When the spillway is in use, a water level below the NAP - 2 m is not required because the water levels upstream will be lowered sufficiently when the Tidal Lake is at NAP - 2 m. Reaching a water level of NAP - 2m would require a long time because the area upstream of the Tidal Lake is large. Furthermore, a water level below NAP -2 m, could lead to problems for nearby harbours, for instance the harbour at Stellendam.

### 3.7.3.3. Uncertainty Surcharge for the design water level

The expectation of the maximum water levels has some level of uncertainty. This is due to uncertainties in the expectations of sea level rise and the levels that occur due to a failure of the Maeslantkering. The maximum water levels are subject to uncertainties regarding the expected sea level rise and the impact of possible failure of the Maeslantkering on the water level in the Tidal Lake. To take these uncertainties into account, the *Handreiking ontwerpen met overstromingskansen 2017* prescribes an uncertainty surcharge for water levels. For waters in the downstream area of the rivers, a surcharge of 0.4 m is stated. The Tidal Lake is defined as a water downstream of the Rhine and Meuse and therefore this 0.4 m is valid for the Tidal Lake. This 0.4 m needs to be added to the water level in the Tidal Lake. This results in a maximum water level in the Tidal Lake of NAP +2.4 m. In Figure 3.7, an overview can be found with the highest and lowest water levels that can occur in the tidal and Energy Storage Lake.

### 3.7.4. Wave Conditions

For the design of the spillway, a distinction is made regarding the origin of the waves. Swell and wind waves generated at the North Sea or wind waves that are generated on the Tidal Lake and Energy Storage Lake.

The relevance of the waves arriving from the North Sea is relatively low. The reason for this is that these waves are limited by two main factors. The first limitation is the closure of the storm surge barrier during storm surge conditions. In these conditions the highest waves are present. Due to the closure of the barrier, the waves from the North Sea cannot enter the Tidal Lake and are not able to reach the spillway. Only during

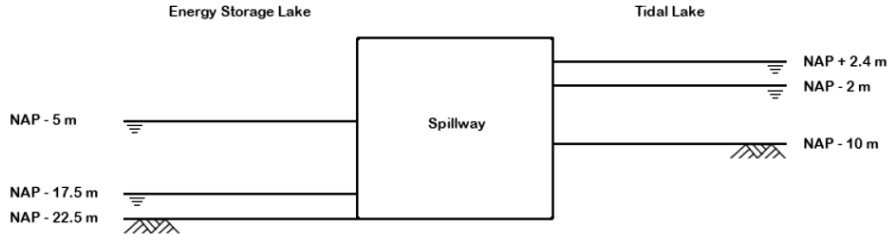


Figure 3.7: Governing water levels

normal conditions, the waves can enter the Tidal Lake. However, during these conditions the wave height is relatively low. The second limiting factor is the diffraction of the waves. In Figure 2.4, the location of the spillway relative to the opening of the storm surge barrier and the sea can be seen. The direction of the incoming waves is mainly parallel to the spillway. The storm surge barrier will cause the waves to diffract in the direction of the spillway. However, due to this diffraction, the waves will lose energy. This loss of energy is displayed in a decreased wave height. This diffraction will lead to a wave height reduction of approximately 90% (Johnson, 1952). Combining these two limitations leads to the conclusion that the waves originating from the sea can be neglected in the design of the spillway.

The wind waves generated on the Tidal Lake and Energy Storage Lake are the governing waves in the design of the spillway. The development of these waves depends on the wind direction, wind velocity, water depth and the available fetch length. Since there is no available data regarding the generated wind waves on both lakes, the wave height is calculated according to the Bretschneider formula, Formula 3.1.

$$\begin{aligned} \tilde{H} &= \tilde{H}_{\infty} \left\{ \tanh(0,343\tilde{d}^{1,14}) \cdot \tanh\left(\frac{4,41 \cdot 10^{-4} \tilde{F}^{0,79}}{\tanh(0,343\tilde{d}^{1,14})}\right) \right\}^{0,572} \\ \tilde{T} &= \tilde{T}_{\infty} \left\{ \tanh(0,10\tilde{d}^{2,01}) \cdot \tanh\left(\frac{2,77 \cdot 10^{-7} \tilde{F}^{1,45}}{\tanh(0,10\tilde{d}^{2,01})}\right) \right\}^{0,187} \end{aligned} \quad (3.1)$$

$$\begin{aligned} \tilde{d} &= \frac{gd}{U_{10}^2}; & \tilde{F} &= \frac{gF}{U_{10}^2} \\ \tilde{H} &= \frac{gH_{m0}}{U_{10}^2}; & \tilde{T} &= \frac{gT_p}{U_{10}} \end{aligned}$$

where:	$H_{m0}$	[m]	=	significant wave height
	$T_p$	[s]	=	peak wave period
	$g$	[m/s <sup>2</sup> ]	=	gravitational acceleration (= 9.81)
	$d$	[m]	=	average water depth of the fetch
	$F$	[m]	=	fetch, distance travelled by wind across open water
	$U_{10}$	[m/s]	=	wind velocity at an attitude of 10 m
	$\tilde{H}_{\infty}$	[-]	=	dimensionless wave height at deep water (= 0.24)
	$\tilde{T}_{\infty}$	[-]	=	dimensionless wave period at deep water (= 7.69)

The calculations for the significant wave height can be found in Appendix D. The wind velocity that is used is the design wind velocity with a probability of occurrence of 1:1000 years. The significant wave height resulting from these calculations are 1.49 m for the Energy Storage Lake and 1 m for the Tidal Lake.

### 3.7.5. Wind Set-up and Set-down

The wind set-up and set-down are both depending on the wind direction, wind velocity, fetch length and the water depth. Apart from these parameters, the wind set-up and set-down is also influenced by the type of water system. In a closed system, for instance a lake, the wind set-up and set-down are different compared to an open system, for instance a river. At one side of a closed system, a set-down occurs while on the other side a set-up is present. The set-down side is located at the side from which the wind is originating and the set-up

is present on the opposite side. In an open system, only one of the two will occur depending on the direction of the wind. The wind set-up and set-down of a closed and open system are described by respectively Formula 3.2a and 3.2b. In Formula 3.2a, the 0.5 is indicating that the gravity centre of the basin is located in the middle of the closed basin. The Energy Storage Lake is a closed system and the Tidal Lake is an open system.

$$\delta h_1 = \frac{0.5 \cdot F \cdot \kappa \cdot u_{10}^2 \cdot \cos(\phi)}{g \cdot h} \quad (3.2a)$$

$$\delta h_1 = \frac{\kappa \cdot u_{10}^2 \cdot \cos(\phi)}{g \cdot h} \delta x \quad (3.2b)$$

where:  $\delta h_1$  [m] = set up or down  
 $\delta x$  [m] = distance from the center of the basin  
 $\kappa$  [-] = friction value ( $\kappa = 3.2 \cdot 10^{-6}$ )  
 $\phi$  [°] = approach angle to the spillway  
 $h$  [m] = water depth  
 $F$  [m] = fetch, distance travelled by wind across open water

As mentioned in Section 3.7.2, the largest wind velocities are parallel to the spillway. Therefore, only at the outer edges of the dune trajectory, the maximum set-up and set-down will occur. The spillway will not be located near the outer edges of the trajectory and therefore, the parallel wind direction is not governing and neglected. If the wind perpendicular to the spillway is taken into consideration and the design velocity of 28 m/s is used in the calculation of the set-up and set-down, the resulting set-up and set-down are relatively low. A wind originating from the Southeast is governing perpendicular wind direction due to the corresponding set-up in the Tidal Lake and set-down in the Energy Storage Lake. This increases the difference in water levels. For the Tidal Lake, this results in +0.21 m and for the Energy Storage Lake in -0.13 m. Compared to the water level difference of 19.9 m without the set-up or down, the values for the set-up and down are low. Taking into account that the design velocity is slightly overestimating in the direction perpendicular to the spillway, the wind set-up and down are neglected in the remainder of this thesis.

### 3.7.6. River Discharge

The inflow of the Tidal Lake depends on the discharges in the Rhine and the Meuse. The impact of the Rhine on the Tidal Lake is significantly greater than the impact of the Meuse. The reason for this is that the Rhine has a discharge that is approximately four times as large as the Meuse. However, not all the water of the Rhine is flowing into the Tidal Lake. A part of the water is flowing into the IJssel near Arnhem. On average, 10% of the water that arrives at Lobith is flowing into the IJssel and 90% is ending up in the Southwest Delta (Rijkswaterstaat, 2019). All of the water from the Meuse flows into the Southwest Delta. In 2000, the Rhine had a governing discharge, with a probability of once every 1250 years, of 16 000 m<sup>3</sup>/s. With 90% reaching the Southwest Delta, this is approximately 14 400 m<sup>3</sup>/s. For the Meuse, the once every 1250 years discharge is 3 900 m<sup>3</sup>/s in 2000. These values can all be found in Section 2.2.4.

The expectations regarding the future discharges of the Rhine and Meuse are also mentioned in Section 2.2.4. It is found that at the end of the lifetime of the spillway, the discharges in the river are expected to increase. The discharge of the Rhine that corresponds with a probability of once every 1250 years by 2100 is between 19 000-22 000 m<sup>3</sup>/s. However, the discharge arriving at Lobith is depending on the flood protection measures that are taken in Germany. Their flood protection is designed for lower discharge and therefore flood events will occur before reaching the Netherlands. As a result of this, the governing discharge at Lobith by 2100 is expected to be 18 000 m<sup>3</sup>/s. Assuming that an equal percentage of 90% will reach the Southwest Delta, this results in an expected discharge of 16 200 m<sup>3</sup>/s. The discharge of the Meuse is expected to increase as well by 2100. The governing discharge of the Meuse is expected to be equal to 4750 m<sup>3</sup>/s by 2100. It needs to be considered that, although both rivers end up in the Southwest Delta, the probability of both reaching their once every 1250 years discharge at the same time is small. An overview of the discharges can be seen in Table 3.3



<b>River</b>	<b>Location</b>	<b>2000</b>	<b>2100</b>
Rhine	Lobith	16 000 m <sup>3</sup> /s	18 000 m <sup>3</sup> /s
Rhine	Southwest Delta	14 400 m <sup>3</sup> /s	16 200 m <sup>3</sup> /s
Meuse	Borgharen	3 900 m <sup>3</sup> /s	4 600 m <sup>3</sup> /s

**Table 3.3:** The governing river discharges in the Netherlands

### 3.7.7. Overview

In Table 3.4, an overview is shown for the natural boundary conditions.

<b>Parameter</b>	<b>Unit</b>
Bed level Energy Storage Lake	NAP -22.5 m
Bed level Tidal Lake	NAP -10 m
Most occurring wind direction	Southwest
Most unfavourable wind direction	Southeast
Design wind velocity	28 m/s
Fetch length Energy Storage Lake	5 000 m
Fetch length Tidal Lake	10 000 m
Maximum water level Energy Storage Lake	NAP -5 m
Minimum water level Energy Storage Lake	NAP -17.5 m
Maximum water level Tidal Lake	NAP +2.4 m
Minimum water level Tidal Lake	NAP -2 m
Significant wave height Energy Storage Lake	1.49 m
Significant wave height Tidal Lake	1 m
Normative Rhine discharge	18 000 m <sup>3</sup> /s
Normative Rhine discharge to Southwest Delta	16 200 m <sup>3</sup> /s
Normative Meuse discharge	4 600 m <sup>3</sup> /s

**Table 3.4:** Overview of parameters

# 4

## Location Selection

In the present design process, multiple types of concepts are generated, verified and evaluated. This chapter concerns the selection of the most suitable location for the spillway. The identification of multiple potentially suitable locations for the spillway can be considered as a form of concept development. The hydraulic design and the structural design loops are described in the next chapters. The selection of the location is the first design loop that is formed within the engineering design cycle. The spillway is the connection between the Tidal Lake and the Energy Storage Lake. Considering the Delta21 layout as discussed in Section 2.3.2, there is only a limited available area in which the spillway can be located. In Figure 4.1, the dune trajectory at which the spillway must be located can be seen. This dune trajectory has a length of approximately 6 km.



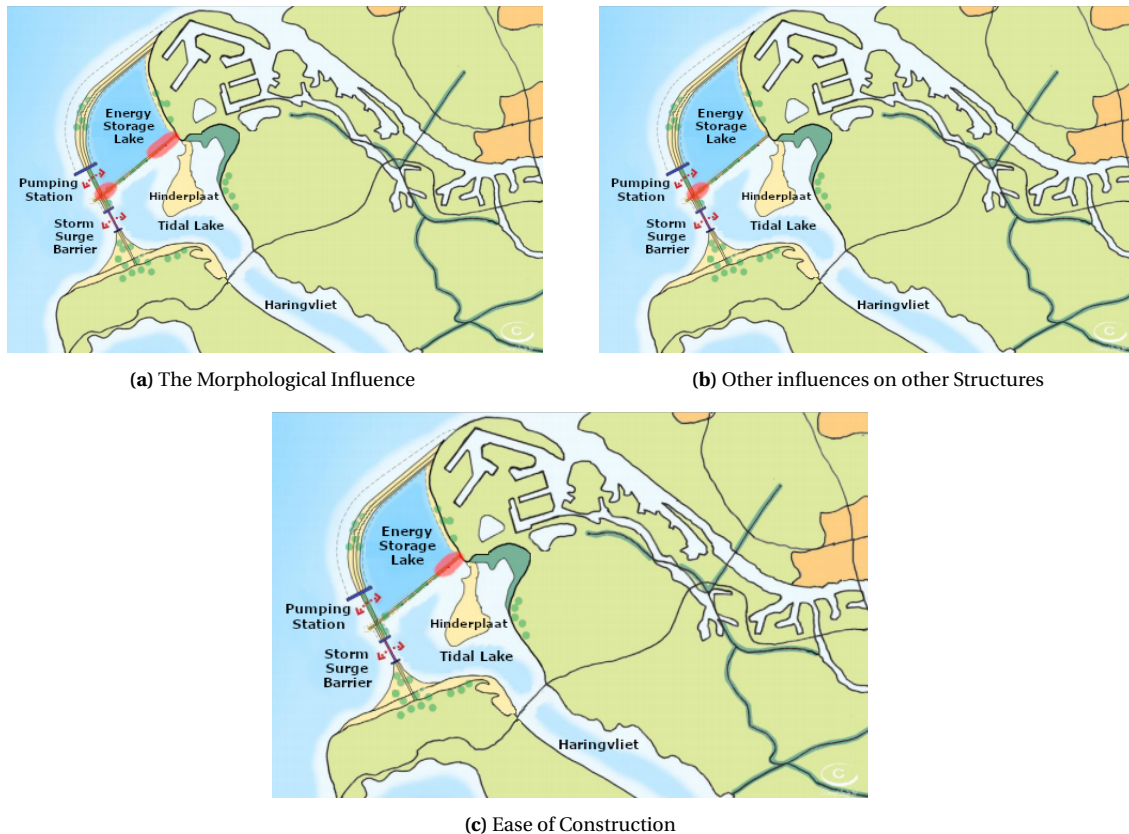
**Figure 4.1:** Potential area for the Spillway

A sieve analysis is carried out to select the final location of the spillway. The sieve analysis has as main objective to eliminate the locations which are not suitable for the spillway based on certain criteria. By eliminating the locations which are not suitable, a location remains which fulfils the requirements (Hertogh et al., 2019). Each criterion is considered separately and afterwards the results of all the criteria are combined. The criteria that are used for the selection of the location are discussed previously in section 3.4 but are also mentioned below:

- The morphological influence
- Influences on other structures
- Ease of construction

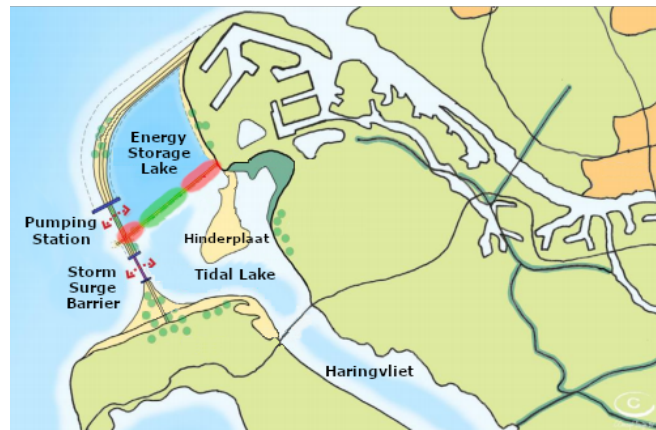
The result of the sieve analysis of each criterion can be found in Figure 4.2. The combined result of the sieve analysis can be seen in Figure 4.3. If the morphological influences of the spillway are considered, it can be concluded that the outer edges of the dune trajectory are not suitable for the placement of the spillway, see

Figure 4.2a. The outer edges of the dune trajectory are near soft retaining structures or areas with shallow water depths. The spillway of Delta21 is associated with high velocities due to the large discharge requirement. If high velocities are located near soft retaining structures this can negatively influence the stability of these structures. A part of Maasvlakte II consists of soft retaining structures and if the spillway is located nearby, measures have to be taken to improve the structures which is not desirable. The same applies to the dune trajectory perpendicular to the dune trajectory of the spillway. This is a soft retaining structure as well. Therefore the outer edges of the dune trajectory are eliminated and shaded red in Figure 4.2a. A part of the Tidal Lake is shallow due to the presence of the Hinderplaat. Although this Hinderplaat is dynamic and moving over time, it is mostly situated as located in Figure 4.2a. Sedimentation can become a problem if the spillway is located too close to the Hinderplaat. Therefore the area which is close to the Hinderplaat is eliminated and shaded red in Figure 4.2a.



**Figure 4.2:** Results of the sieve analysis, red area not suitable for spillway

The second criterion is the influence of the spillway on other structures. The spillway can affect the other structures in two different ways. The first way is the high force which is accompanied by the large velocity and turbulence just behind the spillway. This force influences the design of the other structures and will presumably lead to higher costs. The second way is the current that follows from opening the spillway. The high velocities in combination with the large turbulence can affect the pumping capacity of the pumping station if this station is located nearby. Therefore the location nearby the pumping station is eliminated and shaded red in Figure 4.2b. The last criterion is based on the ease of constructability. In this case, the outer area close to Maasvlakte II is shaded red, see Figure 4.2c. The transport of materials would be easy for this location because it is located near the current infrastructure. But the location will lead to problems if transport over water is required. This location is, as mentioned before, close to the Hinderplaat and therefore navigation can be more complex due to the shallow areas.



**Figure 4.3:** Final Location of the spillway

If all criteria are combined, the sieve analysis shows the suitable area for the location of the spillway. This area is shown in Figure 4.3 as the green shaded area. The length of this dune trajectory is approximately 3 km. The spillway will be located in the middle of the potential area because then the distance to the soft retaining structures is most optimal. However, the exact location of the spillway is depending on the width of the spillway.

# 5

## Generation of Concepts

Now the most suitable location of the spillway has been defined, the hydraulic design loop is elaborated. This chapter describes the generation of the hydraulic concepts. The hydraulic concepts are generated based on different hydraulic characteristics which are discussed in Section 5.1. Each characteristic leads to different design options. Combining these different design options of the characteristics lead to different concepts. Later on, these hydraulic concepts are verified on their discharge capacity and stability in Chapter 6 and evaluated in Chapter 7.

### 5.1. Spillway Characteristics

For the generation of concepts, four different characteristics are taken into consideration. The used characteristics of a spillway are:

- Type of flow
- Type of inlet
- Type of outlet
- Type of cross section

#### 5.1.1. Type of Flow

The flow of a spillway can be distinguished in two types of flow:

- Open channel flow
- Pressurised flow

The type of flow in a spillway is based on the presence of a free surface between the water and the atmosphere. The flow is seen as open channel flow if the free surface is present and is seen as pressurised flow if this free surface is absent. The presence of a free surface layer is partially depending on the type of channel. There are two types of channels: an open channel and a closed channel. In the case of an open channel, the type of flow which is present is already stated in the name. The opposite can not be said about closed channels. In closed channels, for instance a pipe or conduit, the occurrence of a free surface layer is depending on the inflow and outflow conditions. For certain inflow and outflow conditions, the pipe or conduit will be completely filled. In this case, there is no free surface and the flow must be seen as pressurised flow. In the other case, in which the pipe or conduit is not fully filled, the type of flow is open channel flow. The type of flow influences the discharge capacity of the spillway. In a pressurised flow, the resistance of the pipe or conduit leads to a lowering in discharge capacity. In open channel flow, this resistance can be neglected.

### 5.1.2. Type of Inlet

In Section 5.1.1, it is mentioned that the inflow conditions can affect the type of flow in the spillway for closed channels and therefore the discharge in these channels. For open channels, the inflow conditions only affect the discharge of the spillway. The inflow conditions are depending on the design of the inlet. The inlet can be distinguished by two characteristics. Firstly, the inlet can be submerged or unsubmerged and secondly, the inlet can be controlled or uncontrolled. For open channel spillways, the submerged conditions affect the dependence of the discharge of the spillway. In an unsubmerged condition, the discharge is only depending on the upstream water level but in a submerged condition, the discharge is also depending on the downstream condition. For closed channels, the submerged condition at the inlet can lead to either pressurised flow or open channel flow and an unsubmerged condition will lead to open channel flow. The final type of flow in closed channels is also depending on the outlet conditions. Submerged conditions in a closed channel are occurring if the headwater is above the top of the channel. In Figure 5.1a an example of a closed channel can be seen for which water levels above the high astronomical tide (HAT) lead to a submerged condition of the inlet.

Whether an inlet is controlled or uncontrolled is depending on the presence of a gate. With the presence of a gate, the flow can be controlled. The flow in a spillway with a controlled inlet starts flowing when the gate is opened. In an uncontrolled inlet, the flow starts when a certain threshold level is reached. One of the requirements of the spillway of Delta21 is that the flow must be controllable. Therefore, only options in which a gate is present are possible.

Besides the previously mentioned characteristics of the inlet, the inlet of an open channel type of spillway can be distinguished by the shape of the crest as well. The crest of the spillway can either be sharp or broad crested. The type of crest affects the determination of the discharge over the crest. An example of an unsubmerged, sharp crested spillway can be seen in Figure 5.1b.

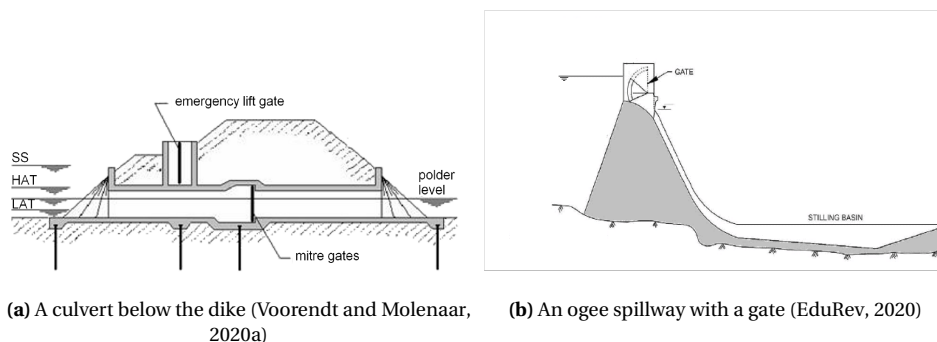


**Figure 5.1:** Examples of types of structures

### 5.1.3. Type of Outlet

The same distinction as for the inlet can be made for the outlet regarding the submerged and unsubmerged condition. If both the outlet and inlet of a closed channel spillway are submerged, pressurised flow will occur. If only the outlet is submerged, part of the flow will be pipe flow and the other part open channel (Benson and World Meteorological Organization, 1968).

### 5.1.4. Type of Cross Section

The type of cross section for the channels is different for each spillway. A cross section can differ in dimension and shape. In this thesis, only two shapes are taken into consideration: circular and rectangular. These shapes are the most commonly used shapes. Other possible shapes are trapezoidal and triangular.

## 5.2. The Concepts

By combining the different characteristics of a spillway, four different concepts are generated. In Section 5.2.1 up to Section 5.2.4, these concepts are described and shown. In Chapter 6, the verification of these concepts can be seen.

### 5.2.1. Concept Siphon

The first concept is the concept Siphon. Around the Energy Storage Lake, dunes will be constructed out of the sand that has been obtained by dredging of the lake. The layout of the dunes can be seen in Figure 5.2.

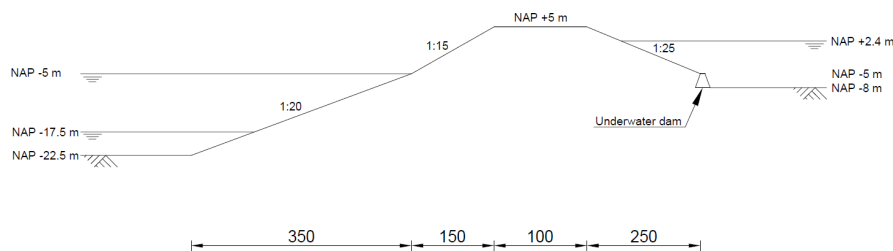


**Figure 5.2:** Dune Layout (NTS)

In the concept Siphon, the dunes will be used to retain the water and on top of the dunes concrete pipes will be constructed to let water flow from the Tidal Lake over the dune into the Energy Storage Lake. Steel pipes are considered but it is assumed that for the large diameter that is required, concrete is less expensive. The inlet and outlet of the spillway will always be submerged and at both sides, a gate is present to control the flow. Due to the ensured submergence of the inlet and outlet, the flow in the spillway is pressurised flow. The pipes of the spillway are going over the dunes and therefore exceeding the maximum water level. To enable this flow, a vacuum pump is required on top of the dune. With the addition of the vacuum pump, a new limitation is added as well. The vacuum pump only functions if the water level difference between the water level in the Energy Storage Lake and the top of the pipeline is not exceeding 10 m. If the increase is above 10 m, the atmospheric pressure cannot push the water up anymore because the pressure in the pipe is becoming negative.

Figure 5.3 illustrates the concept Siphon. The inlet and outlet of the pipe are caissons that contain the gates of the pipe. Both sides require gates to enable maintenance and avoid waves entering the caissons. Near the inlet and outlet, the scour protection will be placed to prevent scour close to the structure. At the inlet, a sediment trap will be placed to decrease the amount of sediment flowing into the spillway and ending up in the Energy Storage Lake. It can be seen in the figure that at the location of the scour protection, the lake is dredged to NAP - 10 m. This is to improve the inflow conditions and decrease the flow velocity near the bed.

The inlet of the concept Siphon will be at NAP - 6 m. In the original dune design, see Figure 5.2, an underwater dam would be placed with a height of 3 m. This dam will be replaced by the inlet caissons and the dune will stop 4 m above the dredged bed level. The top of the pipe at the outlet will be at NAP - 17.5 m, this to ensure the submerged conditions.

The caissons of this concept will be constructed in a construction dock. In the Tidal Lake and the Energy Storage Lake a construction dock will be constructed to decrease the amount of time that is required to construct all the caissons. From these docks, the caisson will be transported to the final location of the spillway.

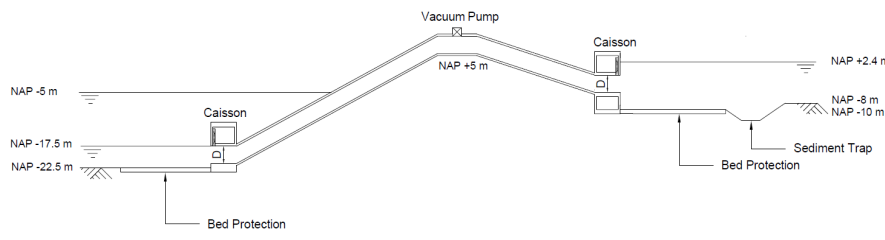


Figure 5.3: Overview concept Siphon (NTS)

### 5.2.2. Concept Underflow

The second concept is the concept Underflow. Again, the dune trajectory at the location of the spillway will be used. The main difference between this concept and the concept Siphon is that for this concept, the use of a vacuum pump is not necessary. The reason for this is the location of the pipe. The pipe will be located below the dune and therefore gravitational flow is possible. The pipes below the dune will be circular since this is more favourable for the soil pressure working on the pipe. Both the inlet and outlet will be caissons which include gates to control and stop the flow. The scour protection needed for this concept will be comparable to the concept Siphon because of the similar inlet and outlet.

The bottom of the inlet of the concept Underflow will be at NAP - 6 m. In the original dune design, see Figure 5.2, an underwater dam would be placed with a height of 3 m. This dam will be replaced by the inlet caissons and the dune will stop 4 m above the dredged bed level. The top of the pipe at the outlet will be at NAP - 17.5 m, this to ensure the submerged conditions.

The caissons of this concept will be constructed in a construction dock. In the Tidal Lake and the Energy Storage Lake a construction dock will be constructed to decrease the amount of time that is required to construct all the caissons. From these docks, the caisson will be transported to the final location of the spillway.

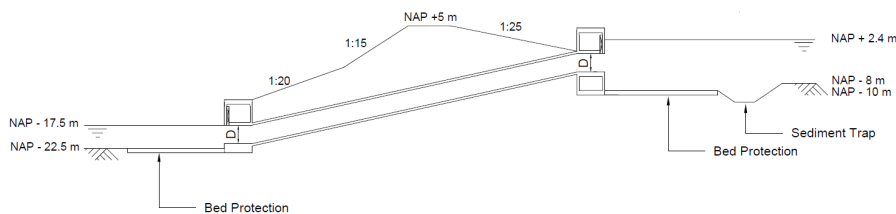


Figure 5.4: Overview Concept Underflow (NTS)

### 5.2.3. Concept Caisson

The third concept is the concept Caisson. In this concept, the dune is replaced by multiple caissons that divide the Tidal Lake and the Energy Storage Lake. The use of caissons is very common to separate two water bodies. A big difference between the first two concepts and this concept is the total width of the structure. The width is in this case the distance between the inlet and the outlet. This concept is a closed channel concept with both the inlet and outlet submerged. Therefore pressurised flow will occur during the use of the spillway. Only in situations of low water levels in the Tidal Lake, open channel flow can occur. However, during these situations, the spillway is closed or only used for low discharges. The conduit has a rectangular shape because of the more efficient use of the flow area compared to the circular shape. More efficiency leads to a lower number of conduits needed to reach the required capacity. Due to the large water level difference between the two lakes, a high flow velocity can occur in the spillway. Therefore there is chosen for two 90° bends in the conduit, to increase the energy loss in the structure. More about this in Chapter 6. Within each caisson, two gates are constructed to ensure the controllability of the flow. During normal conditions, in which the water levels are low and the spillway is not required, both gates will be closed. Both gates must be closed for two reasons. First, to prevent waves from entering the caisson and second, to avoid water being constantly



present in the channel.

The top of the inlet of the concept will be placed at NAP - 2 m. With this configuration, the water level can drop until NAP - 2 m before the inlet becomes unsubmerged. But, a water level of NAP - 2 m is sufficient enough to prevent flood events occurring at Dordrecht. Therefore, when water levels are below NA - 2 m, the spillway is not required. Lowering the top of the inlet will lead to an increase in scour protection because of the higher near bed velocities.

The caissons of this concept will be constructed in a construction dock. Due to the height of the caissons, this construction dock will be located in the Energy Storage Lake. From these docks, the caisson will be transported to the final location of the spillway.

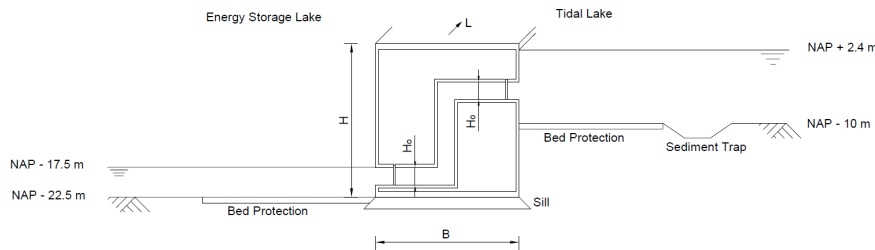


Figure 5.5: Overview concept Caisson (NTS)

#### 5.2.4. Concept Ogee

The fourth concept is completely different compared to the others. This concept is named the concept Ogee. The concept's name comes from the shape of the crest, an ogee shaped crest. Where the previous concepts are based on pressurised flow, this concept is based on open channel flow. The reason for this is that the spillway is open and a free surface between the water and the atmosphere is always present. Only unsubmerged flow can occur due to the top of the crest being above the maximum water level in the Energy Storage Lake. The idea of the concept is that the Energy Storage Lake and Tidal Lake will be separated by a sharp crested concrete weir with a radial gate at the top. If the radial gate is opened, water can flow over the structure into the Energy Storage Lake. Because of the big water level difference, a stilling basin must be located at the end of the spillway. This will decrease the turbulence and flow velocity which is beneficial for the scour protection.

The top of the ogee crest will be located at NAP - 4.5 NAP. The reason to place the top of the crest at NAP - 4.5 m is the maximum water level in the Energy Storage Lake. This maximum level is at NAP - 5 m and therefore submerged conditions are not possible. Lowering the top of the ogee crest will result in a lower ratio between the water level on top of the crest and the height of the spillway compared to the bed level in the Tidal Lake. A lower ratio will lead to a lower discharge coefficient and is not beneficial for the total discharge.

The concept Ogee will be constructed insitu. The reason for this is that transporting the spillway is not feasible. Therefore a building pit needs to be constructed at the location of the spillway. In this building pit, the spillway can be constructed.

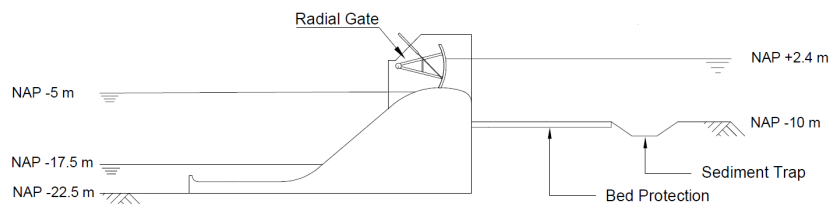


Figure 5.6: Overview concept Ogee (NTS)

# 6

## Verification of Concepts

This chapter verifies whether the developed hydraulic concepts meet the requirements. The dimensions are determined such, that the concepts are able to fulfil their function. First, the dimensions of the flow channels are determined and afterwards, the general dimensions of the spillway are calculated. The dimensions of the outlet are depending on the discharge requirement and are part of the hydraulic design loop. The general dimensions are depending on the stability of the structure and are part of the structural design loop. The reason to combine the hydraulic design loop and a part of the structural design loop is to improve the quality of the evaluation stage. The main dimension affects the costs of the concepts and therefore need to be derived before going into the evaluation stage. Before the calculations are performed, the safety approach and failure mechanisms are explained.

### 6.1. Safety Approach

In the determination of the forces, the old safety standard is used. This standard was commonly used in the Netherlands until 2017. This standard is taking into account the probability of exceedance of a certain event. The new safety standard takes into account the probability of failure of a flood defence system. The probability of failure of a flood defence system depends on the probability of failure of each failure mechanism combined. However, not all possible failure mechanisms are considered in this thesis and therefore the old standard is used. In this old standard, the same probability of exceedance for each failure mechanism is applied.

The verification of a concept must be performed in the ultimate limit state (ULS) and the serviceability limit state (SLS). In the ULS, material and load factors have to be considered in the calculations. In the SLS, these factors are equal to 1.0. In NEN-EN 1997-1 (2016), it is stated which state, the ultimate limit state or serviceability limit state, is governing for each failure mechanism. According to article 6.5 of NEN-EN 1997-1, for the stability calculations, the calculations need to be performed in ULS. This means that in the calculations, the material and load factors are not equal to 1. The load factors for the design of a primary defence structure are retrieved from the *Leidraad Kunstwerken 2003*. As mentioned in Section 3.6.2, the spillway can be categorised as a primary defence structure.

According to *Leidraad Kunstwerken 2003*, the load factors, that are given in Table 6.1, have to be used in the design calculations. In the design, there are two different types of loads: permanent loads and variable loads. Each type of load requires a different load factor. The permanent loads consist of self-weight of the structure, soil pressures and groundwater pressures. In Table 6.1, there are four different categories for the permanent load factors. The first one,  $\gamma_G$ , is used on self weights if this is the only present load. The second one,  $\gamma_{unfav}$ , is used on loads that have an unfavourable effect on the design. The third one,  $\gamma_{fav}$ , is used when a load has a favourable effect on the design. The last one,  $\gamma_N$ , is used on neutral loads. Soil pressures are always neutral loads.

<b>Permanent Load</b>		$\gamma_G$	$\gamma_{Unfav}$	$\gamma_{Fav}$	$\gamma_N$
Self-weight		1.35	1.2	0.9	-
Soil pressure		-	-	-	1.0
Groundwater pressure		-	1.2	0.9	1.0
<b>Variable Load</b>		$\gamma_F$			
Pressure difference due to:	- water levels	1.25			
	- wind waves	1.25			

**Table 6.1:** The load factors according to *Leidraad Kunstwerken 2003*

The variable loads are divided in pressure differences due to water levels and due to wind waves. Although the variable loads are divided into two different types of loads, the load factor for both these loads is equal to 1.25. In Figure 6.1 an example of the use of load factors is shown. In this situation, there is looked at the horizontal movement of the structure. It can be seen that the horizontal forces on the right side are bigger than on the left side. Therefore, the right side is the unfavourable side and the left side is the favourable side. However, the load factor on the left side is 1.25 because it concerns a water level difference with the right side. For the vertical forces, the self-weight is favourable and therefore requires a load factor of 0.9. The uplift pressure is divided into two parts. One part is due to a permanent load and taken as neutral and the other part is a variable load and taken as 1.25.

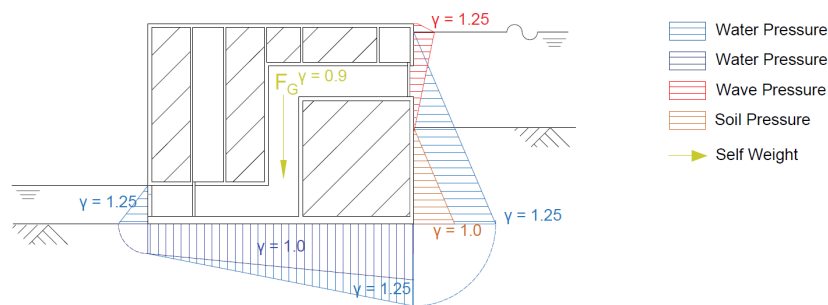


**Figure 6.1:** An example of the use of load factors

## 6.2. Verification Checks

First, the concepts are checked on their hydraulic requirements, the discharge of 20 000 m<sup>3</sup>/s. This check results in the required dimensions for the outlets of the concepts. Afterwards, the main dimensions of the concepts are retrieved by taking into account the stability requirement. The stability of the concepts is checked by the following stability checks:

- Piping
- Sliding Resistance
- Rotational Stability
- Bearing Capacity
- Draught of the Caisson
- Floating Stability

The last two mechanisms, the draught of the caisson and the floating stability, are only taken into consideration for the concepts Siphon, Underflow and Caisson. In Section 6.2.1 up to 6.2.6, the failure mechanism are described in more detail.

### 6.2.1. Piping

Below a structure or dune that separates two water bodies, a flow can occur if there is a water level difference present. This flow will go below the structure of the dune and is referred to as seepage. Seepage does not immediately lead to any kind of failure. However, if the flow velocity reaches a certain level, sediment is removed by the flow. This results in pipes below the structure which, if they extend under the full width of the structure, can lead to instability of the structure. The occurrence of pipes that extend under the full width of the structure is mainly depending on time. The formation of the pipes requires a sufficiently long time to complete. As a result of this, the difference in water level needs to be present for a long time as well.

The required seepage length to prevent problems regarding piping is determined by two methods. The first method is the method of Bligh and the second method is the method of Lane. Bligh's method is most suitable for flow below dikes. For flow below a structure, both methods have to be taken into consideration (Voorendt and Molenaar, 2020b).

<b>Bligh:</b>	<b>Lane:</b>
$L \geq \gamma \cdot C_B \cdot \Delta H$	$L \geq \gamma \cdot C_L \cdot \Delta H$
$L = \sum L_{vert} + \sum L_{hor}$	$L = \sum L_{vert} + \sum \frac{1}{3} L_{hor}$

where:  $L$  [m] = the total seepage distance  
 $L_{vert}$  [m] = the vertical seepage distance  
 $L_{hor}$  [m] = the horizontal seepage distance  
 $C_B$  [-] = Bligh's constant  
 $C_L$  [-] = Lane's constant  
 $\Delta H$  [m] = the water difference  
 $\gamma$  [-] = safety factor (= 1.5)

The constants of Bligh and Lane are depending on the type of soil. At the spillway location, the soil is characterised as coarse sand. This results in a value of  $C_B = 12$  and  $C_L = 5$ . With the maximum water difference of 19.9 m (NAP +2.4 and NAP -17.5), the minimum required seepage length is:

<b>Bligh:</b>	<b>Lane:</b>
$L \geq \gamma \cdot C_B \cdot \Delta H$	$L \geq \gamma \cdot C_L \cdot \Delta H$
$\geq 1.5 \cdot 12 \cdot 19.9$	$\geq 1.5 \cdot 5 \cdot 19.9$
$\geq 358m$	$\geq 149m$

For the concepts Siphon and Underflow, these distances will not cause problems due to the width of the dune. The width of the dune is larger than the required seepage length and therefore the problems due to piping will not occur. Local piping problems around the inlet or outlet can be easily solved by the use of geotextiles below the scour protections. For the concept Caisson and Ogee, the available seepage length below the structure is not sufficient to prevent piping problems.

A common solution to prevent failure due to piping is the use of seepage screens. These screens are placed below the structure and to increase the seepage length. For the concept Caisson and Ogee, the screens should reach up to the clay layer at NAP - 50 m. The flow will not continue in the clay layer and therefore piping can not occur. This will lead to seepage screens of 27.5 m in height. The design of these seepage screens is outside of the scope of this thesis. However, in the evaluation of the concept, an estimation of the price of this screen is included.

Seepage screens have a positive effect on the uplift pressures. Since the screens are outside of the scope, the influence of the screens is neglected. However, the influence of the screens on the uplift pressure will be positive and therefore, neglecting the influence will lead to a more conservative design.

### 6.2.2. Sliding Resistance

The resistance caused by the subsoil should be sufficient enough to resist the horizontal forces on the structure. In a drained situation, which is the case for all concepts because the subsoil is below the water level, the following inequality must be satisfied according to NEN-EN 1997-1, article 6.5.3:

$$\sum H \leq R_d \quad (6.1)$$

In which:

$$R_d = V'_d \cdot \tan(\delta_d)$$

where:  $H$  [kN] = the horizontal forces  
 $R_d$  [kN] = the sliding resistance  
 $V'_d$  [kN] = the sum of the vertical forces  
 $\delta_d$  [°] = the friction angle between subsoil and structure

The unity check that must be met for this failure mechanism is defined as:

$$UC = \frac{\sum H}{R_d} \leq 1 \quad (6.2)$$

### 6.2.3. Rotational Stability

The third failure mechanism is rotational stability. Below a structure on a shallow foundation, only compression stresses can develop. This will occur if the resulting force, caused by all the forces acting on the structure, intersects with the core of the structure. If the resulting force is intersecting outside the core of the structure, tensile stresses are required for stability but those stresses can not develop with sandy soils. The core of the structure is defined as the area that extends  $\frac{1}{6} B$  of the gravity centre line. The eccentricity of the resulting force should be within these boundaries (Voorendt and Molenaar, 2020b).

$$e_R \leq \frac{1}{6} B \quad (6.3)$$

where:  $B$  [m] = the width of the caisson  
 $e_R$  [m] = the eccentricity of the resulting force

The eccentricity of the resulting force is depending on the resulting moment and the resulting vertical force.

$$e_R = \frac{\sum M}{\sum V} \quad (6.4)$$

where:  $\sum M$  [kNm] = the sum of the moments taken at the gravity centre line  
 $\sum V$  [kN] = the sum of the vertical forces

The unity check that must be met is:

$$UC = \frac{\frac{B}{6}}{e_R} \leq 1 \quad (6.5)$$

### 6.2.4. Bearing Capacity

For a structure on a shallow foundation, the bearing capacity of the subsoil must be larger than the acting stresses on the subsoil. According to EN-NEN 1997-1, article D, the following inequality must be met.

$$p'_{max} \leq \sigma_{k,max} \quad (6.6)$$

where:  $p'_{max}$  [kN/m<sup>2</sup>] = the resisting bearing capacity  
 $\sigma_{k,max}$  [kN/m<sup>2</sup>] = the maximum acting stress

The bearing capacity of the subsoil is determined according to EN-NEN 1997-1, article D, with the Brinch Hansen method:

$$p'_{max} = c' N_c s_c i_c + q' N_q s_q i_q + 0.5 \gamma' B' N_\gamma s_\gamma i_\gamma \quad (6.7)$$

where:	$p'_{max}$	[kN/m <sup>2</sup> ]	=	the resisting bearing capacity
	$c'$	[kN/m <sup>2</sup> ]	=	the cohesion value of the soil
	$N_c, N_q, N_\gamma$	[-]	=	the bearing force factor
	$s_c, s_q, s_\gamma$	[-]	=	the foundation shape factor
	$i_c, i_q, i_\gamma$	[-]	=	the horizontal load factor
	$q'$	[kN/m <sup>2</sup> ]	=	the effective stress at the depth net to the foundation
	$\gamma'$	[kN/m <sup>3</sup> ]	=	the effective volumetric weight
	$B'$	[m]	=	the effective width

The acting stresses on the subsoil are determined by:

$$\sigma_{k,max} = \frac{\sum V}{B_{eff}} \quad (6.8)$$

where:	$\sigma_{k,max}$	[kN/m <sup>2</sup> ]	=	the maximum acting stress
	$B_{eff}$	[m]	=	the effective width (= B - 2·e <sub>R</sub> ), with e <sub>R</sub> as Formula 6.4

The unity check that must be met for this failure mechanism is:

$$UC = \frac{\sigma_{k,max}}{p'_{max}} \leq 1 \quad (6.9)$$

### 6.2.5. Draught of the Caisson

The draught of the caisson during transport is relevant because if the draught is too large, the caisson can come in contact with the bed of the river or lake and as a result of this the transport of the caisson will become impossible. Besides this, if the draught is exceeding the height of the caisson, transport will be impossible. The draught of the caisson is determined in the serviceability limit state and therefore the load factors are taken as 1. This means that they can be left out of the formula.

$$d = \frac{F_G}{B \cdot L \cdot \gamma_w} \quad (6.10)$$

where:	$d$	[m]	=	the draught
	$F_G$	[kN]	=	the self weight of the caisson
	$B$	[m]	=	the width of the caisson
	$L$	[m]	=	the length of the caisson
	$\gamma_w$	[kN/m <sup>3</sup> ]	=	the specific weight of water

The draught of the caisson is sufficient if during transport, the keel is 1 m and the draught does not exceed the height of the caisson. For navigability reasons, the distance between the top of the caisson and the water level should be at least 0.5 m.

### 6.2.6. Floating Stability

The caisson is stable during transport if the value of the metacentric height,  $h_m$ , is above 0.5 m.

$$h_m \geq 0.5 \quad (6.11)$$

The metacentric height is defined as:

$$h_m = \overline{GM} = \overline{KB} + \overline{BM} - \overline{KG} \quad (6.12)$$

in which:

$$\begin{aligned}\overline{KB} &= \frac{1}{2}d \\ \overline{BM} &= \frac{I}{V} \\ \overline{KG} &= \frac{\sum V_i \cdot e_i \cdot \gamma_i}{\sum V_i \cdot \gamma_i}\end{aligned}$$

where:  $d$  [m] = the draught of the caisson  
 $I$  [m<sup>4</sup>] = the moment of inertia  
 $V$  [m<sup>3</sup>] = the volume of displaced water  
 $V_i$  [m<sup>3</sup>] = the volume of an element  
 $e_i$  [m] = the distance between the bottom of the caisson and the gravity centre of the element  
 $\gamma_i$  [kN/m<sup>3</sup>] = the specific weight of an element

The unity check for this failure mechanism is:

$$UC = \frac{0.5}{h_m} \leq 1 \quad (6.13)$$

## 6.3. Concept Siphon

### 6.3.1. Dimensions and Number of Pipes

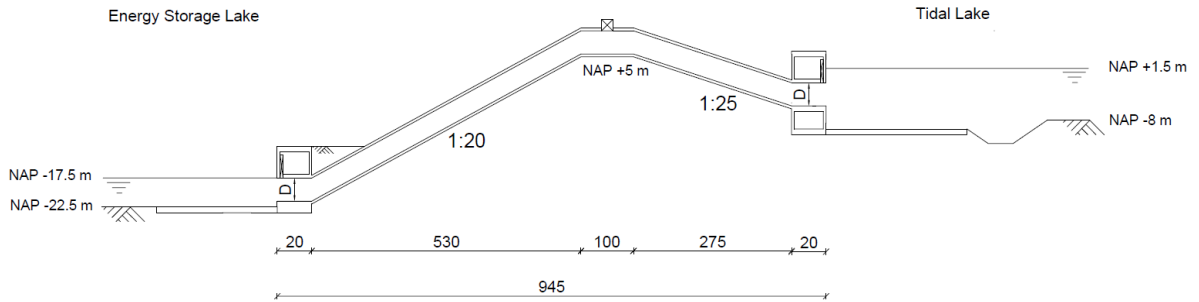


**Figure 6.2:** Concept Siphon governing discharge condition (NTS)

The most important requirement for the spillway is the required discharge capacity of 20 000 m<sup>3</sup>/s. The discharge capacity of the spillway is depending on the dimension and the number of the pipes. In this thesis, the dimension of the pipe is determined by taking into account the required number of pipes for a certain diameter of the pipe. Additionally, the occurring flow velocity in the pipe for a certain diameter is taken into consideration. In the concept Siphon, the inlet and outlet are submerged during the operation of the spillway. Therefore the flow in the spillway is pressurised flow. For this type of flow, the maximum discharge occurs in combination with the highest water level difference. The governing situation for the determination of the discharge can be seen in Figure 6.2. In the governing situation, the water level in the Energy Storage Lake is at NAP -17.5 m and the water level in the Tidal Lake is at NAP 1.5 m. The water level in the Tidal Lake is based on the water level when the barrier closes. For situations in which the water levels are different compared to the governing situation, the capacity of the spillway will be below the 20 000 m<sup>3</sup>/s. For the determination of the discharge in a pressurised spillway, the Bernoulli's equation is applicable:

$$\underbrace{h_{TL} + \frac{p}{\rho g} + \frac{v_{TL}^2}{2g}}_{\text{Energy Head Tidal Lake}} = \underbrace{h_{ESL} + \frac{p}{\rho g} + \frac{v_{ESL}^2}{2g}}_{\text{Energy Head Energy Storage Lake}} + \underbrace{f \frac{L}{D} \frac{v_S^2}{2g} + \sum \zeta \frac{v_S^2}{2g}}_{\text{Head Loss in spillway}} \quad (6.14)$$

where:	$h_{TD}$	[m]	=	the water depth in the Tidal Lake compared to reference level
	$h_{ESL}$	[m]	=	the water depth in the Energy Storage Lake compared to reference level
	$p$	[Pa]	=	the pressure
	$\rho$	[kg/m <sup>3</sup> ]	=	the water density (=1025 kg/m <sup>3</sup> )
	$g$	[m/s <sup>2</sup> ]	=	the gravitational acceleration (= 9.81 m/s <sup>2</sup> )
	$v_{TD}$	[m/s]	=	the flow velocity in the Tidal Lake
	$v_{ESL}$	[m/s]	=	the flow velocity in the Energy Storage Lake
	$v_s$	[m/s]	=	the mean flow velocity in the spillway
	$f$	[-]	=	the Darcy friction factor
	$L$	[m]	=	the length of the pipe
	$D$	[m]	=	the hydraulic diameter of the pipe
	$\zeta$	[-]	=	loss coefficient

The Darcy friction value is calculated by the Colebrook method. This method requires the equivalent roughness of the pipe. This roughness is depending on the absolute roughness of the pipe material. The absolute roughness is the surface roughness of a material and the equivalent roughness is the absolute roughness divided by the internal diameter. Over time, the absolute roughness of the material increases and therefore a higher absolute roughness is required in the calculation of the discharge than the absolute roughness after construction (Walski et al., 1988). For concrete pipes, the value of the absolute roughness is assumed to be 1.0 mm (Munson et al., 2009). The initial length of the pipeline is 945 m, see Figure 6.2. The width of the caisson is not determined yet, this is depending on the stability requirements. For the discharge calculation, a first estimation is used. Later on, this assumption is checked and if necessary, the calculation is repeated. The first assumption of the width of the caisson is 20 m. In Appendix E, the total loss coefficient is calculated and is equal to 2.59 [-]. In Figure 6.3a, the blue line shows the required number of pipes to exceed a total discharge of 20 000 m<sup>3</sup>/s. The red dots show the total discharge that is achieved with that number of pipes. In Figure 6.3b, the flow velocity is shown. The detailed calculations can be found in Appendix E.

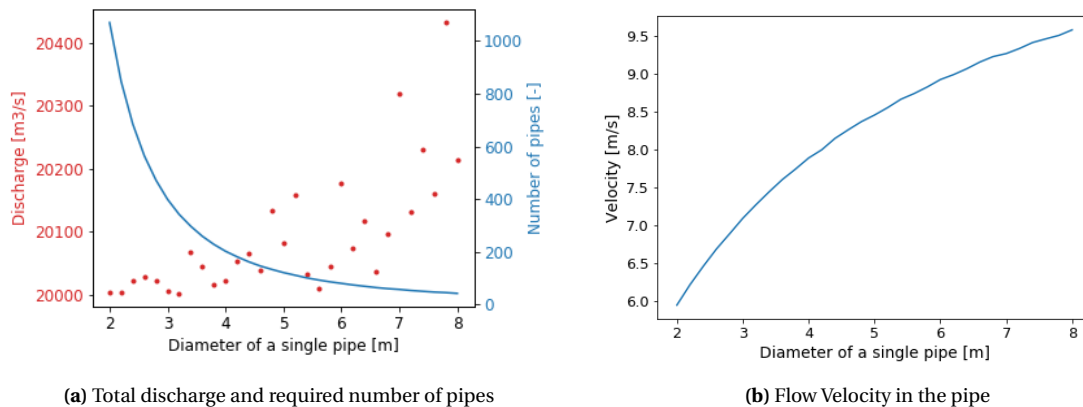


**Figure 6.3:** Results for the concept Siphon for variable pipe diameters

For the spillway, the most optimal diameter is determined by the following items:

- Number of pipes
- Flow velocity in the pipe
- Submerged outlet conditions
- Total length of the spillway

The determination of the optimal diameter is done without calculating the exact cost of each option. It is assumed that if the number of pipes is increasing, the cost will increase as well. The same goes for the total length of the spillway, it is assumed that a larger spillway has larger costs. The flow velocity is taken into account because a larger flow velocity requires a more extensive scour protection. Again, this has a negative influence on the costs.



The most optimal diameter for the pipe is 4 m. This is the largest diameter that ensures submerged outlet conditions at all times. Decreasing the diameter results in a rapid increase in the total number of pipes and total length of the spillway. This can be seen in respectively Figure 6.3a and 6.4. Therefore, decreasing the diameter leads to an increase in cost. The total length of the spillway is based on the number of pipes, the diameter of these pipes and additional space between the pipes (1 m). A pipe diameter of 4 m requires a total of 202 pipes to achieve the maximum discharge capacity of 20 000 m<sup>3</sup>/s. The total discharge during the governing situation is 20 100 m<sup>3</sup>/s. The flow velocity in this situation is 7.89 m/s. For maintenance and failure possibilities, additional pipes are required. To take this into account, the number of pipes is increased by 5%. This results in 10 additional pipes and a total of 212. A more detailed description of the choice of the final dimensions can be found in Appendix E.

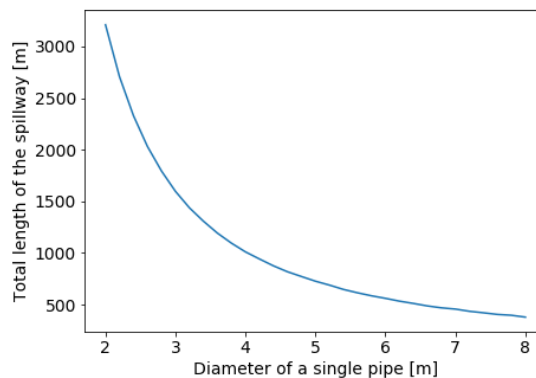


**Figure 6.4:** Total length versus the diameter of a single pipe

The top of the pipe will be at NAP +9 m. The use of a siphon system leads to a limitation in water levels at which the system functions. The maximum rise of a siphon system is 10 m above the water level in the Tidal Lake. Therefore, the minimum water level in the Tidal lake is NAP -1 m. This water level can be lowered if the top of the pipe will be lowered but this leads to the pipe in the dune instead of on top of the dune. However, at the minimum water level of NAP -1 m, the water level at Dordrecht will not exceed the NAP + 2.5 m.

### 6.3.2. Dimensions Inlet and Outlet

The inlet and outlet structures of the concept Siphon are caissons. In these caissons, the gates are located. The dimensions of the caissons are mainly based on the stability requirement. Due to the different circumstances, the inlet and outlet have different dimensions.

#### 6.3.2.1. Energy Storage Lake Side

As mentioned before, the dimensions of the caisson are mainly based on the stability requirement. For the height of the caisson there is also a functional requirement, the gate has to fit in the caisson. In the design of the caisson, the length and height are fixed and the width is found by the failure mechanisms.

- Sliding resistance
- Rotational stability
- Bearing capacity
- Floating stability
- Draught

### The Basis layout of the caisson

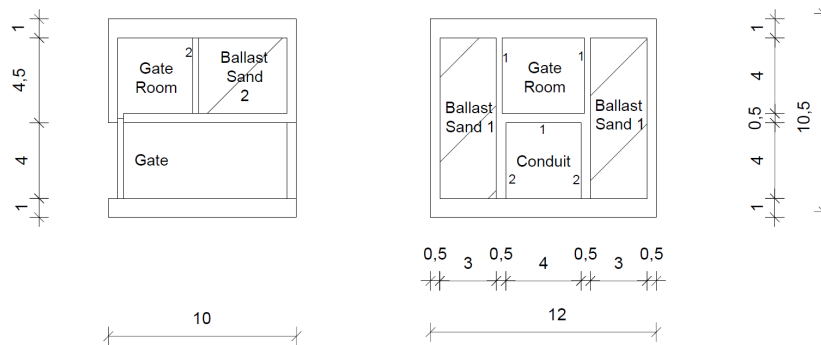


**Figure 6.5:** Side view (left) and front view (right) of the lay-out of the basis caisson.

The required width of the caisson is determined by increasing the width of a basis caisson, see Figure 6.5. The dimensions of the basis caisson are based on the functional requirements. For instance, sufficient room for the gate to fit in the caisson. Besides this, there should be enough room for ballast material to prevent uplift. The initial width of the basis caisson (10 m) is increased with  $\Delta x$  at both sides of the caisson, see Figure 6.6. With each increase, the failure mechanisms of Section 6.2 are checked. Eventually, the minimum required width is found. The results of the checks can be found in the remainder of this section. For the calculations, the forces are given in kN per meter length. The length of the caisson is the direction perpendicular to the flow direction of the water.

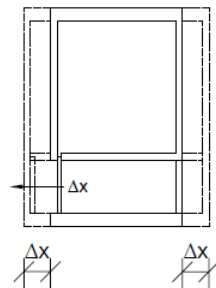


**Figure 6.6:** Increase of width by  $\Delta x$

The self-weight of the basis caisson can be seen in Table 6.2. In the same table, the increase in self-weight for an increase in  $\Delta x$  can be seen. In Appendix F, the detailed calculations for the self-weight can be seen.

Situation	Total [kN]	Total per meter length [kN/m]
<b>Without Ballast</b>		
Basis	12672	1056
Increase with $\Delta x$	1035	86
<b>With Ballast</b>		
Basis	23356	1946
Increase with $\Delta x$	2375	198

**Table 6.2:** Self weight of the caisson

### Load situations

The stability requirements are checked for two different load situations. These two load situations can be seen in Figure 6.7. In the first situation, the water level of the Energy Storage Lake is at NAP - 12 m. This is the

same level as the top of the caisson. In the second situation, the water level is at NAP - 17.5 m, the minimum water level in the Energy Storage Lake. The soil next to the caisson is assumed to be fully saturated because it is below the water level most of the time. Besides this, the influence of a sloped soil instead of a horizontal soil is neglected.



Figure 6.7: The load situation for the concept Siphon

**Sliding Resistance**

In Appendix F, the unity check for the sliding resistance is calculated for both load situations. In these calculations, it is concluded that situation two, Figure 6.7b, is the governing situation. The reason for this is the high resulting horizontal force compared to the other situation. The acting forces in the case of the basis caisson can be seen in Figure 6.8. The forces due to the waves are neglected because these have a positive influence on the stability.

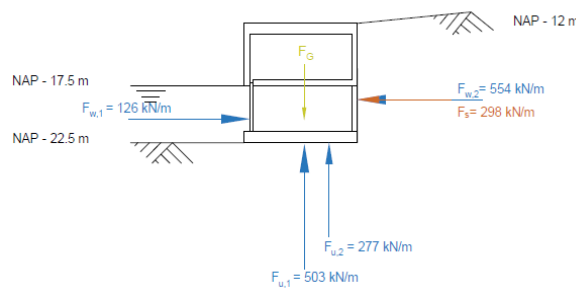


Figure 6.8: Characteristic loads acting on the basis layout of the caisson

The resulting unity checks for each width can be seen in Figure 6.9. It can be seen that the minimum required width is 28 m.

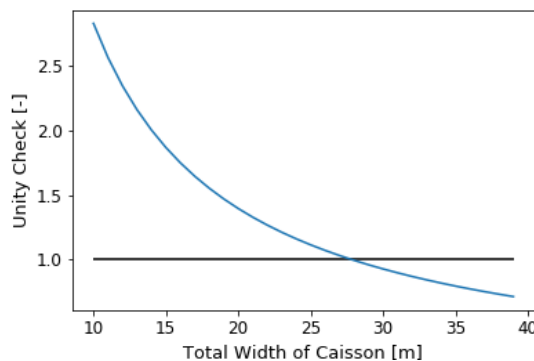
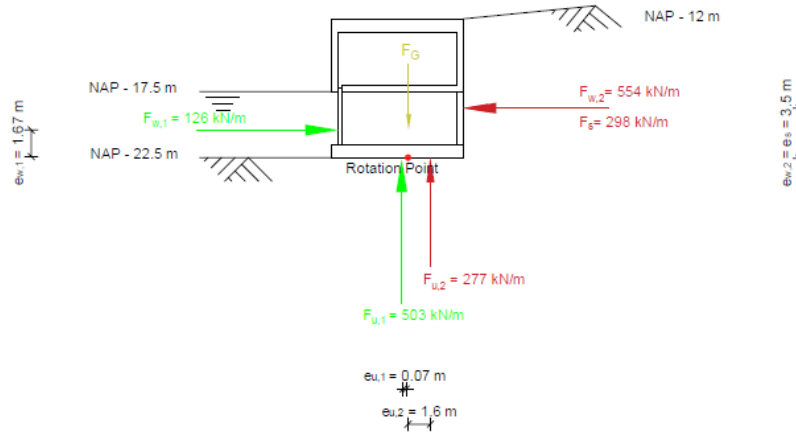


Figure 6.9: Sliding resistance unity check for situation two

**Rotational Stability**

For the rotational stability, the second situation is governing again. The forces acting on the caisson are the same compared to the forces for the sliding resistance. In Figure 6.10, it is illustrated with different colours which forces cause a moment in the same direction. Again, the forces due to waves are neglected.



**Figure 6.10:** Forces causing the resulting moment

The results of the unity check can be seen in Figure 6.11. It can be concluded that a minimum width of 18 m is required.

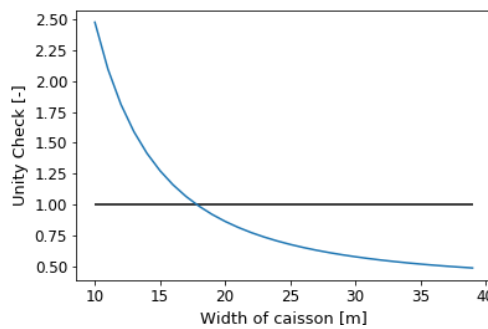


**Figure 6.11:** Rotational stability unity check for situation one

**Bearing Capacity**

The governing situation is situation two, in which low water levels occur. The reason for this is the larger resulting vertical force compared to situation one. This requires a larger bearing capacity due to larger acting stresses. The bearing capacity is calculated with the Brinch Hansen method. The detailed calculations of the acting stresses and the bearing capacity can be found in Appendix F. In Figure 6.12, the unity checks for the bearing capacity can be seen. It can be concluded that the minimum required width is 18 m.

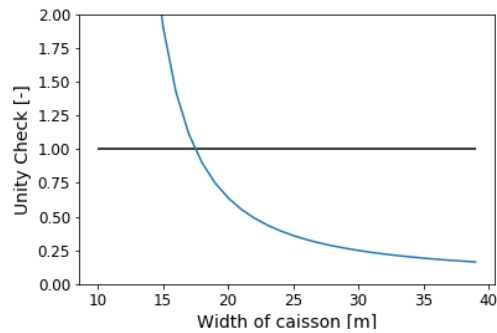


**Figure 6.12:** Bearing capacity versus acting stresses

### The required draught during transport

The occurring water level during transport is taken as the mean water level, NAP + 0 m. This results in a depth of 22.5 m in the Energy Storage Lake. In Figure 6.13, the draught of the caisson can be seen. This draught is calculated in Appendix F. The draught may not exceed the height of the caisson, 10.5 m. It is assumed that during transport, at least 0.5 m of the caisson should be above the water level. Therefore, the maximum draught of the caisson is 10 m. In Figure 6.13, this is illustrated as the horizontal line. It can be concluded that a minimum width of 14 m is required.

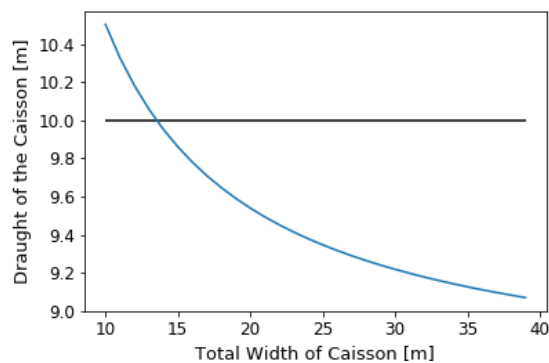


**Figure 6.13:** Draught of the caisson

### Floating Stability

The floating stability is depending on the draught of the caisson, the location of the gravity centre and the moment of inertia of the caisson. In Appendix F, these values and the metacentric height of the caisson are calculated. The results of the metacentric height are shown in Figure 6.14. It can be concluded that floating stability will not be an issue.

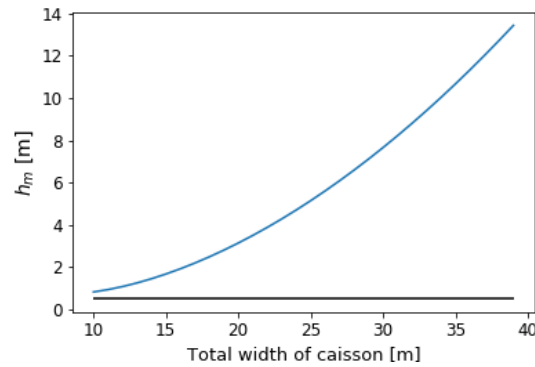


**Figure 6.14:** The metacentric height

### Final Dimensions

The height of the caisson is 10.5 m and the length of the caisson is 48 m. The minimum required widths for each mechanism can be seen in Table 6.3.

<b>Mechanism</b>	<b>Minimum Required Width [m]</b>
Sliding Resistance	28
Rotational Stability	18
Bearing Capacity	18
Draught	14
Floating Stability	-

**Table 6.3:** Minimum required width

The governing mechanism for the determination of the width is the sliding resistance requirement. This requirement requires a width of at least 28 m. The final width of the caisson is set at 28 m. The unity checks for a caisson with a width of 28 m for all the failure mechanisms can be found in Table 6.4.

<b>Mechanism</b>	<b>Unity Check</b>
Sliding Resistance	0.96
Rotational Stability	0.59
Bearing Capacity	0.27
Draught	0.92
Floating Stability	0.07

**Table 6.4:** Unity Checks for the concept Siphon

In Figure 6.15, the final design of the caisson at the Energy Storage Lake side can be seen. The caisson has a height of 10.5 m, a width of 28 m and a length of 48 m. A total of 53 caissons are required which results in a total length of 2544 m.

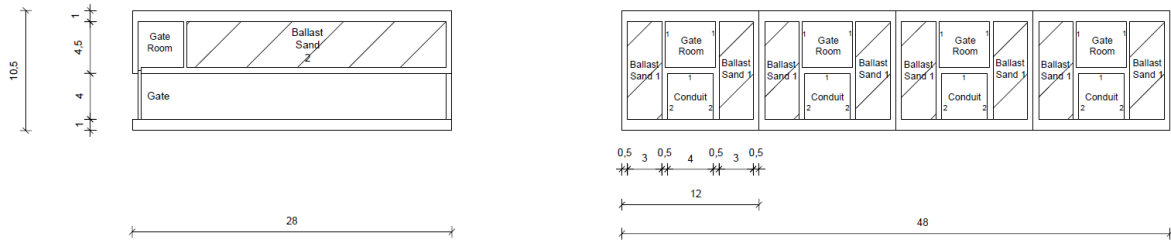


Figure 6.15: Cross sections of the energy storage side caisson

### 6.3.2.2. Tidal Lake Side

For the determination of the width of the caisson in the Tidal Lake, the same method and requirements are used.

#### The Basis layout of the caisson

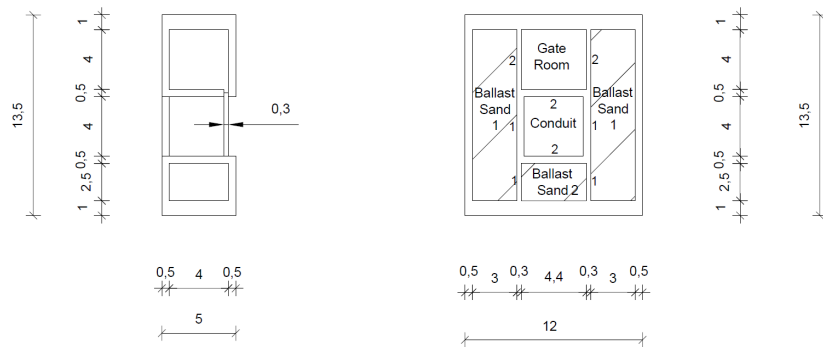


Figure 6.16: The Layout of the Concept Siphon caisson

The lay-out of the basis caisson can be seen in Figure 6.16. The increase of  $\Delta x$  can be seen in Figure 6.17.

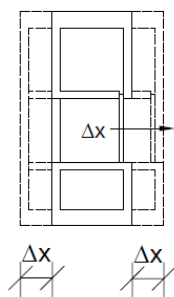


Figure 6.17: Increase of width by  $\Delta x$

The self-weight of the basis caisson can be seen in Table 6.5. In the same table, the increase in self-weight for an increase in  $\Delta x$  can be seen. In Appendix F, the detailed calculations for the self-weight can be seen.

Situation	Total [kN]	Per meter length [kN/m]
<b>Without Ballast</b>		
Basis	9052	754
Increase with $\Delta x$	1213	101
<b>With Ballast</b>		
Basis	15452	1288
Increase with $\Delta x$	2813	234

**Table 6.5:** Self-weight of the caisson

### Load situations

The stability requirements are checked for two different load situations. These two load situations can be seen in Figure 6.18. In the first situation, the water level of the Tidal is at NAP +2.4 m. In the second situation, the water level is at NAP - 2 m, the minimum water level in the Tidal Lake. The soil next to the caisson is assumed to be fully saturated because it is below the water level most of the time. Besides this, the influence of a sloped soil instead of a horizontal soil is neglected.

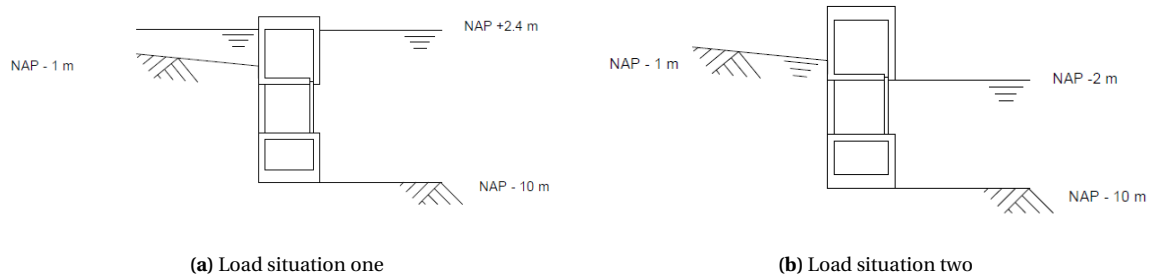


**Figure 6.18:** The load situation for the concept Siphon

### Sliding Resistance

In Appendix F, the unity check for the sliding resistance is calculated for both load situations. In these calculations it is concluded that situation two, Figure 6.18b, is the governing situation. The reason for this is the large uplift pressure which results in a lower resulting vertical pressure. This leads to a lower resistance against horizontal forces. The acting forces can be seen in Figure 6.19.

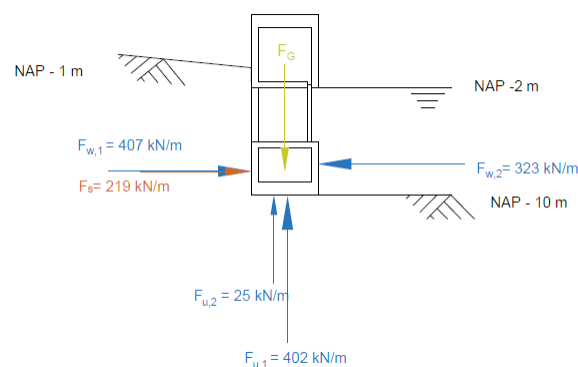


**Figure 6.19:** Characteristic loads acting on the caisson

The results of this unity check can be seen in Figure 6.20. The minimum required with for the sliding resistance is 8 m.



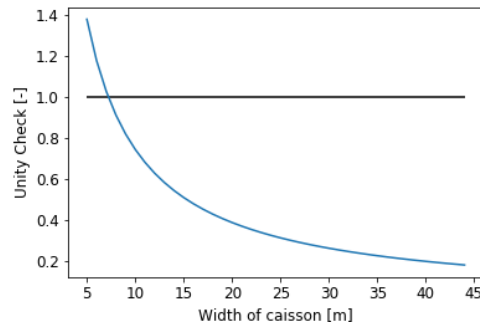


**Figure 6.20:** Unity check of the sliding resistance for situation two

**Rotational Stability**

For the rotational stability, the second situation is governing again. However, the difference between situation one and two are small. The forces acting on the caisson are the same compared to the forces for the sliding resistance. In Figure 6.21 it is illustrated with different colours which forces cause a moment in the same direction. The detailed calculations can be found in Appendix F.

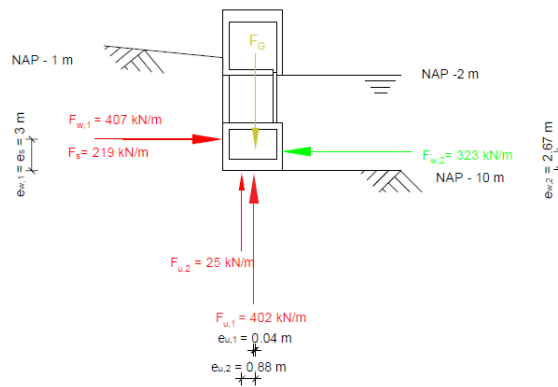


**Figure 6.21:** Forces causing the resulting moment

The results of the unity check can be seen in Figure 6.22. It can be concluded that the minimum required width is 8 m.

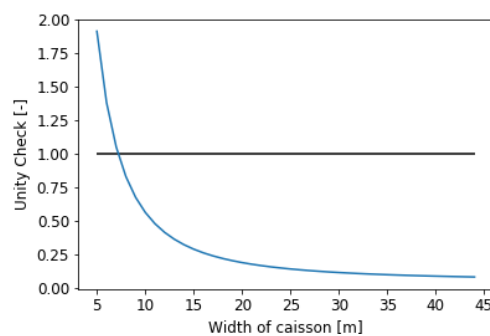


**Figure 6.22:** Unity check for the rotational stability for situation two

### Bearing Capacity

The bearing capacity of the subsoil below the caisson may not be exceeded. The length dimension is taken the same as for the energy lake side, 48 m. Situation two is the governing situation again. The reason for this is the lower uplift pressure. The bearing capacity is calculated with the Brinch Hansen method. The detailed calculations of the acting stresses and the bearing capacity can be found in Appendix F. In Figure 6.23, the unity checks for the bearing capacity can be seen. It can be concluded that the minimum required width is 11 m.

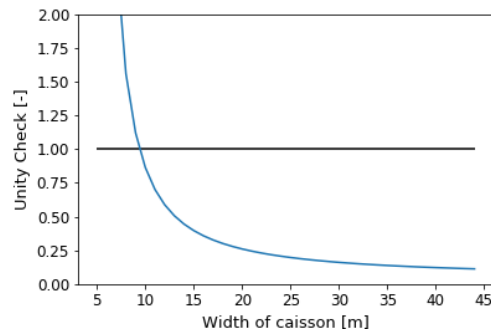


Figure 6.23: Unity check of the bearing capacity for situation two

### The required draught during transport

The occurring water level during transport is taken as the mean water level, NAP + 0 m. This results in a depth of 10 m. In Figure 6.13, the draught of the caisson can be seen. This draught is calculated in Appendix F. The draught may not exceed the height of the caisson, 13.5 m. It is assumed that during transport, at least 0.5 m of the caisson should be above the water level. Therefore, the maximum draught of the caisson is 13 m. In Figure 6.13, this is illustrated as the upper horizontal line. The lower horizontal line illustrates the maximum draught due to the bed levels. It can be concluded that the caisson requires more depth than is available at the location. Therefore it needs to be concluded that this concept is only constructible if the caissons are constructed at the final location in a building pit.

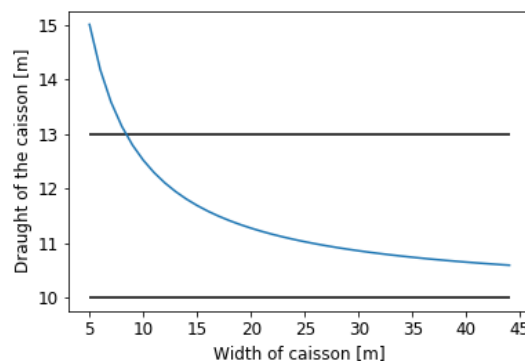


Figure 6.24: Draught of the caisson

### Final Dimensions

The height of the caisson is 13.5 m and the length of the caisson is 48 m. The minimum required widths for each mechanism can be seen in Table 6.6. Transport of the caissons is not possible. The caisson must be constructed at the final location.

Mechanism	Minimum Required Width [m]
Sliding Resistance	8
Rotational Stability	8
Bearing Capacity	11

Table 6.6: Minimum required width

The governing mechanism for the determination of the width is the bearing capacity. This requirement requires a width of at least 1 m. The final width of the caisson is set at 11 m. The unity checks for a caisson with a width of 11 m for all the failure mechanisms can be found in Table 6.7.

Mechanism	Unity Check
Sliding Resistance	0.70
Rotational Stability	0.53
Bearing Capacity	0.82

Table 6.7: Unity Checks for the concept Siphon

In Figure 6.25, the final design of the caisson at the Energy Storage Lake side can be seen. The caisson has a height of 13.5 m, a width of 11 m and a length of 48 m. A total of 53 caissons are required which results in a total length of 2544 m.

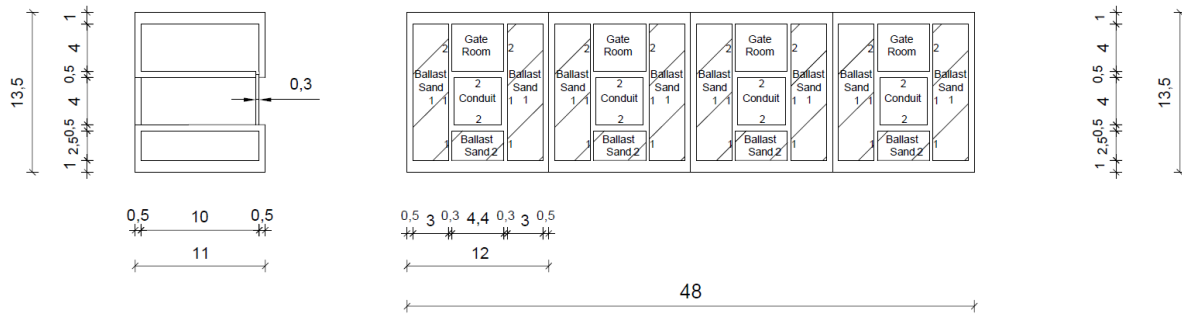


Figure 6.25: Cross sections of the Tidal Lake side caisson

## 6.4. Concept Underflow

### 6.4.1. Dimensions and Number of Pipes

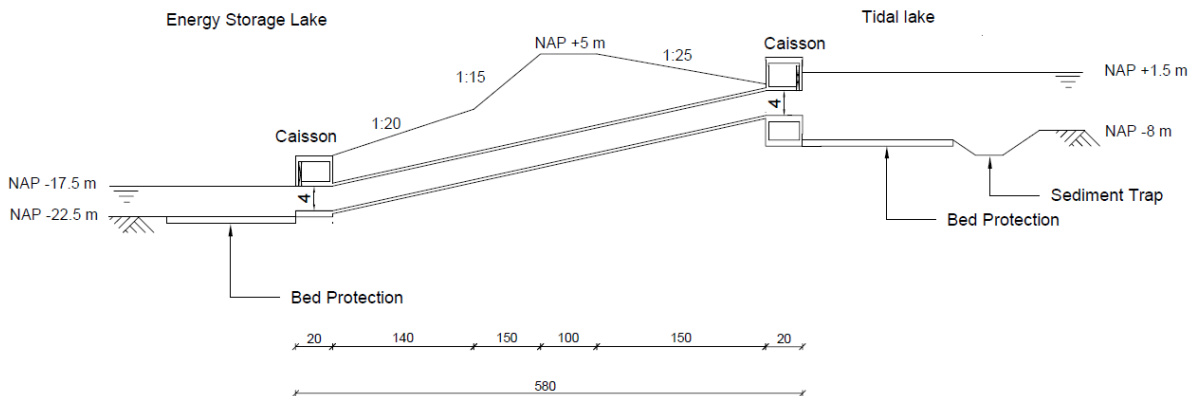
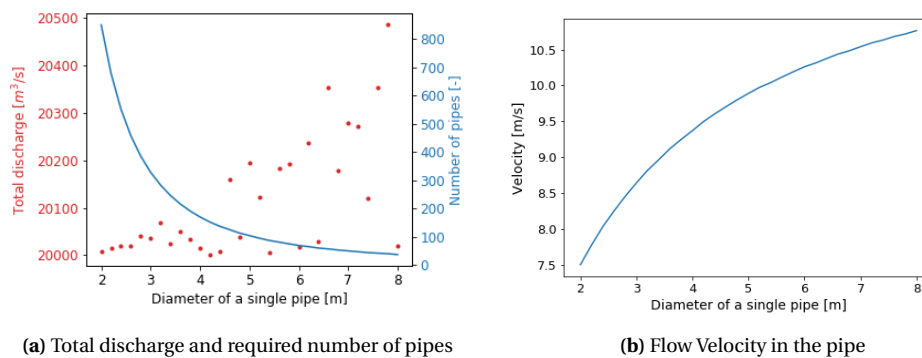


Figure 6.26: Concept Underflow governing discharge condition (NTS)

The maximum discharge for the concept Underflow is reached under the same conditions as the concept Siphon because this concept is also based on pressurised flow. To accomplish pressurised flow, both the inlet and outlet must be submerged. For the governing situation, the same water levels are used as in the concept Siphon, respectively NAP -17.5 m and NAP + 1.5 m in the Energy Storage Lake and the Tidal Lake, see Figure 6.26. Since the inlet and outlet are both submerged, Bernoulli's equation can be used, just like in the concept Siphon.

The length of the pipeline is 580 m, see Figure 6.26, including the assumed width of each caisson (20 m), and the total loss coefficient is 2.42. The required number of pipes and the occurring mean velocity in the pipe can be seen in Figure 6.27a and 6.27b. Detailed calculations can be found in Appendix E. The calculation is also performed for rectangular outlets but circular pipes are preferred. The reason for this is that with circular pipes, the soil pressures can be easier dealt with.



**Figure 6.27:** Results for the Concept Underflow for variable diameter

The same items are used as in the concept Siphon for the determination of the dimensions and number of pipes. The final diameter of the pipe is 4 m. The reason for the 4 m diameter is to avoid the exponential part in Figure 6.27a and 6.28 and to keep the mean velocity as low as possible. Also, the 4 m is the maximum diameter that ensures a submerged outlet. These dimensions lead to a total number of 169 conduits which lead to a maximum discharge of 20 000 m<sup>3</sup>/s. The occurring mean velocity in this design is 9.4 m/s, see Figure 6.27b. For maintenance and failure, additional conduits are required and therefore it is assumed that 5% extra is sufficient. This results in 8 additional conduits and a total of 177. A more detailed description of the choice of the final dimensions can be found in Appendix E.

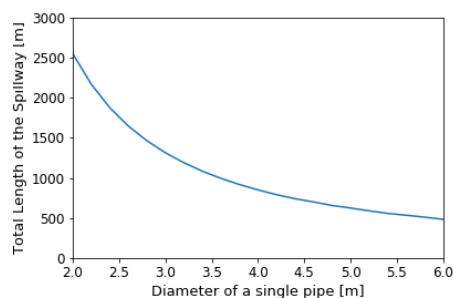


**Figure 6.28:** Total length versus the diameter of a single culvert

### 6.4.2. Dimensions Inlet and Outlet

The dimensions of the pipes that are used for the spillway in the concept Underflow are the same as in concept Siphon. Therefore the same in and outlet structures will be constructed for this concept as for the concept Siphon. In this section, the dimensions are given but the determination process of these dimensions can be found in Section 6.3.2 and Appendix F.

### 6.4.2.1. Energy Storage Lake Side

In Figure 6.29, the final design of the caisson at the Energy Storage Lake side can be seen. The caisson has a height of 10.5 m, a width of 28 m and a length of 48 m. A total of 44 caissons are required which results in a total length of 2112 m.

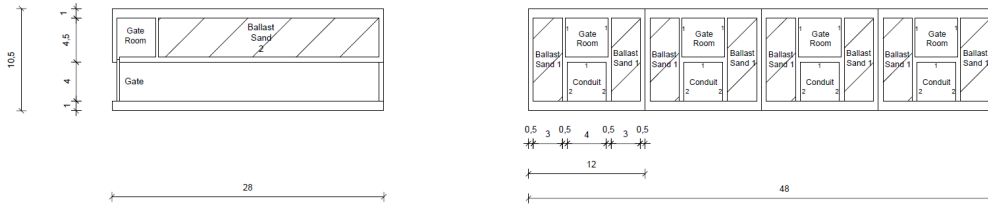


Figure 6.29: Side view (left) and front view (right) of the caisson at the Energy Storage Lake side

### 6.4.2.2. Tidal Lake Side

In Figure 6.30, the final design of the caisson at the Energy Storage Lake side can be seen. The caisson has a height of 10.5 m, a width of 11 m and a length of 48 m. A total of 44 caissons are required which results in a total length of 2112 m.

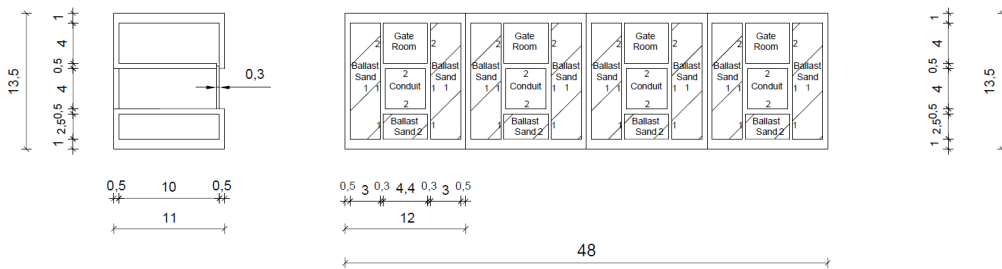


Figure 6.30: Side view (left) and front view (right) of the caisson at the Tidal Lake side

## 6.5. Concept Caisson

### 6.5.1. Dimensions and Number of Conduits

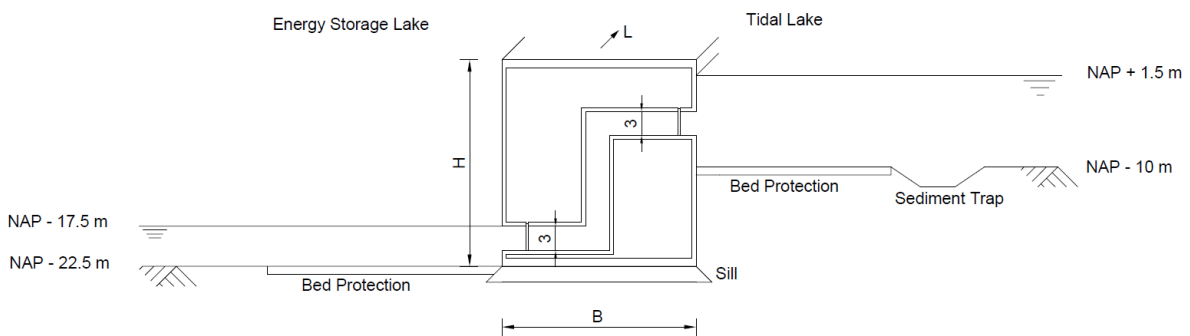


Figure 6.31: The governing discharge situation for the concept Caisson (NTS)

For the concept Caisson, the same governing discharge condition is taken as for the earlier mentioned concepts. This means that the water level in the Energy Storage Lake and the Tidal Lake are respectively, NAP

-17.5 m and NAP + 1.5 m, see Figure 6.31. Formula 6.14 is again applicable for this condition and therefore the discharge is determined with the same method as before.

The internal height of the conduit is 3 m. The reason for this is that this ensures the submerged condition in every situation but also creates space between the outlet and the bed. For the other concepts, this extra space could not be implemented because of the large increase in the number of pipes for those concepts. The length of the conduit, the distance between the inlet opening and outlet opening, is first assumed to be 65 m. Because of the relatively short length of the conduit, the assumed length can differ from the final length because of the minor influence on the head loss. Only for large lengths, like the concept Siphon, the head loss due to the friction of the pipe will play a major role. The total loss coefficient is 4.3 and the corresponding required number of pipes, total discharge and mean velocity can be seen in Figure 6.32a and 6.32b.

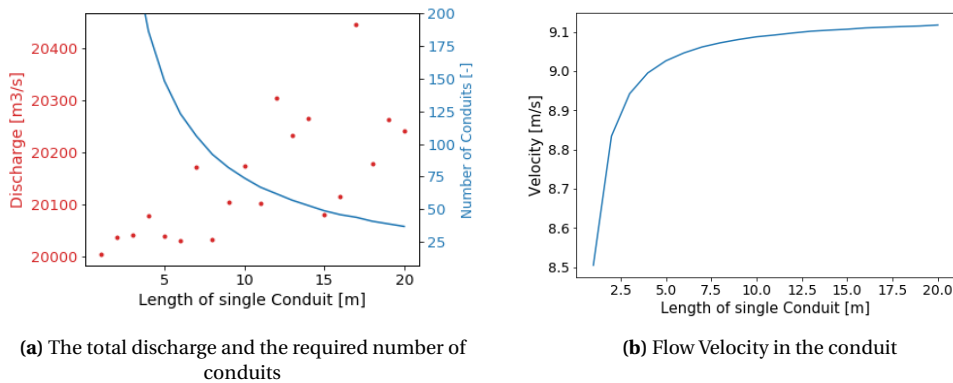


Figure 6.32: Results for the Concept Caisson for variable width

The same items are used to decide on the final dimension as for the concept Siphon and Underflow. The final dimensions of the conduit are an internal height of 3 m and an internal width of 10 m. Again the exponential part in both Figure 6.32a and 6.33 have to be avoided and the mean flow velocity needs to be as low as possible. These dimensions lead to a total number of 74 conduits which lead to a maximum discharge of 20 100 m<sup>3</sup>/s. The occurring mean velocity in this design is 9.1 m/s, see Figure 6.32b. For maintenance and failure, additional conduits are required and therefore it is assumed that 5% extra is sufficient. This results in 4 additional conduits and a total of 78. A more detailed description of the choice of the final dimensions can be found in Appendix E.

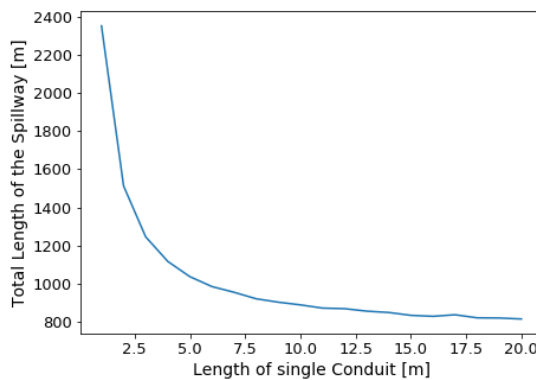


Figure 6.33: Total width versus the width of a single culvert

### 6.5.2. Retaining height of the Caisson

Since the caisson is replacing a part of the dune trajectory, the retaining height of the caisson is important. The Tidal Lake is the governing lake for the calculation of the retaining height due to the larger water levels compared to the Energy Storage Lake. The total height of the caisson is based on the difference between the bed levels of the lakes (12.5 m), the maximum occurring water depth in front of the caisson (12.4 m) and the required freeboard to limit the overtopping discharge. The occurring water depth is different compared to the discharge calculations. The reason behind this is that the maximum discharge capacity must be reached at a lower water level, NAP - 1.5 m. The required freeboard is determined by (Van der Meer et al., 2018):

$$\frac{q}{\sqrt{gH_{m0}^3}} = 0.054 \cdot \exp\left(-2.12 \frac{R_c}{H_{m0}}\right)^{1.3} \quad (6.15)$$

where:  $q$  [m<sup>2</sup>/s] = the overtopping discharge  
 $H_{m0}$  [m] = the significant wave height  
 $R_c$  [m] = the freeboard  
 $g$  [m/s<sup>2</sup>] = the gravitational acceleration (= 9.81 m/s<sup>2</sup>)

The tolerable overtopping discharge,  $q$ , is taken to be 10 l/s/m to ensure that people can stand on the caisson (Van der Meer et al., 2018). The reason for this is that when the spillway is functioning, people should be able to inspect the spillway for instance, in the case of failure of the gate. The detailed calculations of the retaining height and the assumptions regarding the validation of the formula can be found in Appendix G. The required freeboard is equal to 1.03 m. This results in a height of the caisson of 26 m. The different values that determine the height of the caisson can be found in Figure 6.34. An important requirement is that the gate needs to fit in the caisson. In Figure 6.34, it is shown that sufficient room is available for the gate at the top right corner.

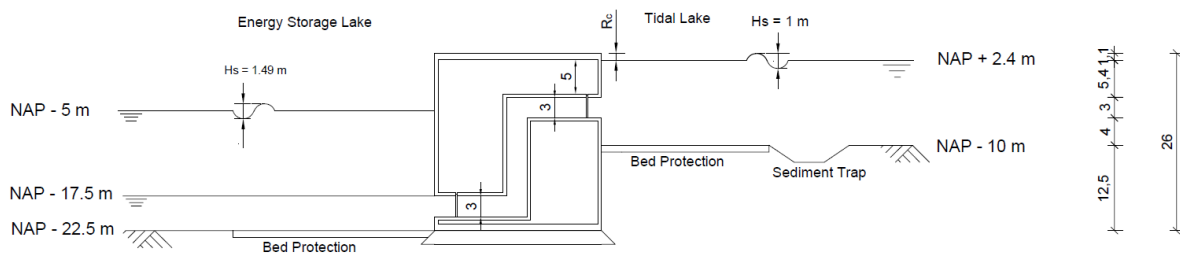


Figure 6.34: Height of the caisson (NTS)

### 6.5.3. Width and Length of the Caisson

The width of the caisson is depending on the same stability requirements used for the caissons in the concept Siphon and Underflow. The width is defined as the distance between the two lakes and the length of the caisson is the distance parallel to the flow direction.

#### 6.5.3.1. The Basis Layout of the Caisson

In the determination of the required width of the caisson, the same method is used as for the concept Siphon and Underflow. A basis caisson is applied, see Figure 6.35a, which will be increased in width by  $\Delta x$  at both sides. The entrance shaft at the Energy Storage Lake side is kept in the middle of the two ballast rooms at the left and therefore moves by  $\frac{1}{2}\Delta x$ . Each time this step is performed, the stability requirements are checked to see if they are fulfilled. The results can be seen in the remainder of this section. For the calculations, the forces are given in kN per meter length. The length of a caisson with a single outlet is 11 m. In total 3 outlets will be placed in one caisson, this results in a total length of 33 m.

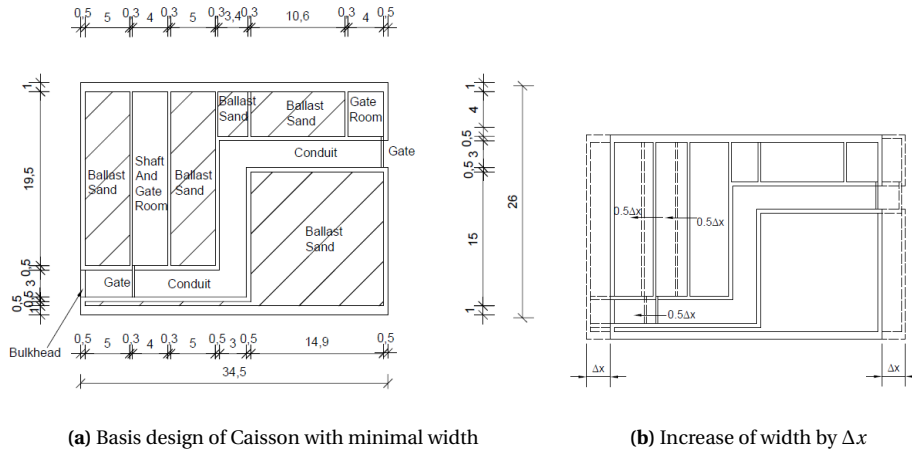


Figure 6.35: The Layout of the Concept Caisson

6.5.3.2. The Use of a Sill

In the concept Caisson, the caisson will be placed on a sill. This sill consists of a mixture of sand and gravel. This sill is required to improve the soil conditions below the caisson. With this improvement, the required self-weight for the sliding resistance will decrease and the bearing capacity will improve. The sill will be placed underwater and therefore the sill is loosely packed. The characteristics of the sand and gravel mixture can be found in Table 6.8. The height of the sill in the concept Caisson is 2 m.

Name	Mixture	Consistency	$\gamma$ [kN/m <sup>3</sup> ]	$\phi$ [Degree]	$c'$ [kPa]
Sill	Gravel (65%) Sand (35%)	Loosely	20	39	0

Table 6.8: Soil characteristics of sill (CETMEF, 2007)

6.5.3.3. Load Situations

In the determination of the width of the caisson, three load situations are taken into account. In all situations, the water level in the Tidal Lake is at the maximum level, NAP + 2.4 m. The reason for this is that the water level in the Energy Storage Lake is always lower than the water level in the Tidal Lake. Consequently, the highest water level differences occur for the largest water level in the Tidal Lake. The water level difference is unfavourable for the stability. In the Tidal Lake, there are three different water levels. The minimum water level, NAP - 17.5 m, the maximum water level, NAP - 5 m and the water level in between these two, NAP - 11.25 m. The situations are shown in Figure 6.36.

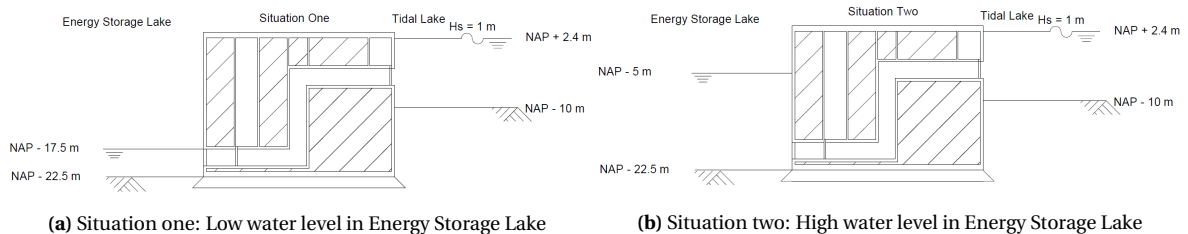


Figure 6.36: The different load situations



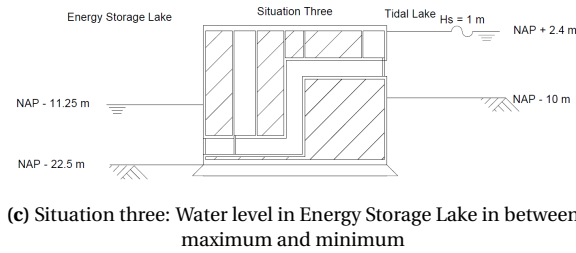


Figure 6.36: The different load situations (cont.)

### 6.5.3.4. Sliding resistance

In Appendix H, the sliding resistance is calculated for all the load situations. The governing situation from these three can be seen in Figure 6.37, situation three. The subsoil below the caisson is the gravel sill.

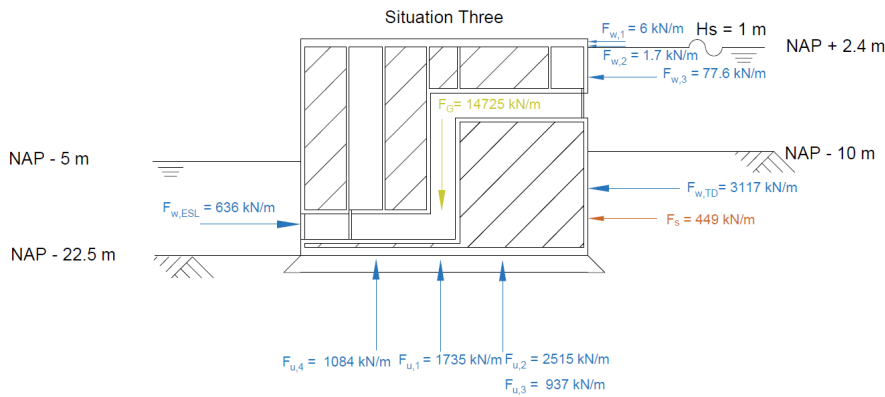


Figure 6.37: The characteristic loads in the governing situation

The results of the unity check for the governing situation can be found in Figure 6.38. The minimum required with is equal to 46.5 m.

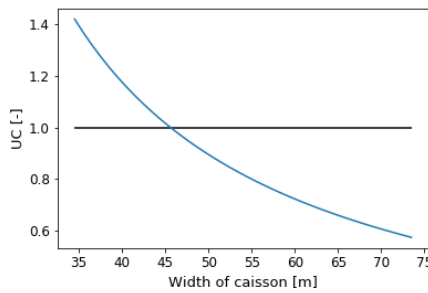
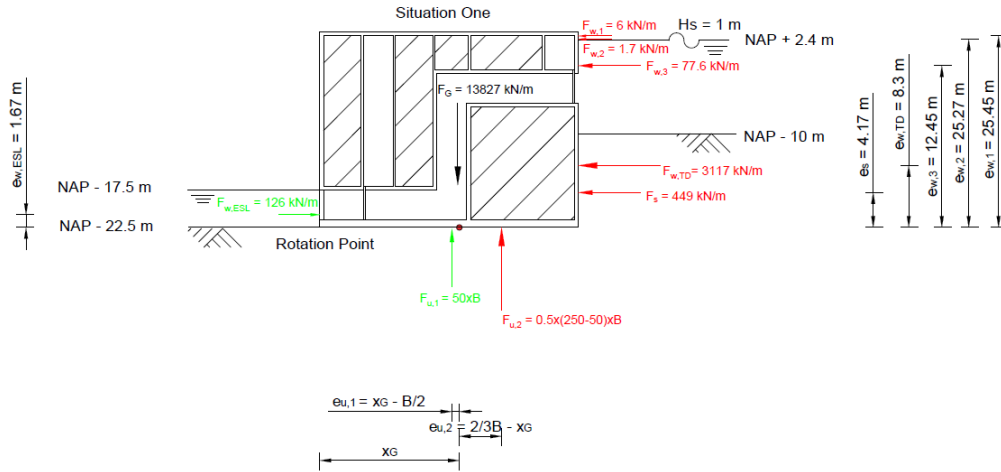


Figure 6.38: Unity check for governing situation

### 6.5.3.5. Rotational Stability

The governing load conditions for the rotational stability is the situation with the highest water level difference. This water level difference results in a larger resulting moment. The maximum water level difference occurs in situation one. The relevant forces for the governing situation can be seen in Figure 6.39.



**Figure 6.39:** Forces and the working arm

The forces that cause a moment in the same direction are coloured the same. In Appendix H, the detailed calculation of the moment around the gravity centre can be found. The results of the unity check can be seen in Figure 6.40. The minimum required width is 42.5 m.

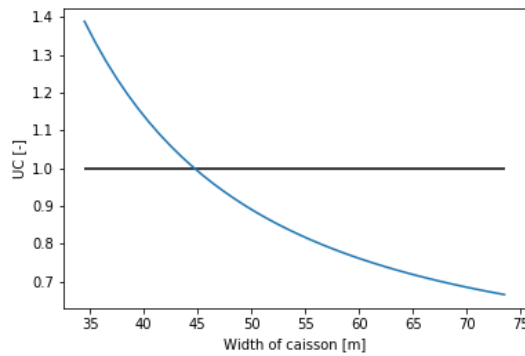


**Figure 6.40:** Unity check rotational stability

### 6.5.3.6. Bearing Capacity

The caisson is placed on a sill with a thickness of 2 m. The detailed calculations for all the bearing capacity can be found in Appendix H. The governing situation for the bearing capacity is situation one. The reason for this is that the uplift pressure in this situation is relatively low and the eccentricity is relatively large. This results in a high resulting vertical force and a low effective width. The bearing capacity is analysed for two layers: the sill and the sand layer. In Figure 6.41, the results of the unity check of the bearing capacity for both layers can be found. It can be seen that the sand layer is the governing layer regarding the bearing capacity. A minimum width of 38.5 m is required to ensure a unity check below 1.0.

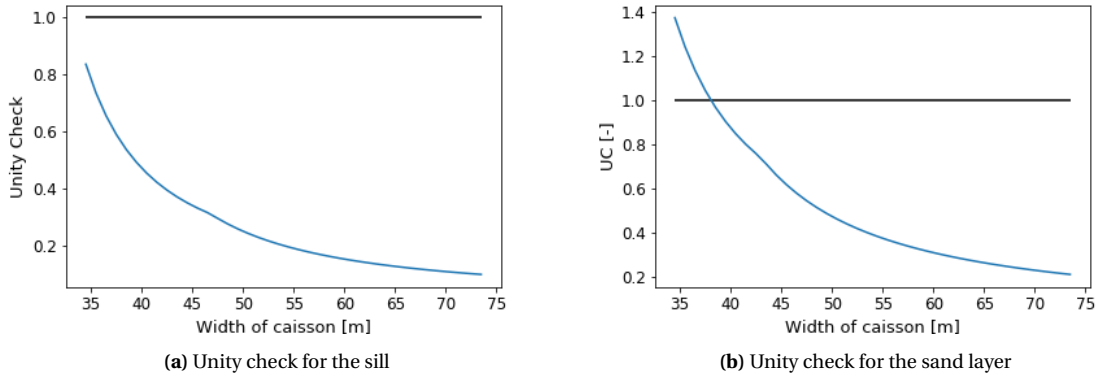


Figure 6.41: The unity checks for the bearing capacity

### 6.5.3.7. Draught

The draught of the caisson is important during the transport and positioning stage. During these stages, the caissons are empty and not filled with ballast. The maximum allowable draught depends on the occurring water levels and the minimum required keel. This required keel is 1 m during transport and 0.5 m during positioning. The caissons are constructed in the Energy Storage Lake. It is assumed that the water level in the Energy Storage Lake is equal to the mean water level in the North Sea and Tidal Lake, NAP + 0 m. This leads to a water depth of 22.5 m. The maximum draught for these stages is respectively 21.5 m and 22 m. In Figure 6.42 it can be seen that this draught will not be exceeded for each width.

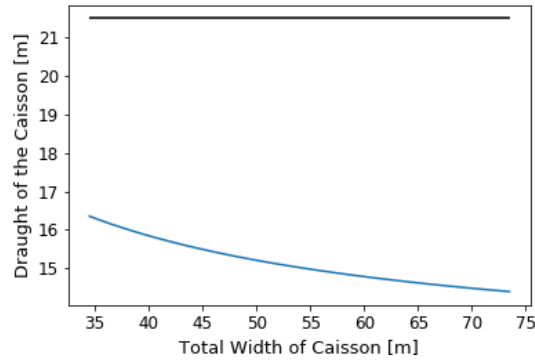


Figure 6.42: Draught of the caisson

### 6.5.3.8. Floating Stability

The caisson is stable during transport if the value of the metacentric height is above the 0.5 m. The metacentric height,  $h_m$ , is defined as:

$$h_m = \overline{GM} = \overline{KB} + \overline{BM} - \overline{KG} \quad (6.16)$$

in which:

$$\begin{aligned} \overline{KB} &= \frac{1}{2}d \\ \overline{BM} &= \frac{I}{V} \\ \overline{KG} &= \frac{\sum V_i \cdot e_i \cdot \gamma_i}{\sum V_i \cdot \gamma_i} \end{aligned}$$

The draught is already shown in the previous section. The values for  $\overline{BM}$  and  $\overline{KG}$  are calculated in Appendix H. The results of  $h_m$  for each width can be seen in Figure 6.43. The minimum required width is 43.5 m to ensure a stable caisson during transport.

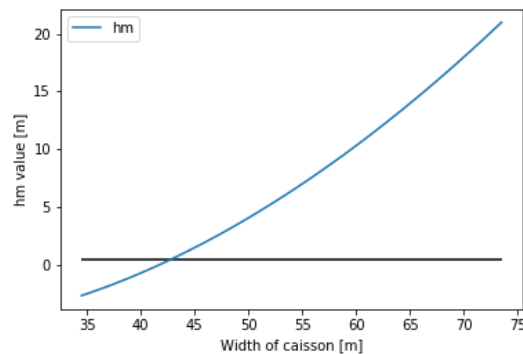


Figure 6.43: The metacentric height ( $h_m$ )

### 6.5.3.9. The final dimensions of the caisson

With the information retrieved from the stability requirements, see Table 6.9, the minimum width of the caisson is determined.

Mechanism	Minimum width [m]
Sliding Resistance	46.5
Rotational Stability	42.5
Bearing Capacity	38.5
Draught	-
Floating Stability	43.5

Table 6.9: Minimum required width

It can be seen that the sliding resistance is the governing mechanism for the minimum required width. The final width will be 49.5 m. The final width is slightly higher than the minimum required width. Unity checks too close to 1.0 are not favourable and therefore the final width is slightly deviant. The unity checks for a width of 49.5 m can be found in Table 6.10.

Mechanism	Unity Check
Sliding Resistance	0.91
Rotational Stability	0.83
Bearing Capacity	0.48
Draught	-
Floating Stability	0.12

Table 6.10: Unity Checks for the concept Caisson

In Figure 6.44a and 6.44b, the design of the concept can be seen. The height of the caisson is 26 m, the width is 49.5 m and the length is 33 m. With a total of 26 caissons, this results in a total length of the spillway of 858 m.

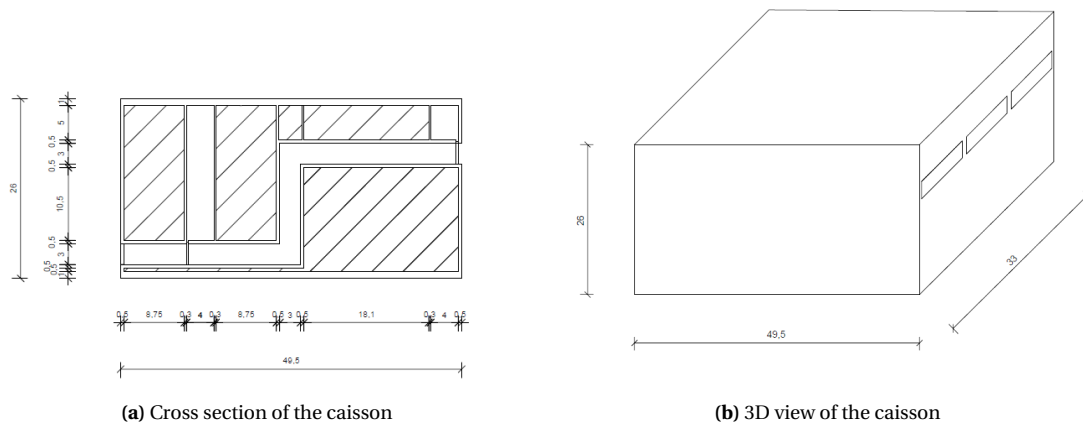


Figure 6.44: Final Layout of the concept Caisson

## 6.6. Concept Ogee

### 6.6.1. Dimension and Number of Openings

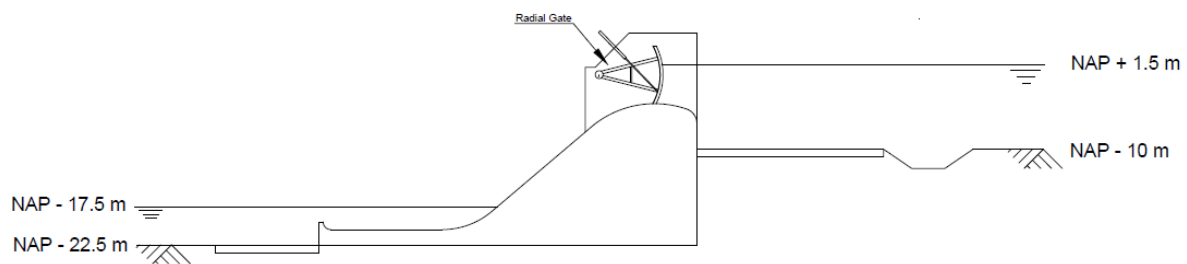


Figure 6.45: Concept Ogee governing discharge condition (NTS)

In concept Ogee, the flow over the spillway is described as open channel flow in which the flow is controlled by a gate. During maximum discharge, the gates will be fully opened and the discharge over the spillway can be described as flow over a sharp crested weir. The applicable formula for uncontrolled flow over a weir is:

$$Q = C_d \cdot L_e \cdot H_e^{\frac{3}{2}} \quad (6.17)$$

where:  $Q$  [m<sup>3</sup>/s] = the discharge over the weir  
 $C_d$  [-] = the discharge coefficient  
 $L_e$  [m] = effective length of the spillway  
 $H_e$  [m] = the hydraulic head above the weir

A difference between the earlier concepts and this concept is the dependence on the water levels in the lake. For open channel flow, the discharge is only depending on the upstream water level. An exception to this is a situation with downstream water levels exceeding the top of the crest. However, this cannot happen for this design due to the crest level being above the maximum water level in the Energy Storage Lake. The maximum discharge must be achieved when the water level in the Tidal Lake is at NAP + 1.5 m, see Figure 6.45.

With the top of the crest at NAP - 4.5 m and the maximum water level at NAP + 1.5 m, the value of  $H_e$  is 6 m. The coefficient of discharge is determined by the ratio between the height of the structure and the water level. The value of  $C_d$  is 2.14. The effective length is depending on the number of flow areas and the shape of the piers and abutments and is derived iteratively. More about this iterative process and the determination of  $C_d$  can be found in Appendix E. The discharge is calculated for multiple widths of a single channel which results in the following, see Figure 6.46.

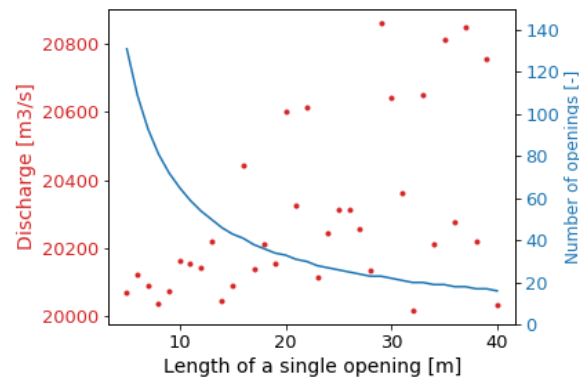


**Figure 6.46:** Total discharge and number of gates

For the determination of the final width of a single flow opening, the following items are taken into account.

- Number of openings needed
- Total width of the spillway
- Reference projects

The line of thinking for these items is that it is assumed that constructing larger openings will be more costly than smaller openings but constructing a large number of small openings will also be costly. The limited space available gives a maximum to the total length of the spillway and it is assumed that the cost will increase with the increase in length. Lastly, there is looked at other projects to see which dimensions are suitable for these projects.

For the first two items there is looked at Figure 6.46 and 6.47. In these figures, the exponential part is avoided because of the sensitivity. A small change in single length leads to a large increase in the number of openings and total length. For the third item, there is looked at multiple reference projects to see what a commonly used width is. Big spillways like the Itaipu and the Garrison have widths of 20 m but the Haringvliet sluices have radial gates with a width of 56 m (Ferguson et al., 1970, Itaipu Binacional, 2020, US Army Corps of Engineers, 2012).

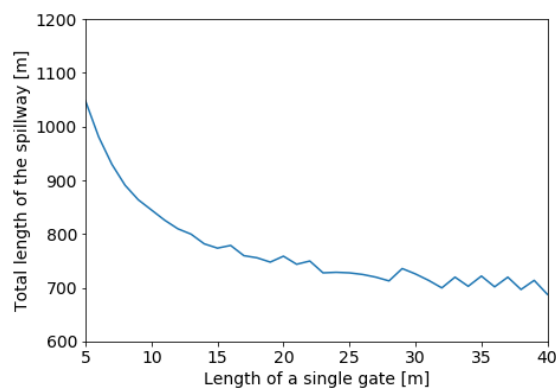


**Figure 6.47:** Total width versus the width of a single gate

The final choice for the length of a single opening is 25 m. To achieve the required discharge, 26 openings are needed. If these 26 openings are fully opened, the spillway can discharge  $20\,300\text{ m}^3/\text{s}$ . To prevent problems due to maintenance or failure, 2 extra gates will be added to ensure the  $20\,000\text{ m}^3/\text{s}$  if one or two gates are out of use due to maintenance or failure.

The reason that the velocity is not taken into account is that the velocity is not changing and only depending on the height of the spillway. The velocity can be defined by Formula 6.18. The total head difference occurs in the extreme situation, the water level in the Tidal Lake at NAP + 1.5 m and the lowest water level of the Energy Storage Lake at NAP - 17.5 m, 19 m. This results in a maximum occurring velocity of 19.3 m/s.

$$v = \sqrt{2g\Delta H} \quad (6.18)$$

where:  $v$  [m/s] = the velocity at the toe of the spillway  
 $\Delta H$  [m] = the total head difference

### 6.6.2. Shape of crest

The shape of the crest of the concept Ogee is important due to the influence on the effectiveness of the spillway. If the shape is not well designed, the spillway will not work efficiently and the probability of damage increases. The design of the crest is carried out by the design formulas of the U.S. Army Corps of Engineers (1990). The shape of the crest of the spillway is depending on the design head  $H$  at the apex and the approach depth  $P$ . The design head is equal to the difference between the maximum water level in the Tidal Lake and the top of the crest. The approach depth is the difference between the top of the crest and the bed level in front. The water level in the Tidal Lake is at NAP + 1.5 m and the top of the crest is at NAP - 4.5 m. This leads to a design head of 6 m and an approach depth of 5.5 m.

The ogee crest is divided into 5 different sections, see Figure 6.48: an upstream section (I), a downstream section (II), a constant slope section (III), a circular section (IV) and a stilling basin (V).

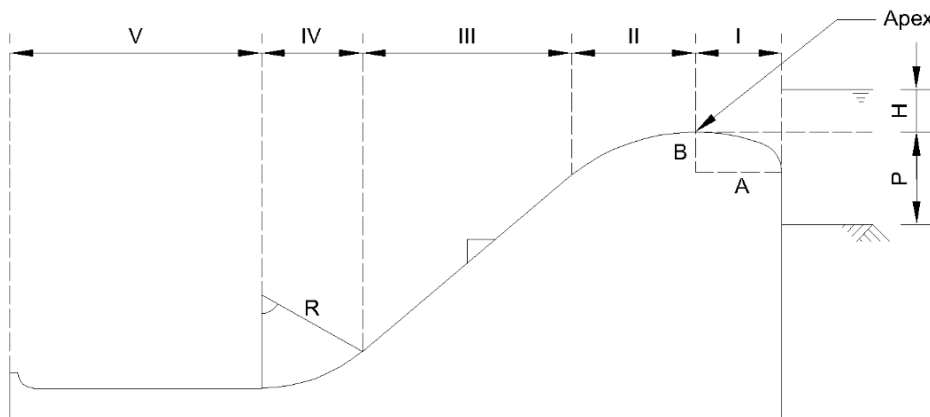


Figure 6.48: Different parts of the ogee crest

Section I and II are given by Formula 6.19 and 6.20, section III is a constant slope and section IV is defined by a circle with radius  $R$ , in which  $R$  is equal to a quarter of the spillway height.

$$Y = -\sqrt{\left(1 - \frac{X^2}{A^2}\right)B^2 + B} \quad (6.19)$$

$$Y = \frac{X^{1.85}}{K \cdot H_d^{0.85}} \quad (6.20)$$

For section I, constants  $A$  and  $B$  are depending on the ratio between  $H$  and  $P$  and for this concept equal to respectively 1.59 and 0.93. For section II,  $K$  is equal to 2. The constant slope in section III is 0.7H:1V. The derivations of these parameters can be found in Appendix I. For section IV, the radius is equal to 4.5 m. This leads to the following shape of the ogee spillway, see Figure 6.49.

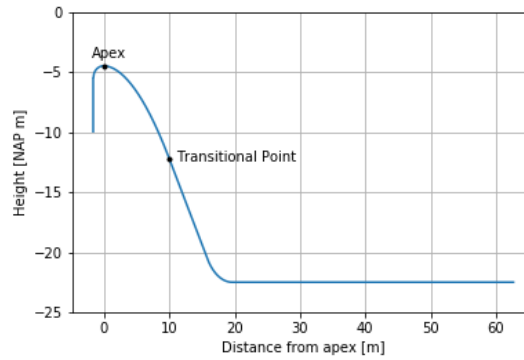


Figure 6.49: Shape of the concept Ogee

### 6.6.3. Stability of the Structure

For the concept Ogee, the first stability check that is carried out is to see if the self-weight of the structure is sufficient to prevent the uplift pressure below the structure. This check is performed first because the self-weight and dimension are smaller compared to the concept Caisson. Apart from that, the concept Ogee is a spillway over a gravity dam. Gravity dams are fully dependent on their self-weight to remain stable. The main component of the concept that provides the self-weight of the structure is the body of the spillway, see Figure 6.50. The part above the body is only present for a small part of the spillway. Therefore the influence of the weight of this part is low.

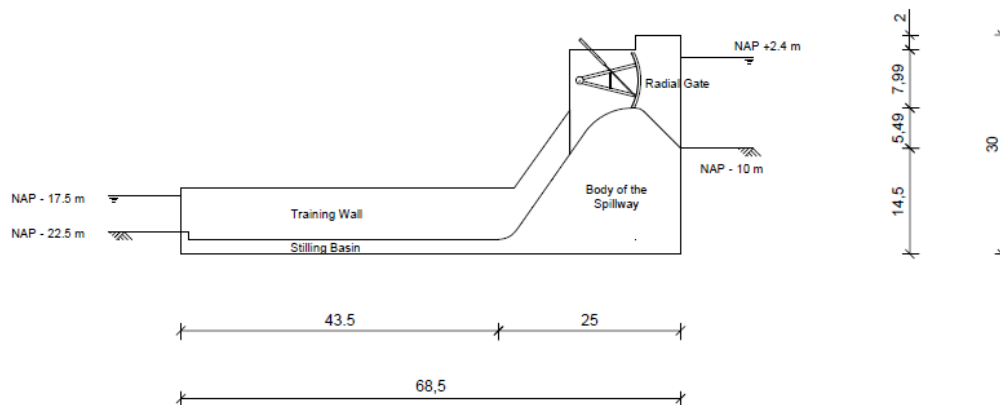


Figure 6.50: Layout of the Concept Ogee

The self-weight of the structure per meter length is equal to 10 132 kN/m, in the ultimate limit state. The detailed calculation for the self-weight can be seen in Appendix J. Besides the self-weight of the spillway, a part of the water causes a force acting downwards. These forces help to counter the uplift pressure. The resulting uplift pressure caused by the water is equal to 10 058 kN/m. It can be concluded that stability is a problem for this concept, because the self-weight is only slightly bigger than the uplift forces. To improve the stability of the spillway, the difference between the forces upwards and downwards has to be increased. The following can be done to achieve this:

- Increase self-weight of the structure
- The use of a drainage gallery
- The use of a pile foundation below the construction



The first point can only be done by decreasing the slope of the spillway. This will increase the volume of the spillway but will also increase the total width of the structure. The uplift pressures will also increase but will increase with a lower value,  $10 \text{ kN/m}^2$ , compared to the value for additional concrete,  $25 \text{ kN/m}^2$ . The second option, the use of a drainage gallery, is a very commonly used solution for uplift problems at large dams. It is only used at large dams because of the high cost of installation of such a gallery. During the construction phase, multiple additional steps have to be taken to construct such a gallery. The third option is the use of a pile foundation. Normally a gravity dam is located above a rock bed layer instead of a sand layer. Therefore the use of a gravity dam spillway is not favourable for the location of Delta21. To improve the location a pile foundation can be used. With the use of a pile foundation, the structure can deal with the uplift pressures and the horizontal forces. Constructing the pile foundation below the water surface at NAP - 22.5 m is a difficult process and ensuring a good connection between the pile foundation and the bottom of the spillway is difficult as well.

The concept Ogee can only be constructed if additional solutions are implemented in the design but it is assumed that this will come with an increase in costs and the constructability of the spillway becomes very complicated due to the possible pile foundation that needs to be constructed at a depth of 22.5 m. Another problem regarding the concept Ogee is the occurring velocity downstream of the spillway, 19.3 m/s. This velocity will cause a hydraulic jump of 10.03 m. This can only take place if the stilling basin is lowered by approximate 5 m and this also increases the difficulty of construction. Therefore, it is decided that the concept Ogee will be dropped in the remainder of this thesis. The main reasons are the difficulty of construction, which leads to an increase in costs and the high velocities at the end of the spillway.

## 6.7. Conclusion of the Verification

All concepts, except the concept Ogee, are feasible to construct and have a discharge capacity exceeding the required capacity. The main hydraulic dimensions of the concepts are obtained by the hydraulic requirement of a discharge of  $20\,000 \text{ m}^3/\text{s}$ . The main dimensions of the concepts are obtained by the stability requirements. For the concept Siphon and Underflow, the main failure mechanisms that determine the width of the structure are sliding resistance for the Energy Storage Lake side and bearing capacity for the Tidal Lake side. Due to an insufficient depth at the Tidal Lake, the caisson can only be constructed in-situ. For the concept Caisson, the main failure mechanism that affects the width is the sliding resistance. The concept Ogee, is not stable in the current condition. Improving the design will increase the cost and the difficulty of construction. Besides this, the flow velocity into the Energy Storage Lake is large ( $\approx 19 \text{ m/s}$ ), which leads to a difficult and expensive scour protection. Combining these reasons leads to the conclusion that this concept is dropped in the remainder of this thesis.

# 7

## Evaluation and Selection

In the previous chapters, the concepts are developed and verified on the hydraulic requirements and the stability requirements are performed. This resulted in the main dimensions of the concepts. In this chapter, the remaining concepts are evaluated by a multi-criteria analysis and a cost estimation and at the end, the best concept is chosen.

### 7.1. The Multi-Criteria Analysis

In the evaluation stage of the engineering design cycle, the remaining concepts are evaluated by a value-cost analysis. In this analysis, the value of the concepts is determined by a multi-criteria analysis (MCA) and the cost are determined by information retrieved from the Ballast Nedam budgeting department. As stated at the end of Chapter 6, the concept Ogee has dropped out and is not considered in the evaluation. In the multi-criteria analysis, different criteria that are obtained by the stakeholder analysis are used to evaluate the concepts. Each criterion results in a certain score for a concept regarding this criterion.

#### 7.1.1. The Criteria

The evaluation criteria are mentioned in detail in Section 3.5 but are also shown and explained below.

- **Ease of operation:**  
Each concept differs regarding the necessary steps that need to be taken during the operations of the spillway. If more steps have to be taken, the system can be considered more complex and receives a lower rating for the ease of operation. For example, a higher number of gates leads to a more extensive system but is still relatively less complex than a system that requires a pumping system.
- **Ease of construction:**  
The ease of construction depends on the design of the construction. Bigger structures are more difficult to transport and to place on the final location. Accessibility of the construction site will be taken into consideration within this evaluation criterion.
- **Serviceability and possibility of inspection:**  
The maintenance of a structure is very important but can be overlooked during the design stage. This can lead to high costs during the operation stage. For this reason, the structure must be easy to maintain. To compare the concept on the serviceability and possibility of inspections, the accessibility of the structure is also taken into account. Besides this, the ease of replacement of components of the spillway is considered.
- **Integration in the environment:**  
For the integration in the environment, the implementation of the structure in the surroundings is taken into consideration. The structure can be part of the environment, which results in a higher score for this specific criterion, or a stand-alone structure that is not integrated into its surroundings, which results in a lower score. In areas in which nature is important, the integration of the structure into its environment is desired.

- **Sustainability:**

The idea of Delta21 is to restore the nature of the Haringvliet basin. For this reason, it is important that the design will have a positive influence on the ecology. A design that uses large volumes of concrete is not sustainable and has a large carbon footprint. This will be considered in this criterion, which regards the sustainability of the spillway concept design. Besides the carbon footprint, the reuse of materials is taken into consideration.

### 7.1.2. The Weighting Factors

Each criterion has its own importance, which can be expressed in weighting factors. A high weighting factor means a higher importance compared to the other criteria. To determine the weighting factors of the criteria, the relative weights of the criteria are determined first and after that, these values are converted to the weighting factors. The determination of the weighting values can be found in Appendix K and the weighting factors can be seen in Table 7.1.

Criteria	Weighting Factor
Ease of operation	38
Ease of construction	28
Serviceability and possibility of inspection	19
Integration in the environment	5
Sustainability	10

**Table 7.1:** Weighting factors of the Multi-Criteria Analysis

### 7.1.3. The Scores of the Concepts

For each criterion, a concept can score a value between 1 and 10 in which 10 is a good value and a 1 is a poor value. The score that is given for a certain criterion is multiplied by the weighting factor of this criterion. In the end, the sum of the scores for each concept is taken for the determination of the most optimal concept according to the evaluation criteria. The detailed explanation of the values given for each criterion can be seen in Appendix K and some important scores are described in the remainder of this section. The total scores of the concepts can be seen in Table 7.2.

	Weighting Factor (WF)	Concept Siphon		Concept Underflow		Concept Caisson	
		Score	Score · WF	Score	Score · WF	Score	Score · WF
<b>Ease of Operation</b>	<b>38</b>	4	152	5	190	6	228
<b>Ease of Construction</b>	<b>28</b>	6	168	6	168	7	196
<b>Serviceability and possibility of inspection</b>	<b>19</b>	7	133	4	76	6	114
<b>Integration in the environment</b>	<b>5</b>	7	35	8	40	5	25
<b>Sustainability</b>	<b>10</b>	6	60	7	70	8	80
	$\Sigma$		<b>548</b>		<b>544</b>		<b>643</b>

**Table 7.2:** The multi-criteria scores per concept

In Table 7.2, it can be seen that concept Caisson scores the best. The main reason for this is the score in the ease of operation. The concept Caisson scores better than the other concepts on this part because the number of gates that have to be opened is lower, which results in a less extensive system for the spillway. Besides this, the concept Caisson does not require additional pumps to let the water flow, which is the case for the concept Siphon. The concept Caisson scores also better on the ease of constructability because the number of caissons is lower compared to the other concepts and the caissons can be transported. However, the concept Caisson consists of caissons with larger dimension. Therefore the construction of the construction dock becomes more challenging. A negative side of the concept Caisson is the integration in the environment. The caissons will be clearly visible and are not part of the surrounding.

## 7.2. The Cost Estimation

The second part of the evaluation phase is the cost estimation. In this part, the costs of each concept are compared. The main reason for including the costs of the concepts into the evaluation is that a concept that scores very well in the multi-criteria analysis is not per definition a good concept if the construction costs are relatively large compared to the other concepts. For the selection of the final concept, the multi-criteria analysis and the cost evaluation have to be considered together.

The cost estimation for each concept is based on the information retrieved from the Tender Infra Projects section of Ballast Nedam. The information that is retrieved is the unit prices for certain actions or materials. In Appendix L, a detailed description about the cost can be found for each concept. The total cost estimations for each concept can be seen in Table 7.3. In the cost of the concepts, the cost of the scour protection is not included. The reason for this is that the flow velocities in the three concepts are comparable. Therefore the cost of the scour protection is assumed to be around the same for each of the concepts.

	Total Cost [€]
<b>Concept Siphon</b>	€1.071.400.000,-
<b>Concept Underflow</b>	€837.240.000,-
<b>Concept Caisson</b>	€474.320.000,-

**Table 7.3:** Total cost of each concept in Euros

The cost of the concepts are based on the cost of the concrete works, dredging works, transport and placement of the caissons and the construction of the construction docks and building pit. For the concept Caisson, an estimation of the cost for the seepage screen is also taken into consideration. Only a limited number of items are included in the cost and therefore some items are not considered. For instance, the scour protection, the mechanism of the gates and life cycle cost. In Appendix L it can be seen that the largest share of the cost are the concrete works and the construction of the pipes. The latter only applies to the concepts Siphon and Underflow. The share of the construction of the concrete pipes is respectively 31% and 48% of the total cost of the concept Siphon and Underflow.

## 7.3. Selection

For the selection of the most optimal concept, the values of the multi-criteria analysis and the costs are plotted against each other, see Figure 7.1. It can be seen that the concept Caisson has the highest multi-criteria value and the lowest costs. Therefore it can be concluded that this is the most optimal concept and this concept will be further elaborated in Chapter 8. Remarkably, the concept with the highest value has the lowest cost estimation. But the reason for this is mainly the impact of the concrete pipes on the costs of the concept Siphon and Underflow.

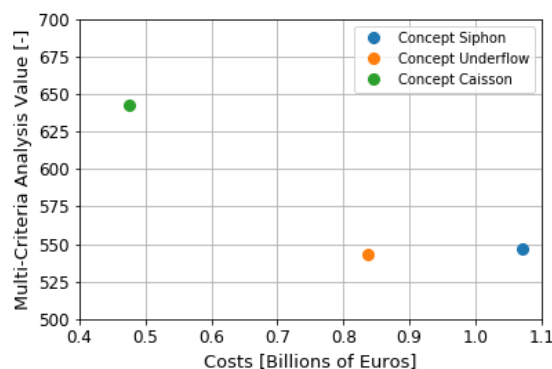


**Figure 7.1:** Costs versus MCA Values

# 8

## Strength Verification and Scour Protection

In this chapter, the strength verification and the scour protection can be found. In the strength verification, the concrete elements are checked on their strength and for the scour protection, a preliminary scour protection design is shown. The strength verification is part of the structural design of the spillway. In Chapter 6, another part of the structural design is already performed, the stability of the spillway.

### 8.1. Strength Verification

In the strength verification, the concrete elements of the caisson are checked if the applied reinforcement is sufficient. First, the classification of the structure is performed and the material properties of the concrete are discussed. Then, the verification checks are performed in this thesis are discussed. Next, the initial lay-out of the caisson is checked and if required, improvements are made to the initial lay-out. Finally, the improved lay-out is checked on the strength of the elements. The proposed reinforcement is determined by the checks in the ultimate limit state and afterwards, the service limit state check is used to see if all checks are sufficient.

#### 8.1.1. Classification of the Structure and Material Properties

For the classification of the structure, two classes are relevant to consider: the exposure class and the structural class. A part of the structure is continuously exposed to seawater and the other part of the structure is only occasionally exposed to seawater. Seawater can lead to erosion problems of the steel reinforcement bars in the concrete. Due to the exposure of seawater, according to NEN-EN 1992-1-1, article 4.4.1.2, the structure can be categorised in exposure classes XS2 and XS3. According to NEN-EN 1992-1-1, Appendix E.1, the minimum required concrete class corresponding to these exposure classes is C35/45. In the remainder of this thesis, the concrete class C50/60 is used because this leads to a higher strength of the elements. The material properties of C50/60 concrete can be found in Table 8.1. The design value in this table is determined with the partial safety factor of 1.5, according to NEN-EN 1992-1-1, article 2.4.2.4.

Concrete Class	$f_{ck}$	$f_{cd}$	$f_{ctd}$	$f_{ctm}$	$E_{cm}$
C50/60	50	33,3	1,9	4,1	37000

**Table 8.1:** The parameters corresponding to the concrete class according to NEN-EN 1992-1-1, Table 3.1

The second relevant class is the structural class. According to NEN-EN 1992-1-1, article 4.4.1.2, the structure is placed in structural class 5 (S5). Due to the design lifetime of the spillway, 100 years, the structure should be classified as structural class 6. But the relatively high concrete class C50/60 leads to a reduction to S5. Both classes, exposure and structural influence the minimum required concrete cover. For a structural class S5 and an exposure class XS2/XS3, this results in a minimum required cover of 50 mm. In Appendix M.4.1, a detailed explanation of the minimum required over is given. The reinforcement steel that is used in the design is B500B and the parameters of this type of steel can be found in Table 8.2.

Steel Type	$f_{yk}$ (tension)	$f_{yk}$ (compression)	$f_{yd}$
B500B	500	500	435

**Table 8.2:** Steel parameters for the reinforcement according to the Manual Hydraulic Structures 2020b

### 8.1.2. Strength Verification Checks

In this chapter, the concrete elements of the concept Caisson are checked on three different items:

- Bending Moment
- Shear Force
- Crack Width

#### 8.1.2.1. Bending Moment

The design bending moment should not exceed the bending moment capacity of the element. The reason this check is performed is that when the design bending moment exceeds the bending moment capacity, the stresses in the steel reinforcement bars exceed the yield stress of the steel. This leads to failure of the element. According to Eurocode 2 the design bending moment must be determined in the ultimate limit state (ULS), this means that load factors have to be used.

$$M_{Ed} \leq M_{Rd}$$

where:  $M_{Ed}$  [kNm] = the design bending moment  
 $M_{Rd}$  [kNm] = the bending moment capacity

The bending moment capacity is depending on the amount of reinforcement and is determined by Formula 8.1 (Braam, 2011).

$$M_{Rd} = A_s \cdot z \cdot f_{yd} \quad (8.1)$$

where:  $A_s$  [mm<sup>2</sup>] = the reinforcement area  
 $z$  [mm] = arm of internal leverage  
 $f_{yd}$  [N/mm<sup>2</sup>] = the design yield strength of the reinforcement

In this thesis, the required reinforcement is determined by a trial and error method. First, the design bending moment is calculated and afterwards, the amount of reinforcement that is required is determined. In the remainder of this chapter, the proposed reinforcement is shown and the results of the unity check for the bending moment can be found.

#### 8.1.2.2. Shear Force

A concrete element can withstand a certain amount of shear force without shear reinforcement due to the shear force capacity of the concrete. If this capacity is exceeded, additional shear force reinforcement is required. According to Eurocode 2, the shear force in the element must be determined in ULS.

$$V_{Ed} \leq V_{Rd,c}$$

$$V_{Ed} \leq V_{Rd}$$

where:  $V_{Ed}$  [kN] = acting shear force  
 $V_{Rd,c}$  [kN] = shear resistance without shear reinforcement  
 $V_{Rd}$  [kN] = shear resistance with shear reinforcement

The shear resistance without reinforcement is determined according to NEN-EN 1992-1-1, article 6.2.2 by Formula 8.2.

$$V_{Rd,c} = (C_{Rd,c} \cdot k \cdot (100 \cdot \rho_1 \cdot f_{ck})^{\frac{1}{3}} + k_1 \cdot \sigma_{cp}) \cdot b_w \cdot d \quad (8.2)$$

with a minimum of:

$$V_{Rd,c,min} = (v_{min} + k_1 \cdot \sigma_{cp}) \cdot b_w \cdot d$$

where:	$V_{Rd,c}$	[kN]	=	shear force resistance
	$V_{Rd,min}$	[kN]	=	minimum shear force resistance
	$C_{Rd,c}$	[-]	=	a coefficient ( $= \frac{0.18}{\gamma_m} = \frac{0.18}{1.5} = 0.12$ )
	$\gamma_m$	[-]	=	material factor of concrete (= 1.5)
	$k$	[-]	=	$1 + \sqrt{\frac{200}{d}} \leq 2.0$ with d in mm
	$\rho_1$	[-]	=	reinforcement ratio
	$f_{ck}$	[N/mm <sup>2</sup> ]	=	characteristic compressive cylinder strength of concrete
	$k_1$	[-]	=	a coefficient (= 0.15)
	$\sigma_{cp}$	[N/mm <sup>2</sup> ]	=	compressive stress in the concrete from axial load ( $\sigma_{cp} = \frac{N_{Ed}}{A_c} < 0,2 \cdot f_{cd}$ )
	$N_{Ed}$	[N]	=	the axial force in the cross-section
	$b_w$	[mm]	=	the smallest width of the cross-section
	$d$	[mm]	=	the effective height of the cross-section
	$v_{min}$	[-]	=	$0.035 \cdot k^{\frac{3}{2}} \cdot \sqrt{f_{ck}}$

The shear resistance with shear reinforcement is according to NEN-EN 1992-1-1, article 6.2.3 given by the minimum value of Formula 8.3 and 8.4.

$$V_{Rd,s} = \frac{A_{sw}}{s} \cdot z \cdot f_{ywd} \cdot \cot(\theta) \quad (8.3)$$

$$V_{Rd} = \frac{\alpha_{cw} \cdot b_w \cdot z \cdot v_1 \cdot f_{cd}}{\cot\theta + \tan(\theta)} \quad (8.4)$$

where:	$V_{Rd,s}$	[N]	=	shear resistance with stirrups governing
	$V_{Rd}$	[N]	=	shear resistance with concrete compressive struts governing
	$A_{sw}$	[mm <sup>2</sup> ]	=	the cross-sectional area of the reinforcement
	$s$	[mm]	=	the spacing of the stirrups
	$f_{ywd}$	[N/mm <sup>2</sup> ]	=	the design yield strength of the shear reinforcement
	$\theta$	[deg]	=	angle between the concrete compression strut and the beam axis
	$\alpha_{cw}$	[-]	=	coefficient taking account of the state of the stress in the compression chord (= 1.0)
	$v_1$	[-]	=	strength reduction factor

Again, in this thesis the required reinforcement is determined by a trial and error method. First, the design shear force is determined and afterwards, the required shear force reinforcement to withstand this force is determined.

### 8.1.2.3. Crack Width

The theoretically crack width, which is depending on the amount of longitudinal reinforcement in the concrete element, may not exceed the maximum allowable crack width. The maximum allowable crack width is set by the tightness class of the structure. The tightness class of the caisson is TC1 in which leakage needs to be limited to a small amount. It is assumed that the cracks will not go through the full height of the elements and according to NEN-EN 1992-3 (2006), article 7.3.1, the National Annex of NEN-EN 1992-1-1 needs to be used for the determination of the theoretically crack width. According to NEN-EN 1992-1-1, article 7.3.1, the maximum allowable crack width is 0.2 mm for exposure Class XS2. More about the exposure class in Section 8.1.1.

$$w_k \leq w_{max} \quad (8.5)$$

The theoretically crack width is determined with Equation 8.6 according to NEN-EN 1992-1-1 and must be performed in the service limit state (SLS).

$$w_k = s_{r,max} \cdot \frac{\sigma_s - k_t \cdot \frac{f_{ct,eff}}{\rho_{p,eff}} \cdot (1 + \alpha_e \cdot \rho_{p,eff})}{E_s} \quad (8.6)$$

where:	$w_k$	[mm]	=	theoretical crack width
	$w_{max}$	[mm]	=	maximum crack width
	$s_{r,max}$	[mm]	=	maximum crack spacing
	$\sigma_s$	[N/mm <sup>2</sup> ]	=	tensile stress in the steel bar
	$k_t$	[-]	=	load duration coefficient
	$f_{ct,eff}$	[N/mm <sup>2</sup> ]	=	mean value of the concrete tensile strength (= $f_{ctm}$ )
	$\rho_{p,eff}$	[-]	=	reinforcement ratio
	$E_s$	[N/mm <sup>2</sup> ]	=	Youngs' modulus of steel (= $200 \cdot 10^3$ N/mm <sup>2</sup> )
	$E_c$	[N/mm <sup>2</sup> ]	=	Youngs' modulus of concrete
	$\alpha_e$	[-]	=	ratio between Youngs' moduli of steel and concrete (= $\frac{E_s}{E_c}$ )

The load duration factor,  $k_t$ , is respectively 0.4 for long-term loading and 0.6 for short-term loading. The use of the long or short-term factor is depending on the load situation. For most of the calculations, the long-term loading is governing. Only if the transport stage of the caisson is governing, short-term loading is governing. The maximum crack spacing is defined by Formula 8.7.

$$s_{r,max} = k_3 c + k_1 k_2 k_4 \frac{\phi}{\rho_{p,eff}} \quad (8.7)$$

where:	$k_1$	[-]	=	bond stress coefficient (= 0.8)
	$k_2$	[-]	=	coefficient for the distribution of the strain over the height of the concrete area (= 0.5)
	$k_3$	[-]	=	coefficient (= 3.4)
	$k_4$	[-]	=	coefficient (= 0.425)
	$c$	[mm]	=	concrete cover
	$\phi$	[mm]	=	diameter of the reinforcement

For the crack width check, the maximum theoretically crack width is calculated for the proposed reinforcement. This proposed reinforcement is, as mentioned before, found by a trial and error method. The maximum theoretically crack width is determined for the proposed reinforcement and if required, additional reinforcement is added.

### 8.1.3. Initial Lay-out

The initial lay-out of the caisson can be seen in Figure 8.1. This lay-out originated from the functional and stability requirements of the spillway, see Chapter 5 and 6. Figure 8.1 shows that some of the elements have a large span (>15 m) but also some elements with a smaller span but with a large column (19.5 m) of ballast sand on it. Some of these elements are only loaded from one side, which results in relatively large bending moments in the elements. Before determining the exact amount of reinforcement, for some of these elements the required reinforcement ratio is calculated by a simplified method, see Section 8.1.4. This is step is performed to see if the initial lay-out can be used or that the required ratio is exceeding the maximum ratio (3.1% for C50/60) and improvements have to be made. Only if the required ratios are below the maximum ratio, a more detailed verification, including the three previously mentioned checks, is performed.



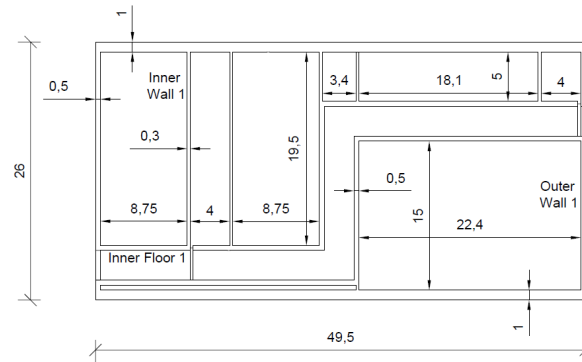


**Figure 8.1:** The initial lay-out of the caisson

#### 8.1.4. Verification of Initial-Layout

As mentioned in Section 8.1.3, the required reinforcement ratios for some of the critical elements is determined by a simplified method. There is chosen to verify two elements in the initial lay-out: internal wall one and internal floor one. Both these elements can be found in Figure 8.1. These elements are either chosen due to the large span or a large amount of ballast sand resting on the element. Within the initial design, there are more elements that can be critical but firstly these two are checked. The first step in this verification is to identify the loads acting on the element and the corresponding bending moments. Secondly, with the use of the theory of elasticity, the required reinforcement ratios are obtained. A more detailed explanation of this method and the calculations can be found in Appendix M. In Table 8.3, the acting bending moments and required reinforcement ratios can be seen. It can be concluded that both elements require a larger amount of reinforcement than the maximum allowable ratio according to Eurocode 2 (*leq*3.1). Therefore, improvements have to be made to the initial lay-out.

Element	Thickness [mm]	Dimensions [m]	Load (ULS) [kN/m <sup>2</sup> ]	Bending Moment [kNm/m]	Required Reinforcement Ratio
Internal Wall One	300	10 x 19.5	250	2782	>3.1%
Internal Floor One	500	8.75 x 10	543	3346	>3.1%

**Table 8.3:** Verification of the Initial Lay-out

#### 8.1.5. Improved Lay-out

The lay-out is improved in two different ways: increasing the thickness of the elements and dividing the caisson in multiple compartments. The increase in thickness of the elements differ per element:

- The internal wall thickness (excluding the culvert walls) increased from 300 mm to 400 mm
- The external wall thickness increased from 500 mm to 600 mm
- The internal floor thickness increased from 300 mm to 600 mm
- The culvert wall thickness is locally increased from 500 mm to 600 mm (Only on the upper left side of the culvert)

All these improvements can be seen in the new lay-out shown in Figure 8.2. The improved lay-out leads to lower loads acting on the elements and an increased resistance. In the lower-left corner of the caisson, small compartments are present. These compartments are required to overcome a large span of certain elements. These compartments will not be filled with ballast material because this would be very difficult to accomplish. The reason there is chosen to create small compartments there instead of increasing the thickness of the bottom slab is that constructing a bottom slab with such a thickness would require additional measures to prevent heating problems.

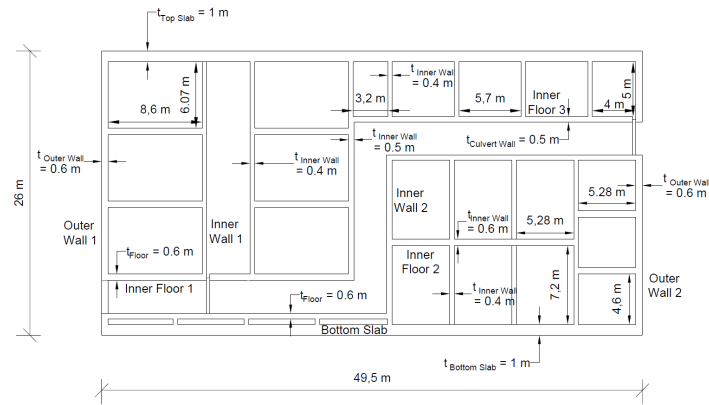


Figure 8.2: The improved lay-out of the caisson

### 8.1.6. Verification of the Improved Lay-Out

In the verification of the initial lay-out, the required reinforcement ratio for the bending moment is used as an indication if the element could withstand the loads. For the improved lay-out, a more detailed verification is performed. In this verification, the earlier mentioned checks, see Section 8.1.2, are checked. In Table 8.5, the proposed reinforcement for each element can be seen. This reinforcement is used in the verification checks and the corresponding unity checks for each element can be seen in Table 8.4. In Appendix M, the detailed calculation of this verification can be found.

Element	Reinforcement		Load			Resistance			Unity Check		
	Diameter $\varnothing$ [mm]	Number of Bars per m [-]	MEd [kNm/m]	VEd [kN/m]	w [mm]	MRd [kNm/m]	VRd [kN/m]	wmax [mm]	Bending Moment [-]	Shear Force [-]	Crack Width [-]
Internal Wall 1	25	9	306	238	0.182	543	396	0.2	0.56	0.60	0.91
Internal Floor 1	32 (Row 1) 25 (Row 2)	10	1114	789	0.181	2233	936	0.2	0.50	0.84	0.91
Internal Wall 2	32	9	458	369	0.188	797	418	0.2	0.58	0.92	0.94
Internal Floor 2	32	8	665	568	0.18	1283	619	0.2	0.52	0.86	0.90
Internal Floor 3	32	9	537	433	0.157	1111	489	0.2	0.52	0.89	0.78
Culvert Wall 1	32 (Row 1) 20 (Row 2)	10	1194	915	0.166	2033	979	0.2	0.59	0.93	0.83
External Wall 1	32	10	771	613	0.170	1510	755	0.2	0.51	0.81	0.85
External Wall 2	32	10	815	795	0.166	1495	1168	0.2	0.55	0.68	0.83
Bottom Slab	32	8	1122	863	0.172	2358	1179	0.2	0.48	0.73	0.86

Table 8.4: Overview of the reinforcement and the unity checks

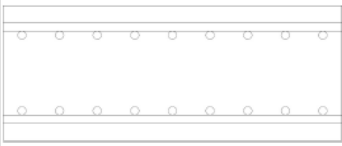
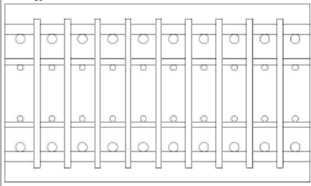
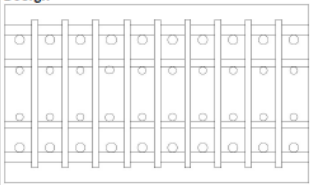
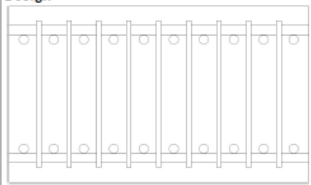
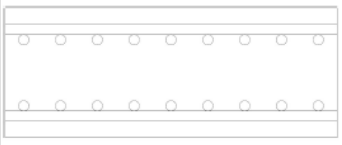
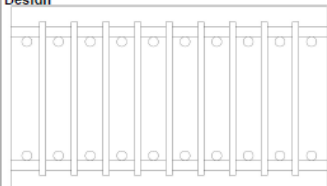
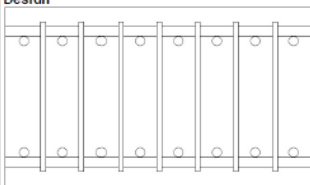
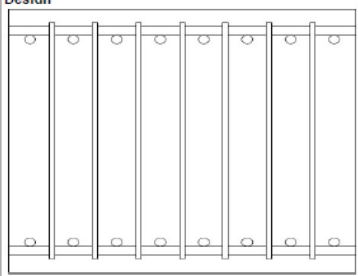
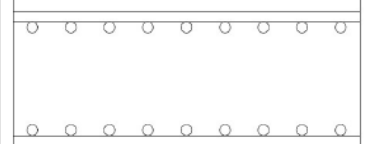
<p>Element Internal Wall One</p> <p>Longitudinal Reinforcement Ø [mm] 25</p> <p>Number of Bars 9</p> <p>Shear Reinforcement Ø [mm] -</p>	<p>Design</p> 	<p>Element Culvert Wall One</p> <p>Longitudinal Reinforcement Ø [mm] 32 &amp; 20</p> <p>Number of Bars 10</p> <p>Shear Reinforcement Ø [mm] 20</p>	<p>Design</p> 
<p>Element Internal Floor One</p> <p>Longitudinal Reinforcement Ø [mm] 32 &amp; 25</p> <p>Number of Bars 10</p> <p>Shear Reinforcement Ø [mm] 20</p>	<p>Design</p> 	<p>Element External Wall One</p> <p>Longitudinal Reinforcement Ø [mm] 32</p> <p>Number of Bars 10</p> <p>Shear Reinforcement Ø [mm] 18</p>	<p>Design</p> 
<p>Element Internal Wall Two</p> <p>Longitudinal Reinforcement Ø [mm] 32</p> <p>Number of Bars 9</p> <p>Shear Reinforcement Ø [mm] -</p>	<p>Design</p> 	<p>Element External Wall Two</p> <p>Longitudinal Reinforcement Ø [mm] 32</p> <p>Number of Bars 10</p> <p>Shear Reinforcement Ø [mm] 20</p>	<p>Design</p> 
<p>Element Internal Floor Two</p> <p>Longitudinal Reinforcement Ø [mm] 32</p> <p>Number of Bars 8</p> <p>Shear Reinforcement Ø [mm] 18</p>	<p>Design</p> 	<p>Element Bottom Slab</p> <p>Longitudinal Reinforcement Ø [mm] 32</p> <p>Number of Bars 8</p> <p>Shear Reinforcement Ø [mm] 18</p>	<p>Design</p> 
<p>Element Internal Floor Three</p> <p>Longitudinal Reinforcement Ø [mm] 32</p> <p>Number of Bars 9</p> <p>Shear Reinforcement Ø [mm] -</p>	<p>Design</p> 		

Table 8.5: Overview of reinforcement in the elements

## 8.2. Scour Protection

### 8.2.1. Determination of the Governing Situation for the Scour Protection

The design of the scour protection is depending on the flow velocities. Before considering the flow velocities, the flow situations are discussed. Two possible situations can occur in the Energy Storage Lake. In the first situation, the spillway is opened and the pumping station is not functioning. This is illustrated in Figure 8.3a. This situation occurs mainly when the spillway is just opened. The water entering the Energy Storage Lake will flow straight to the opposite dune trajectory. Once there, the flow will either bend to the right or will end up on the dunes. In the second situation, the pumping station and the spillway are both functioning. In this situation, the flow in the Energy Storage Lake will be more complex. Part of the flow will go directly to the pumping station but there is a possibility that the other part will flow to the dunes and bend to the right. This situation is illustrated in Figure 8.3b. The precise flow patterns are hard to predict in advance and therefore the shown patterns are assumed. In both figures, the maximum discharge and flow velocity is given for the spillway and the pumping station. The information for the pumping station is retrieved from Paasman (2020). In Figure 8.3, the Hinderplaat is illustrated. The Hinderplaat is a sand bar in front of the Haringvliet sluices and the environmental value of the Hinderplaat is significant. Due to larger flow velocities

caused by the presence of the spillway in comparison to the current situation, the sand bar will probably be affected by the spillway. Sand from the Hinderplaat can eventually end up in the Energy Storage Lake and therefore, the existence of the Hinderplaat can be endangered. On the other hand, the large flow velocities only occur sporadically and the inflow pattern is very diffusive. This reduces the effect of the spillway on the Hinderplaat. The impact of the spillway on the Hinderplaat is outside of the scope of this thesis and therefore not treated in more detail.

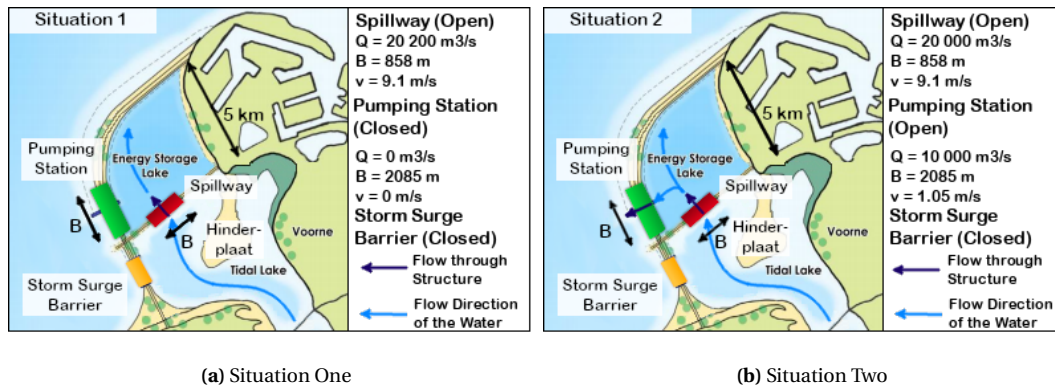
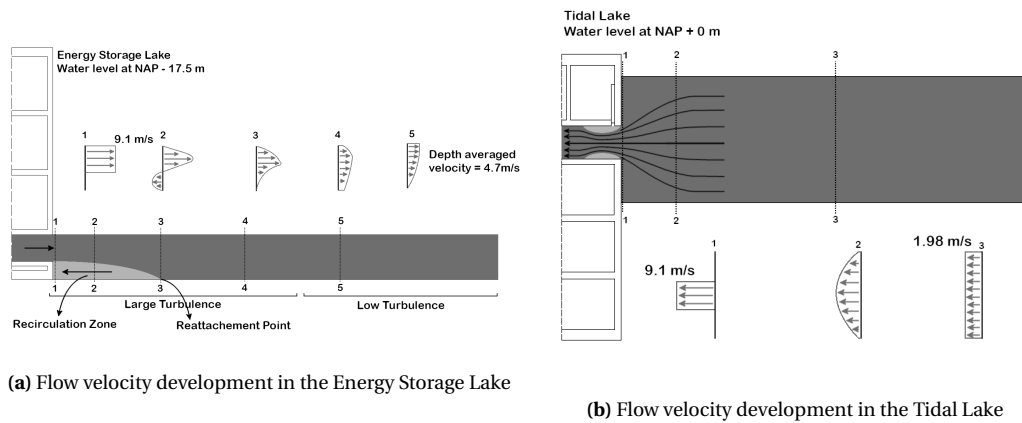


Figure 8.3: The Different flow Situations

In this research, for the design of the scour protection, only the local scour problems are taken into consideration. This means that only scour that endangers the stability of the spillway is treated in this thesis. Erosion of the dunes or the impact of large scour holes on the functioning of the Delta21 concept are not discussed but are relevant for further research. For the design of the scour protection, the flow is assumed to be according to Figure 8.3a. The water will flow towards the opposite dune trajectory. Therefore, the influence of the pumping station on the flow direction is neglected. However, in the calculations of the water level in the Energy Storage Lake, the outflow through the pumping station is taken into account.

The velocities near the spillway, upstream and downstream, are complex and difficult to calculate without doing more detailed research. To estimate the change in velocity flow due to the spillway, other research is used to make a rough estimation of the development of the flow. In Appendix N, these studies are discussed. The most important conclusion is that after passing through the spillway, the turbulence in the water is large but the flow velocity will decrease. All studies show that the decay of the velocity is very site specific and therefore difficult to obtain for the case of the spillway. Although, it can be concluded that the decay will take hundreds of meters. Due to the aforementioned reasons, the depth-averaged flow velocity is taken in the determination of the scour protection. The depth-averaged is the average velocity at any vertical section of a channel cross-section. The depth-averaged velocity is assumed to be equal to the uniform flow velocity. The reason for this is that the discharge remains constant at each location. The turbulence of the flow is taken into account by the use of a turbulence factor.

For the Energy Storage Lake, the governing situation for the maximum depth-averaged flow velocity is the situation in which the discharge is maximum ( $20\,200\text{ m}^3/\text{s}$ ) and the water depth is low (5 m). The width of the spillway is 858 m. This results in a depth-averaged flow velocity of  $4.75\text{ m/s}$  ( $v = \frac{Q}{B \cdot h}$ ). Further downstream the velocity decreases due to an increase in flow width. For the Tidal Lake, the governing situation is the situation in which the water depth is low (10 m) and the discharge is large ( $19\,350\text{ m}^3/\text{s}$ ). The discharge for the Tidal Lake situation is not equal to the Energy Storage Lake situation because to reach  $20\,200\text{ m}^3/\text{s}$ , the water level in the Tidal Lake should be at the maximum value, NAP +1.5 m. This means a larger water depth and therefore a lower velocity. With a large decrease in depth in the Tidal Lake, for instance 1.5 m, the decrease of the discharge is relatively small, a decrease of approximately  $1\,000\text{ m}^3/\text{s}$ . Therefore, a situation with a lower water depth in the Tidal Lake is used compared to the situation for the scour protection of the Energy Storage Lake side. The governing discharge is determined with the Bernoulli equation, similar as in Chapter 6. The maximum depth-averaged flow velocity just downstream of the spillway becomes  $2.27\text{ m/s}$ , see Appendix N. In Figure 8.4, the development of the flow is illustrated.



(a) Flow velocity development in the Energy Storage Lake

(b) Flow velocity development in the Tidal Lake

**Figure 8.4:** The flow velocity development

## 8.2.2. Design of the Scour Protection

### 8.2.2.1. Required Rock Diameters

For the scour protection on both sides of the spillway, a geometrically closed filter is designed. This consists of an armour layer of rock and multiple filter layers of rock and gravel. The diameter of the armour layer should exceed the minimum required diameter obtained by the Shields Equation. The applied rock diameter for the armour layer is obtained from the list of standard gradings. This list can be found in Appendix N.

$$d \geq \frac{K_v^2 \cdot u_c^2}{K_s \cdot \psi_c \cdot C^2} \quad (8.8)$$

where:	$d$	[m]	=	nominal diameter of the grain
	$K_v$	[-]	=	velocity/turbulence factor ( $= \frac{1+3r_{cs}}{1+3r_{cu}}$ )
	$r_{cs}$	[-]	=	vertically averaged turbulence intensity
	$r_{cu}$	[-]	=	relative turbulence intensity in uniform flow (=0.075)
	$u_c$	[m/s]	=	critical, depth-averaged, velocity in uniform flow for incipient motion
	$K_s$	[-]	=	slope factor
	$\psi_c$	[-]	=	the threshold of motion parameter
	$C$	[m <sup>0.5</sup> /s]	=	Chezy Coefficient ( $= 18 \log(12 \frac{h}{k_r})$ )

The Shields formula requires the depth-averaged flow velocity and is therefore applicable for the design of the scour protection. Another option would be the Izbash equation but this requires the flow velocity near the bed which is difficult to obtain. On the Energy Storage Lake side of the spillway, the flow is decelerating. Decelerating flow leads to large turbulence in the water which can be implemented in the Shield equation by the  $K_v$  factor. At the Tidal Lake side, the flow is accelerating and the  $K_v$  factor is zero (Schierck, 2012).

At the Energy Storage Lake side, the highest depth-averaged flow velocity is 4.75 m/s. Using Formula 8.8, leads to a required rock diameter of 0.97 m. The detailed calculation of the required diameter can be seen in Appendix N. Standard gradings are used for the design of the scour protection. More information regarding the standard gradings can be found in Appendix N. From the standard gradings, the diameter of the standard grading HM<sub>A</sub> 3-6t is sufficient for the occurring flow velocities. The nominal diameter of this standard grading is 1.18 m. The standard gradings are retrieved from Schierck (2012). Since the velocity at the outlet is 9.1 m/s, it is likely that the assumed velocity of 4.75 m/s is slightly underestimating the actual flow velocity. Therefore, the first part of the scour protection will be cast into colloidal concrete. This improves the resistance against the flow velocity and can therefore resist higher flow velocities than the assumed 4.75 m/s (Rijkswaterstaat, 2021).

Further downstream of the spillway, both the turbulence and the velocity are decreasing. The latter is decreasing due to the horizontal spreading of the flow. Therefore, the required rock diameter becomes smaller

further downstream of the spillway. In the design of the scour protection, three different parts are taken into consideration. In the first part, 150 m downstream of the spillway, the turbulence is fully present. In the second part, 150 up to 250 m downstream of the spillway, the turbulence is still present but the velocity is decreased. In the third part, more than 250 m downstream, the flow is fully uniform without turbulence. These three parts are based on the assumptions that the turbulence is decreasing and from 150 m distance equal to zero and that the flow will return to a fully uniform flow after 250 m. In further research, these assumptions must be validated. Each part requires a different armour layer. The calculation of the required diameter of the armour layer can be found in Appendix N and the used armour layers can be found in Table 8.6. The thickness of the layers is based on the minimum required thickness, twice the nominal diameter. The required thickness due to tolerances is not taken into account.

As mentioned before, below each armour layer, multiple filter layers can be found. These filter layers are also shown in Table 8.6. The determination of the filter layers is based on the following requirements (Schiereck, 2012):

$$\text{Stability: } \frac{d_{15,F}}{d_{85,B}} < 5, \quad \text{Internal Stability: } \frac{d_{85}}{d_{15}} < 12 - 15, \quad \text{Permeability: } \frac{d_{15,F}}{d_{15,B}} > 5$$

The first requirement prevents movement of the larger grains of the base layer. The second requirement prevents pressure build-up and guarantees the stability of the filter layer as a whole. The third requirement prevents the movement of the smaller grains in the base layer.

Scour Protection x < 150 m						
Layer	Type	Standard Grading	d15 [mm]	dn50 [mm]	d85 [mm]	Thickness Layer [m]
1	Rock	HMa 3-6t	1120	1180	1300	2.4
2	Rock	LMA 10-60	220	240	330	0.5
3	Rock	CP 45/125	42	64	120	0.2
4	Gravel	-	2	4	10	0.2
5	Sand	-	0.3	0.35	0.6	-

Scour Protection between x = 150 m and x = 250 m						
Layer	Type	Standard Grading	d15 [mm]	dn50 [mm]	d85 [mm]	Thickness Layer [m]
1	Rock	HMA 1-6t	880	900	1170	1.4
2	Rock	LMA 10-60	220	240	330	0.2
3	Rock	CP 45/125	42	64	120	0.2
4	Gravel	-	2	4	10	0.2
5	Sand	-	0.3	0.35	0.6	-

Scour Protection from x > 250 m						
Layer	Type	Standard Grading	d15 [mm]	dn50 [mm]	d85 [mm]	Thickness Layer [m]
1	Rock	LMA 40-200	320	340	460	0.7
2	Rock	CP 45/125	42	64	120	0.2
3	Gravel	-	2	4	10	0.2
4	Sand	-	0.3	0.35	0.6	-

**Table 8.6:** The scour protection of the Energy Storage Lake at a certain distance x from the spillway

For the Tidal Lake, the same approach is used. The governing flow velocity just upstream of the spillway is 2.27 m/s. Applying the Shields equation, Formula 8.8, leads to a required diameter of 0.03 m. The required diameter is small compared to the Energy Storage Lake side because the water depth in the Tidal Lake is larger and the velocity is lower. The standard grading CP 45/125 will be used as an armour layer with a nominal diameter of 0.064 m. Due to the small diameter of the armour layer, only one filter layer is required, see Table 8.7. This filter layer also fulfils the previously mentioned stability requirements.

Scour Protection Tidal Lake						
Layer	Type	Standard Grading	d15 [mm]	dn50 [mm]	d85 [mm]	Thickness Layer [m]
1	Rock	CP 45/125	42	64	120	0.2
2	Gravel	-	2	7	15	0.2
3	Sand	-	0.3	0.35	0.6	-

**Table 8.7:** The scour protection of the Tidal Lake

### 8.2.2.2. The Required Protection Length

The required length of the scour protection depends on the depth of the scour hole and how the soil is packed.

$$L_p = \gamma_s \cdot h_s \cdot \frac{\beta_{stab} - \beta_{hole}}{2} \quad (8.9)$$

where:  $L_p$  [m] = protection length  
 $\gamma_s$  [-] = safety factor (= 1.1)  
 $h_s$  [m] = scour hole depth  
 $\beta_{stab}$  [-] = slope after stability is lost  
 $\beta_{hole}$  [-] = slope angle of the scour hole

For the first estimation of the length of the protection, the soil is assumed to be loosely packed. The corresponding slope angle for loosely packed soil is 1:15 m. The slope angle of the scour hole itself is assumed to be approximately 1:2 m (Schierck, 2012). For the scour depth, the equilibrium scour depth is used which is calculated by:

$$h_{se} = \frac{0.5\alpha\bar{u} - \bar{u}_c}{\bar{u}_c} \cdot h_0 \quad (8.10)$$

where:  $h_{se}$  [m] = the scour depth  
 $\alpha$  [-] = amplification factor for the velocity  
 $\bar{u}$  [m/s] = the flow velocity  
 $\bar{u}_c$  [m/s] = the critical flow velocity of the bed material  
 $h_0$  [m] = the water depth

The occurrence of the flow velocities that are used for the calculation of the armour layer dimensions are only present for a short period. The development of a scour hole requires sufficient time and if the velocities only occur for a short period, a couple of hours, the equilibrium depth will not be reached. Using the maximum velocities for the calculation of the equilibrium depth will therefore lead to an overestimation. To prevent this on the Energy Storage Lake Side, a mean value for the flow velocity and water depth is taken. These values are calculated in Appendix N and depending on the development of the discharge of the spillway and the outflow due to the pumping station. The water level in the Energy Storage Lake will increase due to the difference in the discharge of the spillway and the pumping station. Consequently, the discharge and flow velocity will decrease. The obtained mean flow velocity and depth are respectively 1.65 m/s and 12.8 m. According to Formula 8.10, this results in an equilibrium scour depth of 53 m. To prevent stability issues due to scour, a scour protection with a length of 380 m is required using Formula 8.9.

For the Tidal Lake side, using the average values is more difficult. The water depth of the Tidal Lake is mainly depending on the inflow from the Rhine and the Meuse and considering this requires an extensive model. Therefore, the maximum velocity is used to determine the minimum required length. With Formula 8.10, an equilibrium scour depth of 62 m is found and with Formula 8.9, a minimum required length of 440 m is obtained. It must be taken into account that for the Tidal Lake side, the required length is a conservative value due to the overestimation of the scour depth, which is caused by the overestimating of the velocities.

### 8.2.2.3. The Design of the Scour Protection

In the previous section, the required stone diameter and protection length were determined. An overview of all the layers and the length of the protection can be seen in Figure 8.5. In Section 8.2.3, measures that can be considered to improve the design of the scour protection.

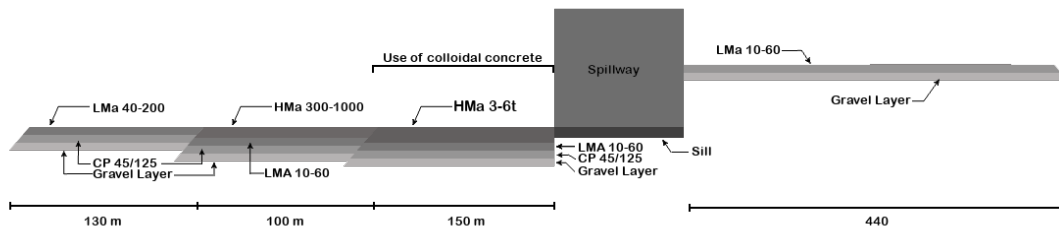


Figure 8.5: Scour protection design

### 8.2.3. Potential Adjustments of the Scour Protection

The design of the scour protection shown in Section 8.2.2.3 is a conceptual design to show a possible solution to the scour problem. Some measures can be considered to improve the design.

- **Use of geotextile**

At the locations with large turbulence and a flow velocity of 4.7 m/s, the geometrically closed filter has a large thickness. To decrease the thickness of the geometrically closed filter a geotextile can be used to replace some layers. This leads to a decrease in the total thickness of the scour protection. A decrease in total thickness leads to a decrease in the amount of soil that has to be dredged.

- **Use of concrete floor**

A second option is the use of a concrete floor at the location where the thickness of the geometrically closed filter is large. For instance at the location of large turbulence. In the Energy Storage Lake the thickness of the geometrically closed filter is exceeding 3 m. The thickness of a concrete floor can be assumed to be below 3 m. Again this results in less soil being dredged. Depending on the prices of dredging, the concrete floor and the geometrically filter it can be cost saving to go for the concrete floor.

- **Increase the number of outlets**

By increasing the number of outlets, the gates can be partly closed during extreme conditions without failing to reach the maximum capacity. By partly closing the gates, more friction is created in the spillway which decreases the flow velocity. A lower flow velocity requires less scour protection. Besides a lower outflow velocity, the width of the spillway is increased. This results in a lower uniform flow velocity and therefore a decrease in the scour depth. A decrease in scour depth can result in a decrease in protection length.

- **Increase the space between outlets**

By increasing the space between the outlets, the impact of the horizontal spreading is bigger at the beginning. Due to the small distance between the outlets, 1 m, the horizontal spreading is quick, within 10 meters, limited to the spreading at the outer edges of the flow. By increasing the space between the outlets, the spreading can also take place between the outlets.



# 9

## Discussion, Conceptual Design and Recommendations

### 9.1. Discussion

Several considerations have been made during the design process which had an impact on the conceptual design. In this section, the considerations with a large contribution to the results of the design process are discussed. The following discussion points are in line with the chapters of this report.

#### **Geo-Technical Boundary Conditions**

The foundation of the concept Caisson is a shallow foundation. The feasibility of a shallow foundation mainly depends on the soil conditions. The governing soil conditions for the design of the shallow foundation are provided by three cone penetration tests nearby the location of the spillway. All three tests illustrate that the soil near the spillway mainly consists of sand, which is beneficial for a structure on a shallow foundation. However, the number of available CPTs is low and the CPTs are not at the exact location of the spillway. This results in some uncertainties regarding the soil conditions at the exact location of the spillway.

#### **Water levels in the Tidal Lake**

One of the key parameters that influences the outcome of the design is the water level in the Tidal Lake. The idea of the Delta21 concept is that the storm surge barrier will close when the water level is at NAP + 1.5 m. This is the moment that the maximum discharge capacity must be achieved. For the stability of the structure, a water level of NAP + 2 m is used (excluding the surcharge uncertainties of *Handreiking ontwerpen met overstroomingskansen 2017*). This level can occur if the Maeslantkering fails to close. In both situations, the water level at Dordrecht is not exceeding NAP + 2.5 m. If the water level in the Tidal Lake changes at which the barrier closes (+1.5m NAP) or when the Maeslantkering fails (+2m NAP), the design would have to be changed. The first can lead to a change in discharge capacity. As a result of this, the channels need to be redesigned. The second point will lead to an increase in the main dimensions of the caisson. This is to ensure the stability of the caisson and keeping the overtopping within the boundaries.

#### **The cost estimation**

The selection of the most optimal concept is based on a multi-criteria analysis and a cost estimation. In the cost estimation, the vast majority of the costs are the concrete works and the construction of the concrete pipes. The construction of the concrete pipes is 31% and 48% of the total cost in respectively the concept Siphon and Underflow. If the cost of the construction of the pipes changes, the effect on the total cost of the two concepts is noticeable. As a result of this, the two concepts can become more beneficial. Another assumption that is done in the cost estimation is the cost of the gates. Since the gates are not treated in much difference, there is an uncertainty in the price of the gates. However, the number of gates in the concepts with

the higher costs is higher. Therefore, if the price of the gates increases, it will potentially not have a different impact on the selection procedure. In the cost estimation, only a limited number of items is taken into account. This can also result in an underestimation of the cost of a certain concept.

### **Dependence on the pumping discharge**

With the selection of a closed channel spillway, the discharge of the spillway becomes related to the discharge of the pumping station. Since the discharge of the spillway is depending on the water level difference in the lakes combined with the energy loss in the spillway, the pumping station will affect the discharge capacity of the spillway. In the present plans of the Delta21 concept, the maximum capacity of the pumping station is half the maximum capacity of the spillway. As a result of this, the water level in the Energy Storage Lake increases and the discharge of the spillway decreases. The influence of the water level in the Energy Storage Lake is bigger than the water level of the Tidal Lake. Due to the difference in discharge between the pumping station and the spillway, the Energy Storage Lake will be filled after 15 to 20 hours. From this point, the discharge of the spillway is limited to the discharge of the pumping station. This means that the spillway can only discharge at a rate of 10 000 m<sup>3</sup>/s. With the choice for a closed channel spillway, the effectiveness of the spillway is both depending on the water levels on both sides as well as the difference in discharge capacity between the spillway and the pumping station.

### **Strength Verification**

The strength verification for the concept Caisson is based on preliminary design calculations. The bending moments in the elements are based on the theory of elasticity, in which all elements are modelled as single plates. In the calculation of the bending moment, the most unfavourable support is considered. This can lead to an overestimation of the bending moment. By modelling the elements as single plates, the coherence between the elements is not taken into consideration. This results in bending moments not being passed on between the different elements. Neglecting this effect influences the outcome of the bending moments. Therefore there is some uncertainty in the calculation of the bending moments in the elements. With the use of the preliminary design equations, the normal forces within the elements are also neglected. This results in a less accurate determination of the capacity of the elements.

### **Scour Protection Design**

The scour protection is designed using the Shields equation. The Shields equation is based on the shear stress. Using the Chezy relation, the Shields equation and the depth-averaged velocity become related. The depth-averaged flow velocity is calculated without the use of extensive models. For the design of the scour protection, the uniform flow velocity is considered as the depth-averaged flow velocity. The reason behind this is that the discharge remains constant over the flow. However, when the water flows out of the spillway, there is a difference in flow velocity between the outflowing water and the water in the lake. Due to this, the flow velocity from water that is originating from the spillway is decelerating. This leads to turbulence upstream of the spillway. A turbulence factor is used to take into account the effects of the decelerating flow. This is a simplified method to work with a complex situation. The result of the simplified method is less accurate than the results of an extensive model. Comparing the design of the scour protection with the other parts of the design process in this thesis, it can be concluded that the scour design is less accurate than the other parts. The main reason for this is the complexity of the flow velocities and turbulence. For the design of the scour protection, this lower accuracy can mean that the flow velocities are underestimated. If this is the case, the rock size in the design will increase or the addition of concrete between the rocks is necessary.

## 9.2. Conceptual Design of the Spillway

Four different concepts are discussed in this report. These concepts are verified on the requirements and evaluated by a cost-value analysis. After the evaluation process, it is concluded that the concept Caisson is the optimal concept. This concept owes its name to the caissons that are used. The conceptual design of the concept Caisson can be seen in Figure 9.1 and 9.2.

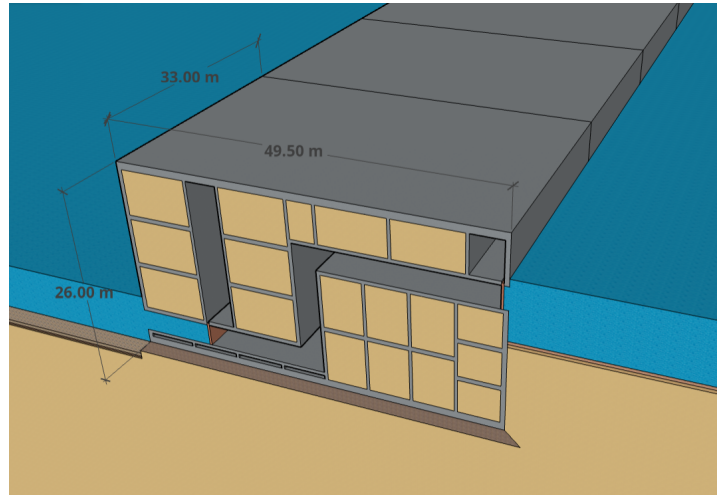


**Figure 9.1:** 3D View of the concept Caisson

The conceptual design of the spillway consists of 26 caissons with a height of 26 m, a width of 49.5 m and a length of 33 m. The bottom of the caisson is placed at NAP - 22.5 m and the top is at NAP + 3.5 m. The top at NAP + 3.5 m is required to prevent significant overtopping. The caisson will be constructed on a sill that consists of gravel and sand to improve the stability of the structure. The total length of the spillway is 858 m. Each caisson consists of 3 channels, this results in a total of 78 channels over the total length of the spillway. From these 78 channels, only 74 are used during the opening of the spillway. The remaining four channels are required to take on the function of channels that are out of use due to maintenance or failure.

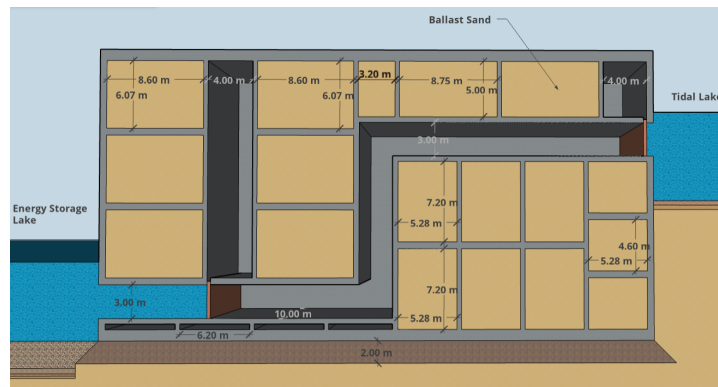


**Figure 9.2:** Front view of the concept Caisson

The channels are rectangular shaped and have a width of 10 m and a height of 3 m. The maximum discharge is 20 200 m<sup>3</sup>/s and is achieved when the Tidal Lake is at NAP + 1.5 m and the Energy Storage Lake at NAP - 17.5 m. This water level difference occurs when the storm surge barrier of Delta21 is closed. This happens when the water level in the Tidal Lake is at NAP + 1.5 m. Before this situation occurs, the Energy Storage Lake has to be emptied with the use of the pumping station. In this situation, the discharge of a single outlet is equal to 273 m<sup>3</sup>/s. With a flow area of 30 m<sup>2</sup>, this results in a maximum flow velocity of 9.1 m/s. When the water level difference is decreasing, the discharge capacity of the spillway will decrease as well.

The caissons are constructed in a construction dock. This dock is built in the Energy Storage Lake. After the caissons are constructed, they are transported to their final location. At this location, the caissons are immersed and afterwards filled with sand. This sand can be retrieved from the dredging works that are required.

The costs of this concept are estimated to be approximately €474.320.000,-. These cost included the concrete works, gates, construction dock, sill, seepage screen, OTA0-process and soil works.

Each caisson is divided into multiple compartments. These compartments are filled with ballast sand, which is obtained from the dredging works, to establish a stable situation during the operational phase of the spillway. The thickness of the concrete elements of the caisson range from 400 mm up to 600 mm. This depends on the location of the element and the governing loads. The thickness of each element can be seen in Figure 9.3. All the elements are reinforced with steel reinforcement bars ranging from  $\varnothing$  20 mm up to  $\varnothing$  32 mm.

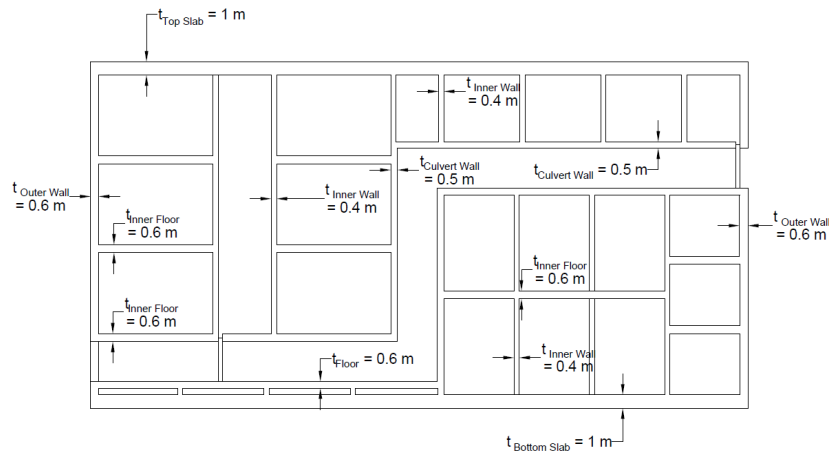


**Figure 9.3:** Overview of the thickness of the elements

When the spillway is operational, sand particles will be moving due to the powerful discharge that occurs. Firstly, sand particles will be removed in front of the spillway in the Tidal Lake and dropped in the Energy Storage Lake at a certain distance from the spillway. Secondly, behind the spillway, in the Energy Storage Lake, sand particles will start to move as well and move away from the spillway. This results in a scour hole behind the spillway. To prevent stability problems for the spillway due to scour, a geometrically closed filter consisting of rock and gravel layers is required. The largest rock diameter that is required in the armour layer of the Energy Storage Lake is 0.97 m and for the Tidal Lake this is 0.06 m. The length of the protection is 379 m and 436 m for respectively the Energy Storage Lake and the Tidal Lake. The design of the scour protection is shown in Figure 9.4.

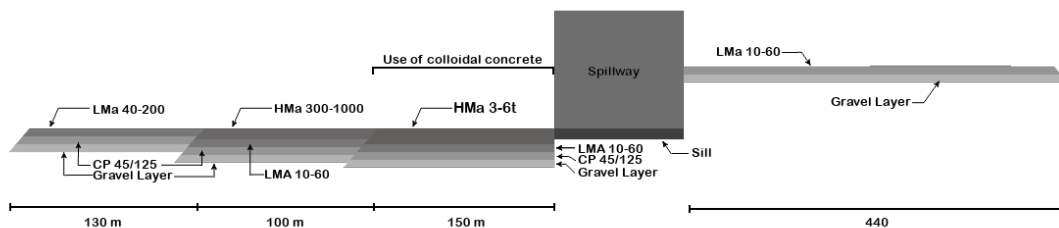


**Figure 9.4:** Conceptual design of the scour protection

During the design process, the following conclusions have been made:

- The water level in the Tidal Lake is the most important parameter in the design of the spillway. This water level affects the main requirement, the discharge capacity of the spillway, the most.

- With gravitational flow, the discharge capacity of 20 000 m<sup>3</sup>/s cannot be guaranteed continuously. This statement holds for all the concepts analysed in this research. Only the addition of pumps in the spillway can guarantee the required discharge capacity continuously.
- In pressurised flow, the discharge depends on the water level difference between both lakes. The pumping station is affecting the water level in the Energy Storage Lake. Therefore, the capacity of the spillway partly depends on the capacity of the pumping station.
- Implementing the design of the scour protection in an early stage of the design process is essential because the large flow velocities just behind the spillway can not be mitigated. Measures have to be taken to prevent failure of stability due to scour.
- In the concepts Siphon and Underflow, the construction of the concrete pipes lead to a significant increase in construction costs. The construction of the pipes is respectively 51% and 34 % of the total cost of the concepts Siphon and Underflow.
- Concept Siphon is only feasible in combination with a vacuum pump.
- Making the flow in the concept Caisson more efficient leads to larger flow velocities and a more expensive scour protection. Therefore, making the flow more efficient is not efficient for the overall design.

### 9.3. Recommendations

Based on this research, the following recommendations for further research are advised:

- **Investigation of the soil conditions:**  
The number of available CPTs in the region of the Delta21 area is scarce, while the conditions of the soil are crucial for the shallow foundation. Therefore it is recommended to execute more CPT at the location of the spillway. By doing so, more information regarding the soil characteristics is retrieved and a more accurate overview of the soil can be obtained.
- **Increasing the discharge capacity of the pumping station:**  
With the discharge requirement of 20 000 m<sup>3</sup>/s for the spillway, the Energy Storage Lake will fill in approximately 15-20 hours. The reason for this is the lower capacity of the pumping station. It could be interesting to investigate the option in which the pumping capacity is increased. This can improve the total effectiveness of the Energy Storage Lake and the spillway because the increase in the water level in the Energy Storage Lake will be slower.
- **Strength Verification:**  
In further research, it is recommended to use computer models to examine the bending moments, shear forces and normal forces within the elements. This will lead to more accurate results.
- **Design of the Gates:**  
The conduit in the conceptual design of the spillway is closed off by two gates. For the implementation of the gates in the caisson, a gate room is designed. In a detailed design, it should be validated if the room has sufficient space to implement the gates.
- **Research on the flow development:**  
The design of the scour protection up and downstream of the spillway depends on the flow velocity. The flow velocities are complex to determine without the use of 2D or 3D numerical models. Therefore additional research has to be performed to obtain more accurate results on the development of the flow velocities and to realise a detailed design for the scour protection.
- **Implementation of the spillway in the Delta21 concept:**  
The main aim of this thesis is to come up with a conceptual design of the spillway of the Delta21 concept. During this thesis, the focus is on the spillway as an individual structure. Due to this, the cooperation between the spillway and the other components is not considered. In further research, the interaction between the spillway and other components has to be investigated.

# **Appendices**

# A

## Stakeholders

In this appendix a stakeholder matrix can be found, Table A.1, and the remainder of the stakeholders are discussed.

### **A.0.1. Primary Stakeholders**

In this section the primary stakeholders are discussed. The primary stakeholders influence the project directly.

#### **Ministry of Agriculture, Nature and Food Quality**

The Ministry of Agriculture, Nature and Food Quality are responsible for the protection and conservation of Natura 2000 areas (Government of The Netherlands, 2020c). These areas are protected nature areas on European scale. One of the main goals of Natura 2000 is to protect the biodiversity in a specific area. The location of Delta21 is within a Natura 2000 area and needs to fulfil multiple requirements on protection and restoration of nature. The project has a negative influence on the nature at the location at which is constructed but at the same time it has a positive influence on the surrounding nature. The biodiversity in the Haringvliet basin will increase and the water quality will improve as well. The ministry is part of the Dutch government and therefore very powerful. Due to the importance of the Natura 2000 areas, the interest of the ministry is high.

#### **Ministry of Economic Affairs and Climate Policy**

The Ministry of Economic Affairs and Climate Policy is involved in this project due to the opportunities with sustainable energies and because of the restoration of the nature in the Haringvliet basin. The ministry is trying to enhance their leading position in energy and invest in a more sustainable Netherlands (Government of The Netherlands, 2020a). The opportunities of sustainable energy can help the government to reach the national climate agreement goals. The main goal of this agreement is to decrease the CO<sub>2</sub> emissions by 49% compared to 1990. To achieve the desired decrease in CO<sub>2</sub> emissions, the percentage of sustainable energy needs to increase to 70% of the total energy in 2030 and 100% in 2050 (Rijksoverheid, 2019). The power and interest of this ministry is equal to the other ministries, very high.

#### **Province of South-Holland**

According to van Heel (2019), the board of the province is positive towards the Delta21 concept. The Province of South Holland is the second level of government authority. They are responsible for the protection of the environment and spatial planning in their province. Delta21 is located in the province of South Holland and most of the effects will be noticeable in their province, therefore their interest are very high. If Delta21 is implemented, an increase in dike height is not necessary anymore. Increasing the dike height also requires an increase in width of the dike, this can now be used for other purposes. Although the province is the second level, the power is still high.

## **Province of North Brabant**

Just like the Province of South Holland, the Province of North Brabant is the second level of government authority. The project is located outside this province but the effects are noticeable in this area. A decrease in the water levels at the mouth of the river, leads also to lower water level in the higher parts of the river. Due to this, the increase of the dike height will not be needed here as well.

## **Port of Rotterdam**

The Port of Rotterdam is very important for the import and export in The Netherlands. therefore the growth of the port is not only important for the port itself but also for the Dutch economy. The location of Delta21 is south of the Maasvlakte II. At the moment there are no plans for an expansion of the port but in the future possible plans can be influenced by the location of Delta21. Due to the importance of the port for the Dutch economy (Kuipers, 2018), the power of the port is high. The interest of the Port is also high because of the location of Delta21.

### **A.0.2. Secondary Stakeholders**

In this section the secondary stakeholders are discussed. The secondary stakeholders do not influence the project directly.

## **Municipality of Rotterdam and Dordrecht**

The municipalities of Rotterdam and Dordrecht are the biggest municipalities that will be affected by Delta21. Rotterdam will be affected by the discharge in the Meuse and Dordrecht will be affected due to the water levels in the city. Dordrecht has some major problems with flooding in the city centre due to high water levels (Lavooij and Berke, 2018c). With the implementation of Delta21 these problems will occur with less frequency. Due to the increase of safety for both Rotterdam and Dordrecht their development can continue because money reserved for dike increase can be spend on another project. The interest of Rotterdam and Dordrecht is respectively high and very high. The difference is due to the frequency of flooding problems in the cities. The power of the municipalities is medium because it is the third level of government authority.

## **Water Authority Hollandse Delta**

The water authority Hollandse Delta is affected directly by the project because the water boards are responsible for the water quality in their area. Besides the water quality they are also responsible for dikes and secondary defence structures (Waterschap Hollandse Delta, 2020). Delta21 will have a positive effect on the work done by the water board. This is due to the increasing water quality by opening the Haringvliet sluices. Due to the increase of water safety by the construction of Delta21, the water safety around the dikes that are part of the water board will increase too.

## **Water Authority Delfland**

The water authority Delfland is affected directly by the project because the inflow of fresh water in their system depends on the fresh water from the Haringvliet basin. Besides this, the increase in flood protection will lead to less increasing of dike heights in their area.

## **Water Authority Schieland and the Krimperwaard**

The water authority Schieland and the Krimperwaard is also affected by the increase of the flood protection. The same as for the other authorities mentioned, an increase of flood protection leads to less improvements for the current flood defences.



---

## **Evides**

Evides is responsible for the drinking water in South Holland. Their inlets for fresh water are partly depending on the fresh water coming from the Haringvliet. If the saltwater intrusion increases, the guarantee of freshwater decreases. For Evides this means that their inlets need to be removed and relocated to ensure the inflow of fresh water. Because the inflow from the Haringvliet is important for Evides, their interest in this project is high. Relocating their inlets is not very difficult so for this reason the power of Evides is Medium.

## **TenneT**

TenneT is responsible for the nation electricity transmission (Lavooij and Berke, 2018a). With one of the main goals of Delta21 being the generation of sustainable energy, the role of TenneT is important. Their interest and power in this project are medium. They will be involved during the project because they have the knowledge that is required.

## **Zuid Hollands Landschap and Droomfonds Project**

Both Zuid Hollands Landschap and the Droomfonds Project have the same goal, protecting the nature in the Haringvliet basin. The difference between the two is that Zuid Holland Landschap is involved in all the nature and environment of South Holland and that Droomfonds is only focused on the Haringvliet. Droomfonds consist of multiple environmental and animal organisations which all are trying to improve the Haringvliet area. The interest of these groups is medium to high but because their power is low, their role in this project is also low.

## **Other Municipalities**

The other municipalities that are involved in the project are mentioned in Table A. These municipalities are close to the Delta21 project side. These municipalities are secondary stakeholders because they are not directly affected by the project. The reason for this is that these municipalities are not responsible for the flood protection of the Haringvliet and only responsible for the protection of their cities. Although their responsibility stops at the border of their cities, the flood protection of their city will increase by Delta21.

## **Citizens**

The citizens are also a secondary stakeholder. They are not directly affected in their daily life by Delta21. At the end they will be safer due to the improvements but that is not something they will notice. Maybe for some citizens it will create a safer living environment which will lead to a happier life.

Stakeholder	Key, Primary or Secondary	Involvement by Subject	Interest	Power	Point of View	Effect on stakeholder
Ministry of Infrastructure and Water Management	Key	Client	Very High	Very High	Responsible for policy on flood protection	An increase in flood protection in the Delta area
Rijkswaterstaat	Key	Client	Very High	Very High	Responsible for construction and maintenance of flood defence structures	New structures to maintain, increase in safety, cost of project can become high
Ministry of Agriculture, Nature and Food Quality	Primary	Environment	Very High	Very High	Responsible for protection of Natura 2000 area	Natura 2000 area is removed, improvement are made in the environment in the Haringvliet basin
Ministry of Economic Affairs and Climate Policy	Primary	Energy and Environment	Very High	Very High	Responsible for policy on Energy and Climate	New possibilities of generating sustainable energy to reach Paris agreement goals, restoration of nature in Haringvliet Area
Province South-Holland	Primary	Spatial planning and Environmental protection	Very High	High	Responsible for protection of environment in their Province and spatial planning of their province	More room for spatial planning due to no increase in dike height, Better flood protection in province
Province North Brabant	Primary	Spatial planning and Environmental protection	High	High	Responsible for protection of environment in their Province and spatial planning of their province	More room for spatial planning due to no increase in dike height, Better flood protection in province
Municipality of Rotterdam	Primary	Urban Development	High	Medium	Responsible for Development of Rotterdam and flood protection	Development of Rotterdam can continue in a safer environment due to increase of water safety
Municipality of Dordrecht	Primary	Urban Development	Very High	Medium	Responsible for Development of Dordrecht and flood protection	Development of Dordrecht can continue in a safer environment due to increase of water safety
Water Authority Hollandse Delta	Primary	Environment and Flood protection	High	Medium	Maintenance of dikes and dams, Water level and quality control	More to maintain and increase of water quality of Haringvliet basin. Easier to manage water levels.
Water Authority Delfland	Primary	Environment and Flood protection	High	Medium	Maintenance of dikes and dams, Water level and quality control	Dikes in area do not need increase of retaining height, new structures to maintain, increase in water quality
Water Authority Schieland Krimpervwaard	Primary	Environment and Flood protection	High	Medium	Maintenance of dikes and dams, Water level and quality control	Dikes in area do not need increase of retaining height
Port of Rotterdam	Primary	Economics and Growth	High	High	Keep their dominant position as Port in the World	Expanding in south direction (South of Maasvlakte II) not possible. Possibilities with sustainable energy of Delta21
Evides	Primary	Fresh water inlets at Haringvliet	High	Medium	Guaranteed inflow of fresh water	Increase of saltwater intrusion in Haringvliet. Possible movement of inlet further land inwards of the basin
Tennet	Primary	Energy	Medium	Medium	Responsible for national electricity transmission	New opportunities in sustainable energy in Rotterdam area
Zuid-Holland Landschap	Primary	Environment	Medium	Low	Protection and restoration of Haringvliet area	Restoration of nature in Haringvliet area
Droomfonds Project <sup>1</sup>	Primary	Environment	Medium	Low	Protection and restoration of Haringvliet area	Restoration of nature in Haringvliet area
Other Municipalities <sup>2</sup>	Secondary	Urban Development	Low	Low	Responsible for Development and flood protection of their cities	Increase of flood protection in their municipalities
Citizens	Secondary	Safety	Low	Very Low	Working and living in safe environment	Increase of flood protection in their work and living area

Table A.1: The Stakeholder Matrix

<sup>1</sup> Droomfonds Project consist of the following parties: WNF, Natuurmonumenten, ARK Natuurontwikkeling, Vogelbescherming, Sportvisserij Nederland, Staatsbosbeheer

<sup>2</sup> Municipalities of Goeree-Overflakkee, Westvoorne, Hellevoetsluis, Nissewaard, Hoeksche Waard and Brielle

# B

## Geotechnical Soil Profile

At the location of Delta21 project side, multiple cone penetration test have been performed in the past. The bed level of the Energy Storage Lake is planned at NAP - 22.5 m. Therefore it is important that only cone penetration tests with a depth exceeding the 22.5 m are examined. Most of the test that are performed in this area only reach to a depth of 20 m and are therefore not relevant. For the location of the spillway this leads to only three relevant cone penetration tests. These tests are done at sufficient depth and close to the possible location of the spillway.

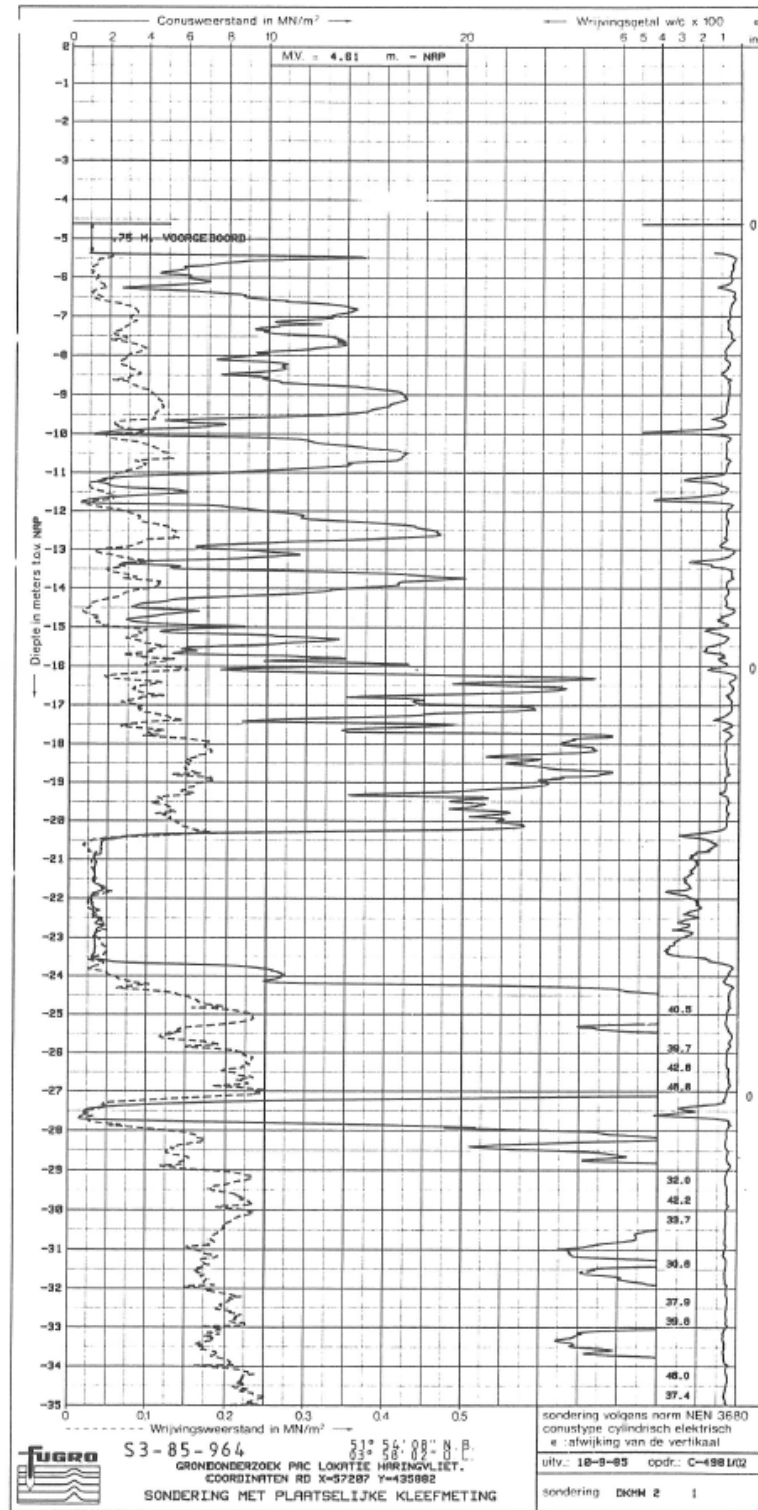
- CTP 1: S36H00033\_00
- CTP 2: S36H00034\_00
- CTP 3: S36H00035\_00

The exact location of these test can be seen in Figure B.1 and in Section B.1 to B.3 the results are shown. In Section B.4, the cone penetration tests are converted to soil layers.



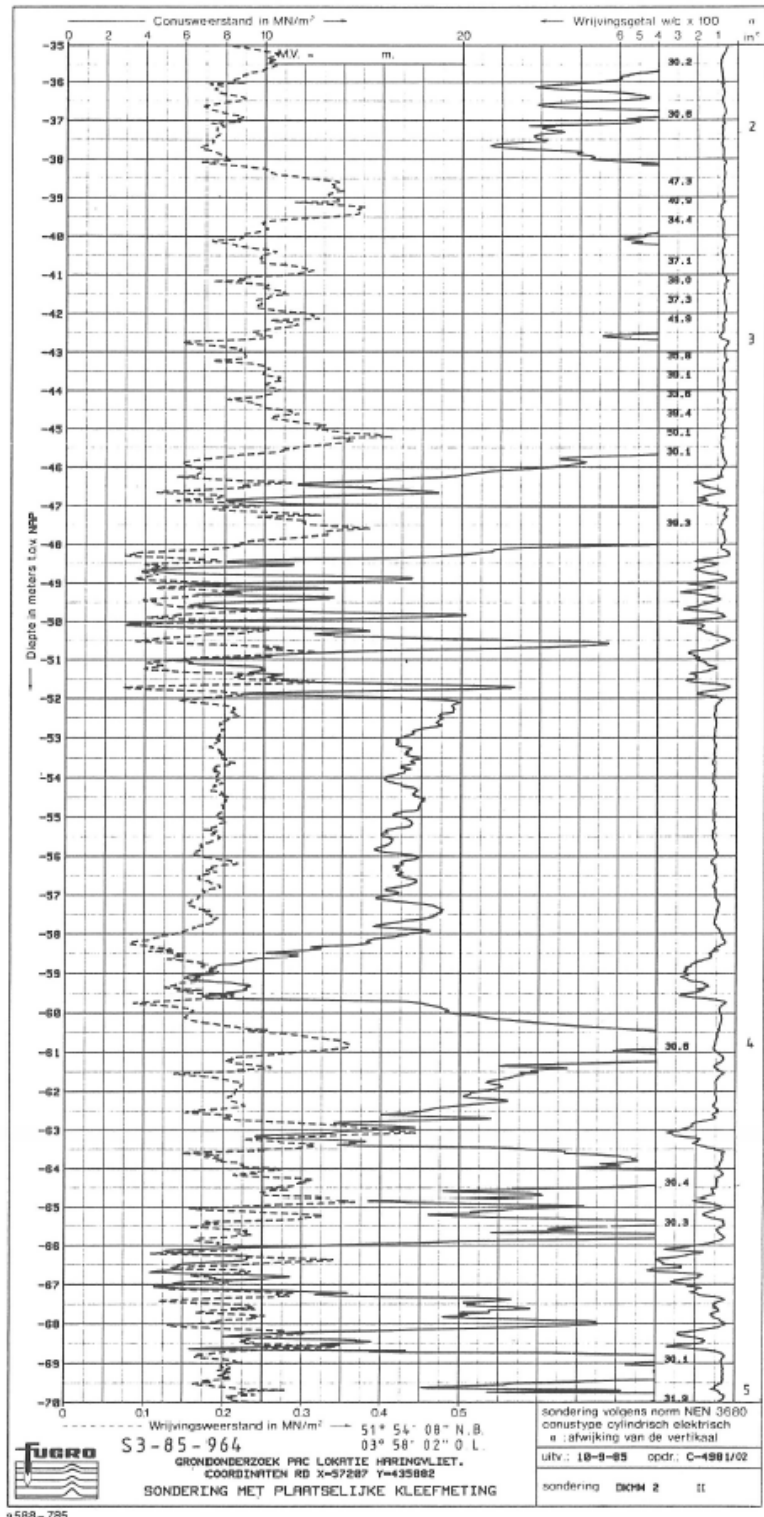
Figure B.1: Locations of the Cone Penetration Test

**B.1. CPT 1: S36H00033\_00**

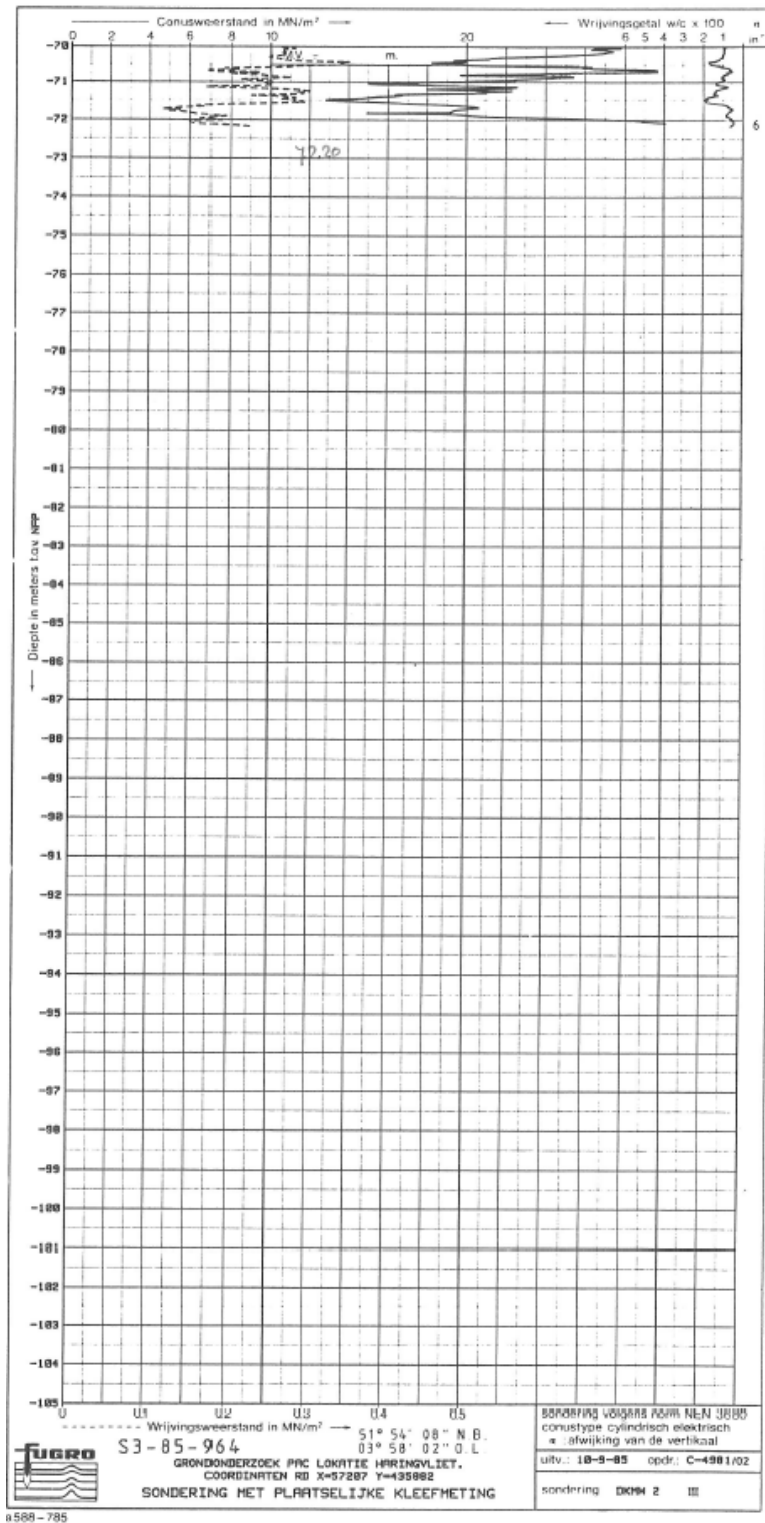


s588-785

(a)



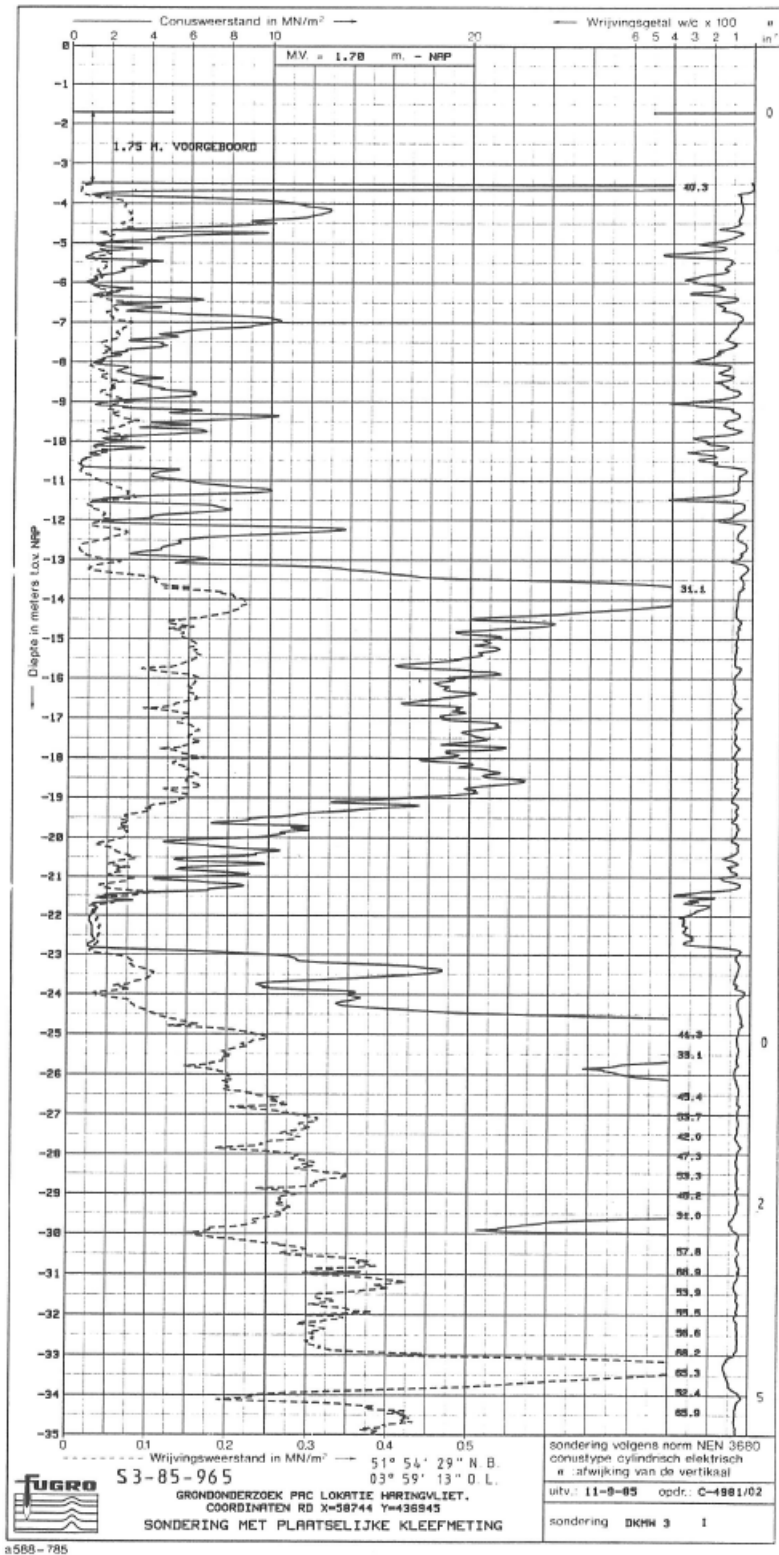
(b)



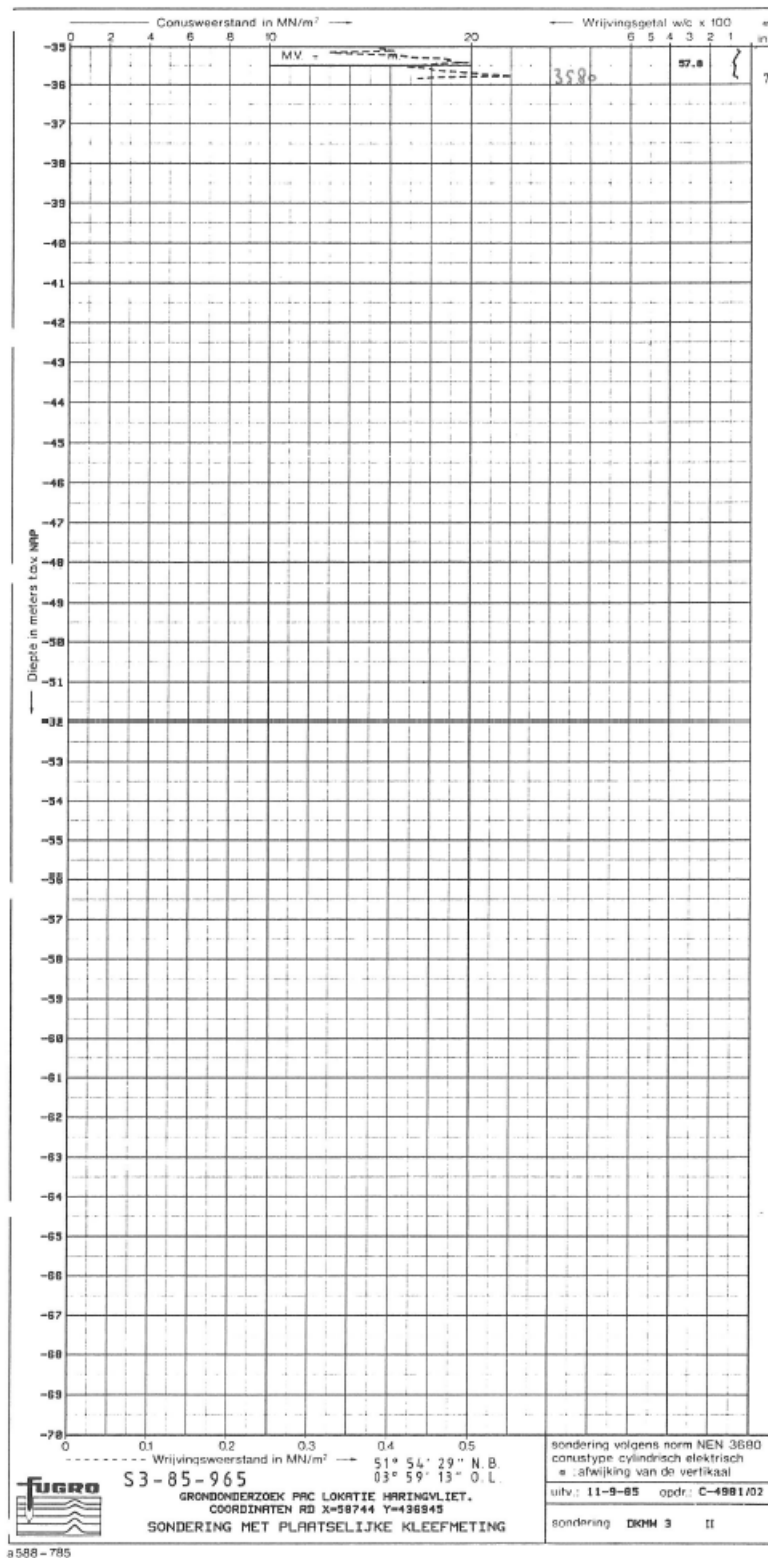
(c)

Figure B.2: CPT S36H00033\_00 (Fugro, 2020)

**B.2. CPT 2: S36H00034\_00**



(a)

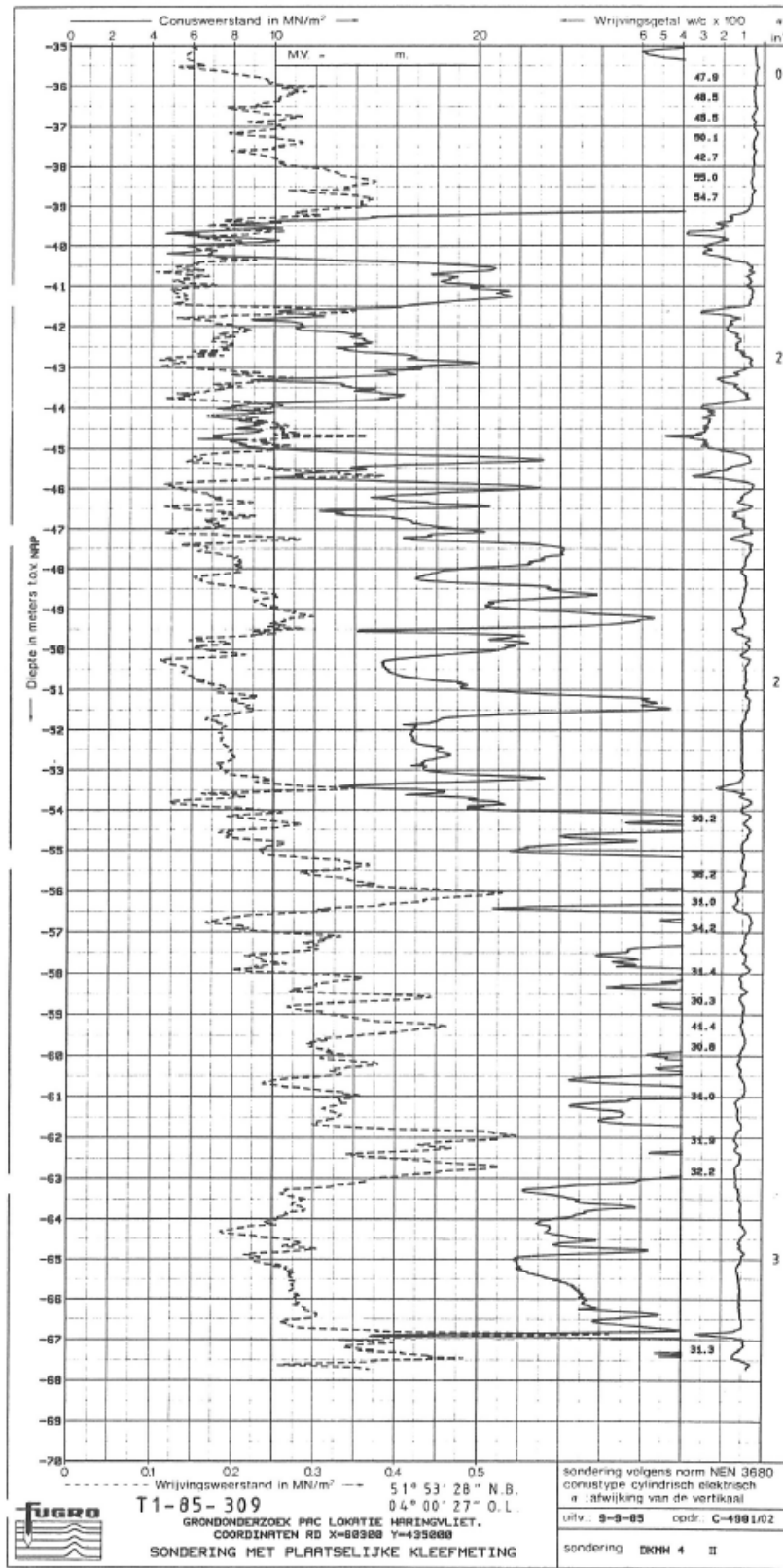


(b)

Figure B.3: CPT S36H00034\_00 (Fugro, 2020)







a588-785

(d)

Figure B.3: CPT S36H00035\_00 (Fugro, 2020)

### B.4. Soil Profiles

The cone penetration show the friction number of the soil at a certain depth. These friction numbers show which type of soil is present at a certain depth. By using this information the soil profiles are created, see Figure B.4.

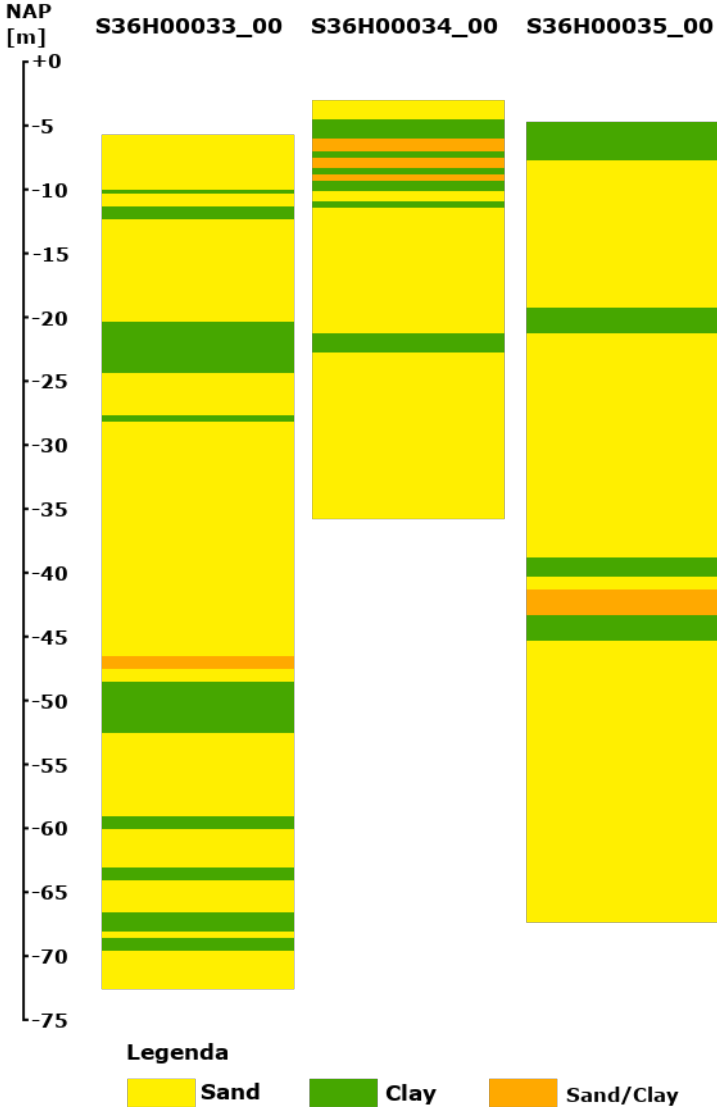


Figure B.4: Soil profiles at the Delta21 location

# C

## Wind Calculations

In this appendix, the design wind velocity is calculated and the occurrence of the wind is discussed. The design wind velocity is required for the calculation of the wind waves in both lakes and the wind set-up and set down.

### C.1. Conversion of Design Wind Velocity

For the design wind velocity, the wind velocity with a return period of once every 1 000 years is used. The reason for this is that the safety standard of the spillway is 1:1000 per year, see Section 3.6. This is 170 km/h (= 47.2 m/s) at 2 km height according to the KNMI taking climate change into consideration. The relevant wind velocity is the velocity 10 m above ground level. The conversion of the wind velocity can be done by the following formulas according to the NEN-EN1991 2011a:

$$v_b = \frac{v_m(z)}{c_r(z) \cdot c_o(z)} \quad (\text{C.1})$$

where:  $v_b$  [m/s] = the basis Velocity at height 10 m  
 $z$  [m] = the height above the ground  
 $v_m(z)$  [m/s] = the velocity at height  $z$   
 $c_r(z)$  [-] = the roughness factor  
 $c_o(z)$  [-] = the orography factor (=1.0)

At  $z > 200$  m, the velocity is assumed to be the same. This leads to  $v_m(200) = v_m(2000) = 170$  km/h. The roughness factor if  $z$  is above  $z_{\min}$  is described as:

$$c_r(z) = k_r \cdot \ln\left(\frac{z}{z_0}\right)$$

with:  $k_r = 0.19 \left(\frac{z_0}{z_{0,II}}\right)^2$

where:  $c_r(z)$  [-] = roughness factor  
 $k_r$  [-] = terrain factor  
 $z_0$  [m] = factor depending on terrain type  
 $z_{0,II}$  [m] = = 0.05

The spillway is located in terrain I which leads to a  $z_0$  of 0.01 m. The  $k_r$  value becomes 0.17 and the roughness factor is equal to 1.68. This results in a design velocity of 28 m/s.

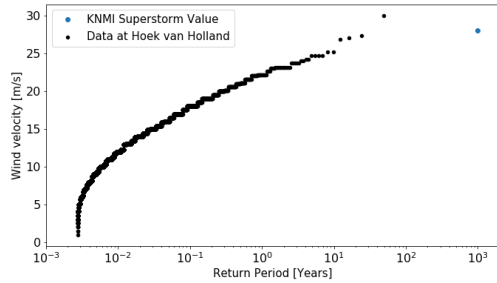
$$k_r = 0.19 \left( \frac{z_0}{z_{0,II}} \right)^2 = 0.19 \left( \frac{0.01}{0.05} \right)^2 = 0.17$$

$$c_r(z) = k_r \cdot \ln \left( \frac{z}{z_0} \right) = 0.17 \cdot \ln \left( \frac{200}{0.01} \right) = 1.68$$

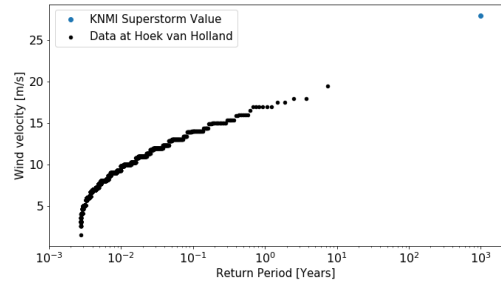
$$v_b = \frac{v_m(z)}{c_r(z) \cdot c_o(z)} = \frac{42.7}{1.68 \cdot 1} = 28 \text{ m/s}$$

## C.2. Wind Occurrence

The wind measurements from the KNMI are taken at Hoek van Holland. The dataset consists of data from 1970 until 2020. In Figure C.1a and C.1b, the return periods of the wind velocity from all directions and from the direction perpendicular to the spillway. The design value for a superstorm according to the KNMI are also shown in both figures. It can be seen that the design value is in line of expectation for the situation in which all wind directions are taken into account. For the other situation, perpendicular wind directions, it can be seen that the design value of the super storm of the KNMI is a bit of an overestimation. Although it slightly overestimates the occurring wind velocity, the velocity of 28 m/s is taken as governing wind velocity.



(a) Return period of the wind velocity (All Directions)



(b) Return period of the wind velocity (Perpendicular to Spillway)

## C.3. Wind Set-up

The wind set-up and down for an open system can be described with the following formula (Jonkman et al., 2018):

$$\frac{\delta h_1}{\delta x} = \frac{\kappa \cdot u_{10}^2 \cdot \cos(\phi)}{g \cdot h} \quad (\text{C.2})$$

where:  $h_1$  [m] = the wind set up  
 $x$  [m] = distance from the start of the set up  
 $\kappa$  [-] = the friction factor ( $= 3.2 \cdot 10^{-6}$ )  
 $u_{10}$  [m/s] = the wind Velocity at height of 10 m  
 $\phi$  [°] = the angle of approach, perpendicular = 0  
 $h$  [m] = the water depth

For a closed system, for example a lake, the following formula needs to be used:

$$\delta h_1 = \frac{0.5 \cdot F \cdot \kappa \cdot u_{10}^2 \cdot \cos(\phi)}{g \cdot h} \quad (\text{C.3})$$

In which F is the Fetch, in this case the length of the lake. The water depths that are used in the set up calculation are shown in Figure C.2.

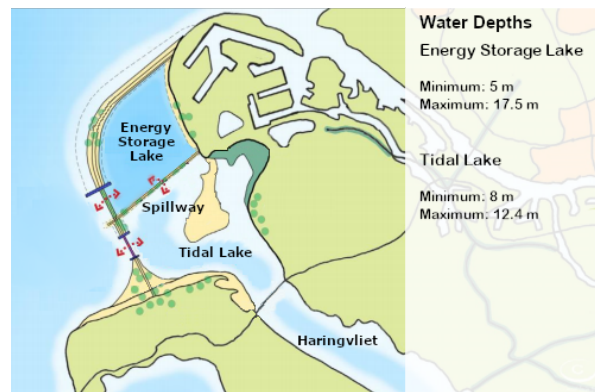


**Figure C.2:** Water depths in the Lakes

For the Energy Storage Lake a wind set down during low water level conditions is the most relevant situation. For the Tidal Lake, the relevant situation is a set up during high water level conditions. Both situations occur for a Southeast wind direction. For the Energy Storage Lake this leads to a fetch of 5 km and for the Tidal Lake to a fetch of 10 km. The Energy Storage Lake is taken as a closed system with a shape of a square. For the Tidal Lake, a rectangle shape is taken and the lake can be seen as an open system. With the design velocity of 28 m/s this leads to the following set up and down:

Location	Maximum Set-up [m]
Energy Storage Lake	-0.13
Tidal Lake	+0.21

The values of the wind set-up are low and combining that with the fact that the design wind velocity leads to an overestimation of the wind set-up, the wind set-up will be neglected.

# D

## Wave Calculations

In this appendix, the calculations of the waves near the spillway can be seen. The obtained wave height is used in the calculation of the retaining height of the concept Caisson but also used in the stability calculations of the concepts.

### D.1. Bretschneider Equation

The wave climate on the energy storage lake and the tidal lake are caused by the wind. Both climates start in the lake itself and there is no influence by the sea due to the dikes and the storm surge barrier. To determine the design wave height and period for the wind waves in the two lakes, the following formulas of Bretschneider are used (Voorendt and Molenaar, 2020b):

$$\tilde{H} = \tilde{H}_{\infty} \left\{ \tanh(0,343\tilde{d}^{1,14}) \cdot \tanh\left(\frac{4,41 \cdot 10^{-4} \tilde{F}^{0,79}}{\tanh(0,343\tilde{d}^{1,14})}\right) \right\}^{0,572} \quad (\text{D.1})$$

$$\tilde{T} = \tilde{T}_{\infty} \left\{ \tanh(0,10\tilde{d}^{2,01}) \cdot \tanh\left(\frac{2,77 \cdot 10^{-7} \tilde{F}^{1,45}}{\tanh(0,10\tilde{d}^{2,01})}\right) \right\}^{0,187} \quad (\text{D.2})$$

With:

$$\tilde{d} = \frac{gd}{U_{10}^2}$$

$$\tilde{F} = \frac{gF}{U_{10}^2}$$

where:	$\tilde{H}$	[-]	=	dimensionless wave height
	$\tilde{T}$	[-]	=	dimensionless wave period
	$\tilde{H}_{\infty}$	[-]	=	dimensionless wave height at deep water (= 0.24)
	$\tilde{T}_{\infty}$	[-]	=	dimensionless wave period at deep water (= 7.69)
	$\tilde{d}$	[-]	=	dimensionless depth
	$\tilde{F}$	[-]	=	dimensionless fetch
	$g$	[m/s <sup>2</sup> ]	=	gravitational acceleration (= 9.81)
	$d$	[m]	=	average water depth of the fetch
	$F$	[m]	=	fetch, distance travelled by wind across open water
	$U_{10}$	[m/s]	=	wind velocity at an attitude of 10 m

With the dimensionless wave height and wave period at deep water,  $\tilde{H}_{\infty}$  and  $\tilde{T}_{\infty}$ , the significant wave height and the peak period are determined by using the following formulas:

$$\tilde{H} = \frac{gH_{m0}}{U_{10}^2} \rightarrow H_{m0} = \frac{\tilde{H}U_{10}^2}{g} \quad (\text{D.3})$$

$$\tilde{T} = \frac{gT_p}{U_{10}} \rightarrow T_p = \frac{\tilde{T}U_{10}}{g} \quad (\text{D.4})$$

where:  $H_{m0}$  [m] = significant wave height, estimated from a wave spectrum  
 $T_p$  [s] = peak wave period

## D.2. Energy Storage Lake

Firstly, the fetch and the averaged water depth are determined. The fetch is 5 km and can be seen in Figure D.1.



Figure D.1: The relevant fetch length

For the averaged water depth, the maximum occurring water level is considered. This water level can be found in Section 3.7.3. The maximum occurring water level in the energy storage lake is NAP - 5 m. This leads to a respectively averaged depth of 17.5 m because the bed level of the energy storage lake is at NAP - 22.5 m, see Section 3.7.1. The wind velocity at an attitude of 10 m is derived in Section C.3 and is equal to 28 m/s. Using these parameters, the value of  $\tilde{d}$  and  $\tilde{F}$  are derived.

$$\tilde{d} = \frac{gd}{U_{10}^2} = \frac{9.81 \cdot 17.5}{28^2} = 0.22 [-]$$

$$\tilde{F} = \frac{gF}{U_{10}^2} = \frac{9.81 \cdot 5000}{28^2} = 62.5 [-]$$

Next, the values of  $\tilde{H}$  and  $\tilde{T}$  are derived.

$$\begin{aligned} \tilde{H} &= \tilde{H}_{\infty} \left\{ \tanh(0,343\tilde{d}^{1,14}) \cdot \tanh\left(\frac{4,41 \cdot 10^{-4} \tilde{F}^{0,79}}{\tanh(0,343\tilde{d}^{1,14})}\right) \right\}^{0,572} \\ &= 0.24 \left\{ \tanh(0,343 \cdot 0.22^{1,14}) \cdot \tanh\left(\frac{4,41 \cdot 10^{-4} \cdot 62.5^{0,79}}{\tanh(0,343 \cdot 0.22^{1,14})}\right) \right\}^{0,572} \\ &= 0.019 \\ \tilde{T} &= \tilde{T}_{\infty} \left\{ \tanh(0,10\tilde{d}^{2,01}) \cdot \tanh\left(\frac{2,77 \cdot 10^{-7} \tilde{F}^{1,45}}{\tanh(0,10\tilde{d}^{2,01})}\right) \right\}^{0,187} \\ &= 7.69 \left\{ \tanh(0,10 \cdot 0.22^{2,01}) \cdot \tanh\left(\frac{2,77 \cdot 10^{-7} \cdot 62.5^{1,45}}{\tanh(0,10 \cdot 0.22^{2,01})}\right) \right\}^{0,187} \\ &= 1.4 \end{aligned}$$

Finally, the values for the significant wave height and peak period are determined.



$$H_{m0} = \frac{\tilde{H}U_{10}^2}{g} = \frac{0.019 \cdot 28^2}{9.81} = 1.49 \text{ m}$$

$$T_p = \frac{\tilde{T}U_{10}}{g} = \frac{1.4 \cdot 28}{9.81} = 4 \text{ s}$$

The significant wave height and the peak period in the energy storage lake are equal to respectively 1.49 m and 4 s. Other relevant parameters associated with the waves are the wavelength and the wave number. The wavelength depends on the water condition in the lake. The water conditions can either be shallow, transitional or deep water conditions. This depends on the ratio of the water depth over the wavelength. Therefore, first deep water conditions are assumed. For deep water the wavelength is described by:

$$L_0 = \frac{gT_{m-1,0}^2}{2\pi}$$

where:  $L_0$  [m] = the deep water wavelength  
 $T_{m-1,0}$  [s] = the wave period

The period that is used in the calculation of the wavelength is spectral wave period,  $T_{m-1,0}$ . The relation between the peak period  $T_p$  and  $T_{m-1,0}$  is given by (Van der Meer et al., 2018):

$$T_{m-1,0} = \frac{T_p}{1.1}$$

The peak period of the Energy Storage Lake is 4 s. This results in a spectral period of 3.64 s. The corresponding deep water wavelength is:

$$L_0 = \frac{gT^2}{2\pi} = \frac{9.81 \cdot 3.63^2}{2\pi} = 20.7 \text{ m}$$

The water conditions are valid if the ratio of the water depth over the wavelength is greater than 0.5.

$$\frac{h}{L_0} = \frac{17.5}{20.7} = 0.85 > 0.5$$

The wave number is calculated by the ratio of  $2\pi$  over the wavelength. For the Energy Storage Lake, this results in a wave number of 0.3.

$$k = \frac{2\pi}{20.7} = 0.3 \text{ [-]}$$

An overview of the wave characteristics of the Energy Storage Lake can be found in Table D.1.

### D.3. Tidal Lake

Firstly, the fetch and the averaged water depth are determined. The fetch can be seen in Figure D.1, 5 km. For the averaged water depth, the maximum occurring water level is considered. This water level can be found in Section 3.7.3. The maximum occurring water level in tidal lake is NAP + 2.4 m because the bed level of the tidal lake is at NAP - 10 m, see Section 3.7.1. This leads to a respectively averaged depth of 12.4 m. The wind velocity at an attitude of 10 m is equal to the velocity for the energy storage lake, 28 m/s. Using these parameters, the value of  $\tilde{d}$  and  $\tilde{F}$  are derived.

$$\tilde{d} = \frac{gd}{U_{10}^2} = \frac{9.81 \cdot 12.4}{28^2} = 0.155 \text{ [-]}$$

$$\tilde{F} = \frac{gF}{U_{10}^2} = \frac{9.81 \cdot 2000}{28^2} = 25 \text{ [-]}$$

Next, the values of  $\tilde{H}$  and  $\tilde{T}$  are derived.

$$\begin{aligned}
\tilde{H} &= \tilde{H}_\infty \left\{ \tanh(0,343\tilde{d}^{1,14}) \cdot \tanh\left(\frac{4,41 \cdot 10^{-4} \tilde{F}^{0,79}}{\tanh(0,343\tilde{d}^{1,14})}\right) \right\}^{0,572} \\
&= 0.24 \left\{ \tanh(0,343 \cdot 0.155^{1,14}) \cdot \tanh\left(\frac{4,41 \cdot 10^{-4} \cdot 25^{0,79}}{\tanh(0,343 \cdot 0.155^{1,14})}\right) \right\}^{0,572} \\
&= 0.012 \\
\tilde{T} &= \tilde{T}_\infty \left\{ \tanh(0,10\tilde{d}^{2,01}) \cdot \tanh\left(\frac{2,77 \cdot 10^{-7} \tilde{F}^{1,45}}{\tanh(0,10\tilde{d}^{2,01})}\right) \right\}^{0,187} \\
&= 7.69 \left\{ \tanh(0,10 \cdot 0.155^{2,01}) \cdot \tanh\left(\frac{2,77 \cdot 10^{-7} \cdot 25^{1,45}}{\tanh(0,10 \cdot 0.155^{2,01})}\right) \right\}^{0,187} \\
&= 1.09
\end{aligned}$$

Finally, the values for the significant wave height and peak period are determined.

$$\begin{aligned}
H_{m0} &= \frac{\tilde{H}U_{10}^2}{g} = \frac{0.012 \cdot 28^2}{9.81} = 1m \\
T_p &= \frac{\tilde{T}U_{10}}{g} = \frac{1.09 \cdot 28}{9.81} = 3.12s
\end{aligned}$$

The corresponding wavelength and wave number are:

$$\begin{aligned}
T_{m-1,0} &= \frac{T_p}{1.1} = \frac{3.12}{1.1} = 2.84s \\
L = L_0 &= \frac{gT^2}{2\pi} = \frac{9.81 \cdot 2.84^2}{2\pi} = 12.6m \\
\frac{h}{L} &= \frac{12.4}{12.6} = 0.98 > 0.5 \rightarrow \text{Therefore, } L_0 \text{ is valid to use} \\
k &= \frac{2\pi}{15.2} = 0.5
\end{aligned}$$

### D.3.1. Overview

An overview of the wave characteristics of the Energy Storage Lake and the Tidal Lake can be found in Table D.1

Location	$H_s$ [m]	$T_p$ [s]	$T_{m-1,0}$ [s]	L [m]	k [-]
Energy Storage Lake	1.49	4.00	3.64	20.07	0.3
Tidal Lake	1.00	3.12	2.84	15.20	0.5

**Table D.1:** Wave characteristics in the Tidal Lake

# E

## Discharge Calculations

The main requirement of the spillway of Delta21 is the discharge requirement. In this appendix, the two different types of flow are described and the discharge capacities of the four concepts are calculated.

### E.1. Pressurised flow

#### E.1.1. The Bernoulli Equation

In pressurised flow conditions, the Bernoulli equation, Formula E.1, is applicable.

$$\frac{1}{2}\rho v^2 + \rho gh + p = \text{constant} \quad (\text{E.1})$$

where:  $\rho$  [kg/m<sup>3</sup>] = the density of the fluid  
 $v$  [m/s] = the mean flow velocity  
 $g$  [m/s<sup>2</sup>] = the gravitational acceleration (= 9.81)  
 $h$  [m] = the water depth compared to reference level  
 $p$  [Pa] = the pressure

For the determination of the discharge in the spillway, Formula E.1 is rewritten in terms of energy head  $H$ , see Formula E.2.

$$\frac{v^2}{2g} + h + \frac{p}{\rho g} = H \quad (\text{E.2})$$

With Formula E.2, the mean velocity in the spillway is determined by the differences in the energy heads in the tidal lake,  $H_{TD}$ , and the energy storage lake,  $H_{ESL}$ . The difference between the two are caused by the head loss between the inlet and the outlet of the spillway  $H_L$ , see Formula E.4.

$$H_{TD} = H_{ESL} + H_L \quad (\text{E.3})$$

The head loss between the inlet and the outlet can be divided into two different types of losses. The first type is the distributed loss, caused by the friction of the pipe or conduit and the second type is the local loss, which is caused by additional components like valves, bends and expansions. In Section E.1.2 and Section E.1.3, more about the distributed and local losses can be found.

$$H_L = \underbrace{f \frac{L}{D} \frac{v^2}{2g}}_{\text{Distributed loss}} + \underbrace{\sum \zeta \frac{v^2}{2g}}_{\text{Local loss}} \quad (\text{E.4})$$

where:	$f$	[-]	=	the Darcy friction factor
	$L$	[m]	=	the length of of the pipe
	$D$	[m]	=	the hydraulic diameter of the pipe
	$v$	[m/s]	=	the mean flow velocity
	$g$	[m/s <sup>2</sup> ]	=	the gravitational acceleration (= 9.81 m/s <sup>2</sup> )
	$\zeta$	[-]	=	the loss coefficient

Substituting Formula E.2 and E.4 into Formula E.3 results in Formula E.5 that is used to calculate the mean velocity in the spillway,  $v_s$ . The subscripts 1 and 2 corresponds to respectively the Tidal Lake and the Energy Storage Lake.

$$\frac{v_1^2}{2g} + h_1 + \frac{p_1}{\rho g} = \frac{v_2^2}{2g} + h_2 + \frac{p_2}{\rho g} + f \frac{L}{D} \frac{v_s^2}{2g} + \sum \zeta \frac{v_s^2}{2g} \quad (\text{E.5})$$

If the mean flow velocity is known, the discharge is calculated with the relation between the cross-sectional area of flow and the velocity:

$$Q = v_s \cdot A$$

where:	$Q$	[m <sup>3</sup> /s]	=	the discharge
	$v_s$	[m/s]	=	the mean flow velocity in the spillway
	$A$	[m <sup>2</sup> ]	=	the cross-sectional area of flow

### E.1.2. Distributed Head Losses

As mentioned before, the distributed head losses are caused by the friction within the pipe or conduit and can be described by Formula E.6.

$$h_{L,dis} = f \frac{L}{D} \frac{v^2}{2g} \quad (\text{E.6})$$

The Darcy friction factor is determined by the Colebrook equation, see Formula E.7. This is an implicit formula which requires an iterative process to calculate the friction value. This iterative process can easily be performed by computer programs like Python.

$$\frac{1}{\sqrt{f}} = -2.0 \log \left( \frac{\epsilon}{3.7D} + \frac{2.51}{Re \sqrt{f}} \right) \quad (\text{E.7})$$

With:

$$Re = \frac{\rho v D}{\mu}$$

where:	$f$	[-]	=	the Darcy friction factor
	$\epsilon$	[mm]	=	the equivalent roughness
	$D$	[m]	=	the hydraulic diameter
	$Re$	[-]	=	the Reynolds number
	$\rho$	[kg/m <sup>3</sup> ]	=	the water density (=1025 kg/m <sup>3</sup> )
	$v$	[m/s]	=	the mean flow velocity
	$\mu$	[kg/ms]	=	the dynamic viscosity of the fluid (= $1 \cdot 10^{-3}$ kg/ms)

The equivalent roughness depends on the type of material that is used, see Table E.1. For new concrete pipe, the equivalent roughness will be low but due to erosion, the equivalent roughness will increase over time. For maximum occurring velocity, the smooth condition is governing and for the discharge capacity, the rougher condition is governing. For the smooth condition a equivalent roughness of 0.5 is assumed and for the rougher condition a equivalent roughness of 1.0 is assumed.

Pipe or Conduit Type	Equivalent Roughness $\epsilon$ [mm]
Riveted steel	0.9-9.0
Concrete	0.3-3.0
Wood stave	0.18-0.9
Cast iron	0.26
Galvanized iron	0.15
Plastic, glass	0.0 (smooth)

**Table E.1:** Equivalent Roughness (Munson et al., 2009)

### E.1.3. Local Head Losses

The local head losses are caused by additional components that are used in the pipeline or conduit. The head loss due to the minor losses can be described by Formula E.8.

$$h_{L,local} = \sum \zeta \frac{v^2}{2g} \quad (\text{E.8})$$

In which  $\zeta$  is the loss coefficient of an additional component or change in pipe. In Table E.2 an overview is given of possible loss coefficients.

<b>Bends</b>	$\zeta$
90° degree mitered	1.1
90° degree threaded	1.5
45° degree threaded	0.4
<b>Gates</b>	
Gate fully open	0.15
Gate 25% closed	0.26
Gate 50% closed	2.1
Gate 75% closed	17
<b>Inlet</b>	
Round	0.2
Straight	0.5
<b>Outlet</b>	
All Types	1.0

**Table E.2:** Overview possible head loss coefficients (Munson et al., 2009)

Another relevant type of local head loss which needs to be considered is the energy loss due to the trash grid at the inlet of the structure. The head loss due to a trash grid depends on the dimensions of the grid and the shape of the grid. The  $\zeta_{Trash}$  value for certain shapes and dimension can be seen in Figure E.1.  $\zeta_{Trash}$  can vary from 0 to 1.2 depending on the design. For a first assumption of the  $\zeta_{Trash}$  value, 0.6 is taken. The reason behind this assumption is that it is higher than the most ideal situation but also covers a large part of the non-ideal shapes.

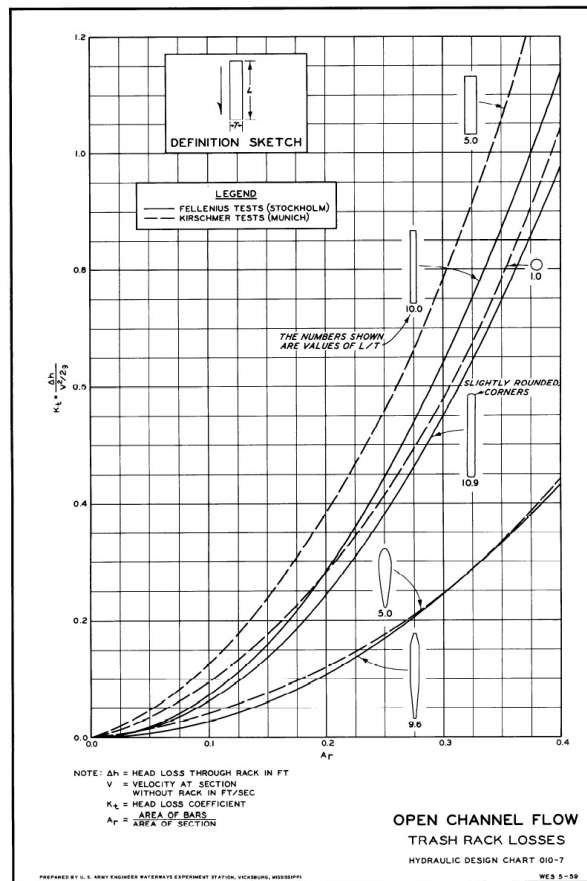


Figure E.1: Head loss value due to trash grid (Army Engineer Waterways Experiment Station, 1977)

### E.1.4. Concept Siphon

#### E.1.4.1. The Governing Situation

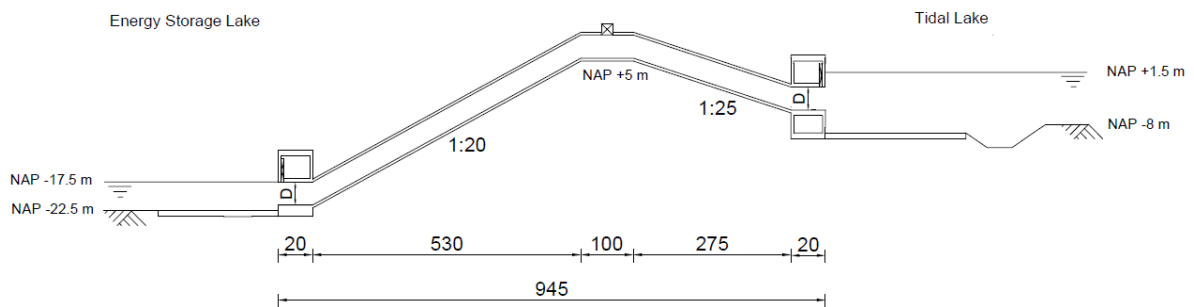


Figure E.2: Concept Siphon governing discharge condition (NTS)

For the calculation of the flow velocity in the spillway for the concept Siphon, Formula E.5 is used. The pressures at both lakes are the same and equal to the atmospheric pressure and therefore can be removed from the equation. Besides this, it can be assumed that at a certain distance away from the spillway, the velocity in both lakes is equal to zero and therefore the velocity part of each lake can be removed from the equation. This results in the simplified Formula E.9.

$$h_1 = h_2 + f \frac{L}{D} \frac{v_s^2}{2g} + \sum \zeta \frac{v_s^2}{2g} \tag{E.9}$$

In which the mean flow velocity is depending on the difference in water levels between both lakes. The water level of the Tidal Lake is at NAP + 1.5 m and the Energy Storage Lake is at NAP - 17.5 m, see Figure E.2. The difference between the two is equal to 19 m and therefore the following can be said:

$$f \frac{L}{D} \frac{v^2}{2g} + \sum \zeta \frac{v^2}{2g} = 19 \quad (\text{E.10})$$

#### E.1.4.2. The Local Head Losses

In this concept, the radius of the pipe is taken as variable. The friction factor is determined by an iterative process, using Formula E.7. The length of the pipe is assumed to be 945 m due to the mild slopes of the dunes, see Figure E.2. For the equivalent roughness a value of 1.0 is taken. This value takes into account the increase in roughness over time.

#### E.1.4.3. The Distributed Losses

The hydraulic diameter that is needed for the distributed head losses is equal to the diameter of the pipe and the total loss coefficient that is used consists of:

- 4 2° Elbows
- 1 Vacuum pump
- 2 Gates, fully open
- 1 Straight inlet
- 1 Outlet
- 1 Trash rack

Within this concept, there are two types of head losses that are not discussed in Section E.1.3. The head loss due to the vacuum pump that is places at the highest point of the siphon system and the head loss due to low degree elbows. The value of the vacuum pump loss coefficient is assumed to have the same value as a gate that is fully open. This means this value is equal to 0.15. For the 2° elbow, the loss coefficient is assumed to be very low and equal to 0.01. The total loss coefficient for the concept Siphon is 2.29.

$$\begin{aligned} \zeta_{\text{total}} &= 4 \cdot \zeta_{\text{elbow}} + \zeta_{\text{vacuum pump}} + 2 \cdot \zeta_{\text{gate, open}} + \zeta_{\text{inlet, straight}} + \zeta_{\text{outlet}} + \zeta_{\text{trash rack}} \\ &= 4 \cdot 0.01 + 0.15 + 2 \cdot 0.15 + 0.5 + 1 + 0.6 \\ &= 2.59 \end{aligned}$$

#### E.1.4.4. The Flow Velocity and the Discharge

Rewriting Formula E.10 to Formula E.11, the velocity in the spillway can be calculated.

$$\Delta H = f \frac{L}{D} \frac{v^2}{2g} + \sum \zeta \frac{v^2}{2g} \rightarrow v = \sqrt{\frac{\Delta H}{f \frac{L}{2gD} + \frac{\zeta_{\text{total}}}{2g}}} \quad (\text{E.11})$$

Taking as an example a pipe with a diameter of 4 m. This leads to the following equations that needs to be solved iteratively, with only v and f as unknowns:

$$\begin{aligned} v &= \sqrt{\frac{19}{f \frac{945}{2 \cdot 9.81 \cdot 4} + \frac{2.59}{2 \cdot 9.81}}} \\ \frac{1}{\sqrt{f}} &= -2.0 \log \left( \frac{0.001}{3.7} + \frac{2.51}{\frac{1025 \cdot v \cdot 4}{1 \cdot 10^{-3}} \sqrt{f}} \right) \end{aligned}$$

Solving this iterative for a pipe with a diameter of 4 m leads to a velocity of 7.89 m/s and a friction factor of 0.0144. With the relation between the area and the velocity ( $v = \frac{Q}{A}$ ) the discharge is determined.

$$v = \frac{Q}{A} \rightarrow Q = v \cdot A = v \cdot \frac{1}{4} \cdot \pi \cdot D^2 = 7.89 \cdot \frac{1}{4} \cdot \pi \cdot 4^2 = 99.12 \text{ m}^3/\text{s}$$

The minimum required discharge capacity is 20 000 m<sup>3</sup>/s and therefore the required number of pipes is:

$$N = \frac{Q_{\text{required}}}{Q} = \frac{20000}{99.12} = 202$$

To ensure a maximum discharge capacity of 20 000 m<sup>3</sup>/s a minimum of 202 pipes is needed. The steps taken for a pipe with a diameter of 4 m are taken for multiple diameters. The results of these different diameters can be seen in see Figure E.3a and see Figure E.3b.

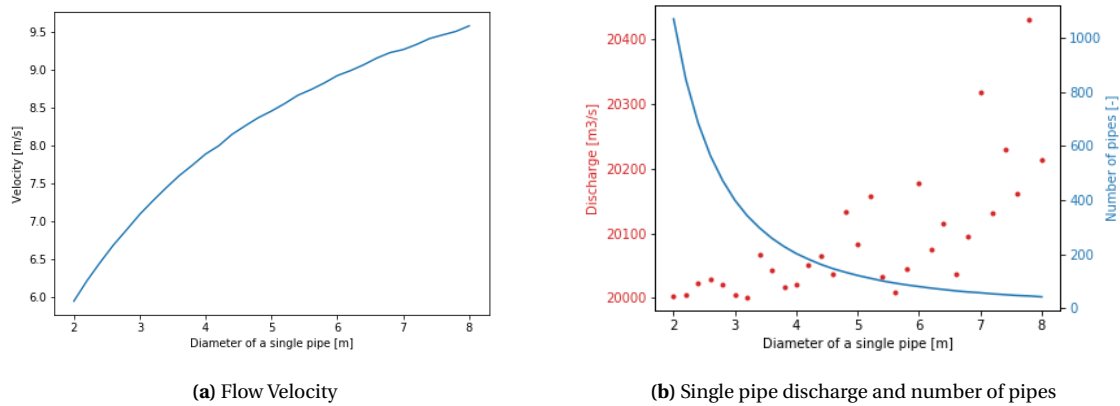


**Figure E.3:** Results for the Concept Siphon for variable diameter

#### E.1.4.5. Discharge Final Dimension

The diameter of the pipes of the final design of the concept Siphon are 4 m. A total of 202 pipes are required in the design to reach the discharge requirement. The pipes have a length of 945 m and the total loss coefficient is 2.59. This results in a discharge of 20 000 m<sup>3</sup>/s.

$$v = \sqrt{\frac{\Delta H}{f \frac{L}{2 \cdot g \cdot D} + \frac{\zeta}{2 \cdot g}}} = \sqrt{\frac{19}{f \frac{945}{2 \cdot 9.81 \cdot 4} + \frac{2.59}{2 \cdot 9.81}}} \rightarrow f = 0.0144 [-], v = 7.89 \text{ m/s (Iterative process)}$$

$$Q = N \cdot A \cdot v = 202 \cdot \frac{1}{4} \pi \cdot 4^2 \cdot 7.89 = 20\,000 \text{ m}^3/\text{s}$$



## E.1.5. Concept Underflow

### E.1.5.1. The Governing Situation

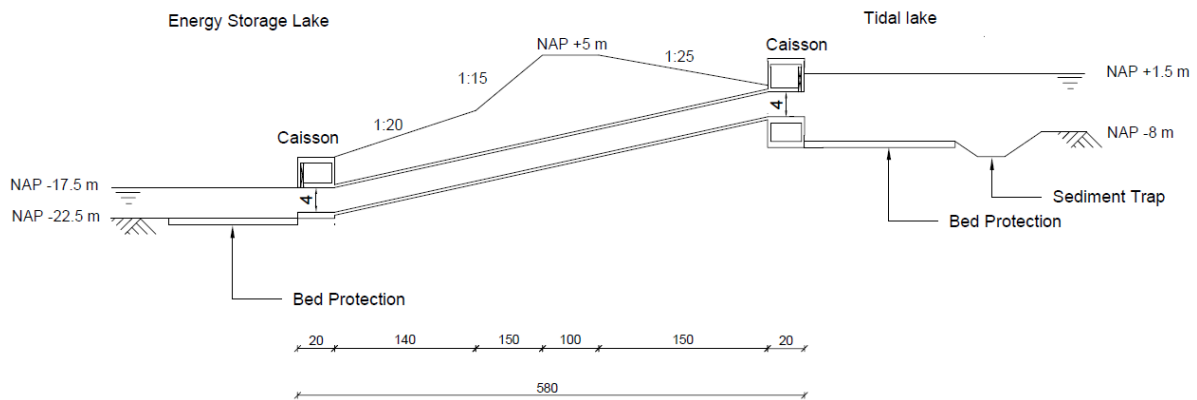


**Figure E.4:** Concept Underflow governing discharge condition (NTS)

To calculate the discharge for the concept Underflow, the same formula is used as for the concept Siphon, Formula E.10.

### E.1.5.2. The Local Head Losses

In this concept, the radius of the pipe and the width of the box culvert is taken as variable. The friction factor is determined by an iterative process using Formula E.7. The length of the pipe, including the inlet and outlet caissons, is assumed to be 580 m due to the mild slopes of the dunes. The initial assumption for the width of the inlet and outlet is 20 m. The equivalent roughness has the same value as in the earlier concept. Besides the earlier mentioned input values, the hydraulic diameter is needed for the rectangular conduit. The hydraulic diameter of a rectangular shape is calculated by:

$$D = \frac{4A}{P} = \frac{2h \cdot w}{h + w} \quad (\text{E.12})$$

where:  $D$  [m] = the hydraulic diameter  
 $A$  [m] = the cross-sectional area of flow  
 $P$  [m] = the wetted perimeter  
 $h$  [m] = the height of the inlet  
 $w$  [m] = the length of the inlet

### E.1.5.3. The Distributed Losses

The total loss coefficient for the concept Underflow consists of:

- 2 2° Elbows
- 2 Gates, fully open
- 1 Straight inlet
- 1 Outlet
- 1 Trash rack

This leads to the following value of the total loss coefficient.

$$\begin{aligned} \zeta_{\text{total}} &= 2 \cdot \zeta_{\text{elbow}} + 2 \cdot \zeta_{\text{gate, open}} + \zeta_{\text{inlet, straight}} + \zeta_{\text{outlet}} + \zeta_{\text{trash rack}} \\ &= 4 \cdot 0.01 + 2 \cdot 0.15 + 0.5 + 1 + 0.6 \\ &= 2.42 \end{aligned}$$

The total loss coefficient for the concept Underflow is 2.42.

### E.1.5.4. The Flow Velocity and Discharge

With the use of Formula E.11, the velocity is determined in relation to the length or diameter of the conduit or pipe. For the calculations of the pipe in this concept the method is the same as the concept Siphon. The results can be seen in respectively Figure E.5a and E.5b. For the rectangular conduit the method an additional step is taken. First the hydraulic diameter is determined before continuing with the same method. As example a rectangular conduit with 4 m height and 4 m length is taken to show the calculation of the hydraulic diameter.

$$D = \frac{4A}{P} = \frac{2h \cdot w}{h + w} = \frac{2 \cdot 4 \cdot 4}{4 + 4} = 4$$

The results of the rectangular conduit can be seen in respectively Figure E.6a and E.6b. It can be seen that the rectangular shape is more favourable for the number of conduits but a rectangular shape is less favourable for placing under a soil layer. Circular shapes can handle soil pressure better. The differences between the rectangular and circular shapes in number of conduits is relatively small and therefore the circular shape is chosen. With as main reason the resistance against soil pressure.

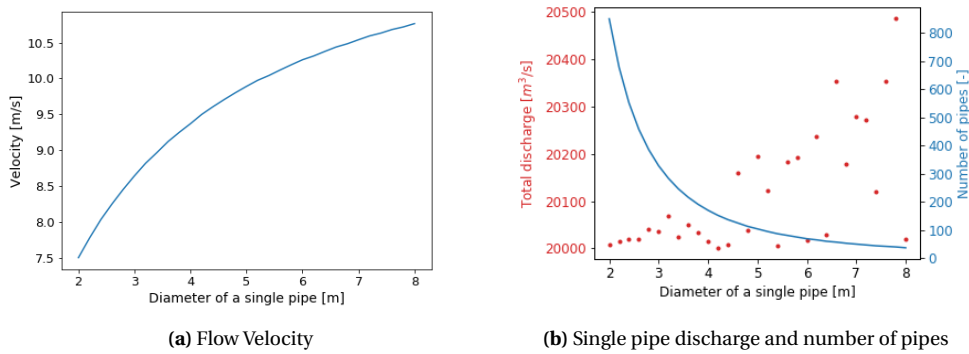


Figure E.5: Results for the Concept Underflow for variable radius

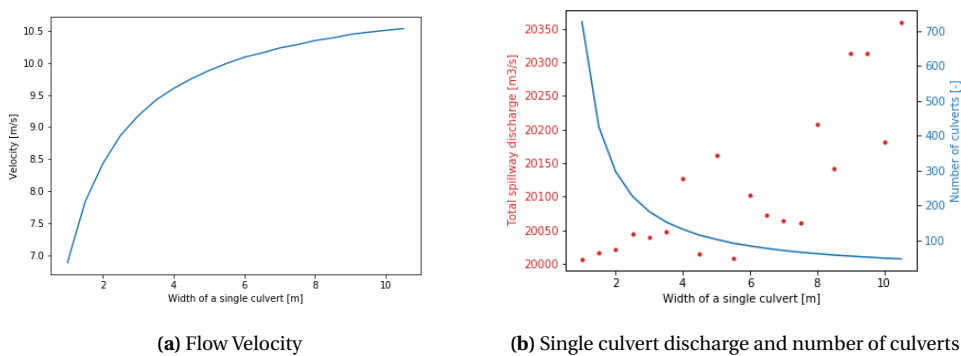


Figure E.6: Results for the Concept Underflow for variable width

### E.1.5.5. Discharge Final Dimension

The diameter of the pipes of the final design of the concept Underflow are 4 m. A total of 169 pipes are required in the design to reach the discharge requirement. The pipes have a length of 580 m and the total loss coefficient is 2.42. This results in a discharge of 20 000 m<sup>3</sup>/s.

$$v = \sqrt{\frac{\Delta H}{f \frac{L}{2 \cdot g \cdot D} + \frac{\zeta}{2 \cdot g}}} = \sqrt{\frac{19}{f \frac{580}{2 \cdot 9.81 \cdot 4} + \frac{2.42}{2 \cdot 9.81}}} \rightarrow f = 0.0126 [-], v = 9.4 \text{ m/s (Iterative process)}$$

$$Q = N \cdot A \cdot v = 169 \cdot \frac{1}{4} \pi \cdot 4^2 \cdot 9.4 = 20\,000 \text{ m}^3/\text{s}$$

### E.1.6. Concept Caisson

#### E.1.6.1. The Governing Situation

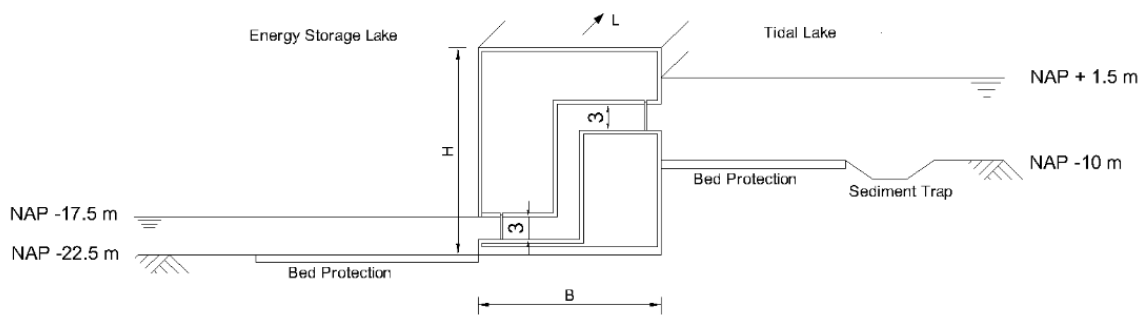


Figure E.7: Concept Caisson governing discharge condition (NTS)

#### E.1.6.2. The Local Head Losses

The concept Caisson consist of a concrete conduit with a height of 3 m. The width is taken as variable. For the calculation of the mean flow velocity, the length of the conduit is assumed to be 65 m. The equivalent roughness has the same value as in the earlier concepts and the hydraulic diameter is calculated with Formula E.12.

#### E.1.6.3. The Distributed Losses

The total loss coefficient for the concept Caisson consist of:

- 2 90° mitered bends
- 2 Gates, fully open
- 1 Rounded inlet
- 1 Outlet
- 1 Trash rack

This leads to a total loss coefficient of 4.3.

$$\begin{aligned} \zeta_{\text{total}} &= 2 \cdot \zeta_{\text{bend}} + 2 \cdot \zeta_{\text{gate, open}} + \zeta_{\text{inlet}} + \zeta_{\text{outlet}} + \zeta_{\text{trash rack}} \\ &= 2 \cdot 1.1 + 2 \cdot 0.15 + 0.2 + 1 + 0.6 \\ &= 4.3 \end{aligned}$$

### E.1.6.4. The Flow Velocity and Discharge

With the use of Formula E.11, the flow velocity is calculated in relation to the width of the conduit, see Figure E.8a. With the relation between the area and the velocity ( $v = \frac{Q}{A}$ ) the discharge is calculated, see Figure E.8b. In the same figure, the number of caissons is indicated to reach the required discharge capacity of 20 000 m<sup>3</sup>/s.

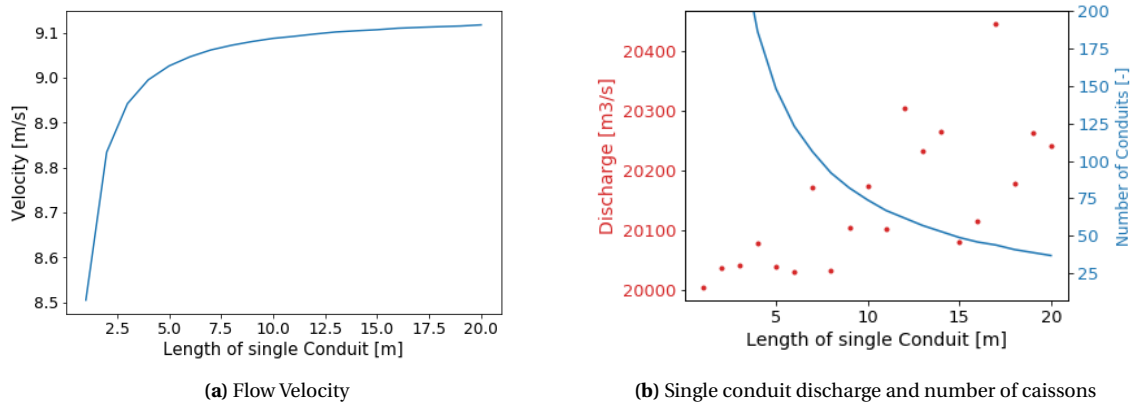


Figure E.8: Results for the Concept Caisson for variable width

### E.1.6.5. Discharge Final Dimension

The height and width of the outlets are respectively 3 and 10 m. A total of 74 outlets are required in the design to reach the discharge requirement. The outlets have a length of 65 m and the total loss coefficient is 4.3. This results in a discharge of 20 200 m<sup>3</sup>/s.

$$D = \frac{4A}{P} = \frac{2h \cdot w}{h + w} = \frac{2 \cdot 3 \cdot 10}{10 + 3} = 4.61 \text{ m}$$

$$v = \sqrt{\frac{17.5}{f \frac{65}{2 \cdot 9.81 \cdot 4.61} + \frac{4.3}{2 \cdot 9.81}}} \rightarrow f = 0.0152 \text{ [-]}, v = 9.1 \text{ m/s (Iterative process)}$$

$$Q = N \cdot A \cdot v = 74 \cdot 30 \cdot 9.1 = 20\,200 \text{ m}^3/\text{s}$$

## E.2. Open Channel Flow

Open channel flow occurs in open channels but also in cases in which a pipe or conduit is not entirely filled. For the situations in which water flows over an ogee crest, the discharge can be described by weir equation, see Formula E.13. This flow is described as uncontrolled flow over a sharp-crested weir.

$$Q = C_d \cdot L_e \cdot H_e^{\frac{3}{2}} \quad (\text{E.13})$$

where:  $Q$  [m<sup>3</sup>/s] = the discharge over the weir  
 $C_d$  [-] = the discharge coefficient  
 $L_e$  [m] = effective length of the spillway  
 $H_e$  [m] = the hydraulic head above the weir

The value for  $C_d$ , can be seen in Figure E.9a. If the flow is controlled by means of a gate, Formula E.13 is changed to the orifice equation, see Formula E.14.

$$Q = C_g \cdot d \cdot L_e \sqrt{2gH_e} \quad (\text{E.14})$$

where:  $Q$  [m<sup>3</sup>/s] = the discharge over the weir  
 $C_g$  [-] = the gated discharge coefficient  
 $d$  [m] = the gate opening  
 $L_e$  [m] = the effective length of the spillway  
 $H_e$  [m] = the hydraulic head above the weir

The value of  $C_g$  can be seen in Figure E.9b.

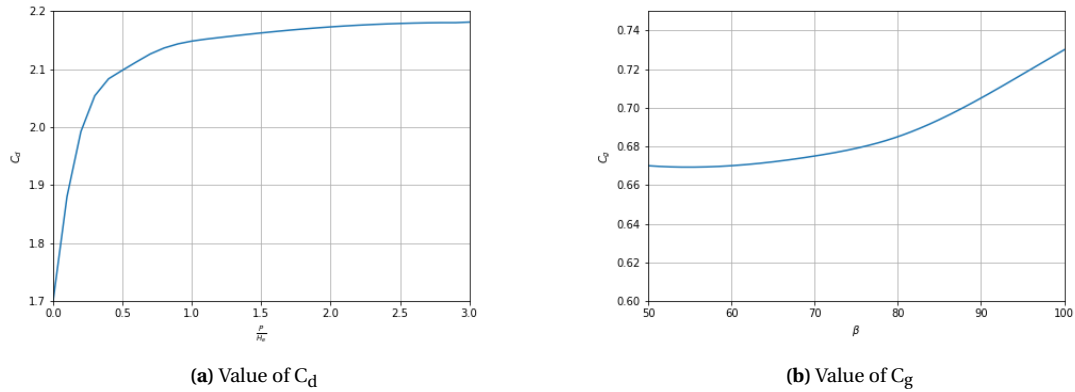


**Figure E.9:** Coefficients of discharge U.S. Army Corps of Engineers (1990)

The effective length is calculated according to Formula E.15.

$$L_e = L - 2(N \cdot K_p + K_a)H_e \quad (\text{E.15})$$

where:  $L_e$  [m] = the effective length of the spillway  
 $L$  [m] = the total length of the spillway  
 $N$  [-] = the number of piers  
 $K_p$  [-] = the pier contraction coefficient  
 $K_a$  [-] = the abutment contraction coefficient  
 $H_e$  [m] = the hydraulic head above the weir

The values for the pier contraction coefficient and the abutment contraction coefficient can be seen in Table E.3.

Type of pier	$K_p$
Rectangular Nosed	0.02
Round Nosed	0.01
Cut-Water Nosed	0.00
Type of Abutment	$K_a$
Sharp Edged	0.2
Round Edged	0.1

**Table E.3:** Pier and abutment coefficients

### E.2.1. Concept Ogee

#### E.2.1.1. The opening dimensions and the discharge capacity

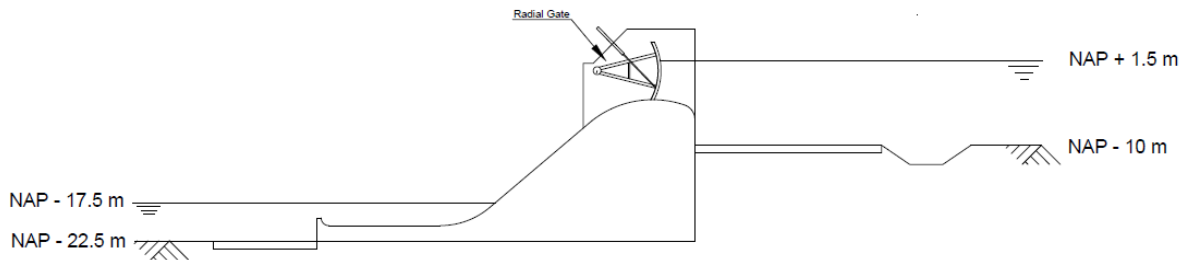


Figure E.10: Concept Ogee governing discharge condition (NTS)

In concept Ogee, the flow over the spillway can be seen as open channel flow in which the flow is controlled by a gate. When the maximum discharge is required, the gate will be fully open and the flow can be seen as uncontrolled. Therefore Formula E.13 applies for this concept.

The top of the ogee crest will be located at NAP - 4.5 m and the maximum water level in the tidal like is NAP + 1.5 m. Due to this,  $H_e$  is equal to the water level on the crest, which is 6 m. For the coefficient of discharge the ratio of the height of the spillway and the water level on the crest is taken.

$$\frac{P}{H_e} = \frac{5.5}{6} = 0.92$$

This results in a  $C_d$  of 2.14. The effective length is determined with an iterative process. First a certain width between two piers is taken. This width is taken as total length and after that this length is used to calculate the discharge. This discharge is compared with the required discharge to see the required number of channels. Next, the  $K_a$  and  $K_p$  values are determined by looking at the design. The design will consist of round nosed piers and sharp-edged abutments. This leads to values of respectively 0.01 and 0.2. After this, the effective length is calculated and the discharge that corresponds with that length. With this discharge the number of channels is calculated and this is repeated until the number of channels is the same as the try before. Doing this for multiple widths results in the following discharges, see Figure E.11b.

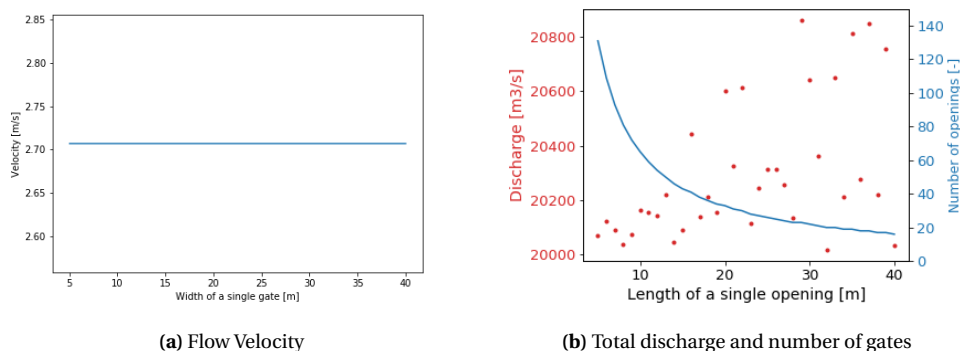


Figure E.11: Results for the Concept Ogee for variable width

**E.2.1.2. Discharge Final Dimension**

The final design of concept Ogee consists of 26 gates with an width of 25 m. The top of the crest is at NAP - 4.5 m. With a water level of NAP + 1.5, the hydraulic head above the weir ( $H_e$ ) is 6 m. The height of the weir (P) is equal to 5.5 m and therefore  $C_d$  is equal to 2.14.

$$L_e = L - 2(N \cdot K_p + K_a)H_e = 26 \cdot 25 - 2(26 \cdot 0.01 + 0.2) \cdot 6 = 646.7 \text{ m}$$

$$Q = C_d \cdot L_e \cdot H_e^{\frac{3}{2}} = 2.14 \cdot 646.7 \cdot 6^{\frac{3}{2}} = 20\,300 \text{ m}^3/\text{s}$$

# F

## Stability Concept Siphon

In this appendix, the calculations corresponding to the determination of the dimensions of the concept Siphon can be seen. First the dimensions for the caisson at the Energy Storage Lake side are obtained and afterwards, the dimensions of the caisson at the Tidal Lake side.

### F.1. Design of the Caisson at the Energy Storage Lake side

#### F.1.1. Basis Layout and Expansion

For the determination of the optimal width of the caisson, a basis layout of the caisson is used and increased in width by  $\Delta x$ . The basis layout of the caissons has a height of 10.5 m, a width of 10 m and the length of a caisson with a single conduit is 12 m. This can be seen in Figure F.1.

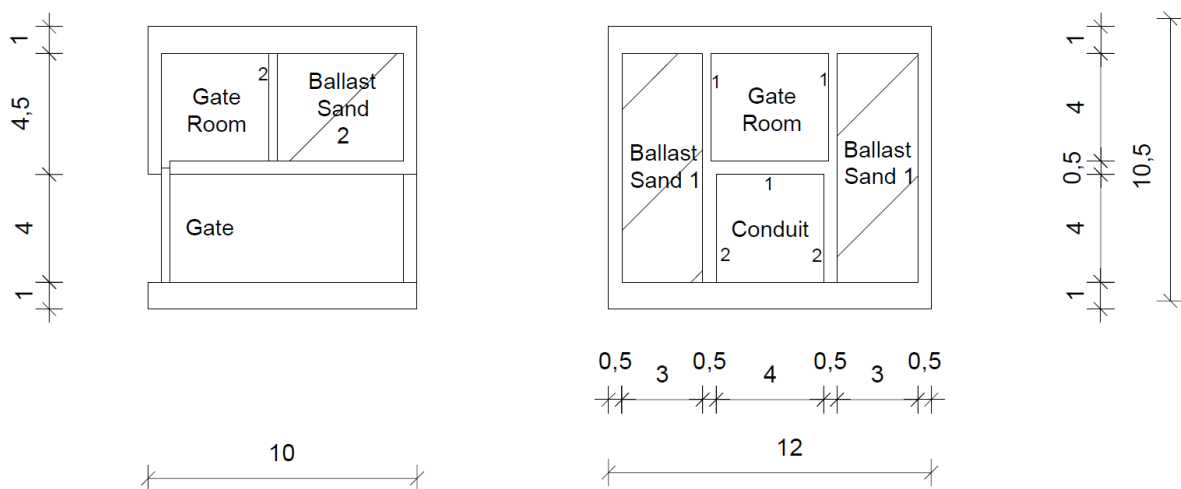


**Figure F.1:** The Layout of the Concept Siphon caisson

The self-weight of the basis caisson consists of multiple elements. In the calculations of the self-weight, the specific weight of concrete and steel are respectively  $25 \text{ kN/m}^3$  and  $78 \text{ kN/m}^3$ . The self-weight of the ballast material (sand) is  $20 \text{ kN/m}^3$ . The self-weight of the elements of the caisson can be seen in F.1.



Element	Number of Elements [-]	Total Volume [m <sup>3</sup> ]	Weight [kN]
Outer Wall L-direction	2	85	2125
Outer Wall B-direction	2	82	2050
Slab	2	240	6000
Inner Wall 1	2	21.6	540
Inner Wall 2	1	4.8	120
Conduit Wall 1	1	22.5	563
Conduit Wall 2	2	36	900
Ballast 1	2	459	9180
Ballast 2	1	75.2	1504
Gate	1	4.8	374
<b>Total (With Ballast)</b>			23356
<b>Total (Without Ballast)</b>			12672

**Table F.1:** Self Weight of the Caisson

For the calculations in the remainder of this appendix, the self-weight per meter length is used instead of the total self-weight of a caisson. This leads to a self-weight excluding ballast of 1056 kN/m and including ballast 1946 kN/m.

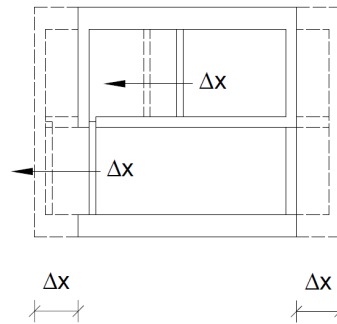


**Figure E.2:** Increase in width by  $\Delta x$

To determine the optimal width of the caisson, the basis layout is increased by  $\Delta x$ , see Figure E.2. The additional weight for each increase of  $\Delta x$  can be seen in Table E.2.

Element	Additional Volume [m <sup>3</sup> ]	Additional Force [kN]
Slabs	24	600
Ballast	67	1340
Outer Wall	8.5	212.5
Culvert Wall	6.5	162.5
Inner Wall	2.4	60
<b>Total (With Ballast)</b>		2375
<b>Total (Without Ballast)</b>		1035

**Table E.2:** Increase in self-weight by the increase in width of  $\Delta x$

The increase in self weight per meter length excluding ballast is equal to 86 kN/m and including ballast it is equal to 198 kN/m.

### F.1.2. Sliding Resistance

The sum of the horizontal forces may not exceed the sliding resistance, otherwise the structure will move in horizontal direction. More information about the method used for the sliding resistance can be found in Chapter 6.

$$\sum H \leq R_d \quad (\text{F1})$$

in which:

$$R_d = V'_d \cdot \tan(\delta_d)$$

### F.1.2.1. Situation One

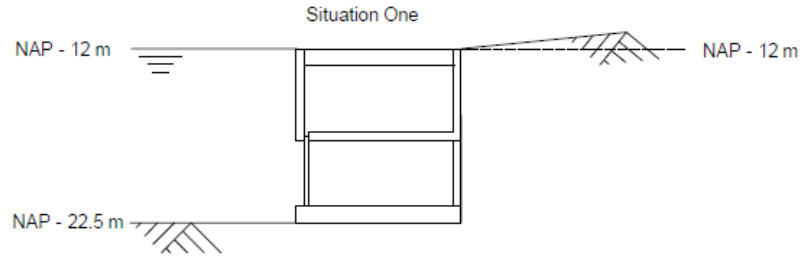


**Figure F.3:** Load situation one

Load situation one can be seen in Figure F.3. The loads acting on the caisson consist of water pressures and soil pressure. Wave pressures are not taken into account because the situation without waves is less favourable. The reason for this is the direction of the wave force. The water pressure is determined by the use of Formula F.2.

$$p_w = h \cdot \gamma_w \quad (\text{F2})$$

in which:

$$\gamma_w = \rho_{w,s} \cdot g$$

where:

$p_w$	[kPa]	=	the water pressure
$h$	[m]	=	the water depth
$\rho_{w,s}$	[kg/m <sup>3</sup> ]	=	the density of salt water (=1025)
$g$	[m/s <sup>2</sup> ]	=	the gravitational acceleration (=9.81)

For situation one, the water pressure at the bottom of the caisson is:

$$p_w = h \cdot \gamma_w = 10.5 \cdot 10.06 = 106 \text{ kPa}$$

This is shown in Figure F.4. The horizontal soil pressure is determined according to NEN-EN 1997-1 and the soil pressures are taken as neutral. The reason for this is that in NEN-EN 1997-1, it is stated that if displacements are not determined, neutral soil pressures should be taken.

$$\sigma_v = h_g \cdot \gamma'_z \quad (\text{F3})$$

$$\sigma_h = \sigma_v \cdot k_n \quad (\text{F4})$$

in which:

$$k_n = (1 - \sin(\phi_d)) \cdot \sqrt{OCR}$$

where:

$\sigma_v$	[kN/m <sup>2</sup> ]	=	the vertical soil pressures
$\sigma_h$	[kN/m <sup>2</sup> ]	=	the horizontal soil pressures
$\gamma'_z$	[kN/m <sup>3</sup> ]	=	specific weight of the soil
$h_g$	[m]	=	the height of the soil
$\phi_d$	[°]	=	the design value of the internal friction
$OCR$	[-]	=	the overconsolidation ratio

The OCR value is assumed to be equal to 1. The height of the soil layer is 10.5 m. The  $\gamma'_z$  for sand is equal to 9.95 kPa/m and the design value of the internal friction is 27°, see Section 3.7.1. This leads to the following soil pressures, which can also be seen in Figure H.3:

$$K_n = (1 - \sin(\phi_d)) \cdot \sqrt{OCR} = (1 - \sin(27)) \cdot \sqrt{1} = 0.54$$

$$\sigma_v = h_g \cdot \gamma'_z = 10.5 \cdot 9.95 = 104.4 \text{ kN/m}^2$$

$$\sigma_h = \sigma_v \cdot k_n = 104.4 \cdot 0.54 = 56.8 \text{ kN/m}^2$$

The water and soil pressures acting on the caisson can be seen in Figure E.4.

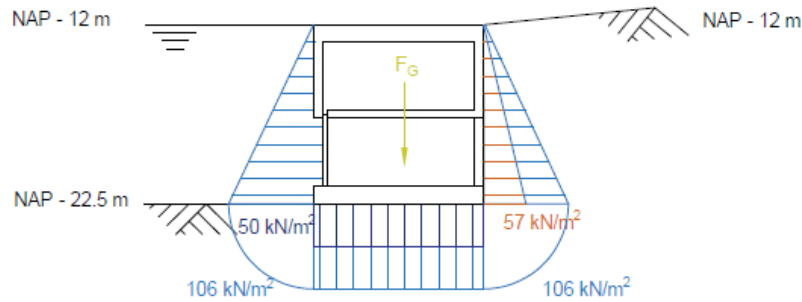


**Figure E.4:** Pressures acting on the caisson

These pressures can be transformed into forces by calculating the area of the pressure. These forces are shown in Figure E.5.

$$F_s = \sigma_h \cdot h_g \cdot \frac{1}{2} = 56.8 \cdot 10.05 \cdot \frac{1}{2} = 298 \text{ kN/m}$$

$$F_{w,1} = F_{w,2} = p_w \cdot h_w \cdot \frac{1}{2} = 106 \cdot 10.5 \cdot \frac{1}{2} = 555 \text{ kN/m}$$

$$F_{u,1} = 50.3 \cdot B = 50 \cdot 10 = 503 \text{ kN/m}$$

$$F_{u,2} = (p_w - 50) \cdot B = (106 - 50) \cdot 10 = 553 \text{ kN/m}$$

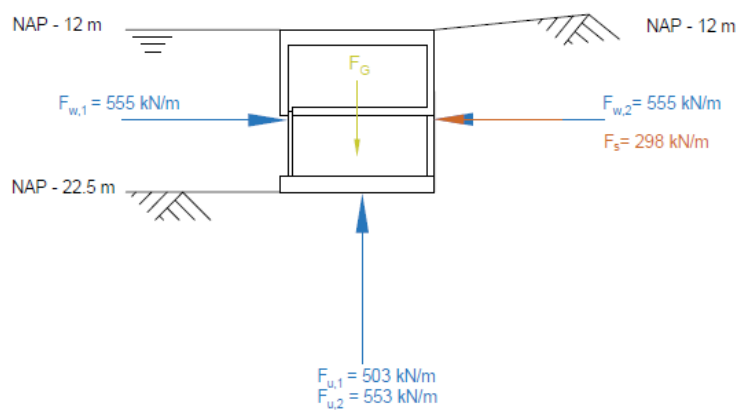


**Figure E.5:** Forces acting on caisson

To determine the unity check for the sliding resistance, the sum of the vertical and horizontal forces are taken. In the calculation of the sum of the horizontal and vertical forces, load factors are used.

$$V'_d = F_G \cdot \gamma_{fav} - F_{u,1} \cdot \gamma_N - F_{u,2} \cdot \gamma_F \quad (E5)$$

$$\sum H = F_s \cdot \gamma_N + F_{w,1} - F_{w,2} \quad (E6)$$

where:  $F_G$  [kN] = the force due to the self-weight  
 $\gamma_{fav}$  [-] = the load factor for favourable forces (=0.9)  
 $F_u$  [kN] = the force due to the uplift  
 $\gamma_F$  [kN] = the load factor for forces (=1.25)  
 $F_s$  [kN] = the force due to the soil  
 $\gamma_N$  [kN] = the neutral load factor (=1.00)

The sum of the vertical forces is depending on the width of the structure and is therefore different for each width. The calculations are done for the basis layout of the caisson. With the use of python the addition of  $\Delta x$  is taken into account in the calculations.

$$\begin{aligned} V'_d &= F_G \cdot \gamma_{fav} - F_{u,1} \cdot \gamma_N - F_{u,2} \cdot \gamma_F \\ &= 1946 \cdot 0.9 - 500 \cdot 1.0 - 560 \cdot 1.25 \\ &= 558 \text{ kN/m} \\ \sum H &= F_s \cdot \gamma_N + F_{w,1} - F_{w,2} \\ &= 298 \cdot 1.0 + 555 - 555 \\ &= 298 \text{ kN/m} \end{aligned}$$

The sliding resistance is depending on the friction angle between the subsoil and the structure,  $\delta_d$ . According to NEN-EN 1997-1, article 6.5.3,  $\delta_d$  is approximately  $\frac{2}{3}$  of  $\phi_d$ . The characteristic value of  $\phi$  for sand can be found in Section 3.7.1 and is equal to  $32.5^\circ$ . The safety factor for  $\phi$  is 1.2 according to NEN-EN 1997-1.

$$\begin{aligned} \phi_d &= \frac{\phi_{c,soil}}{\gamma_\phi} = \frac{32.5}{1.2} = 18^\circ \\ \delta_d &= \frac{2}{3} \phi_d = \frac{2}{3} \cdot 27 = 18^\circ \end{aligned}$$

The sliding resistance for this situation is:

$$R_d = V'_d \cdot \tan(\delta_d) = 558 \cdot \tan(18) = 182 \text{ kN/m}$$

The unity check for the basis layout is:

$$UC = \frac{\sum H}{R_d} = \frac{298}{182} = 1.64$$

It can be concluded that the basis layout of the caisson does not meet the stability requirement. With the use of python this calculation is repeated for the other widths of the caisson. The results of these unity checks can be seen in Figure E.6 and it can be concluded that the minimum required width is 17 m.

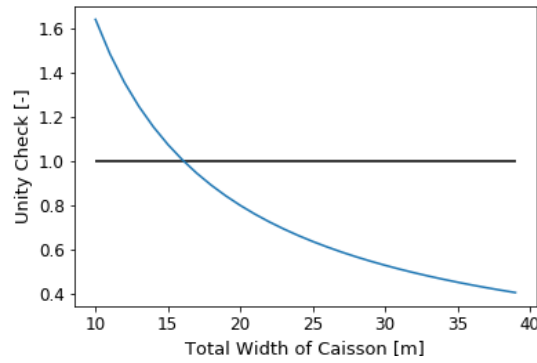


**Figure E.6:** Unity Check Sliding Resistance

**F.1.2.2. Situation Two**

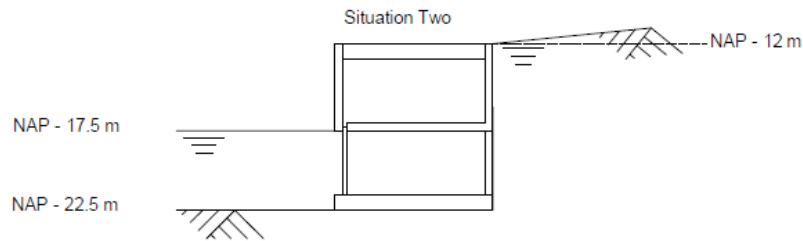


**Figure E.7:** Load situation Two

Figure E.7 shows load situation two. For this situation, the same calculation steps are performed as for situation one. Therefore the detailed calculations for pressures are not shown for this situation. The pressures acting on the caisson can be seen in Figure E.8a and the forces can be seen in Figure E.8b.

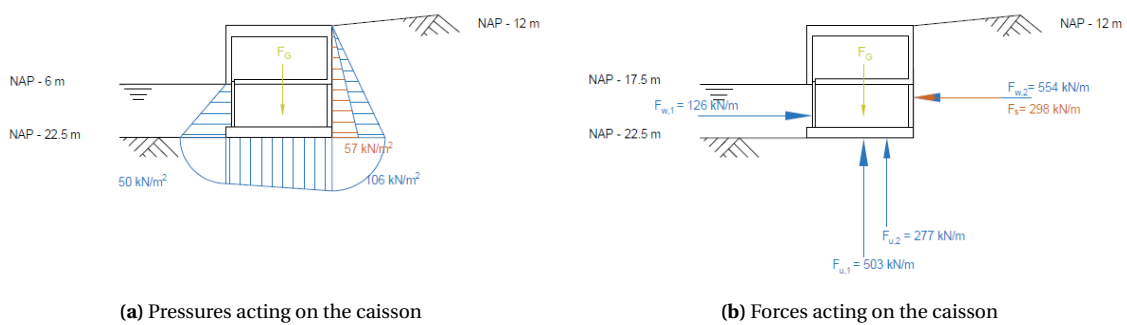


**Figure E.8:** Pressures and forces acting on the caisson

In this load situation, the difference in water level has influence on the sum of the horizontal forces.

$$\begin{aligned}
V'_d &= F_G \cdot \gamma_{\text{fav}} - F_{u,1} \cdot \gamma_N - F_{u,2} \cdot \gamma_F \\
&= 1946 \cdot 0.9 - 503 \cdot 1.0 - 277 \cdot 1.25 \\
&= 903 \text{ kN/m} \\
\sum H &= F_s \cdot \gamma_N - (F_{w,1} - F_{w,2}) \cdot \gamma_F \\
&= 298 \cdot 1.0 - (126 - 555) \cdot 1.25 \\
&= 834 \text{ kN/m}
\end{aligned}$$

This results in the following sliding resistance:

$$R_d = V'_d \cdot \tan(\delta_d) = 903 \cdot \tan(18) = 294 \text{ kN/m}$$

Comparing the resistance against the load leads to the following unity check:

$$UC = \frac{\sum H}{R_d} = \frac{834}{294} = 2.8$$

The basis layout does not meet the stability requirement. The unity checks for the other widths of the caisson can be seen in Figure E.9.

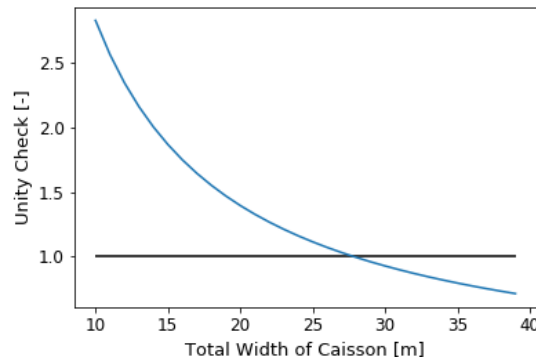


**Figure E.9:** Unity Check Sliding Resistance

### F.1.3. Rotational Stability

If the eccentricity of the resulting force is exceeding the boundaries of the core of the caisson, the caisson will rotate. Therefore, the eccentricity may not exceed the boundaries of the core. More information about the method used for the rotational stability can be found in Chapter 6.

$$-\frac{1}{6}B \leq e_R \leq \frac{1}{6}B \quad (\text{E7})$$

with:

$$e_R = \frac{\sum M}{\sum V}$$

#### F.1.3.1. Horizontal position of the gravity centre

For the vertical forces, the location of the gravity centre is important. The distance to the gravity centre from a certain reference point, in this case the left outer wall, can be determined by:

$$x_G = \frac{\sum V_i \cdot e_i \cdot \gamma_i}{\sum V_i \cdot \gamma_i} \quad (\text{E8})$$

where:  $x_G$  [m] = the distance of the gravity centre from the rotation point  
 $V_i$  [m<sup>3</sup>] = the volume of a single element  
 $e_i$  [m] = the distance of the element from the rotation point  
 $\gamma_i$  [kN/m<sup>3</sup>] = the density of the element

For the basis layout of the caisson, the volumes of each element and the distances from the left side of the caisson can be found in Table F.3.

Element	Number	Total Volume $V_i$ [m <sup>3</sup> ]	Distance $e_i$ [m]	$\gamma_i$
Outer Wall 1	2	85	5	25
Outer Wall 2	1	27	0.25	25
Outer Wall 3	1	27	9.75	25
Outer Wall 4	2	21	0.25	25
Outer Wall 5	2	21	9.75	25
Bottom Slab	1	120	5	25
Top Slab	1	120	5	25
Inner Wall 1	2	21.6	5	25
Inner Wall 2	1	4.8	4.65	25
Culvert Wall 1	2	36	5	25
Culvert Wall 2	1	22.5	5	25
Gate	1	4.8	0.65	78
Ballast 1	2	459	5	20
Ballast 2	1	75.2	7.15	20

**Table F.3:** Volume and distances of elements

This results in the following location of the gravity centre compared to the left side (side with the gate) of the caisson.

$$x_G = \frac{\sum V_i \cdot e_i \cdot \gamma_i}{\sum V_i \cdot \gamma_i} = 5.07 \text{ m}$$

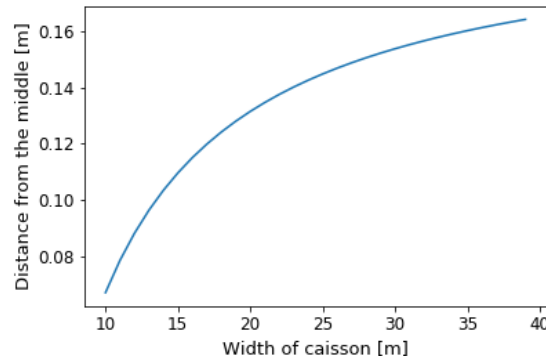


**Figure F.10:** Distance between middle of caisson and gravity centre

The location of the gravity centre compared to the left side of the caisson can be seen in Figure F.10 for each width. The values in the graph show that the centre of gravity is close to the middle of the caisson. The reason for the asymmetry is the gate room, which causes less ballast sand on that side of the caisson.

### F.1.3.2. Situation One

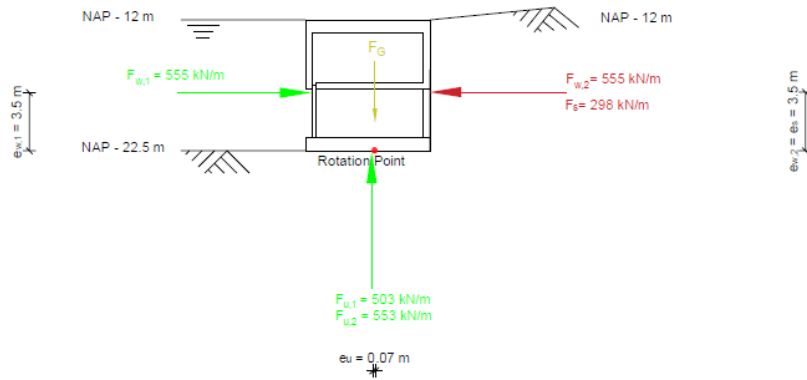


**Figure F.11:** Forces and distances

Situation one for the rotational stability is the same as situation one for the sliding resistance. The forces acting on the caisson can be seen in Figure F.11, in which forces with the same colour cause a moment in the same direction. Besides the forces, the distance to the gravity centre are given. The sum of the vertical forces and moments are determined with Formula F.9 and F.10.

$$\sum V = F_G \cdot \gamma_{fav} - F_{u,1} \cdot \gamma_N - F_{u,2} \cdot \gamma_F \quad (F.9)$$

$$\sum M = \sum M_H - \sum M_V \quad (F.10)$$

with:

$$\sum M_H = F_s \cdot e_s \cdot \gamma_N$$

$$\sum M_V = F_{u,1} \cdot e_u \cdot \gamma_N + F_{u,2} \cdot e_u \cdot \gamma_F$$

Using the forces and distances given in Figure F.11 leads to the following:

$$\begin{aligned} \sum M_H &= F_s \cdot e_s \cdot \gamma_N \\ &= 298 \cdot 3.5 \cdot 1.0 = 1043 \text{ kNm/m} \\ \sum M_V &= F_{u,1} \cdot e_u \cdot \gamma_N + F_{u,2} \cdot e_u \cdot \gamma_F \\ &= 500 \cdot 0.07 \cdot 1.0 + 560 \cdot 0.07 \cdot 1.25 = 84 \text{ kNm/m} \\ \sum M &= \sum M_H - \sum M_V \\ &= 1043 - 84 = 959 \text{ kNm/m} \\ \sum V &= F_G \cdot \gamma_{fav} - F_{u,1} \cdot \gamma_N - F_{u,2} \cdot \gamma_F \\ &= 1946 \cdot 0.9 - 503 \cdot 1.0 - 560 \cdot 1.25 = 558 \text{ kN/m} \end{aligned}$$

The eccentricity corresponding to these values is:

$$e_R = \frac{\sum M}{\sum V} = \frac{959}{558} = 1.73 \text{ m}$$

The unity check for the basis layout is equal to:

$$UC = \frac{e_R}{\frac{1}{6}B} = \frac{1.73}{\frac{1}{6}10} = 1.04$$



It can be concluded that the basis layout is not meeting the requirement. The unity checks for the other widths of the caisson can be seen in Figure F.12.

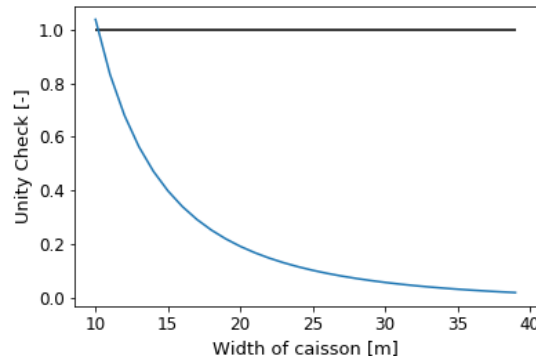


Figure F.12: Unity Check Rotational Stability

### F.1.3.3. Situation Two

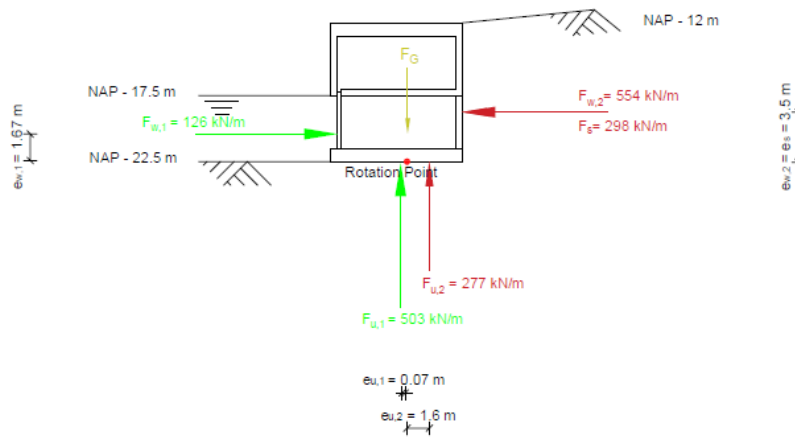


Figure F.13: Forces and distances

For situation two the forces and distances can be seen in Figure F.13. The difference between situation one and two is the sum of the moments in the horizontal and vertical direction. This is changed to:

$$\begin{aligned} \sum M_H &= F_s \cdot e_s \cdot \gamma_N + (F_{w,2} \cdot e_{w,2} - F_{w,1} \cdot e_{w,1}) \cdot \gamma_F \\ &= 298 \cdot 3.5 \cdot 1.0 + (554 \cdot 3.5 - 125 \cdot 1.67) \cdot 1.25 = 3206 \text{ kNm/m} \\ \sum M_V &= F_{u,1} \cdot e_{u,1} \cdot \gamma_N - F_{u,2} \cdot e_{u,2} \cdot \gamma_F \\ &= 503 \cdot 0.07 \cdot 1.0 - 277 \cdot 1.6 \cdot 1.25 = 517 \text{ kNm/m} \\ \sum M &= \sum M_H + \sum M_V \\ &= 3206 + 517 = 3723 \text{ kNm/m} \\ \sum V &= F_G \cdot \gamma_{fav} - F_{u,1} \cdot \gamma_N - F_{u,2} \cdot \gamma_F \\ &= 1946 \cdot 0.9 - 503 \cdot 1.0 - 277 \cdot 1.25 = 893 \text{ kN/m} \end{aligned}$$

The eccentricity and unity check corresponding to this load situation for the basis layout is:

$$e_R = \frac{\sum M}{\sum V} = \frac{3723}{893} = 4.18m$$

$$UC = \frac{e_R}{\frac{1}{6}B} = \frac{4.18}{1.67} = 2.5$$

The results for all the widths of the caisson can be seen in Figure F.14.

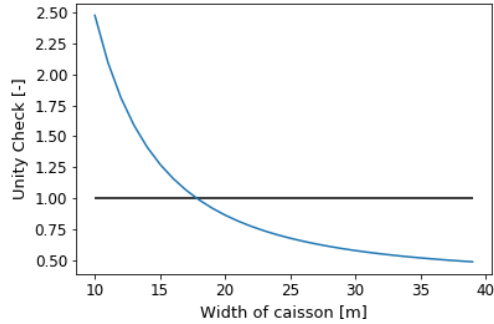


Figure F.14: Unity Check Rotational Stability

### F.1.4. Bearing Capacity

The bearing capacity of the soil,  $p'_{max}$ , must be larger than the acting stresses due to the self weight of the caisson and the forces acting on the caisson,  $\sigma_{k,max}$ . More information about the method used for the bearing capacity can be found in Chapter 6.

$$p'_{max} \geq \sigma_{k,max}$$

with:

$$p'_{max} = c' N_c s_c i_c + q' N_q s_q i_q + 0.5 \gamma' B' N_\gamma s_\gamma i_\gamma \quad \text{and} \quad \sigma_{k,max} = \frac{\sum V}{B_{eff}}$$

#### F.1.4.1. Load situation

The governing load situation for the bearing capacity is situation two, see Figure F.13. The reason for this is the higher resulting moment and therefore the higher eccentricity of the resulting force. This situation has the following moments and forces:

$$\begin{aligned} \sum M_H &= F_s \cdot e_s \cdot \gamma_N + (F_{w,2} \cdot e_{w,2} - F_{w,1} \cdot e_{w,1}) \cdot \gamma_F \\ &= 298 \cdot 3.5 \cdot 1.0 + (554 \cdot 3.5 - 126 \cdot 1.67) \cdot 1.25 = 3206 \text{ kNm/m} \\ \sum M_V &= -F_{u,1} \cdot e_{u,1} \cdot \gamma_N + F_{u,2} \cdot e_u \cdot \gamma_F \\ &= -503 \cdot 0.07 \cdot 1.0 + 277 \cdot 1.6 \cdot 1.25 = 517 \text{ kNm/m} \\ \sum M &= \sum M_H + \sum M_V \\ &= 3206 + 517 = 3725 \text{ kNm/m} \end{aligned}$$

$$\begin{aligned}
\sum V_1 &= F_G \cdot \gamma_{unfav} - F_{u,1} \cdot \gamma_N - F_{u,2} \cdot \gamma_F \\
&= 1936 \cdot 1.2 - 503 \cdot 1.0 - 277 \cdot 1.25 = 1475 \text{ kN/m} \\
\sum V_2 &= F_G \cdot \gamma_{fav} - F_{u,1} \cdot \gamma_N - F_{u,2} \cdot \gamma_F \\
&= 1936 \cdot 0.9 - 503 \cdot 1.0 - 277 \cdot 1.25 = 894 \text{ kN/m} \\
\sum H &= F_s \cdot \gamma_N - (F_{w,1} - F_{w,2}) \cdot \gamma_F \\
&= 298 \cdot 1.0 - (126 - 554) \cdot 1.25 = 834 \text{ kN/m}
\end{aligned}$$

For the eccentricity of the resulting force, the self weight of the caisson has to be taken favourable and therefore a load factor of 0.9.

$$e_R = \frac{\sum M}{\sum V_2} = \frac{3725}{894} = 4.18 \text{ m}$$

The effective width is therefore equal to:

$$B' = B - 2e_R = 10 - 2 \cdot 4.18 = 1.64 \text{ m}$$

### F.1.4.2. Bearing capacity of sand layer

The bearing capacity of the subsoil below the caisson may not be exceeded. To calculate the bearing capacity of the subsoil, the Brinch Hansen method is used, Formula F.11.

$$p'_{max} = c' N_c s_c i_c + q' N_q s_q i_q + 0.5 \gamma' B' N_\gamma s_\gamma i_\gamma \quad (\text{F.11})$$

where:	$p'_{max}$	[kN/m <sup>2</sup> ]	=	the resisting bearing capacity
	$c'$	[kN/m <sup>2</sup> ]	=	the cohesion value of the soil
	$N_c, N_q, N_\gamma$	[-]	=	the bearing force factor
	$s_c, s_q, s_\gamma$	[-]	=	the foundation shape factor
	$i_c, i_q, i_\gamma$	[-]	=	the horizontal load factor
	$q'$	[kN/m <sup>2</sup> ]	=	the effective stress at the depth net to the foundation
	$\gamma'$	[kN/m <sup>3</sup> ]	=	the effective volumetric weight
	$B'$	[m]	=	the effective width

The bearing force factors depend on the angle of internal friction of the soil,  $\phi'$ . A higher angle of internal friction leads to a higher bearing capacity. The relation between the angle of internal friction and the bearing force factors are:

$$\begin{aligned}
N_c &= (N_q - 1) \cot(\phi') \\
&= (13.32 - 1) \cot(27) = 24.1 \\
N_q &= \frac{1 + \sin(\phi')}{1 - \sin(\phi')} \exp^{\pi \tan(\phi')} \\
&= \frac{1 + \sin(27)}{1 - \sin(27)} \exp^{\pi \tan(27)} = 13.32 \\
N_\gamma &= 2(N_q - 1) \tan(\phi') \\
&= 2(13.32 - 1) \tan(27) = 12.6
\end{aligned}$$

For the sand layer ( $\phi_d = 27^\circ$ ) this results in  $N_c = 24.1$ ,  $N_q = 13.32$  and  $N_\gamma = 12.6$ . The foundation shape factors depends on the shape of the foundation. For rectangular foundations, the shape factors are defined as, in which the width (B) is the shortest side of the foundation:

$$\begin{aligned}
s_c &= 1 + 0.2 \frac{B'}{L} \\
&= 1 + 0.2 \frac{10 - 2 \cdot 4.18}{52} = 1.01 \\
s_q &= 1 + \frac{B'}{L} \sin(\phi') \\
&= 1 + \frac{10 - 2 \cdot 4.18}{52} \sin(27) = 1.02 \\
s_\gamma &= 1 - 0.3 \frac{B'}{L} \\
&= 1 - 0.3 \frac{10 - 2 \cdot 4.18}{52} = 0.99
\end{aligned}$$

The width of the basis layout is 10 m and the length is 4 times the length of a single pipe in the caisson, 52 m (4x13m). This leads to a  $s_c$ ,  $s_q$  and  $s_\gamma$  of respectively 1.01, 1.02, 0.99. The factors for horizontal load are depending on the value of the horizontal load, the orientation of the force and the cohesion of the soil,  $c'$ . The cohesion of sand is equal to 0.

$$\begin{aligned}
i_c &= i_q - \frac{1 - i_q}{N_c \cdot \tan(\phi')} \\
&= 0.19 - \frac{1 - 0.19}{24.1 \cdot \tan(27)} = 0.13 \\
i_q &= \left(1 - \frac{H}{V + Ac' \cot(\phi')}\right)^m \\
&= \left(1 - \frac{834}{894}\right)^{1.97} = 0.19 \\
i_\gamma &= \left(1 - \frac{H}{V + Ac' \cot(\phi')}\right)^{m+1} \\
&= \left(1 - \frac{834}{894}\right)^{2.97} = 0.08
\end{aligned}$$

with:

$$m = \frac{2 + \frac{B'}{L'}}{1 + \frac{B'}{L'}} = \frac{2 + \frac{10 - 2 \cdot 4.18}{52}}{1 + \frac{10 - 2 \cdot 4.18}{52}} = 1.97$$

With the use of all these parameters the bearing capacity of the soil is determined. The cohesion of sand is equal to 0 as mentioned before and the effective stress at the depth net to the foundation is also 0.

$$\begin{aligned}
p'_{max} &= c' N_c s_c i_c + q' N_q s_q i_q + 0.5 \gamma' B' N_\gamma s_\gamma i_\gamma \\
&= 0.5 \gamma' B' N_\gamma s_\gamma i_\gamma \\
&= 0.5 \cdot 10 \cdot 1.64 \cdot 12.6 \cdot 0.99 \cdot 0.08 = 8.71 \text{ kN/m}^2
\end{aligned}$$

This calculation is done for all the other possible widths of the caisson, see Figure F.15.

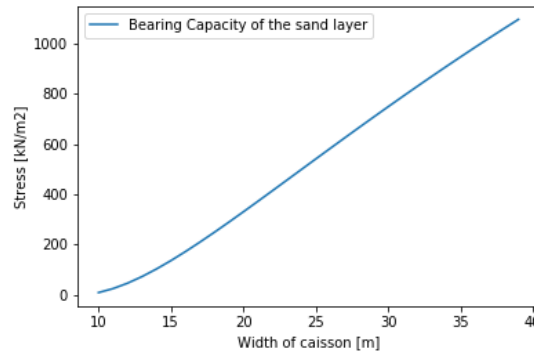


Figure F.15: Bearing capacity of the sand layer

### F.1.4.3. Acting Stresses

This bearing capacity is compared to the maximum acting stress on the soil due to the caisson. This maximum acting stress is determined by Formula F.12.

$$\sigma_{k,max} = \frac{\sum V}{B'} \quad (\text{F.12})$$

For the acting stress on the soil, the self-weight of the caisson has to be taken unfavourable,  $\gamma_{unfav} = 1.2$ . This leads to a  $\sigma_{k,max}$  of 899 kN/m<sup>2</sup>.

$$\sigma_{k,max} = \frac{\sum V_1}{B'} = \frac{1475}{1.64} = 899 \text{ kN/m}^2$$

This calculation is done for each width of the caisson, see Figure F.16

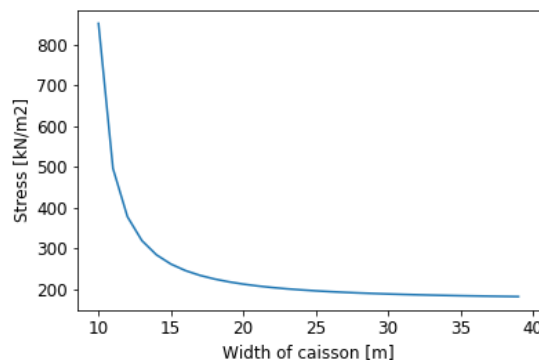


Figure F.16: Acting stresses on soil

Comparing the acting stresses to the bearing capacity leads to the following figure, see Figure F.17a. The unity check of the bearing capacity is shown in Figure F.17b. It can be concluded that a minimum of 17 m width is required to meet the bearing capacity requirement.

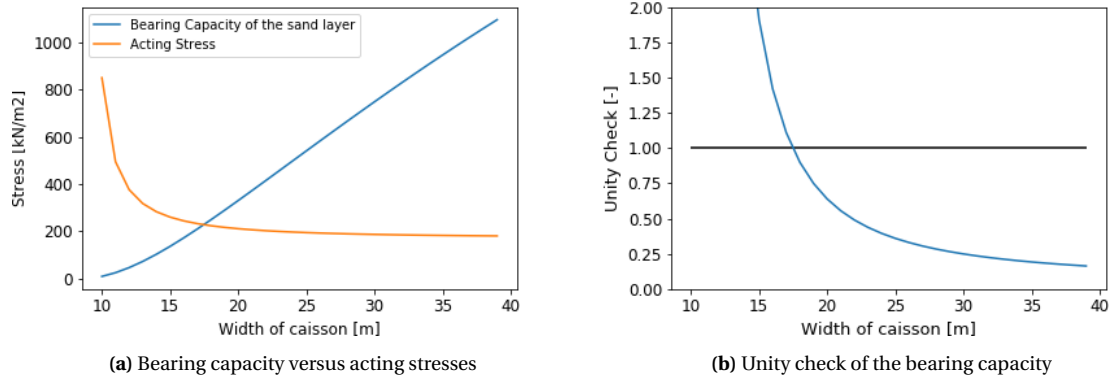


Figure F.17: Bearing capacity of the caisson

### F.1.5. Draught

For the transportation of the caisson, the draught is important. The draught should not exceed the height of the caisson and sufficient clearance should be available during transport and positioning. The minimum clearance during transport should be 1 m and the top of the caisson should be at least 0.5 m above the water level. The draught of the caisson is determined with Formula F.13.

$$d = \frac{F_G}{B \cdot L \cdot \gamma_w} \tag{F.13}$$

- where:
- $d$  [m] = the draught of the caisson
  - $F_G$  [kN] = the self weight of the caisson
  - $B$  [m] = the width of the caisson
  - $L$  [m] = the length of the caisson
  - $\gamma_w$  [kN/m<sup>3</sup>] = the specific weight of salt water (=10.06)

The self-weight of the caisson during transport and positioning is the weight excluding the ballast, 1056 kN/m for the basis layout.

$$d = \frac{F_G}{B \cdot L \cdot \gamma_w} = \frac{1056}{10 \cdot 1 \cdot 10.06} = 10.49m$$

In Figure F.18, the draught of the caisson can be seen for each width. It can be concluded that the clearance requirement is no problem and the minimal width for the draught compared to the height of the caisson is 14 m.

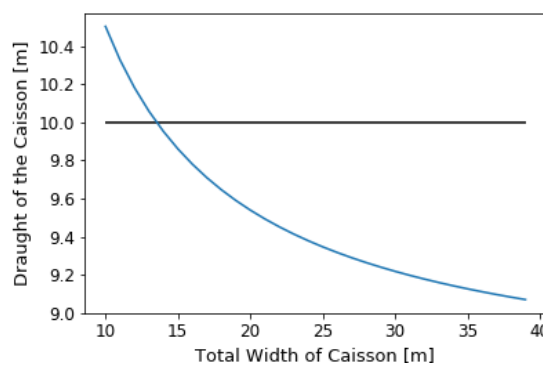


Figure F.18: Draught of the Caisson

### F.1.6. Floating Stability

During transportation and immersion the caisson needs to be stable. The stability during transport and immersion is determined by the metacentric height. If this height is above 0.5 m, there is no static stability problem. The metacentric height is defined as:

$$h_m = \overline{GM} = \overline{KB} + \overline{BM} - \overline{KG} \geq 0.5 \quad (\text{E14})$$

in which:

$$\begin{aligned} \overline{KB} &= \frac{1}{2}d \\ \overline{BM} &= \frac{I}{V} \\ \overline{KG} &= \frac{\sum V_i \cdot e_i \cdot \gamma_i}{\sum V_i \cdot \gamma_i} \end{aligned}$$

The draught can be seen in Section F.1.5 and equal to 10.4 m for the basis layout. This results in a  $\overline{KB}$  of 5.2 m. The value of  $\overline{BM}$  is determined with:

$$\begin{aligned} \overline{BM} &= \frac{I}{V} = \frac{\frac{1}{12}L \cdot B^3}{L \cdot B \cdot d} = \frac{\frac{1}{12} \cdot B^2}{d} \\ &= \frac{\frac{1}{12} \cdot 10^2}{10.4} = 0.8m \end{aligned}$$

For the value of  $\overline{KG}$ , the vertical location of the gravity centre is needed. The location of the gravity centre is determined on the same way as in Section F.1.3, only difference is that the choice of reference location. This time the bottom of the caisson is used as reference.

Element	Number	Total Volume $V_i$ [m <sup>3</sup> ]	Distance $e_i$ [m]	$\gamma_i$
Outer Wall 1	2	85	5.25	25
Outer Wall 2	1	27	7.25	25
Outer Wall 3	1	27	7.25	25
Outer Wall 4	2	21	3	25
Outer Wall 5	2	21	3	25
Bottom Slab	1	120	0.5	25
Top Slab	1	120	10	25
Inner Wall 1	2	21.6	7.5	25
Inner Wall 2	1	4.8	7.5	25
Culvert Wall 1	2	36	3	25
Culvert Wall 2	1	22.5	5.25	25
Gate	1	4.8	3	78

**Table F.4:** Volume and distances of elements

With the use of these values, the value of  $\overline{KG}$  is determined.

$$\overline{KG} = \frac{\sum V_i \cdot e_i \cdot \gamma_i}{\sum V_i \cdot \gamma_i} = 5.23m$$

The metacentric height for the basis layout is equal to:

$$\begin{aligned} h_m = \overline{GM} &= \overline{KB} + \overline{BM} - \overline{KG} \\ &= 5.2 + 0.8 - 5.23 = 0.77m \end{aligned}$$

The basis layout is stable during transport because the metacentric height is above the 0.5 m. For all the other widths, the metacentric height can be found in Figure F.19. It can be concluded that the caisson is always stable.

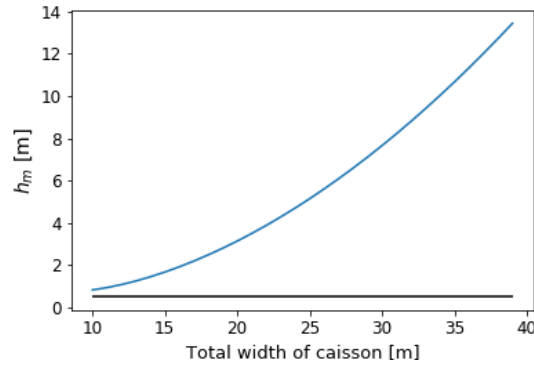


**Figure F.19:** Metacentric height of the Caisson

### F.1.7. Final Dimensions

In Table E.5, the minimum required width for each mechanism can be seen. It can be concluded that the sliding resistance is the governing situation. The minimum required width corresponding to this governing mechanism is 28 m. Therefore the caisson will have a width of 28 m and the bottom of the caisson will be roughened to increase the resistance on sliding.

Mechanism	Minimum Required Width [m]
Sliding Resistance	28
Rotational Stability	18
Bearing Capacity	18
Draught	14
Floating Stability	-

**Table E.5:** Minimum required width

The length of the caisson will be the length of 4 times the basic length (=13 m), which leads to a total length of 52 m. The height of the caisson is 16.5 m.

Mechanism	Unity Check
Sliding Resistance	0.96
Rotational Stability	0.59
Bearing Capacity	0.27
Draught	0.92
Floating Stability	0.07

**Table E.6:** The unity checks for the final design

## F.2. Design of the caisson at the Tidal Lake Side

### F.2.1. Basis Layout and Expansion

Just like the energy storage lake side, the width of the caisson at the Tidal Lake side is determined with a basis caisson. The height of the basis caisson is 13.5 m, the width is 5 m and the length of a caisson with a single caisson is 12 m. The length of the caisson on the tidal lake side should be equal to the energy storage lake side otherwise, the conduits will not align. The height of the caisson is the minimum height that is required to fit the gate into the gate chamber. The layout of the caisson can be seen in Figure F.20.



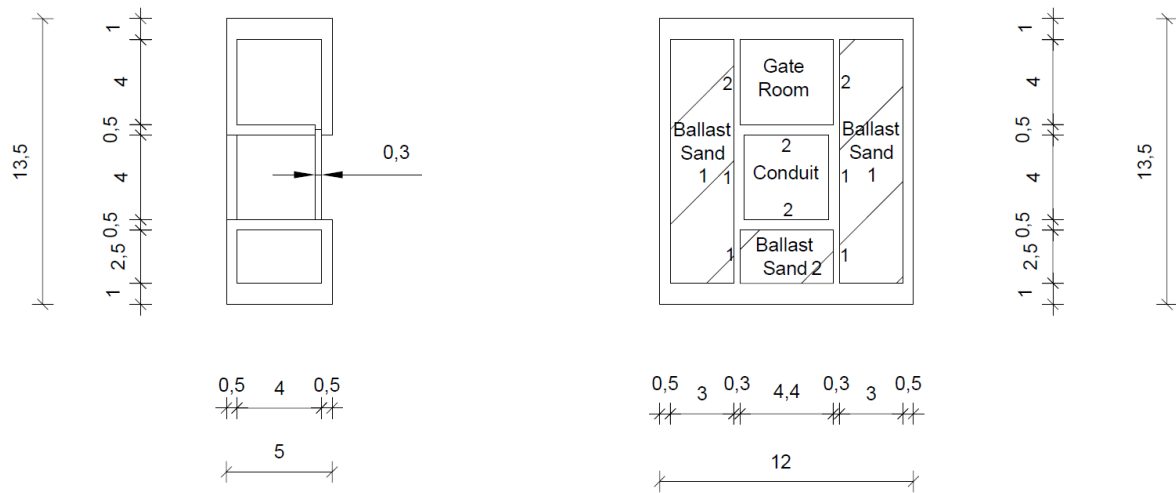


**Figure E.20:** The Layout of the Concept Siphon caisson

The self-weight of the basis caisson consists of the same elements as the caisson of the Energy Storage Lake side. In Table E.7 the self-weight of the elements of the caisson is shown.

Element	Number of Elements [-]	Volume [m <sup>3</sup> ]	Weight [kN]
Outer Wall L-direction	2	57.5	1437.5
Outer Wall B-direction	2	118	2950
Slab	2	120	3000
Inner Wall 1	2	9.6	240
Inner Wall 2	2	6	150
Culvert Wall 1	2	20	500
Culvert Wall 2	2	16	400
Ballast 1	2	276	5520
Ballast 2	1	44	880
Gate	1	4.8	374.4
<b>Total (With Ballast)</b>			<b>15452</b>
<b>Total (Without Ballast)</b>			<b>9052</b>

**Table E.7:** Self Weight of the Caisson

For the calculations the self-weight per meter length is used instead of the total self-weight of a caisson. This leads to a self-weight excluding ballast of 754 kN/m and including ballast 1288 kN/m.

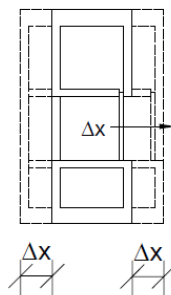


**Figure E.21:** Increase of width by  $\Delta x$

To determine the optimal width of the caisson, the width of the basis layout is increased by  $\Delta x$ , see Figure E.21. The addition weight for each increase of  $\Delta x$  can be seen in Table E.8.

Element	Additional Volume [m <sup>3</sup> ]	Additional Force [kN]
Slabs	24	600
Ballast	80	1600
Outer Wall	11.5	287.5
Culvert Wall	9	225
Inner Wall	3.9	97.5
	<b>Total (With Ballast)</b>	2813
	<b>Total (Without Ballast)</b>	1213

**Table F.8:** Increase in self weight by expansion of  $\Delta x$

The increase in self-weight per meter length excluding ballast is equal to 101 kN/m and including ballast it is equal to 234 kN/m.

### F.2.2. Sliding Resistance

The sum of the horizontal forces may not exceed the sliding resistance, otherwise the structure will move in horizontal direction. More information about the method used for the sliding resistance can be found in Chapter 6.

$$\sum H \leq R_d \tag{E15}$$

in which:

$$R_d = V'_d \cdot \tan(\delta_d)$$

#### F.2.2.1. Situation One

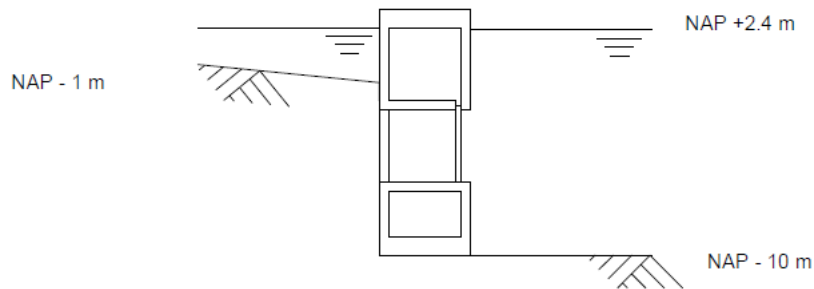


**Figure F.22:** Load Situation One

The first load situation considers the water level in the Tidal Lake at NAP + 2.4 m, see Figure F.22. The forces due to the waves are not taking into account because they have a positive effect on the stability. On the dune side of the caisson, the horizontal forces consists of the soil pressure and the water pressure. The pressures and forces can be seen in Figure F.23.

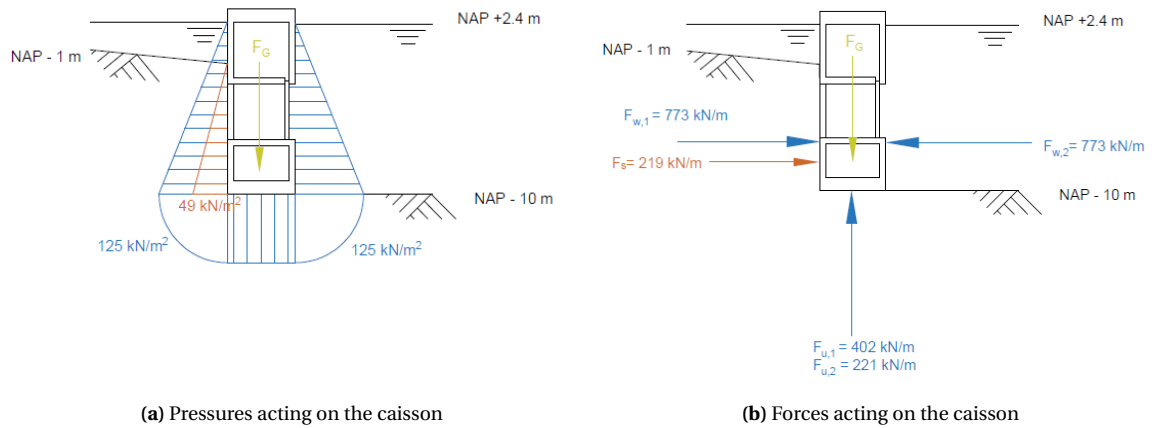


**Figure F.23:** Pressures and forces acting on the caisson

With these forces the sum in vertical and horizontal direction are calculated including the load factors.

$$\begin{aligned}
 V'_d &= F_G \cdot \gamma_{fav} - F_{u,1} \cdot \gamma_N - F_{u,2} \cdot \gamma_F \\
 &= 1288 \cdot 0.9 - 402 \cdot 1.0 - 221 \cdot 1.25 \\
 &= 480 \text{ kN/m} \\
 \sum H &= F_s \cdot \gamma_N + F_{w,1} - F_{w,2} \\
 &= 219 \cdot 1.0 + 773 - 773 \\
 &= 219 \text{ kN/m}
 \end{aligned}$$

The vertical forces lead to a sliding resistance of:

$$R_d = V'_d \cdot \tan(\delta_d) = 480 \cdot \tan(21.67) = 156 \text{ kN/m}$$

The unity check for the basis layout is:

$$UC = \frac{\sum H}{R_d} = \frac{196}{156} = 1.26$$

The results of the unity check for all other widths can be seen in Figure F.24. It can be concluded that for this situation, the minimum width is 7 m.

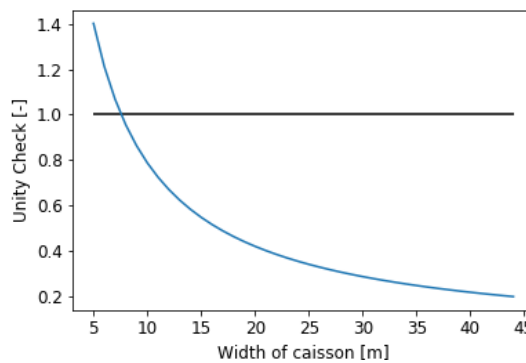


**Figure F.24:** Unity check sliding resistance situation one

**F.2.2.2. Situation Two**

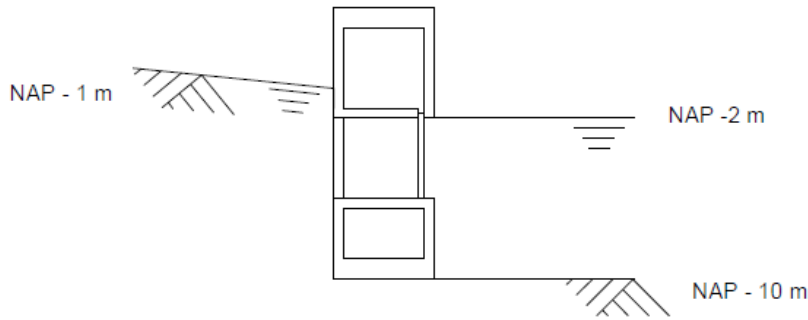
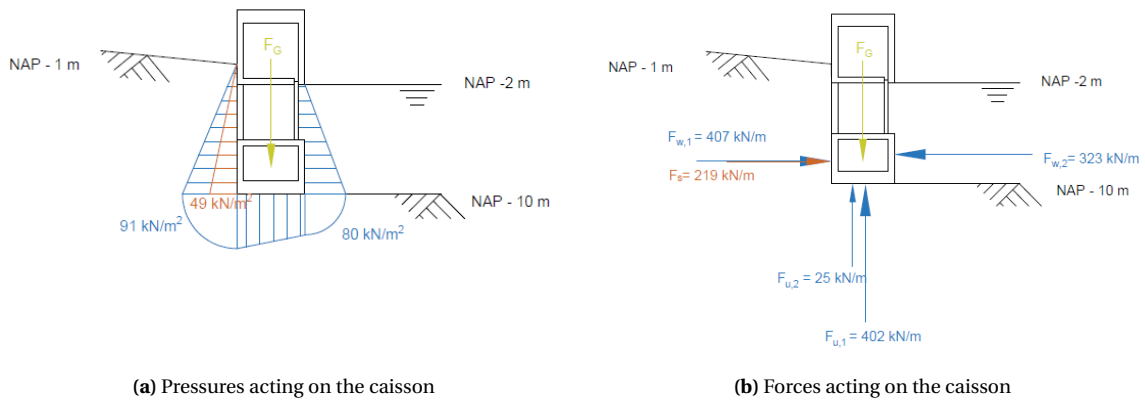


**Figure E.25: Load Situation One**

The second load situation considers the lower water level in the Tidal Lake of NAP - 2 m, see Figure E.25. Again, the other horizontal forces at the water side are caused by the waves. On the dune side of the caisson, the horizontal forces consists of the soil pressure and the water pressure in the soil. It is assumed that the soil below the conduit is saturated. The pressures and forces can be seen in Figure E.26.



**(a) Pressures acting on the caisson**

**(b) Forces acting on the caisson**

**Figure E.26: Pressures and forces acting on the caisson**

For this situation, the same formulas as in situation one are used.

$$\begin{aligned}
 V'_d &= F_G \cdot \gamma_{fav} - F_{u,1} \cdot \gamma_N - F_{u,2} \cdot \gamma_F \\
 &= 1288 \cdot 0.9 - 402 \cdot 1.0 - 25 \cdot 1.25 \\
 &= 725 \text{ kN/m} \\
 \sum H &= F_s \cdot \gamma_N + F_{w,1} - F_{w,2} \\
 &= 219 \cdot 1.0 + 407 - 322 \\
 &= 324 \text{ kN/m}
 \end{aligned}$$

The vertical forces lead to a sliding resistance of:

$$R_d = V'_d \cdot \tan(\delta_d) = 725 \cdot \tan(21.67) = 236 \text{ kN/m}$$

The unity check for the basis layout is:

$$UC = \frac{\sum H}{R_d} = \frac{324}{236} = 1.38$$

The results of the unity checks for the other widths can be seen in Figure F.27. It can be concluded that a minimum width of 8 m is required.

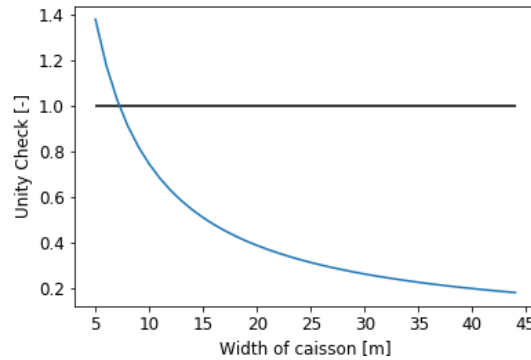


Figure F.27: Unity check sliding resistance situation two

### F.2.3. Rotational Stability

If the eccentricity of the resulting force is exceeding the boundaries of the core of the caisson, the caisson will rotate. Therefore, the eccentricity may not exceed the boundaries of the core. More information about the method used for the rotational stability can be found in Chapter 6.

$$-\frac{1}{6}B \leq e_R \leq \frac{1}{6}B \tag{E.16}$$

with:

$$e_R = \frac{\sum M}{\sum V}$$

#### F.2.3.1. Horizontal location of the gravity centre

For the vertical forces, the location of the gravity centre is important. The location of the gravity centre compared to a certain reference point, in this case the left outer wall, can be determined by:

$$x_G = \frac{\sum V_i \cdot e_i \cdot \gamma_i}{\sum V_i \cdot \gamma_i} \tag{E.17}$$

where:  $x_G$  [m] = the distance of the gravity centre from the rotation point  
 $V_i$  [m<sup>3</sup>] = the volume of a single element  
 $e_i$  [m] = the distance of the element from the rotation point  
 $\gamma_i$  [kN/m<sup>3</sup>] = the density of the element

For the basis layout of the caisson, the volumes of each element and the distances from the left side of the caisson can be found in Table F.9.

Element	Number	Total Volume $V_i$ [m <sup>3</sup> ]	Distance $e_i$ [m]	$\gamma_i$
Outer Wall 1	2	57.5	2.5	25
Outer Wall 2	1	27	0.25	25
Outer Wall 3	1	27	4.75	25
Outer Wall 4	1	18	0.25	25
Outer Wall 5	1	18	4.75	25
Outer Wall 6	2	7	0.25	25
Outer Wall 7	2	7	4.75	25
Bottom Slab	1	60	2.5	25
Top Slab	1	60	2.5	25
Inner Wall 1	2	3	2.5	25
Inner Wall 2	2	4.8	2.5	25
Culvert Wall 1	2	10	2.5	25
Culvert Wall 2	1	8	2.5	25
Gate	1	4.8	4.35	78
Ballast 1	2	276	2.5	20
Ballast 2	1	44	2.5	20

**Table E.9:** Volume and distances of elements

This results in the following location of the gravity centre compared to the left side (Dune side) of the caisson.

$$x_G = \frac{\sum V_i \cdot e_i \cdot \gamma_i}{\sum V_i \cdot \gamma_i} = 2.54m$$

In Figure E.28, the distance between the gravity centre and the middle of the caisson (B/2) can be seen. Positive values mean that the gravity centre is on the right side of the middle.

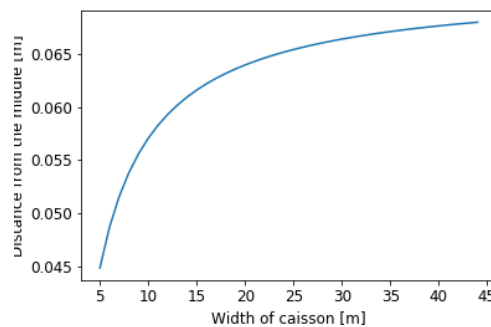


**Figure E.28:** Distance between the gravity centre and B/2

### E.2.3.2. Situation One

In the rotational stability, the forces are equal to the forces in the sliding resistance. However, the arm of the forces is relevant in the calculation of the moment. The arm of the forces can be seen in Figure E.29.

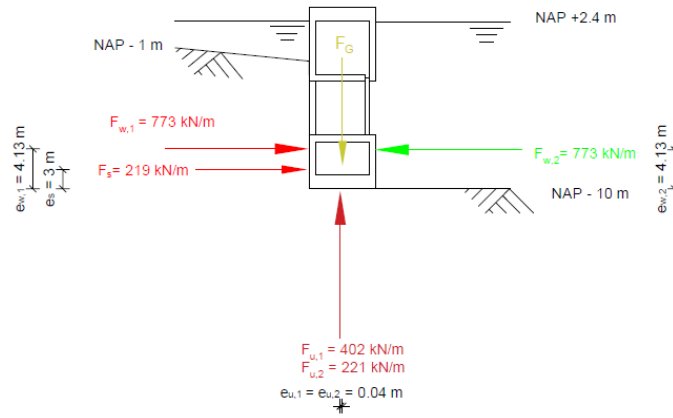


Figure E.29: Forces and distances

For the rotational stability, the sum of the forces and the moments are determining the eccentricity. These are retrieved by using the following formulas.

$$\begin{aligned} \sum M_H &= F_s \cdot e_s \cdot \gamma_N \\ &= 219 \cdot 3 \cdot 1.0 = 658 \text{ kNm/m} \\ \sum M_V &= F_{u,1} \cdot e_u \cdot \gamma_N + F_{u,2} \cdot e_u \cdot \gamma_F \\ &= 402 \cdot 0.04 \cdot 1.0 + 221 \cdot 0.04 \cdot 1.25 = 30 \text{ kNm/m} \\ \sum M &= \sum M_H + \sum M_V \\ &= 658 + 30 = 688 \text{ kNm/m} \\ \sum V &= F_G \cdot \gamma_{fav} - F_{u,1} \cdot \gamma_N - F_{u,2} \cdot \gamma_F \\ &= 1288 \cdot 0.9 - 402 \cdot 1.0 - 221 \cdot 1.25 = 480 \text{ kN/m} \end{aligned}$$

The eccentricity corresponding to these values is:

$$e_R = \frac{\sum M}{\sum V} = \frac{688}{480} = 1.43 \text{ m}$$

The unity check for the basis layout is equal to:

$$UC = \frac{e_R}{\frac{1}{6}B} = \frac{1.43}{\frac{1}{6}5} = 1.72$$

In Figure E.30, the value of the unity check for each width for the rotational stability can be found. It can be concluded that the minimum required width to overcome rotational stability problems is 7 m.

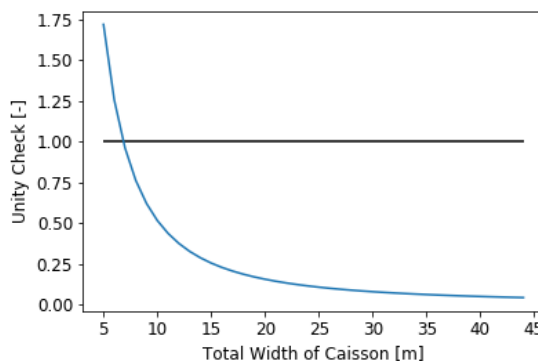
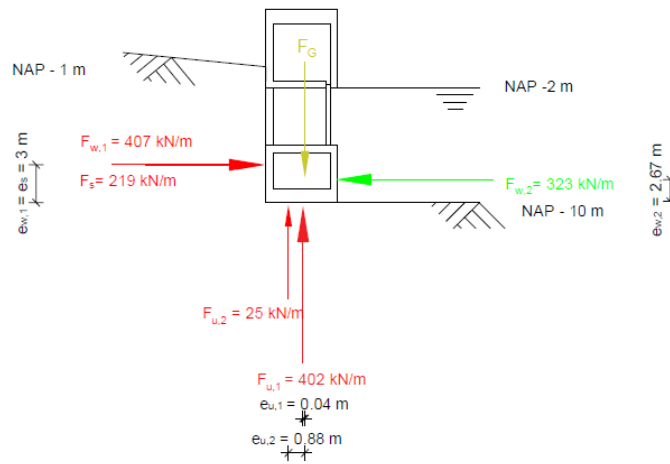


Figure E.30: Unity check rotational stability situation two

### F.2.3.3. Situation Two

In Figure F31, the forces and their corresponding arm can be seen.



**Figure F31:** Forces and distances

This results in the following moments and resulting forces.

$$\begin{aligned} \sum M_H &= F_s \cdot e_s \cdot \gamma_N + F_{u,1} \cdot e_{u,1} \cdot \gamma_N + F_{u,2} \cdot e_{u,2} \cdot \gamma_F \\ &= 219 \cdot 3 \cdot 1.0 + 407 \cdot 3 \cdot 1 + 322 \cdot 2.67 \cdot 1.25 = 1113 \text{ kNm/m} \\ \sum M_V &= F_{u,1} \cdot e_u \cdot \gamma_N + F_{u,2} \cdot e_u \cdot \gamma_F \\ &= 402 \cdot 0.04 \cdot 1.0 + 25 \cdot 0.88 \cdot 1.25 = 46 \text{ kNm/m} \\ \sum M &= \sum M_H + \sum M_V \\ &= 1113 + 46 = 1159 \text{ kNm/m} \\ \sum V &= F_G \cdot \gamma_{fav} - F_{u,1} \cdot \gamma_N - F_{u,2} \cdot \gamma_F \\ &= 1288 \cdot 0.9 - 402 \cdot 1.0 - 25 \cdot 1.25 = 725 \text{ kN/m} \end{aligned}$$

The eccentricity corresponding to these values is:

$$e_R = \frac{\sum M}{\sum V} = \frac{1159}{725} = 1.6 \text{ m}$$

The unity check for the basis layout is equal to:

$$UC = \frac{e_R}{\frac{1}{6}B} = \frac{1.6}{\frac{1}{6}5} = 1.92$$

In Figure F32, the value of the unity check for each width for the rotational stability can be found. It can be concluded that the minimum required width to overcome rotational stability problems is 8 m.



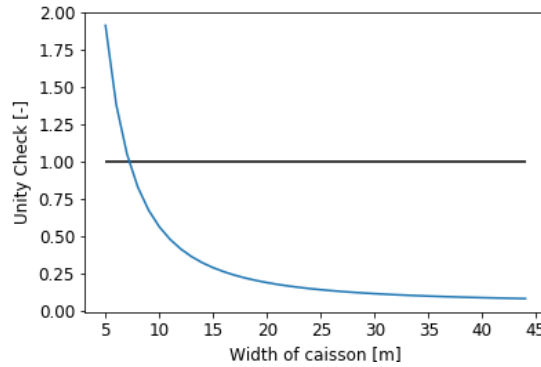


Figure F.32: Unity check rotational stability situation two

### F.2.4. Bearing Capacity

The bearing capacity of the soil,  $p'_{max}$ , must be larger than the acting stresses due to the self weight of the caisson and the forces acting on the caisson,  $\sigma_{k,max}$ . More information about the method used for the bearing capacity can be found in Chapter 6.

$$p'_{max} \geq \sigma_{k,max}$$

with:

$$p'_{max} = c' N_c s_c i_c + q' N_q s_q i_q + 0.5 \gamma' B' N_\gamma s_\gamma i_\gamma \quad \text{and} \quad \sigma_{k,max} = \frac{\sum V}{B_{eff}}$$

#### F.2.4.1. Governing Situation

Situation two is the governing situation for the bearing capacity due to the low uplift pressure which leads to a high resulting downward force. The forces and moments in this situation are shown below:

$$\begin{aligned} \sum M_H &= 1113 \text{ kNm/m} \\ \sum M_V &= 46 \text{ kNm/m} \\ \sum M &= 1159 \text{ kNm/m} \\ \sum V &= 725 \text{ kN/m} \quad (\text{Self Weight Favourable}) \\ \sum H &= 324 \text{ kN/m} \end{aligned}$$

For the eccentricity of the resulting force, the self weight is a favourable load but for the remainder of the bearing capacity, the self weight is unfavourable.

$$\begin{aligned} \sum V &= F_G \cdot \gamma_{fav} - F_{u,1} \cdot \gamma_N - F_{u,2} \cdot \gamma_F \\ &= 1288 \cdot 1.2 - 402 \cdot 1.0 - 25 \cdot 1.25 = 1112 \text{ kN/m} \quad (\text{Self Weight Unfavourable}) \end{aligned}$$

The eccentricity of the resulting force in situation two is equal to:

$$e_R = \frac{\sum M}{\sum V} = \frac{1159}{725} = 1.6 \text{ m}$$

The effective width for the basis layout is therefore equal to;

$$B' = B - 2e_R = 5 - 2 \cdot 1.6 = 1.8 \text{ m}$$

### F.2.4.2. Bearing capacity of sand layer

The bearing capacity of the subsoil below the caisson may not be exceeded. To calculate the bearing capacity of the subsoil, the Brinch Hansen method is used, Formula F.18. As mentioned for the Energy Storage Lake side, the first two parts of the equations can be neglected.

$$p'_{max} = c' N_c s_c i_c + q' N_q s_q i_q + 0.5 \gamma' B' N_\gamma s_\gamma i_\gamma \quad (F.18)$$

The factors of the formula are depending on the length and the width of the foundation but also on the horizontal forces acting on the foundation. The foundation has the same length as the energy storage lake side (52 m) but has a width of 5 m for the basis layout. The values for the N factor are only depending on the type of soil and is not changing for this side. Therefore  $N_c = 24.1$ ,  $N_q = 13.32$  and  $N_\gamma = 12.6$ . The other parameters are recalculated:

$$s_c = 1 + 0.2 \frac{B'}{L} = 1 + 0.2 \frac{5 - 2 \cdot 1.6}{52} = 1.02$$

$$s_q = 1 + \frac{B'}{L} \sin(\phi') = 1 + \frac{5 - 2 \cdot 1.6}{52} \sin(27) = 1.02$$

$$s_\gamma = 1 - 0.3 \frac{B'}{L} = 1 - 0.3 \frac{5 - 2 \cdot 1.6}{52} = 0.99$$

$$m = \frac{2 + \frac{B'}{L}}{1 + \frac{B'}{L}} = \frac{2 + \frac{5 - 2 \cdot 1.6}{52}}{1 + \frac{5 - 2 \cdot 1.6}{52}} = 1.96$$

$$i_c = i_q - \frac{1 - i_q}{N_c \cdot \tan(\phi')} = 0.51 - \frac{1 - 0.51}{24.1 \cdot \tan(27)} = 0.047$$

$$i_q = \left(1 - \frac{H}{V}\right)^m = \left(1 - \frac{324}{1112}\right)^{1.96} = 0.51$$

$$i_\gamma = \left(1 - \frac{H}{V}\right)^{m+1} = \left(1 - \frac{324}{1112}\right)^{2.96} = 0.36$$

With the use of all these parameters the bearing capacity of the soil is determined.

$$p'_{max} = 0.5 \gamma' B' N_\gamma s_\gamma i_\gamma$$

$$= 0.5 \cdot 10 \cdot 1.8 \cdot 12.6 \cdot 0.99 \cdot 0.36 = 39.94 \text{ kN/m}^2$$

This calculation is done for all the other possible widths of the caisson, see Figure F.33.

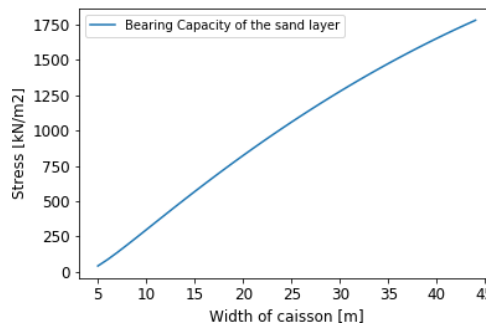


Figure F.33: Bearing capacity of the sand layer

### F.2.4.3. Acting Stresses

This bearing capacity is compared to the maximum acting stress on the soil due to the caisson. This maximum acting stress is determined by Formula F.19.

$$\sigma_{k,max} = \frac{\sum V}{B'} \tag{E.19}$$

For the acting stress on the soil, the self weight of the caisson has to be taken unfavourable,  $\gamma_{unfav} = 1.2$ . This leads to a  $\sigma_{k,max}$  of 885 kN/m<sup>2</sup>

$$\sigma_{k,max} = \frac{\sum V}{B'} = \frac{1112}{1.8} = 618 \text{ kN/m}^2$$

This calculation is done for each width of the caisson, see Figure E.34.

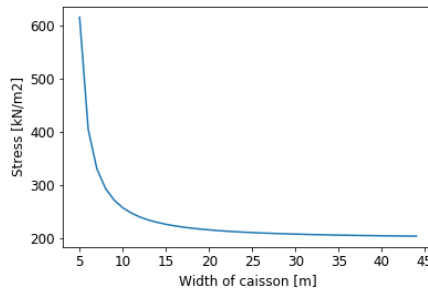
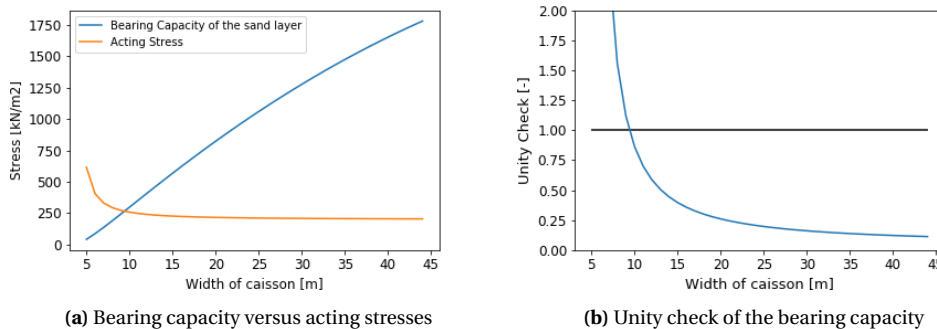


Figure E.34: Acting stresses on soil

Comparing this to the values of the bearing capacity, Figure E.35a and Figure E.35b, it can be concluded that a minimum width of 10 m is needed.



(a) Bearing capacity versus acting stresses

(b) Unity check of the bearing capacity

Figure E.35: Bearing capacity of the caisson

### F.2.5. Draught

The self weight of the caisson during transport and positioning is the weight excluding the ballast, 754 kN/m for the basis layout.

$$d = \frac{F_G}{B \cdot L \cdot \gamma_w} = \frac{754}{5 \cdot 1 \cdot 10.06} = 15 \text{ m}$$

In Figure E.36, the draught of the caisson can be seen for each width. It can be concluded that there is not sufficient clearance during transport. Transporting the caisson will not be an feasible option.

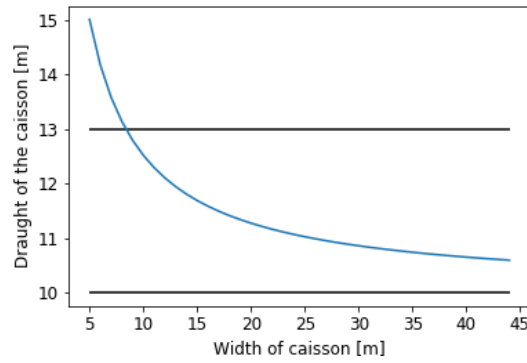


Figure E.36: Draught of caisson

### F.2.6. Final Dimensions

For the stability requirements, the following minimal widths are required to ensure stability:

Mechanism	Minimal Width [m]
Sliding Resistance	8
Rotational Stability	8
Bearing Capacity	10

Table F.10: Minimum required width

The governing mechanism is the bearing capacity of the soil. Therefore the minimum width should be 10 m. For the final design there is chosen for a width of 10 m. This leads to the following unity checks:

Mechanism	Unity Check
Sliding Resistance	0.78
Rotational Stability	0.57
Bearing Capacity	0.86

Table F.11: Unity Checks

The length of the caisson will be equal to the length of the energy storage lake side and therefore 4x13m (= 52m). The height of the caisson will be 13.5 m.

# G

## Retaining Height

The spillway is part of the primary flood defence line and therefore the height of the structure is very important. During normal conditions, the spillway should retain water and therefore a sufficient height is needed. The required retaining height depends on the design of the structure. For the open channel flow concepts and the caisson concept there is looked at the retaining height of a vertical structure. Although the waves in the energy storage lake (1.48 m) are higher than the waves in the tidal lake (1 m), the tidal lake side is governing due to the higher occurring water levels. Therefore only this side will be used for the calculation of the height of the structure.

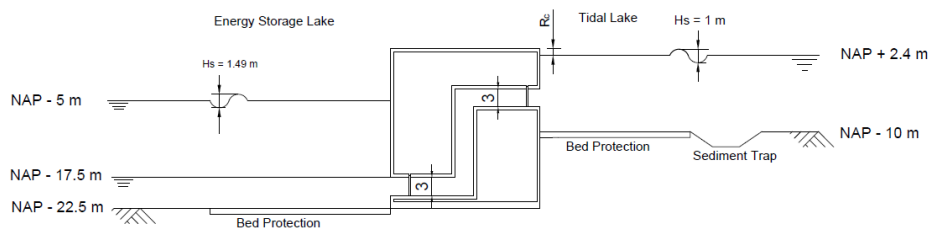


**Figure G.1:** The location of the freeboard ( $R_c$ )

The top of the structure of the concept Caisson and concept Ogee is depending on the required freeboard,  $R_c$ , that is needed to avoid excessive overtopping. The freeboard can be seen in Figure G.1. The freeboard is depending on the water level, the incoming waves and the wind set up. The latter can be neglected as mentioned before. To determine the freeboard, the following points needed to be investigated according to EurOtop 2018:

1. Is there a influencing foreshore?
2. Are the waves impulsive or non impulsive?

The first point is depending on the water condition: shallow, transitional or deep water. In shallow and transitional water, the foreshore has an influence. Only if there is a influencing foreshore, it should be checked if the waves are impulsive or not. In Appendix D, it is determined that deep water conditions are present. Therefore, there is no influencing foreshore and the distinction between impulsive or non impulsive waves is not relevant anymore. As a result of this, the freeboard is calculated with:

$$\frac{q}{\sqrt{gH_{m0}^3}} = 0.054 \cdot \exp\left(-2.12 \frac{R_c}{H_{m0}}\right)^{1.3} \quad (\text{G.1})$$

where:  $q$  [m<sup>2</sup>/s] = the overtopping discharge  
 $H_{m0}$  [m] = the significant wave height  
 $R_c$  [m] = the freeboard  
 $g$  [m/s<sup>2</sup>] = the gravitational acceleration (= 9.81 m/s<sup>2</sup>)

The tolerable overtopping discharge,  $q$ , is limited by the use of the structure. For the concepts with vertical walls, the tolerable overtopping discharge is limited by the maximum allowable overtopping when people are standing on it. The reason for this is that during a storm, inspection must be possible if required due to problems in operation. This results in a tolerable overtopping discharge of 10 l/s/m for waves with  $H_{m0}$  of approximately 1 m (Van der Meer et al., 2018).

$$\frac{q}{\sqrt{gH_{m0}^3}} = 0.054 \cdot \exp\left(-2.12 \frac{R_c}{H_{m0}}\right)^{1.3}$$

$$\rightarrow \frac{0.01}{\sqrt{9.81 \cdot 1^3}} = 0.054 \cdot \exp\left(-2.12 \frac{R_c}{1}\right)^{1.3}$$

$$\rightarrow R_c = 1.03 \text{ m}$$

So the required freeboard for a vertical structure is 1.03 m.

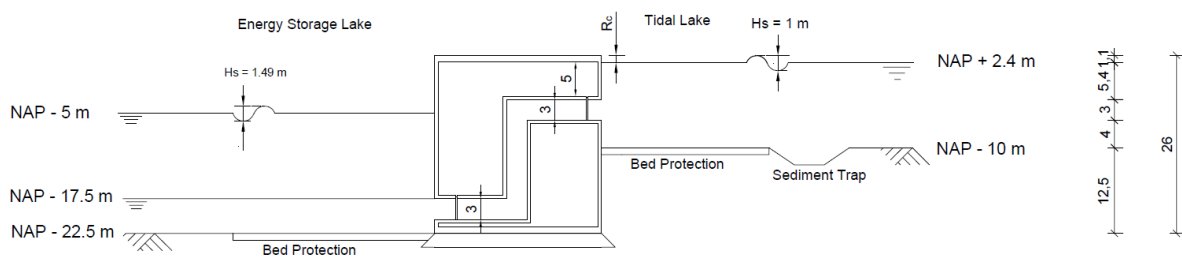


**Figure G.2:** Height of the caisson(NTS)

# H

## Stability Concept Caisson

In this appendix, the stability calculations for the concept Caisson can be found. The basis lay-out of the caisson is introduced and afterwards all the calculations are performed for this basis lay-out. By using the computer software of Python, the calculations are repeated for all other dimensions of the caisson. With the solutions found in this appendix, the dimensions of the caisson are determined.

### H.1. Basis Layout and Expansion

Figure H.1 shows the lay-out of the basis caisson. The width of this caisson is 34.5 m and the height is 26 m. The length of the caisson with a single conduit in it is 11 m. In the figure, the location of the conduit, ballast rooms and gate rooms can be seen. The ballast in the caissons will be saturated sand.

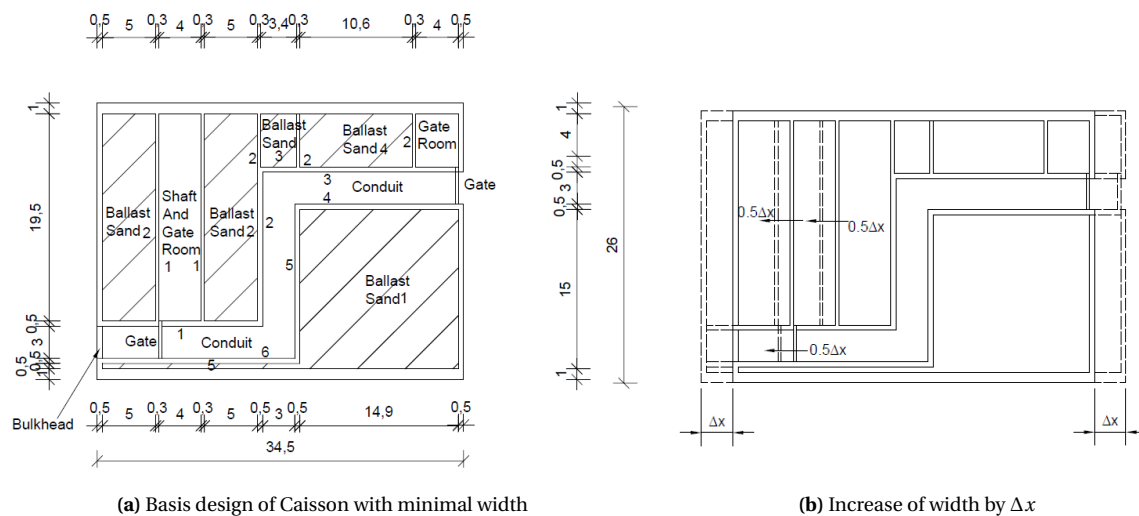


**Figure H.1:** The Layout of the Concept Caisson

The self-weight of the basis layout can be seen in Table H.1.

Element	Number of Elements [-]	Volume [m <sup>3</sup> ]	Weight [kN]
Outer Wall L-direction	2	210	5 250
Outer Wall B-direction	2	828	20 700
Slab	2	759	18 975
Inner Wall 1	2	117	2 925
Inner Wall 2	3	45	1 125
Culvert Wall 1	1	75.5	1 887.5
Culvert Wall 2	1	72.5	1 812.5
Culvert Wall 3	1	93	2 325
Culvert Wall 4	1	72	1 800
Culvert Wall 5	1	75	1 875
Culvert Wall 6	1	93	2 325
Ballast 1	1	2 235	44 700
Ballast 2	2	1 950	39 000
Ballast 3	1	170	3 400
Ballast 4	1	530	10 600
Ballast 5	1	93.75	1 875
Gate	2	18	1 404
<b>Total (With Ballast)</b>			161 979
<b>Total (Without Ballast)</b>			62 404

Table H.1: Self Weight of the Caisson

The self-weight of the basis caisson is equal to 161 979 kN if the caisson is filled with ballast. Without ballast the self-weight is equal to 62 404 kN. For the calculations, the self-weight per meter length is relevant which leads to respectively 14 725 kN/m and 5 673 kN/m.

With the expansion in width by  $\Delta x$ , the self-weight of the caisson will increase as well. The increase in self weight due to the expansion can be seen in Table H.2.

Element	Additional Volume [m <sup>3</sup> ]	Additional Force [kN]
Slabs	22	550
Ballast	200	4 000
Outer Wall	24	600
Culvert Wall	10	250
<b>Total (With Ballast)</b>		5 400
<b>Total (Without Ballast)</b>		1 400

Table H.2: Increase in self weight by expansion of  $\Delta x$ 

The increase in self-weight including the ballast material is 5 400 kN per  $\Delta x$  which is equal to 491 kN/m and for the situation excluding the ballast material, the increase is 1 400 kN or 127 kN/m.

## H.2. Sliding Resistance

The sum of the horizontal forces may not exceed the sliding resistance, otherwise the structure will move in horizontal direction. More information about the method used for the sliding resistance can be found in Chapter 6.

$$\sum H \leq R_d \quad (\text{H.1})$$

in which:

$$R_d = V'_d \cdot \tan(\delta'_d)$$



### H.2.1. Situation One

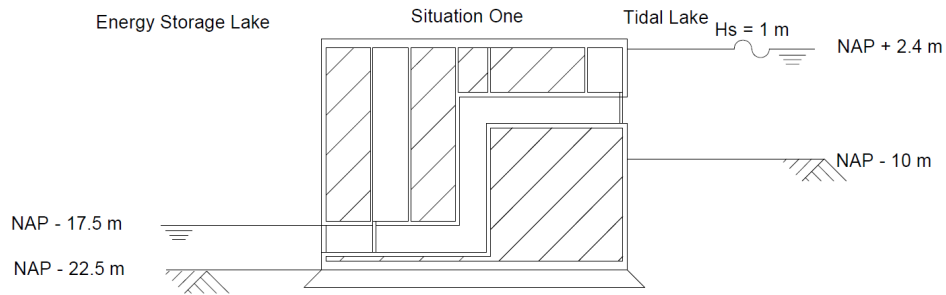


Figure H.2: Situation One

In situation one, the horizontal forces are caused by the water pressure, soil pressure and the wave pressure. The water pressures are determined by  $p_w = \rho_w \cdot h_w \cdot g$ , just like for the concept Siphon. Again, the soil pressures are neutral and a  $K_n$  value of 0.58 can be used.

$$p_{w,esl} = 1025 \cdot 5 \cdot 9.81 = 50 \text{ kN/m}^2$$

$$p_{w,TD} = 1025 \cdot 24.9 \cdot 9.81 = 250 \text{ kN/m}^2$$

$$p_{s,TD} = 0.58 \cdot 12.5 \cdot (20 - 10.25) = 71 \text{ kN/m}^2$$

These pressures can be seen in Figure H.3.

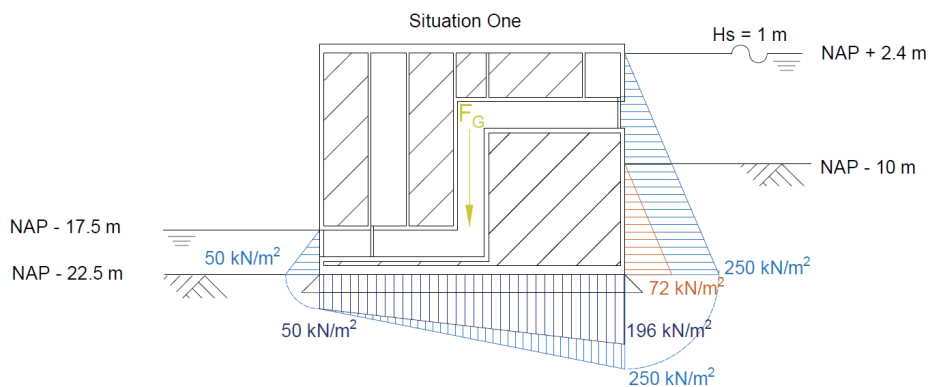


Figure H.3: Water and soil pressures on the caisson for situation one

The wave pressures are determined by using the Sainflou method. In this method the pressures due to the wave are simplified, see Figure H.4, and therefore slightly higher than in real. In the Sainflou method, the pressures are calculated by Formula H.2 and H.3

$$p_0 = \frac{\rho_{w,s} g H_{in}}{\cosh(kh)} \quad (\text{H.2})$$

$$p_1 = \rho_{w,s} g (H_{in} + h_0) \quad (\text{H.3})$$

in which:

$$h_0 = \frac{1}{2} k H_{in}^2 \coth(kh)$$

where:  $p_0$  [kPa] = the wave pressure at the bed level  
 $p_1$  [kPa] = the wave pressure at the water level  
 $\rho_{w,s}$  [kg/m<sup>3</sup>] = the density of salt water (=1025)  
 $H_{in}$  [m] = the incoming wave height  
 $k$  [-] = the wave number

The  $H_{in}$  from the Tidal Lake is 1 m, the corresponding wave number is 0.5 and the water depth in the Tidal Lake is 12.4 m.

$$h_0 = \frac{1}{2} k H_{in}^2 \coth(kh) = \frac{1}{2} \cdot 0.5 \cdot 1^2 \coth(0.5 \cdot 12.4) = 0.25 \text{ m}$$

$$p_0 = \frac{\rho_{w,s} g H_{in}}{\cosh(kh)} = \frac{1025 \cdot 9.81 \cdot 1}{\cosh(0.5 \cdot 12.4)} = 0.04 \text{ kN/m}^2$$

$$p_1 = \rho_{w,s} g (H_{in} + h_0) = 1025 \cdot 9.81 \cdot (1 + 0.25) = 12.6 \text{ kN/m}^2$$

Due to the height of the caisson, part of the wave will go over the caisson and therefore the pressure at the top is not equal to zero. The available freeboard ( $R_c$ ) is 1.1 m and is determined in Appendix G.

$$p_2 = \frac{p_1}{H_{in} + h_0} \cdot R_c = \frac{12.6}{1 + 0.25} \cdot 1.1 = 1.5 \text{ kN/m}^2$$

The wave pressures can be seen in Figure H.4.

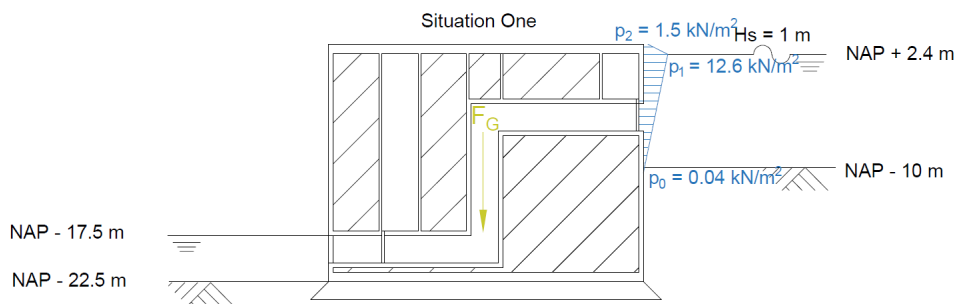


Figure H.4: Wave loads on the caisson for situation one

The forces acting on the caisson can be seen in Figure H.5.

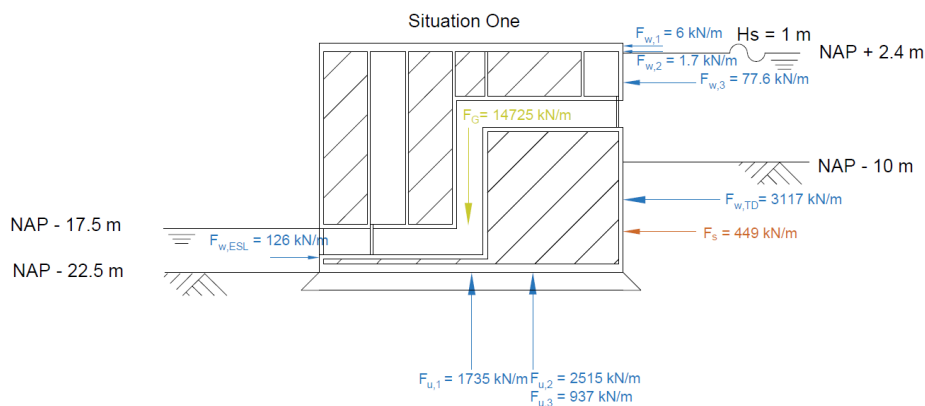


Figure H.5: Forces acting on the caisson

By adding up the forces in Figure H.5, the value for  $V_d'$  and  $\sum H$  can be found. By determining these values the load factors are taken into account.

$$\begin{aligned}
 V'_d &= F_G \cdot \gamma_{\text{fav}} - F_{u,1} \cdot \gamma_N - F_{u,2} \cdot \gamma_N - F_{u,3} \cdot \gamma_F \\
 &= 14725 \cdot 0.9 - 1735 \cdot 1.0 - 2515 \cdot 1.0 - 936 \cdot 1.25 \\
 &= 7832 \text{ kN/m} \\
 \sum H &= (-F_{w,ESL} + F_{w,TD} + F_{w,1} + F_{w,2} + F_{w,3}) \cdot \gamma_F + F_s \cdot \gamma_N \\
 &= (-126 + 3117 + 6 + 1.7 + 77.6) \cdot 1.25 + 449 \cdot 1.0 \\
 &= 4295 \text{ kN/m}
 \end{aligned}$$

The resistance of the soil, in this case the sill, is determined by the friction angle between the structure and the subsoil ( $\delta$ ). This angle is approximately  $\frac{2}{3}$  of the angle of internal friction ( $\phi$ ) according to NEN-EN 2019-1 article 6.5.3. The angle of internal friction for the sill is  $39^\circ$ , see Section 3.7.1.

$$\begin{aligned}
 \phi_d &= \frac{\phi_s}{\gamma_\phi} = \frac{39}{1.2} = 32.5 \\
 \delta_d &= \frac{2}{3} \cdot \phi_d = \frac{2}{3} \cdot 32.5 = 21.67
 \end{aligned}$$

This results in a  $R_d$  value of:

$$R_d = V'_d \cdot \tan(\delta_d) = 7832 \cdot \tan(21.67) = 3112 \text{ kN/m}$$

The unity check for this failure mechanism is equal to:

$$UC = \frac{H}{R_d} = \frac{4295}{3112} = 1.38$$

In Figure H.6, the unity check can be found for other widths of the caisson.

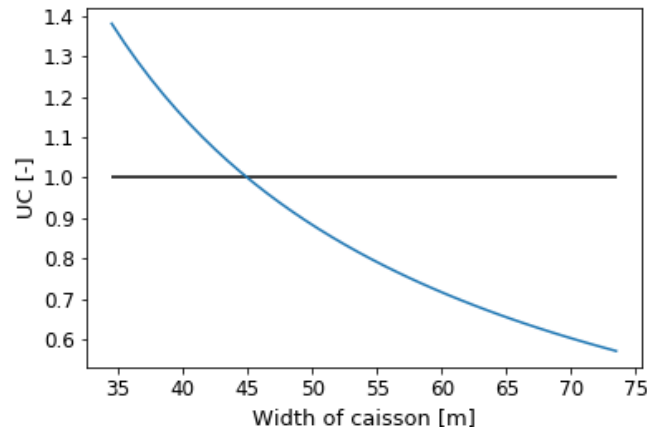


**Figure H.6:** Unity Check for situation one

It can be concluded that a minimum width of 45.5 m is required to ensure a unity check below 1.0.

**H.2.2. Situation Two**

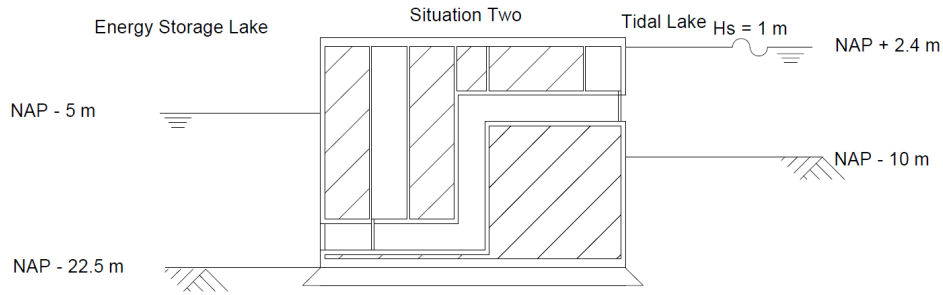


**Figure H.7:** Situation Two

The difference between situation one and two, is the water level in the Energy Storage Lake, respectively NAP -17.5 m and NAP - 5 m. This leads to a change in horizontal and vertical pressures, see Figure H.8, and forces, see Figure H.9.

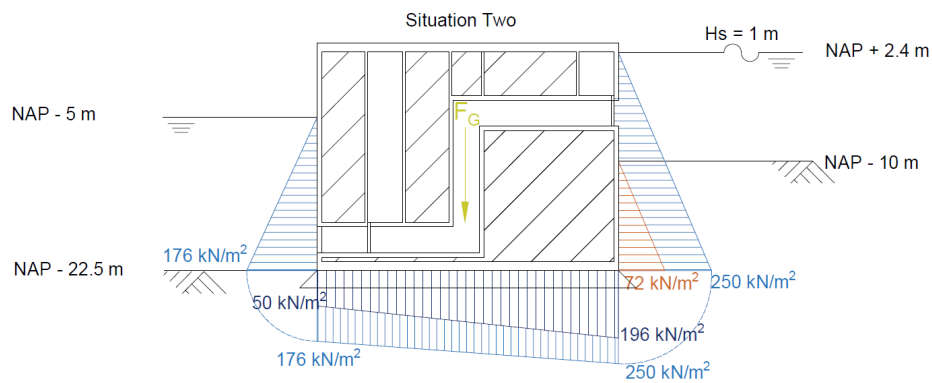


**Figure H.8:** Water and soil pressure on the caisson for situation two

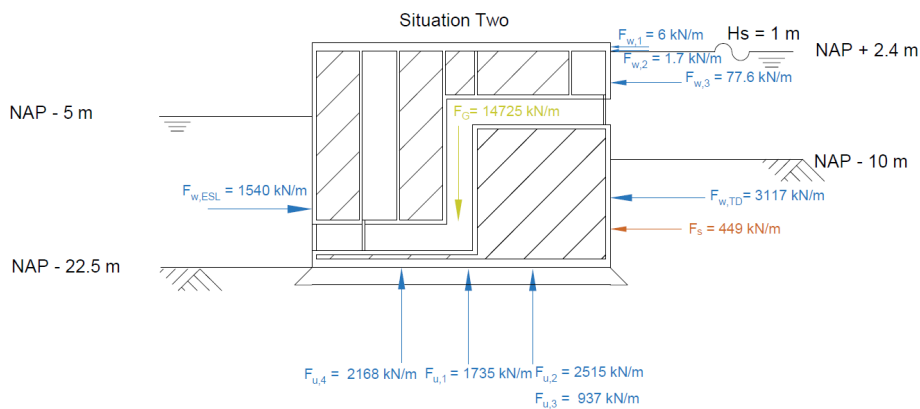


**Figure H.9:** Forces acting on the caisson

The value for  $V_d'$ , the resistance force,  $R_d$ , and  $\sum H$  change to:

$$\begin{aligned}
 V'_d &= F_G \cdot \gamma_{\text{fav}} - F_{u,1} \cdot \gamma_N - F_{u,2} \cdot \gamma_N - F_{u,3} \cdot \gamma_F - F_{u,4} \cdot \gamma_F \\
 &= 14725 \cdot 0.9 - 1735 \cdot 1.0 - 2515 \cdot 1.0 - 936 \cdot 1.25 - 2168 \cdot 1.25 \\
 &= 5122 \text{ kN/m} \\
 R_d &= V'_d \cdot \tan(\delta_d) \\
 &= 5122 \cdot \tan(21.67) = 2035 \text{ kN/m} \\
 \sum H &= (-F_{w,ESL} + F_{w,TD} + F_{w,1} + F_{w,2} + F_{w,3}) \cdot \gamma_F + F_s \cdot \gamma_N \\
 &= (-1540 + 3117 + 6 + 1.7 + 77.6) \cdot 1.25 + 449 \cdot 1.0 \\
 &= 2528 \text{ kN/m}
 \end{aligned}$$

This results in a unity check of:

$$UC = \frac{H}{R_d} = \frac{2528}{2035} = 1.24$$

The unity checks for the other widths can be seen in Figure H.10.

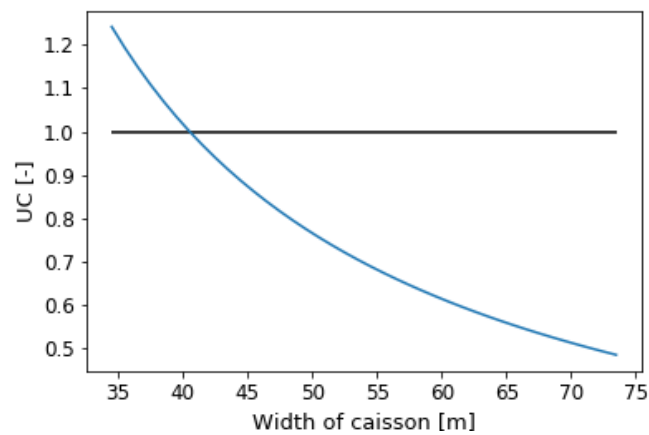


Figure H.10: Unity Check for situation two

The minimum required width for the caisson for situation two is 41.5 m.

### H.2.3. Situation Three

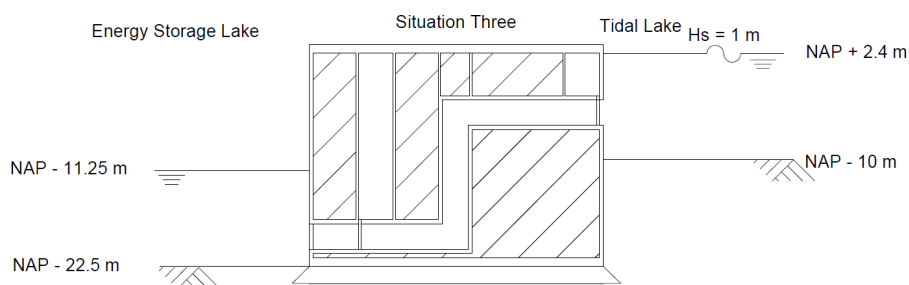


Figure H.11: Situation Three

The difference between situation one and two, is the water level in the Energy Storage Lake, respectively NAP - 17.5 m and NAP - 5 m. This leads to a change in horizontal and vertical pressures, see Figure H.12, and forces, see Figure H.13.

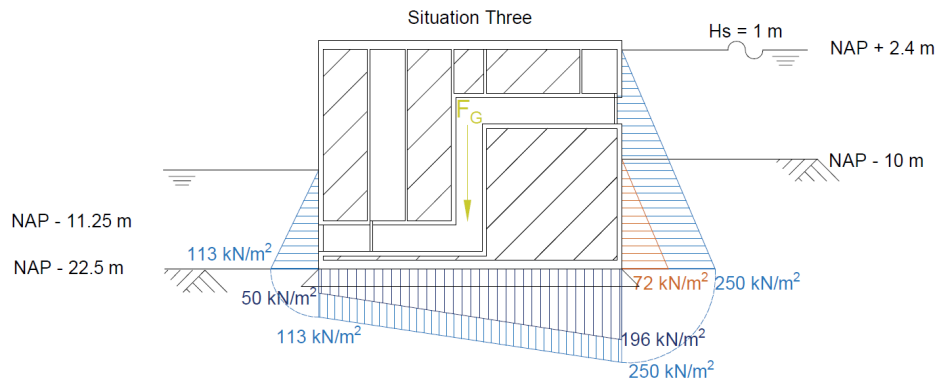


Figure H.12: Water and soil pressure on the caisson for situation three

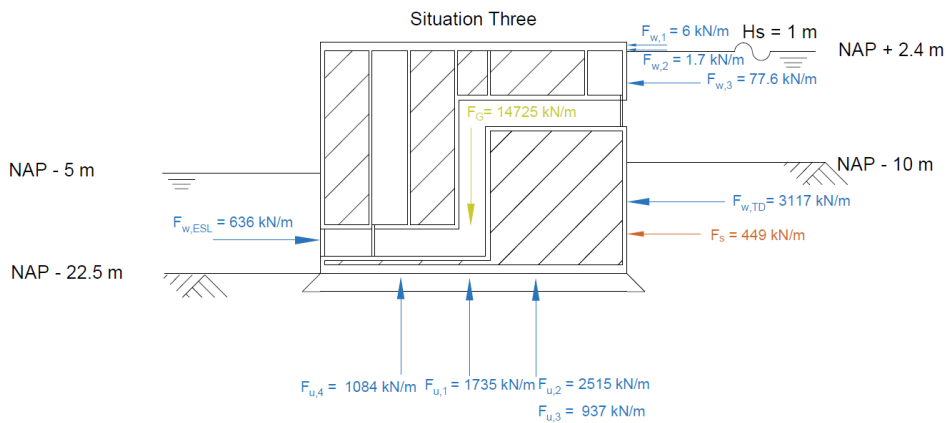


Figure H.13: Forces acting on the caisson

The value for  $V'_d$ , the resistance force,  $R_d$ , and  $\sum H$  change to:

$$\begin{aligned}
 V'_d &= F_G \cdot \gamma_{fav} - F_{u,1} \cdot \gamma_N - F_{u,2} \cdot \gamma_N - F_{u,3} \cdot \gamma_F - F_{u,4} \cdot \gamma_F \\
 &= 14725 \cdot 0.9 - 1735 \cdot 1.0 - 2515 \cdot 1.0 - 936 \cdot 1.25 - 1084 \cdot 1.25 \\
 &= 6477 \text{ kN/m} \\
 \delta_d &= \frac{2 \phi_{c,sill}}{3 \gamma_\phi} = \frac{2 \cdot 39}{3 \cdot 1.2} = 21.67^\circ \\
 R_d &= V'_d \cdot \tan(\delta_d) \\
 &= 6477 \cdot \tan(21.67) = 2573 \text{ kN/m} \\
 \sum H &= (-F_{w,ESL} + F_{w,TD} + F_{w,1} + F_{w,2} + F_{w,3}) \cdot \gamma_F + F_s \cdot \gamma_N \\
 &= (-636 + 3117 + 6 + 1.7 + 77.6) \cdot 1.25 + 449 \cdot 1.0 \\
 &= 3657 \text{ kN/m}
 \end{aligned}$$

This results in an unity check of:

$$UC = \frac{H}{R_d} = \frac{3657}{2573} = 1.42$$

The unity checks for the other widths can be seen in Figure H.14. The minimum required width for the caisson in situation three is 46.5 m.

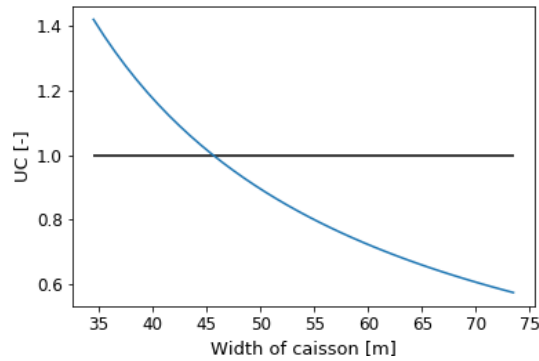


Figure H.14: Unity Check for situation three

### H.3. Rotational Stability

If the eccentricity of the resulting force is exceeding the boundaries of the core of the caisson, the caisson will rotate. Therefore, the eccentricity may not exceed the boundaries of the core. More information about the method used for the rotational stability can be found in Chapter 6.

$$-\frac{1}{6}B \leq e_R \leq \frac{1}{6}B \tag{H.4}$$

with:

$$e_R = \frac{\sum M}{\sum V}$$

#### H.3.1. Governing Load Situation

The governing situation for this stability requirement is the situation with the highest resulting moment. The highest resulting moment is occurring in the situation with the highest water level difference. In this case, situation one is governing due to the water level difference. Therefore, the other situations are not calculated.

##### H.3.1.1. Acting Loads

The load situation for situation one is given in Figure H.15. The values for the forces are the same as for sliding resistance, Section H.3.

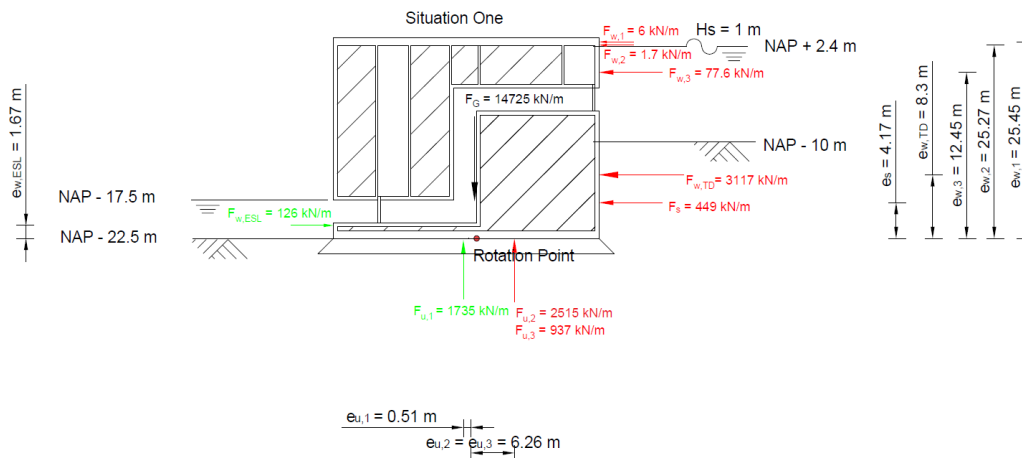


Figure H.15: Forces and the working arm

### H.3.1.2. Horizontal Location of the Gravity Centre

For the rotational stability requirement, the horizontal location of the gravity centre is required. This location is determined by Formula H.5.

$$x_G = \frac{\sum V_i \cdot e_i \cdot \gamma_i}{\sum V_i \cdot \gamma_i} \quad (\text{H.5})$$

In Table H.3, the volumes of each element and the distances from the energy lake side of the caisson can be seen.

Element	Number	Total Volume	Distance	Gamma
Outer Wall 1	1	100	0.25	25
Outer Wall 2	1	77.5	34.25	25
Outer Wall 3	1	27.5	34.25	25
Outer Wall 4	2	414	17.25	25
Outer Wall 5	1	5	0.25	25
Bottom Slab	1	379.5	17.25	25
Top Slab	1	379.5	17.25	25
Inner Wall 1	1	58.5	5.56	25
Inner Wall 2	1	58.5	9.95	25
Inner Wall 3	1	15	15.75	25
Inner Wall 4	1	15	19.45	25
Inner Wall 5	1	15	29.85	25
Culvert Wall 1	1	75.5	8.05	25
Culvert Wall 2	1	72.5	14.85	25
Culvert Wall 3	1	93	24.7	25
Culvert Wall 4	1	77	26.3	25
Culvert Wall 5	1	70	18.85	25
Culvert Wall 6	1	93	7.8	25
Gate 1	1	9	0.65	78
Gate 2	1	9	33.85	78
Ballast 1	1	2235	26.55	20
Ballast 2	1	975	3	20
Ballast 3	1	975	12.6	20
Ballast 4	1	170	24.4	20
Ballast 5	1	530	16.9	20
Ballast 6	1	93.75	9.8	20

**Table H.3:** Volume and distances of elements

This leads to a horizontal location of the gravity centre for the basis layout of:

$$x_G = \frac{\sum V_i \cdot e_i \cdot \gamma_i}{\sum V_i \cdot \gamma_i} = 17.76$$

The gravity centre of the caisson is a bit to the right compared with the middle of the caisson. For each width, the gravity centre is changing, see Figure H.16. It is getting closer to the middle of the caisson ( $B/2$ ) if the width is increasing.



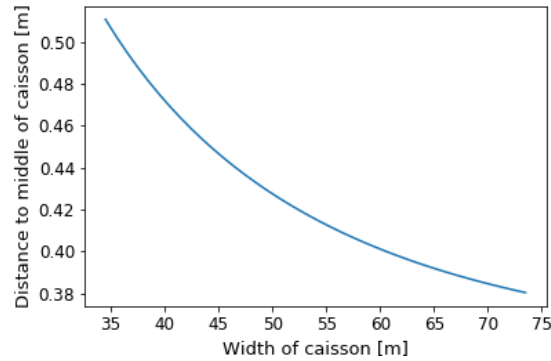


Figure H.16: Distance from middle of caisson ( $B/2$ ) to gravity centre line

### H.3.2. Resulting Moment and Vertical Force

With the forces and distances given in Figure H.15 the resulting moment and vertical force can be determined. Taking into account the given load factors, this leads to:

$$\begin{aligned}\sum M_H &= (F_{w,1} \cdot e_{w,1} + F_{w,2} \cdot e_{w,2} + F_{w,2} \cdot e_{w,2} + F_{w,TD} \cdot e_{w,TD}) \cdot \gamma_F + F_s \cdot e_s \cdot \gamma_N - F_{w,ESL} \cdot e_{w,ESL} \cdot \gamma_F \\ &= (6 \cdot 24.45 + 1.7 \cdot 25.27 + 77.6 \cdot 12.45 + 3317 \cdot 8.3) \cdot 1.25 + 449 \cdot 4.17 - 125 \cdot 1.67 \\ &= 35812 \text{ kNm/m} \\ \sum M_V &= (F_{u,2} \cdot e_{u,2} + F_{u,3} \cdot e_{u,3}) \cdot \gamma_F - F_{u,1} \cdot e_{u,1} \cdot \gamma_N \\ &= (2515 \cdot 6.26 + 936 \cdot 6.26) \cdot 1.25 - 1735 \cdot 0.51 \cdot 1.0 \\ &= 23961 \text{ kNm/m} \\ M &= M_H + M_V \\ &= 35812 + 23961 \\ &= 59774 \text{ kNm/m}\end{aligned}$$

The sum of the vertical forces is already determined for the sliding resistance and is equal to 7832 kN/m. The eccentricity for this situation is equal to 7.63.

$$e_R = \frac{M}{V} = \frac{59774}{7832} = 7.62$$

### H.3.3. The Unity Check

The unity check for this stability is determined and equal to 1.33.

$$UC = \frac{e_R}{\frac{1}{6}B} = \frac{7.63}{5.75} = 1.33$$

The results of the unity check for the other widths can be seen in Figure H.17. The minimum required width is equal to 42.5 m.

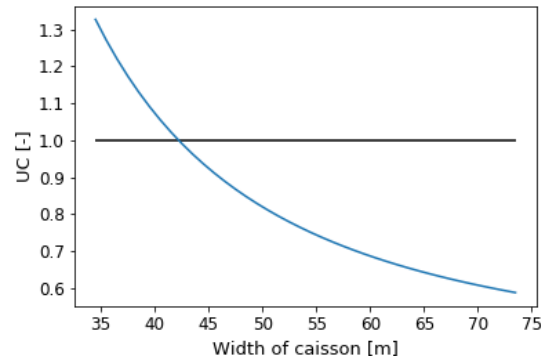


Figure H.17: Unity check rotational stability

## H.4. Bearing Capacity

The bearing capacity of the soil,  $p'_{max}$ , must be larger than the acting stresses due to the self weight of the caisson and the forces acting on the caisson,  $\sigma_{k,max}$ . More information about the method used for the bearing capacity can be found in Chapter 6.

$$p'_{max} \leq \sigma_{k,max}$$

with:

$$p'_{max} = c' N_c s_c i_c + q' N_q s_q i_q + 0.5 \gamma' B' N_\gamma s_\gamma i_\gamma \quad \text{and} \quad \sigma_{k,max} = \frac{\sum V}{B_{eff}}$$

For the bearing capacity load situation One is governing. The reason for this is that the uplift pressure is low and the moment and therefore the eccentricity high. There are two soil layers that are analysed regarding the bearing capacity.

- **Soil Layer One:** The sill below the caisson
- **Soil Layer Two:** The sand layer below the sill

### H.4.1. The Acting forces

#### H.4.1.1. Soil Layer One

The forces acting on the sill and the caisson are already determined. Only important change is that the self weight of the caisson is now an unfavourable load and therefore a load factor of 1.2 is required instead of 0.9.

$$\begin{aligned} H &= 4295 \text{ kN/m} \\ V &= F_G \cdot \gamma_{fav} - F_{u,1} \cdot \gamma_N - F_{u,2} \cdot \gamma_N - F_{u,3} \cdot \gamma_F \\ &= 14725 \cdot 1.2 - 1735 \cdot 1.0 - 2515 \cdot 1.0 - 936 \cdot 1.25 \\ &= 12250 \text{ kN/m} \end{aligned}$$

The effective width of the caisson is depending on the eccentricity of the resulting force. The eccentricity in situation one is 7.63 m.

$$B' = B - 2 \cdot e_R = 34.5 - 2 \cdot 7.63 = 19.24 \text{ m}$$

The maximum acting stress on the sill due to the caisson is determined with Formula H.6. The reason that the sum of the vertical forces is only divided by the effective width is that the sum of the vertical forces is in kN/m.

$$\sigma_{k,max} = \frac{\sum V}{B'} \quad (\text{H.6})$$

Using the loads of situation one, this leads to a acting stress of 636.7 kN/m<sup>2</sup>

$$\sigma_{k,max} = \frac{\sum V}{B'} = \frac{12250}{19.24} = 636.7 \text{ kN/m}^2$$

The results for the other widths can be seen in Figure H.18.

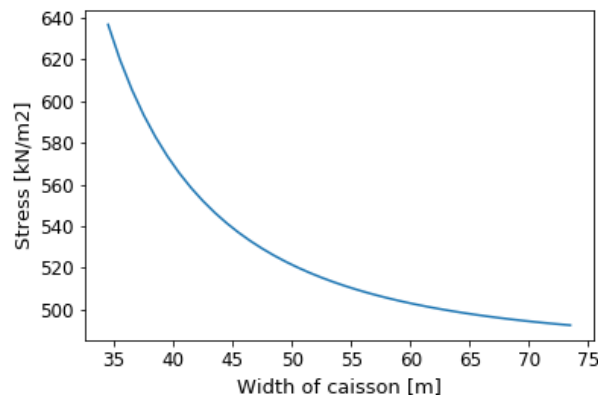


Figure H.18: Acting stresses on the sill

#### H.4.1.2. Soil Layer Two

For the second soil layer, the weight of the sill has to be added to the vertical force. The sill has a height of 2 m and at the edges the angle of the sill is 45°. Therefore the additional weight due to the sill is equal to 710 kN/m.

$$\begin{aligned} F_{G,sill} &= (h_{sill} \cdot B + 2 \cdot 0.5 \cdot h_{sill} \cdot \tan(45)) \cdot \gamma'_{sill} \\ &= (2 \cdot 34.5 + 2 \cdot \tan(45)) \cdot (20 - 10.06) \\ &= 706 \text{ kN/m} \end{aligned}$$

This leads to a resulting vertical force of:

$$\begin{aligned} V &= (F_G + F_{G,sill}) \cdot \gamma_{fav} - F_{u,1} \cdot \gamma_N - F_{u,2} \cdot \gamma_N - F_{u,3} \cdot \gamma_F \\ &= (14725 + 706) \cdot 1.2 - 1735 \cdot 1.0 - 2515 \cdot 1.0 - 936 \cdot 1.25 \\ &= 13097 \text{ kN/m} \end{aligned}$$

The effective width is increasing as well because the sill has a larger width than the caisson. The effective width increase with 4 m ( $2 \cdot h_{sill} \cdot \tan(45)$ ). This leads to an effective width of 23.24 m. The acting stresses on the second soil layer can be seen in Figure H.19.

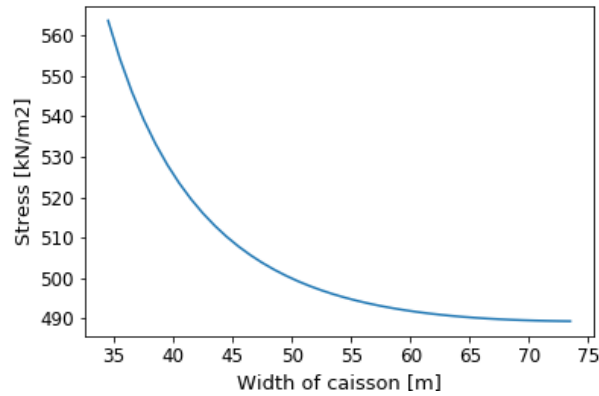


Figure H.19: Acting stresses on sand layer

## H.4.2. The Bearing Capacity of the Layer

### H.4.2.1. Soil Layer One

The bearing capacity of the subsoil is determined by the Brinch Hansen method, Formula H.7. The first two parts can be neglected due to the cohesion of sand ( $c' = 0$ ) and the effective stress at the depth of the foundation ( $q' = 0$ ).

$$p'_{max} = \underbrace{c' N_c s_c i_c}_{=0} + \underbrace{q' N_q s_q i_q}_{=0} + 0.5 \gamma' B' N_\gamma s_\gamma i_\gamma \quad (\text{H.7})$$

where:	$p'_{max}$	[kN/m <sup>2</sup> ]	=	the resisting bearing capacity
	$c'$	[kN/m <sup>2</sup> ]	=	the cohesion value of the soil
	$N_c, N_q, N_\gamma$	[-]	=	the bearing force factor
	$s_c, s_q, s_\gamma$	[-]	=	the foundation shape factor
	$i_c, i_q, i_\gamma$	[-]	=	the horizontal load factor
	$q'$	[kN/m <sup>2</sup> ]	=	the effective stress at the depth net to the foundation
	$\gamma'$	[kN/m <sup>3</sup> ]	=	the effective volumetric weight
	$B'$	[m]	=	the effective width

The bearing force factors depend on the angle of internal friction of the soil,  $\phi'$ . A higher angle of internal friction leads to higher values for the bearing force capacity. The relation between the angle of internal friction and the bearing force factors are:

$$N_c = (N_q - 1) \cot(\phi')$$

$$N_q = \frac{1 + \sin(\phi')}{1 - \sin(\phi')} \exp^{\pi \tan(\phi')}$$

$$N_\gamma = 2(N_q - 1) \tan(\phi')$$

For the sill ( $\phi_d = 32.5^\circ$ ) this results in a  $N_c = 37.02$ ,  $N_q = 24.58$  and  $N_\gamma = 30.05$ . The foundation shape factors depends on the shape of the foundation. For rectangular foundations, the shape factors are defined as, in which the width (B) is the shortest side of the foundation:

$$s_c = 1 + 0.2 \frac{B'}{L}$$

$$s_q = 1 + \frac{B'}{L} \sin(\phi')$$

$$s_\gamma = 1 - 0.3 \frac{B'}{L}$$

The effective width and length are respectively 19.24 m and 33 m. The length is based on 3 single conduits in one caisson (3x11 = 33m). This results in  $s_c = 1.33$ ,  $s_q = 1.31$  and  $s_\gamma = 0.85$ . The factors for horizontal load are depending on the value of the horizontal load and the orientation of the force. The horizontal and vertical forces for situation one are calculated in the earlier stability requirements.

$$i_c = i_q - \frac{1 - i_q}{N_c \cdot \tan(\phi')}$$

$$i_q = \left(1 - \frac{H}{V + Ac' \cot(\phi')}\right)^m$$

$$i_\gamma = \left(1 - \frac{H}{V + Ac' \cot(\phi')}\right)^{m+1}$$

with:

$$m = \frac{2 + \frac{B'}{L}}{1 + \frac{B'}{L}}$$

With the vertical and horizontal forces acting on the caisson, the following factors for horizontal loads are found:  $i_c = 0.47$ ,  $i_q = 0.49$  and  $i_\gamma = 0.32$ . This result in a bearing capacity of:

$$p'_{max} = 0.5 \gamma' B' N_\gamma s_\gamma i_\gamma = 0.5 \cdot (20 - 10.05) \cdot 19.24 \cdot 30.05 \cdot 0.85 \cdot 0.32 = 761 \text{ kN/m}^2$$

In Figure H.20, the bearing capacity for the other widths can be found.

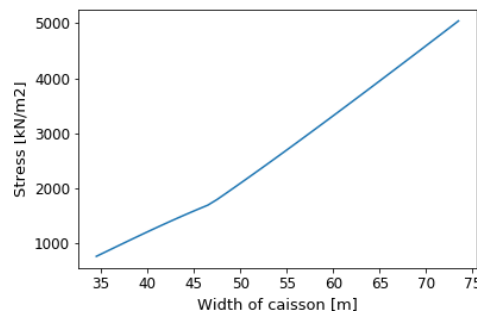


Figure H.20: Bearing capacity of the sill

#### H.4.2.2. Soil Layer Two

For the second soil layer, the first two parts can be neglected again for the same reasons.

$$p'_{max} = 0.5 \gamma' B' N_\gamma s_\gamma i_\gamma$$

For the sand layer ( $\phi_d = 18^\circ$ ) the bearing force factors are respectively  $N_c = 24$ ,  $N_q = 13.3$  and  $N_\gamma = 12.6$ . The effective width and length are respectively 23.24 m and 33 m. This results in  $s_c = 1.35$ ,  $s_q = 1.32$  and  $s_\gamma = 0.79$ . With the vertical and horizontal forces acting on the caisson, the following factors for horizontal loads are found:  $i_c = 0.49$ ,  $i_q = 0.53$  and  $i_\gamma = 0.36$ . This results in a bearing capacity for the basis caisson of:

$$p'_{max} = c' N_c s_c i_c + q' N_q s_q i_q + 0.5 \gamma' B' N_\gamma s_\gamma i_\gamma = 0.5 \cdot (20 - 10.05) \cdot 23.24 \cdot 12.6 \cdot 0.79 \cdot 0.36 = 411 \text{ kN/m}^2$$

In Figure H.21, the bearing capacity for the other widths can be found.

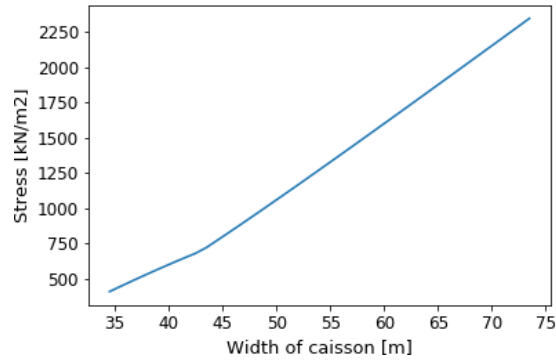


Figure H.21: Bearing capacity of the sand layer

### H.4.3. The Unity Check

#### H.4.3.1. Soil Layer One

The unity check that is done for both soil layers is:

$$\text{Unity Check} = \frac{\sigma_{k,max}}{p'_{max}}$$

This results in a unity check of 0.84 for soil layer one.

$$UC = \frac{636.7}{761} = 0.84$$

The results for the other widths can be found in Figure H.22. It can be concluded that the sill always full fills the requirement.

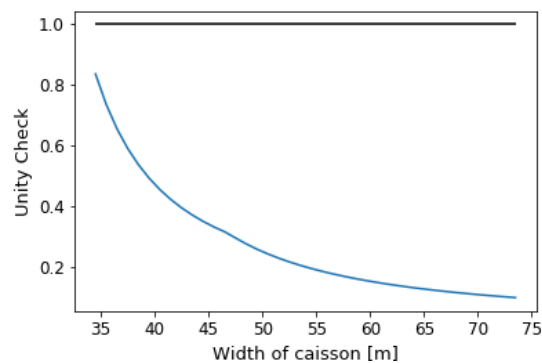


Figure H.22: Results bearing capacity for the sill

### H.4.3.2. Soil Layer Two

The unity check for the second soil layer for the basis layout of the caissons is:

$$UC = \frac{564}{411} = 1.37$$

The results for the other widths can be found in Figure H.23. It can be concluded that the required minimum width is 38.5 m for situation one.

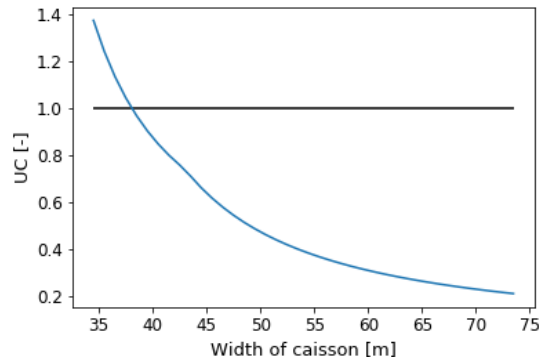


**Figure H.23:** Results bearing capacity for the sand layer

## H.5. Draught

The self weight of the caisson during transport and positioning is the weight excluding the ballast, 5673 kN/m for the basis layout. The draught corresponding to this self weight is:

$$\begin{aligned} d &= \frac{F_G}{B \cdot L \cdot \gamma_w} \\ &= \frac{5673}{34.5 \cdot 1 \cdot 10.06} = 16.35m \end{aligned}$$

In Figure E18, the draught of the caisson can be seen for each width. It can be concluded that the clearance requirement and the minimum freeboard are no problem.

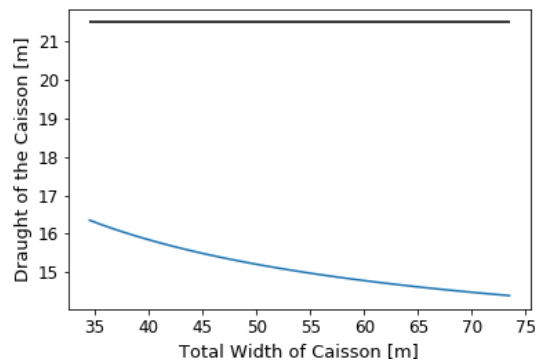


**Figure H.24:** Draught of the caisson

## H.6. Floating stability

During transportation and immersion the caisson needs to be stable. The stability during transport and immersion is determined by the metacentric height. If this height is above 0.5 m, there is no static stability problem. The metacentric height is defined as:

$$h_m = \overline{GM} = \overline{KB} + \overline{BM} - \overline{KG} \quad (\text{H.8})$$

in which:

$$\begin{aligned} \overline{KB} &= \frac{1}{2}d \\ \overline{BM} &= \frac{I}{V} \\ \overline{KG} &= \frac{\sum V_i \cdot e_i \cdot \gamma_i}{\sum V_i \cdot \gamma_i} \end{aligned}$$

where:  $d$  [m] = the draught of the caisson  
 $I$  [m<sup>4</sup>] = the moment of inertia  
 $V$  [m<sup>3</sup>] = the volume of displaced water  
 $V_i$  [m<sup>3</sup>] = the volume of an element  
 $e_i$  [m] = the distance between the bottom of the caisson and the gravity centre of the element  
 $\gamma_i$  [kN/m<sup>3</sup>] = the specific weight of an element

The draught of the caisson is calculated in Section H.5 and therefore  $\overline{KB}$  is already known for each width. For the basis layout  $\overline{KB}$  is 8.18 m. For  $\overline{BM}$ , the displaced volume of water is already determined in Section H.5. The moment of inertia of the area that intersects with the water is calculated with:

$$I = \frac{1}{12} \cdot L \cdot B^3$$

As mentioned before, L is equal to 1 because there is looked at per meter width in the length direction and B is variable.  $\overline{BM}$  can also be written as:

$$\begin{aligned} \overline{BM} &= \frac{\frac{1}{12} \cdot L \cdot B^3}{L \cdot B \cdot d} = \frac{\frac{1}{12} \cdot B^2}{d} \\ &= \frac{\frac{1}{12} \cdot 34.5^2}{16.35} = 6.07 \text{ m.} \end{aligned}$$

$\overline{KG}$  is the distance between the gravity centre of the caisson and the bottom of the caisson. The location of the gravity centre of the caisson is determined by multiplying the volume of each element by its specific weight and the distance to the bottom. This value is divided by the total volume of the caisson. the volumes and distances can be seen in Table H.4.



Element	Number	Total Volume	Distance	Gamma
Outer Wall 1	1	100	14.5	25
Outer Wall 2	1	77.5	8.75	25
Outer Wall 3	1	27.5	23.25	25
Outer Wall 4	2	414	13	25
Outer Wall 5	1	5	1.25	25
Bottom Slab	1	379.5	0.5	25
Top Slab	1	379.5	25.5	25
Inner Wall 1	1	58.5	15.25	25
Inner Wall 2	1	58.5	15.25	25
Inner Wall 3	1	15	22.5	25
Inner Wall 4	1	15	22.5	25
Inner Wall 5	1	15	22.5	25
Culvert Wall 1	1	75.5	5.25	25
Culvert Wall 2	1	72.5	12.25	25
Culvert Wall 3	1	93	19.75	25
Culvert Wall 4	1	77	16.25	25
Culvert Wall 5	1	70	9	25
Culvert Wall 6	1	93	1.75	25
Gate 1	1	9	3.5	78
Gate 2	1	9	18	78

**Table H.4:** Volume and distances of elements

With the use of Table H.4, the value for  $\overline{KG}$  can be determined.

$$\overline{KG} = \frac{\sum V_i \cdot e_i \cdot \gamma_i}{\sum V_i \cdot \gamma_i} = 16.6m$$

Combining the values for  $\overline{KB}$  and  $\overline{BM}$  and extracting the value of  $\overline{KG}$ , leads to the value of  $h_m$ .

$$h_m = \overline{KB} + \overline{BM} - \overline{KG} = 8.18 + 6.07 - 16.6 = -2.37m$$

The value for  $h_m$  is determined for each width and can be seen in Figure H.25. It can be concluded that the minimum required width is 43.5 m.

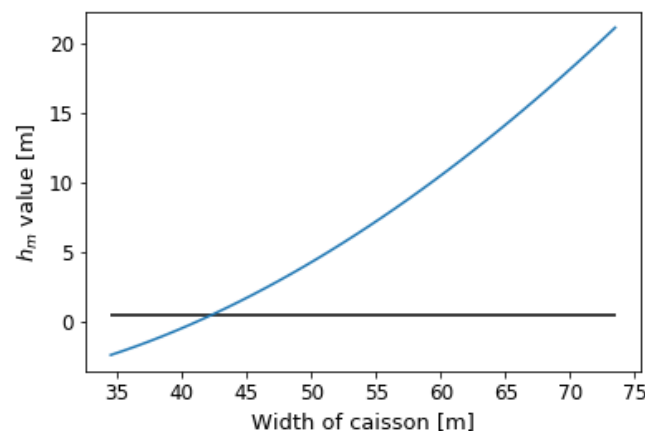


**Figure H.25:** The metacentric height of the caisson,  $h_m$



# Dimensions of the concept Ogee

The ogee crest profile is determined with the use of the design head of the spillway. The design head of the spillway is defined as the total head at the crest including the velocity head. For the design of the spillway, the total head is equal to the maximum water level in the tidal lake when the Europort barrier is functioning, NAP + 1.5 m.

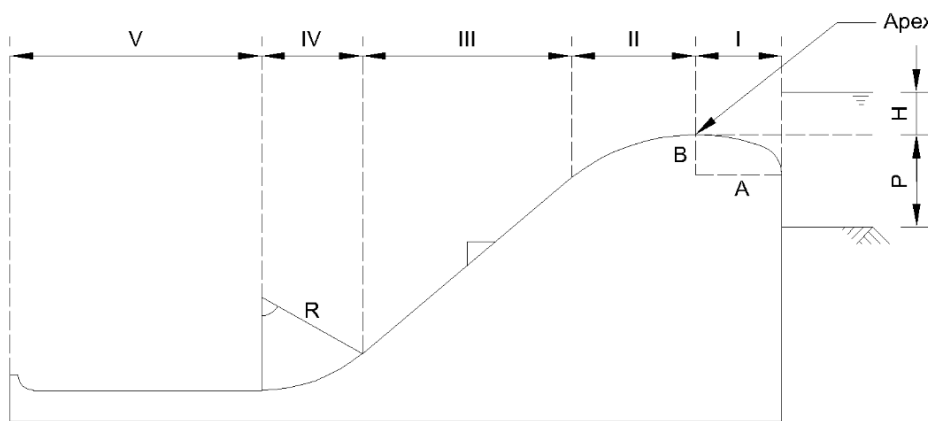


Figure I.1: Different parts of the ogee crest

The ogee crest is divided in five different sections:

- Section I: Upstream part, curved
- Section II: Downstream part, curved
- Section III: Constant slope
- Section IV: Circular part
- Section V: Stilling basin

The different sections can be seen in Figure I.1. Section I is defined by Formula I.1 and section II by Formula I.2 (U.S. Army Corps of Engineers, 1990). Section I depends on two parameters, A and B. These parameters can be seen in Figure I.2.  $P/H_d$  is equal to 0.92 and this leads to a value of A of  $0.265H_d$  and for B of  $0.155H_d$ , which is respectively 1.59 and 0.93.

$$Y = -\sqrt{\left(1 - \frac{X^2}{A^2}\right)B^2} + B \tag{I.1}$$

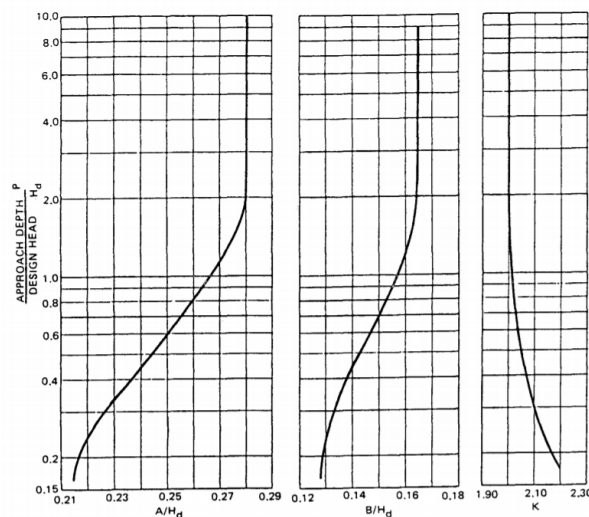


Figure I.2: Values of A,B and K (U.S. Army Corps of Engineers, 1990)

Section II depends on the value of K, which can also be seen in Figure I.2. With  $P/H_d$  equal to 0.93, the value of K can be set at 2. Section I is valid between  $X = -1.59$  and  $X = 0$  and section II is valid between  $X = 0$  and the transition point.  $X = 0$  is at the apex of the crest. The transition point is the location in which the slope of section II is the same as the slope of the rest of the spillway. The positive directions of the axis can be seen in Figure I.3.

$$Y = \frac{X^{1.85}}{K \cdot H_d^{0.85}} \quad (I.2)$$

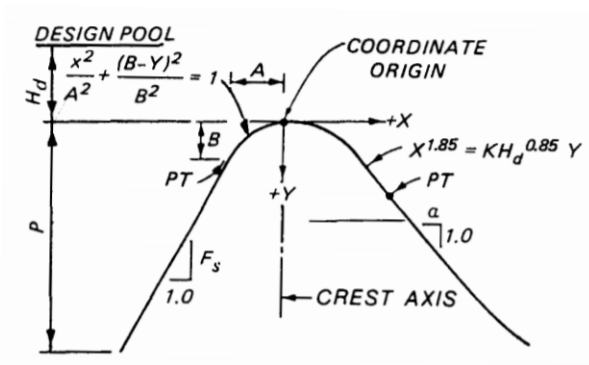


Figure I.3: Definition Sketch (U.S. Army Corps of Engineers, 1990)

Formula I.2 is applicable between the apex ( $X = 0$ ) and the transition point. To determine the transition point, the derivative of Formula I.2 is used which can be seen in Formula I.3. The slope of the spillway is taken as 0.7H:1V. This results in the X coordinate 9.48. This means that section II is valid between  $X = 0$  and  $X = 9.48$ .

$$\frac{dY}{dX} = \frac{1.85X^{0.85}}{2.0H_d^{0.85}} \quad (I.3)$$

As mentioned, section II is followed up by a constant slope. Which can be described by:

$$Y = -1.43X + C \quad (I.4)$$

With C being determined by using the transition point between the downstream formula part and the constant slope part. Using this transition point leads to C being equal to 6.22. After the constant slope, the shape of the spillway will be circular. This circle has a radius of  $\frac{P}{4}$ , in which P is the height of the spillway compared

to the depth of the tidal lake, 18 m. This results in a radius of 4.5 and can be draw with an angle equal to the constant slope, 55°.

The last part of the spillway is the stilling basin. At this moment, the length of this basin will be estimated by the use of the water depth after the hydraulic jump that will occur at the end of the spillway. There are different types of stilling basins but the simplest case will be applied at this moment. This means that the length of the still basin can be estimated by multiplying the water depth downstream of the jump by 4.2. The depth downstream of the jump is calculated with the Formula I.6. In which  $y_2$  is the water depth downstream of the hydraulic jump,  $y_1$  the water depth upstream of the hydraulic jump and  $F_1$  the Froude number upstream of the jump.

$$y_2 = \frac{y_1}{2} (\sqrt{1 + 8F_1^2} - 1) \quad (I.5)$$

The Froude number and the depth upstream of the jump are both depending on the velocity. This velocity is determined by  $v = \sqrt{2gH}$  in which H is the difference between the water level of the tidal lake and the energy storage lake, 19m. This results in a velocity of 19.3 m/s. The water depth upstream of the jump is determined by:

$$y_1 = \frac{Q/B_t}{v} \quad (I.6)$$

With B being the total width of the structure, excluding the piers. This is equal to 672 m and results in a  $y_1$  of 1.54 m. The Froude number is derived with:

$$F = \frac{v}{\sqrt{g \cdot y_1}} \quad (I.7)$$

This results in a Froude number of 4.97. Using Formula I.5 leads to a water depth downstream of the jump of 10.08 m and a total length of the basin of 42 m.

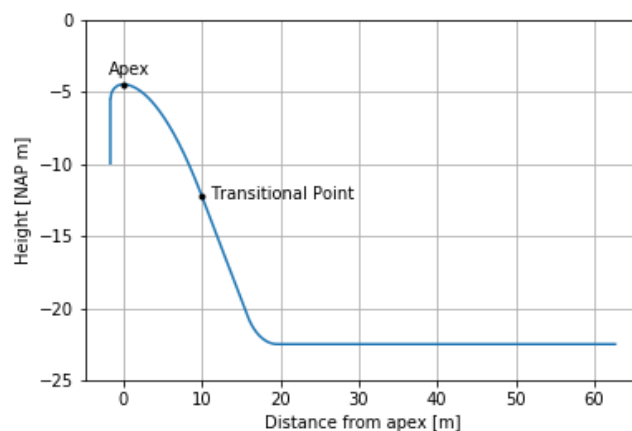


**Figure I.4:** Shape of the Ogee Spillway

# J

## Stability Concept Ogee

In this Appendix, the stability calculations for the concept Ogee can be found. First the self-weight of the structure is calculated and afterwards the pressures are determined.

### J.1. Self weight of spillway

In Figure J.1, the body of the spillway is separated in different parts to determine the self weight of the structure. In the figure, the dimensions can be seen.

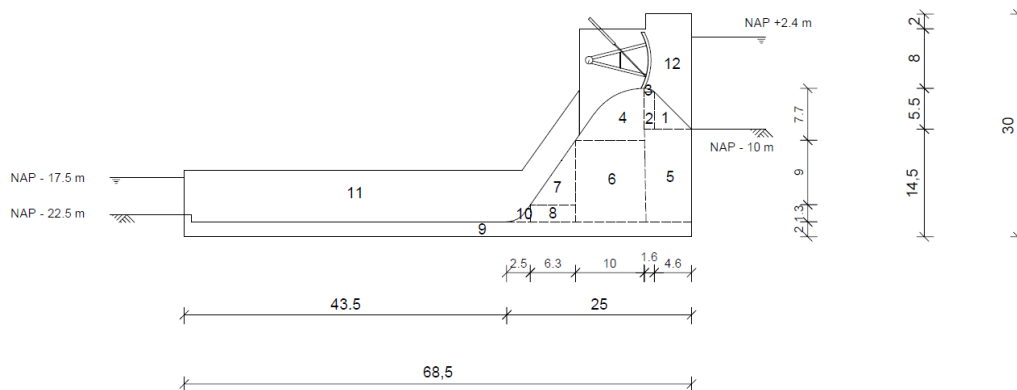


**Figure J.1:** Different parts of the spillway

For each part the area is calculated:

$$A_1 = 0.5 \cdot 4.6 \cdot 5.5 = 12.65m^2$$

$$A_2 = (5.5 - 0.93) \cdot 1.6 = 7.3m^2$$

$$A_3 = \int_{-1.59}^0 -\sqrt{\left(1 - \frac{x^2}{1.59^2}\right)} \cdot 0.93^2 + 0.93 dx = 1.16m^2$$

(Formula can be found in Appendix I)

$$A_4 = \int_0^{9.48} \frac{x^{1.85}}{2 \cdot 6^{0.85}} dx = 50m^2$$

(Formula can be found in Appendix I)

$$A_5 = 6.2 \cdot 12.5 = 77.5m^2$$

$$A_6 = 10 \cdot 10.3 = 103m^2$$

$$A_7 = 6.3 \cdot 9 \cdot 0.5 = 28m^2$$

$$A_8 = 6.3 \cdot 1.3 = 8.19m^2$$

$$A_9 = 68.5 \cdot 2 = 137m^2$$

$$A_{10} = 3 \cdot 1.73 - \int_0^{2.45} (\sqrt{3^2 - x^2} + 1.73) dx = 1m^2$$

(Area outside of a circle)

This leads to a total area of 426 m<sup>2</sup>. Using the specific weight of concrete, 25 kN/m<sup>3</sup>, leads to 10650 kN/m. For part 11 and 12, some assumptions are made. Part 11 is assumed to be a wall with thickness 0.5 m, a height of 6 m and a length of 43.5 m. This results in a volume of 130.5 m<sup>3</sup> or 3262.5 kN. Part 12 is assumed to have a self weight of 7500 kN. This includes the weight of the concrete walls and the mechanical parts for the gates. The length of a single opening is 25 m and the piers are assumed to be 3 m in length. Taking 1.5 pier per part, it leads to a length of 29.5 m. Part 11 and 12 are set to self weight per meter, which leads to 370 kN/m total. The gate is assumed to have a weight of 7000 kN, which is 238 kN/m. This leads to a total weight of 11258 kN/m.

## J.2. Pressures acting on the spillway

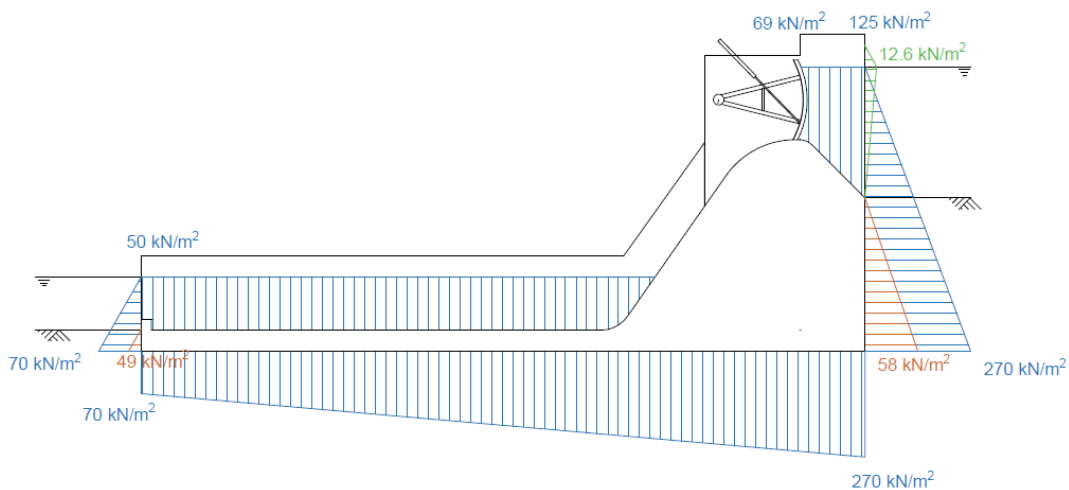
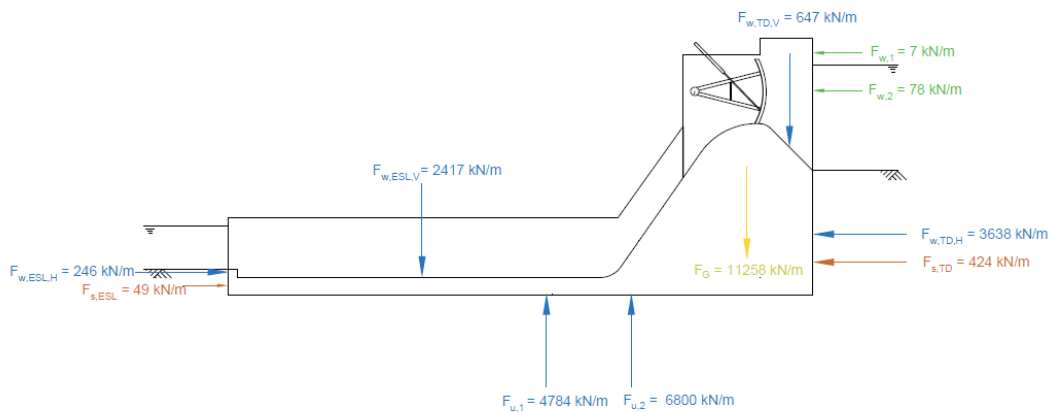


Figure J.2: Pressures acting on the spillway



**Figure J.3:** Forces acting on the spillway

In Figure J.2, the pressures acting in the governing situation can be seen. The water pressures and waves pressure are determined as done before in the calculations of the concept Caisson. For the soil pressures, the calculation has changed. With soil at both sides of the spillway, the soil is divided in active soil and passive soil. The active side is the tidal lake side. Here the structure moves away from the soil. The energy storage lake side is passive because the spillway is moving into the soil. The active and passive soil pressure are determined by:

$$\sigma_{s,TD} = h_{g,TD} \cdot \gamma'_{sand} \cdot K_a$$

$$\sigma_{s,ESL} = h_{g,ESL} \cdot \gamma'_{sand} \cdot K_p$$

in which:

$$K_a = \frac{1 - \sin(\phi_d)}{1 + \sin(\phi_d)}$$

$$K_p = \frac{1 + \sin(\phi_d)}{1 - \sin(\phi_d)}$$

With  $\phi_d$  equal to  $25^\circ$ , this leads to a  $K_a$  and  $K_p$  of respectively 0.4 and 2.5. For the soil pressures this leads to a soil pressure at the energy storage lake side of  $49 \text{ kN/m}^2$  and at the tidal lake side  $59 \text{ kN/m}^2$ . In Figure J.3, the forces acting on the spillway can be seen.

The total vertical resulting force is determined with Formula J.1 and the resulting horizontal force is determined with Formula J.2.

$$\sum V = F_G \cdot \gamma_{fav} + (F_{w,ESL,V} + F_{w,TD,V}) \cdot \gamma_F - F_{u,1} - F_{u,2} \cdot \gamma_F \quad (J.1)$$

$$\sum H = (F_{s,TD} - F_{s,ESL}) \cdot \gamma_N + (F_{w,TD,H} - F_{w,ESL,H}) \cdot \gamma_F + (F_{w,1} + F_{w,2}) \cdot \gamma_F \quad (J.2)$$

This leads to a resulting vertical uplift force of  $74 \text{ kN/m}$  and a resulting horizontal force of  $4721.25 \text{ kN/m}$ . Positive values are to the right and downwards. The resulting vertical force is very low and taking into account the assumptions that are made, it is very risky. Therefore the structure can not deal with the uplift forces. Besides that, the resulting horizontal force can not be countered by the vertical force and sliding will be a problem.

# K

## Multi-Criteria Analysis

In this appendix, the multi-criteria analysis is described. First the weighting factors for the analysis are determined and afterwards the concept are given scores for each criterion.

### K.1. Relative Weighting factors of the criteria

For the determination of the weighting factors of the evaluation criteria, the relative weighting factors are determined first. The relative weighting factors are determined by comparing two criteria with each other. The criterion in the first column is compared to the criteria in the first row. If the criterion in the column is more important than the criterion in the row, a value of 1 is awarded. If the criterion in the row is more important, a value of 0 awarded. The importance of the criteria is based on the requirements of the spillway in combination with the interest of the stakeholders. In Table K.1, this process can be seen.

	a	b	c	d	e	Total
Ease of Operation	a	1	1	1	1	4
Ease of Construction	b	0	1	1	1	3
Serviceability and possibility of inspection	c	0	0	1	1	2
Integration in the environment	d	0	0	0	0	0
Sustainability	e	0	0	0	1	1

Table K.1: Relative weighting factors

It can be concluded that the ease of operation is the most valuable criteria. The operation process of the spillway is the most important process in the functioning of the spillway. If the operational process is extensive and complicated, it will decrease the effectiveness of the process and increase the duration of the process. The second most valuable criteria is the ease of construction. A concept which is difficult to construct is not favourable. Normally, the ease of construction is taken into account in the cost but because of the very rough cost estimation, this is also taken as an important criterion in the multi-criteria analysis.

### K.2. Weighting factors of the criteria

With the values of the relative weighting factors, the weighting factors of each criterion can be determined. This is done by dividing the score of each criterion by the total score of all the criteria. Before doing this, the criterion with 0 points is awarded 1 point, otherwise a weighting factor of 0 will occur. This would imply that this criterion has no meaning in this evaluation. To achieve a fair distinction between the criteria, the other values are multiplied by 2. The weighting factors of the criteria are shown in Table K.2. For simplicity reasons, the weighting factors are multiplied by 100 to end up with round values in the multi-criteria analysis.



		Score	Weighting Factor
Ease of Operation	a	8	$\frac{8}{21} = 0,38$
Ease of Construction	b	6	$\frac{6}{21} = 0,28$
Serviceability and possibility of inspection	c	4	$\frac{4}{21} = 0,19$
Integration in the environment	d	1	$\frac{1}{21} = 0,05$
Sustainability	e	2	$\frac{2}{21} = 0,10$
		$\Sigma = 21$	$\Sigma = 1.00$

Table K.2: Weighting Factor of each Criteria

### K.3. Scores of the Concepts

Each concept is rated between 1 and 10 for each criterion. In which a 1 is the lowest score and a 10 the highest. At the end of the multi-criteria analysis, the concept with the highest score can be seen as the most optimal concept according to the evaluation criteria.

	Weighting Factor (WF)	Concept Siphon		Concept Underflow		Concept Caisson	
		Score	Score· WF	Score	Score·WF	Score	Score·WF
Ease of Operation	38	4	152	5	190	6	228
Ease of Construction	28	6	168	6	168	7	196
Serviceability and possibility of inspection	19	7	133	4	76	6	114
Integration in the environment	5	7	35	8	40	5	25
Sustainability	10	6	60	7	70	8	80
	$\Sigma$		548		544		643

Table K.3: The multi-criteria scores per concept

#### K.3.1. Ease of Operation

##### Concept Siphon - 4

Out of the three concepts, the concept Siphon has the lowest value looking at the ease of operation. The reason for this is the required vacuum pump to let the water flow from the Tidal Lake to the Energy Storage Lake. The use of the vacuum pump is an additional step in the process and in the other concepts not needed because the water level in the Tidal Lake is always higher than the Energy Storage Lake. Another point which leads to a low score is the dependence on both water levels.

##### Concept Underflow - 5

The concept Underflow has a main disadvantage compared to the best scoring concept, that the number of gates that need to be opened to reach the maximum discharge is very high. Therefore it scores lower than the concept Caisson but the number of gates is lower than for the concepts siphon and does not require a vacuum pump and scores therefore higher than concept Siphon.

##### Concept Caisson - 6

The concept Caisson is rated slightly better than the concept Underflow because in the operational phase less gates have to be opened to achieve the maximum discharge capacity. Both concepts require two gates to be opened to let the water flow but the total number of gates is lower in the concept Caisson. Just like the other two concepts, the caisson concept is depending on both water levels.

#### K.3.2. Ease of Construction

##### Concept Siphon - 6

Compared to the concept Caisson, the score is lower because the Tidal Lake part can only be constructed in situ. To construct in situ a large building pit has to be made which is not favourable compared to a small construction dock in which caisson can be made and floated to their final location.

##### Concept Underflow - 6

Although the concept is very similar to the concept Siphon, there are two differences. The first one is the number of caissons that is needed and the second is the location of the pipeline. Less caissons leads less

construction work and therefore the ease of construction scores higher for this concept on this difference. But with the pipeline below the dune, additional dredging work has to be done and afterwards a part of this dredged area has to be filled with sand again. This leads to more work and decreases the ease of construction. At the end, this results in a same rating as the concept Siphon

**Concept Caisson - 7**

This concept has the highest score looking at the ease of construction. The reason for this is the low number of caissons that need to be constructed and each caisson is able to float. Therefore, only one construction dock is needed to construct the caisson. The construction of this construction dock can be difficult due to the height of the caisson. The height can also cause some difficulties during transport.

**K.3.3. Serviceability and possibility of inspection****Concept Siphon - 7**

In concept Siphon, the pipeline is above the dune which makes it easy to inspect or replace. In case of leakage or other failures, it is easy to find the broken pipeline. Besides this, the number of pipes is high and therefore if one is out of order due to inspection, only a low decrease in capacity will occur.

**Concept Underflow - 4**

Concept Underflow is by far the most difficult concept looking at serviceability and possibility of inspection. The reason for this is the location of the pipeline. The pipeline can be found below the dune and therefore difficult to reach. In case of leakage or other failure, the dike has to be removed before the pipe can be replaced. This dike removal is difficult and cannot be done during the storming seasons. Besides this, if the dike is removed, the spillway cannot be used at all.

**Concept Caisson - 6**

Easy access to the conduit is available in this concept and therefore the possibility of inspection is good. If one of the conduits needs inspection, this conduit can be closed individually and has no influence on the rest of the conduits. The reason for a lower score than the concept Siphon is that the access of the Siphon concept is easier.

**K.3.4. Integration in the environment****Concept Siphon - 7**

The concept Siphon is rated a 7 for the integration in the environment. The reason for this, is the use of the dune trajectory. Due to this, the concept is more integrated in the environment. The downside of this concept is, that the pipelines are laying on the dune and therefore the score is lower than the underflow concept. A positive side of this concept is the caisson in the Energy Storage Lake, which is not always visible because it is under water. This improves the integration with the environment.

**Concept Underflow - 8**

Concept Underflow is the highest rated concept regarding the integration in the environment. The reason for this is that only the caisson on the Tidal Lake side will be visible and this caisson is relatively small compared to the caisson in the concept Caisson. The pipeline is constructed below the dune and will therefore be not visible. This results in a design in which most of the visible parts is nature which is very common around the North Sea.

**Concept Caisson - 5**

The concept Caisson is rated the lowest regarding the integration in the environment. The reason for this is the visibility of the spillway and the different look compared to the surrounding environment. The concept Caisson has a concrete look which does not fit in the environment.

**K.3.5. Sustainability****Concept Siphon - 6**

The carbon footprint of the concept Siphon is the worst compared to the other concepts. The reason for this is the large amount of concrete that is necessary for the construction of the caissons. At the moment, 8% of the CO<sub>2</sub> emission in the world is due to the production of cement, the main ingredient of concrete (Rodgers,

2018). Therefore, a large volume of concrete leads to a large carbon footprint which is not wanted in the current climate crisis. Besides this large amount of concrete, the number of caissons is larger compared to the other concepts which leads to more transport which also results in an increase in CO<sub>2</sub>. An advantage compared to the concept caisson is the reuse of dredged sand. A large amount of sand can be used in the construction of the dunes.

**Concept Underflow - 7**

Compared to the concept Siphon, the number of caissons required is lower and therefore the amount of concrete is lower. This lower number of concrete leads to a lower carbon footprint. Combining this with the decrease in number of transports required, this leads to a better concept regarding the sustainability criteria than the concept Siphon. The amount of sand that can be reused is higher which is more sustainable as well.

**Concept Caisson - 8**

The concept Caisson has the lowest value for the reuse of sand that is retrieved from dredging the Energy Storage Lake. But an important difference between this concept and the other two concepts is the use of concrete. Although the concept is based on a concrete caisson and no use of the dune trajectory, the amount of concrete is lower and therefore the carbon footprint of the construction is lower. This leads to a more sustainable design than the other concepts. For this reason, this concept is the highest rated concept regarding sustainability.



# Cost Evaluation

In this appendix, the cost estimation that is used in the evaluation and selection of the concepts is described. This is done for each concept separately.

## L.1. Concept Siphon

The cost of the concept Siphon are divided in nine different parts.

- Concrete Works
- Ballast Material
- Gates
- Pipeline
- Construction Dock
- Building Pit
- OTA0-Process
- Dredging Work
- Dune Construction

For all these different parts, unity prices are retrieved from the section Tender Infra Projects of Ballast Nedam. Behind the unit prices some assumptions can be found. These assumptions are elaborated in more detail in the remainder of this appendix.

### Concrete Works

For the concrete, an unit price of €500,- per m<sup>3</sup> is taken. This unit price is assumed to be equal for all elements of the caisson.

### Ballast Material

The required ballast material is already available on the location due to the required dredging activities for the energy storage lake. Therefore the cost of the ballast material is only based on the placement of the ballast material in the caissons.

### Gates

For the gates it is assumed that a single gate cost approximate €125.000,-. This cost is a rough estimation since, a detailed design of the gate and the gate mechanics is not part of this thesis.

### Pipeline

For the pipeline, an extrapolation is made from the known prices of concrete pipes with a diameter of 2200

mm and a thickness of 210 mm. This resulted in a price of €600,- per  $m^3$ . There are 212 pipelines required with a length of 900 m and a thickness of 400 mm. The results in  $863\,159\,m^3$  of concrete pipeline.

### Construction Dock

The cost for the construction dock are based on the price for a combination wall and the construction of a gate. There is chosen for a combination wall because of the large depth. The combination wall is approximate €42.175,- per meter and the gate is approximate €500.000,-. In the construction dock, it is considered that 4 caissons can be constructed at once. This leads to a construction dock with a perimeter of 364 m. The length of the dock is 111 m. This includes the length of 2 caissons, 96 m (2x48) and 5 m space between the caissons self and the walls of the dock. The width of the dock is 71 m. This includes 2 times the width of the caisson, 56 m (2x28) and the 5 m free space between the caissons and the caissons and the wall.

### Building Pit

At the tidal lake side, a building pit has to be created because the caissons are not able to float. It is assumed that sheet pile walls are bought to construct a pit for 4 caissons. These walls are reused each time. Totally this process repeats itself 13 times. Afterwards, one small building pit has to be constructed for the last caisson. The dimensions of the building pit are 20 m by 192 m and a depth of 14 m. The cost of the building pit is €35,- per  $m^2$ .

### OTAO-Process

The OTAO-process (in Dutch: **O**pdrijven, **T**ransportereren, **A**fzinken en **O**nderstromen **O**pleggen) is the process in which the caissons are transported from the construction dock to the final location. Part of this process is also the placement of the caissons at the final location. With 53 caissons, the OTAO process repeats itself 53 times. Each OTAO process costs €1 750 000,-.

### Dredging Work

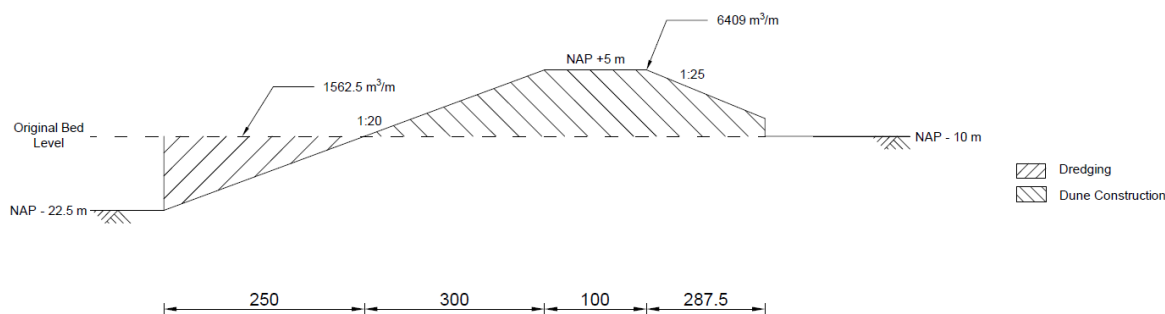


Figure L.1: Dredging and dune construction volumes for spillway

The dredging work of the concept Siphon consists of removing sand to create the lower part of the dune. In Figure L.1, the area that has to be dredged is presented. This area leads to a volume of  $1562.5\,m^3/m$  that needs to be dredged. The total length of the spillway is 2544 m. This results in a total volume of approximately  $3\,975\,000\,m^3$ . The cost of the dredging and dune construction works are €10,- per  $m^3$ .

### Dune Construction

In Figure L.1, the volume of sand that needs to be placed to construct the dune is illustrated. It can be seen that  $6409\,m^3/m$  needs to be placed. Considering the total length of the spillway, 2544 m, the total volume that needs to be placed is approximately  $16\,300\,000\,m^3$ .

The total cost for the concept Siphon can be seen in Table L.1.

	Volume		Unit Price		Total Cost [€]
<b>Concrete Work</b>	362 244	m <sup>3</sup>	€500,-	per m <sup>3</sup>	€181.120.000,-
<b>Ballast Material</b>	538 480	m <sup>3</sup>	€10,-	per m <sup>3</sup>	€5.380.000,-
<b>Gates</b>	424	Gates	€125.000,-	per Gate	€53.000.000,-
<b>Pipeline</b>	863 159	m <sup>3</sup>	€600,-	per m <sup>3</sup>	€517.900.000,-
<b>Construction Dock</b>	364	m <sup>1</sup>	€42.175,-	per m <sup>1</sup>	€15.850.000,-
	1	Gate	€500.000,-	per Gate	
<b>Building Pit</b>	75 843	m <sup>2</sup>	€35,-	per m <sup>2</sup>	€2.650.000,-
<b>OTAO-Process</b>	53	Caissons	€1.750.000,-	per Caisson	€92.750.000,-
<b>Dredging Work</b>	3 975 000	m <sup>3</sup>	€10,-	per m <sup>3</sup>	€39.750.000,-
<b>Dune Construction</b>	16 300 000	m <sup>3</sup>	€10,-	per m <sup>3</sup>	€163.000.000,-
				Σ	<b>€1.071.400.000</b>

Table L.1: Cost of concept Siphon

## L.2. Concept Underflow

For the concept Underflow, the same nine different parts of the cost are used. Only if there is a change in assumption, this is mentioned in the remainder of this section. Otherwise the assumptions are equal to the assumptions for the concept Siphon.

### Dredging Work

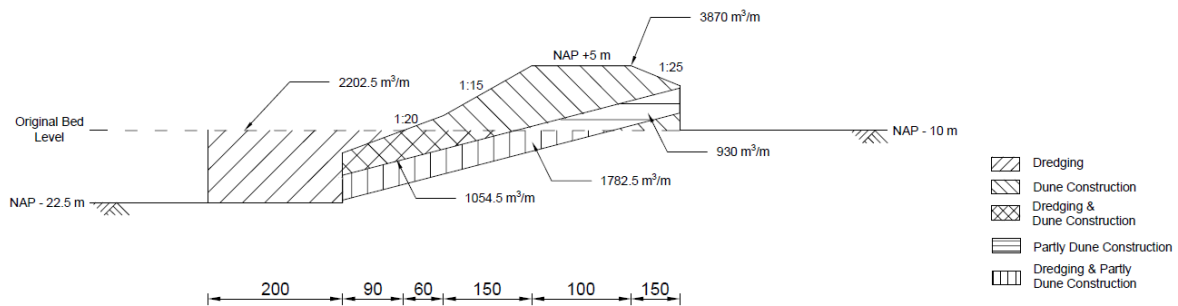
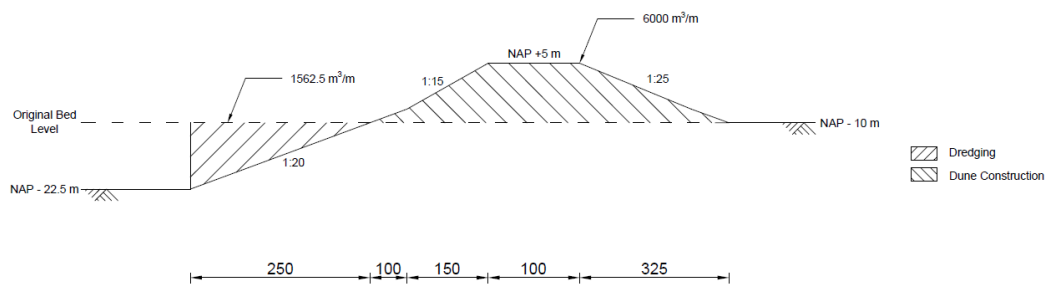


Figure L.2: Dredging and dune construction volumes for spillway trajectory

In concept Underflow, more dredging work has to be performed compared to concept Siphon. The reason for this is that the pipes will be placed below the dune. Consequently, the sand has to be removed first before the pipes can be placed. In Figure L.2, the dredging volumes are shown. A total of 5039.5 m<sup>3</sup>/m has to be dredged. The length of the spillway is 2112 m and as a result of this, the total amount of dredged sand is approximately 10 643 000 m<sup>3</sup>. Each concept has a different total length. For concepts with a shorter length, a dune has to be constructed in the remaining part. In Figure L.3, the dredged volumes for the dune are presented. It can be found that 1562.5 m<sup>3</sup>/m has to be dredged. The remaining part has a length of 432 m (2544-2112 = 432 m). This leads to a total volume of 675 000 m<sup>3</sup>. This is added to the earlier calculated volume and leads to 11 318 000 m<sup>3</sup>.

### Dune Construction



**Figure L.3:** Dredging and dune construction volumes for the normal dune trajectory

After the placement of the pipes, the dune can be constructed. In Figure L.2, the construction volumes can be found. A total of  $7637 \text{ m}^3/\text{m}$  has to be constructed. Over the total length this leads to a volume of  $16\,129\,000 \text{ m}^3$ . However, it has to be taken into account that at the location of the pipes, no sand is required. Therefore, the volume of the pipes is subtracted. There are 177 pipes with a diameter of 5 m and a length of 540 m. This results in a volume of  $8\,478 \text{ m}^3$  per pipe and a total of  $1\,501\,000 \text{ m}^3$ . Subtracting this leads to the total volume that has to be constructed:  $14\,628\,000 \text{ m}^3$ . In the remaining part of the trajectory, the dune has to be constructed. In Figure L.3, it can be seen that this requires  $6000 \text{ m}^3/\text{m}$  and over 432 m this leads to  $2\,592\,000 \text{ m}^3$ . Overall, this results in a total of  $17\,220\,000 \text{ m}^3$ .

The total cost for the concept Siphon can be seen in Table L.2.

	Volume		Unit Price		Total Cost [€]
<b>Concrete Work</b>	300 731	$\text{m}^3$	€500,-	per $\text{m}^3$	€150.370.000,-
<b>Ballast Material</b>	447 040	$\text{m}^3$	€10,-	per $\text{m}^3$	€4.470.000,-
<b>Gates</b>	352	Gates	€125.000,-	per Gate	€44.000.000,-
<b>Pipeline</b>	429 951	$\text{m}^3$	€600,-	per $\text{m}^3$	€257.970.000,-
<b>Construction Dock</b>	364	$\text{m}^1$	€42.175,-	per $\text{m}^1$	€15.850.000,-
	1	Gate	€500.000	per Gate	
<b>Building Pit</b>	62 964	$\text{m}^2$	€35,-	per $\text{m}^2$	€2.200.000,-
<b>OTAO-Process</b>	44	Caissons	€1.750.000,-	per Caisson	€77.000.000,-
<b>Dredging Work</b>	11 318 000	$\text{m}^3$	€10,-	per $\text{m}^3$	€113.180.000,-
<b>Dune Construction</b>	17 220 000	$\text{m}^3$	€10,-	per $\text{m}^3$	€172.200.000,-
				$\Sigma$	<b>€837.240.000,-</b>

**Table L.2:** Cost of concept Underflow

## L.3. Concept Caisson

In the cost estimation of the concept Caisson, some different parts are used to distinguish the costs. The cost for the sill, seepage screen are added and the costs of the pipeline and building pit are removed. Again, only if there is a change in the assumption, this is mentioned in this section. Otherwise the same assumptions are valid.

### Gates

The gates of the concept Caisson are bigger than the gates in the other two concepts. Therefore the costs of a single gate are estimated at €250.000,-

### Construction Dock

The cost for the construction dock are based on the price for a combination wall and the construction of a gate. There is chosen for a combination wall because of the large depth. The combination wall is approximate €45.000,- per meter and the gate is approximate €500.000,-. In the construction dock, it is considered that 4 caissons can be constructed at once. This leads to a construction dock with a perimeter of 364 m. The length of the dock is 81 m. This includes the length of 2 caissons, 66 m (2x49.5) and 5 m space between the caissons self and the walls of the dock. The width of the dock is 114 m. This includes 2 times the width of the caisson, 99 m (2x49.5) and the 5 m free space between the caissons and the caissons and the wall. The depth of the construction dock will be approximately 22.5 m.

### Sill

Below the caisson, a sill needs to be constructed. This sill will consist of sand/gravel mixture. The costs of such a mixture is approximately €25,- per m<sup>3</sup>

### Seepage Screen

To overcome the problems occurring due to the piping below the caisson, a sheet pile wall has to be placed. In this thesis, the sheet pile wall is not analysed in detail but for the cost an estimation has to be made. It is assumed that the sheet pile wall costs approximately €50.000,- per m. This is based on the cost of a combined wall. Although a sheet pile wall is not the same as a combined wall, it is assumed that the cost of the seepage screen is more in the range of the combined wall than the sheet pile wall used for the building pits. The reason for this is the required depth and the compressed sand layer, which increases the difficulty of the placement.

### Dredging Work

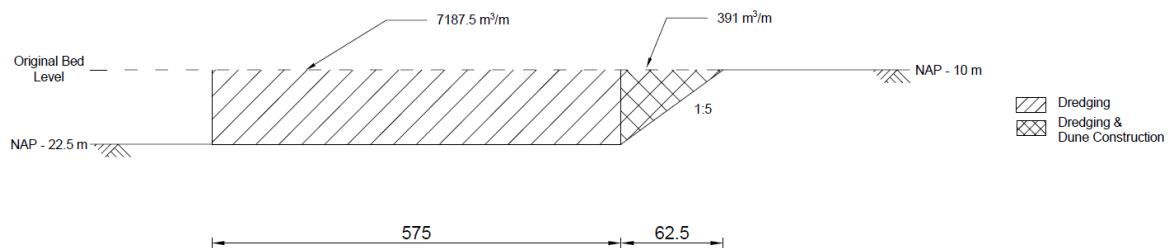


Figure L.4: Dredging and dune construction volumes for the spillway

In Figure L.4, the dredging volumes can be found. Due to the smaller width of the structure, a larger part of the soil has to be dredged to a depth of NAP - 22.5 m. Comparing the location of the caisson with the dune, the caisson is placed in the middle of the highest part of the dune. Therefore, a volume of 7187.5 m<sup>3</sup>/m has to be dredged. Besides this, an area has to be dredged to ensure a stable slope next to the location of the caisson. This slope is assumed to be 1:5. This results in an additional amount of 391 m<sup>3</sup>/m that needs to be dredged. The total dredging volume is 7578.5 m<sup>3</sup>/m. The spillway has a length of 858 m and this leads to a total volume of 6 502 000 m<sup>3</sup>. In the remainder part (1686 m), the dune is constructed and this requires 2 634 000 m<sup>3</sup>. For the construction of the concept Caisson, a total volume of 9 136 000 m<sup>3</sup> must be removed.

### Dune Construction

In the concept Caisson, only a small amount of sand has to be placed next to the structure. This amount is 391 m<sup>3</sup>/m and a total of 335 000 m<sup>3</sup>. In the remaining part (1686 m), the dune is constructed and therefore a total amount of 10 116 000 m<sup>3</sup> is required. The total volume that is required for the dune construction is 10 451 000 m<sup>3</sup>.



The total cost for the concept Caisson can be seen in Table L.3

	<b>Volume</b>		<b>Unit Price</b>		<b>Total Cost [€]</b>
<b>Concrete Work</b>	252 915	m <sup>3</sup>	€500,-	per m <sup>3</sup>	€126.460.000,-
<b>Ballast Material</b>	622 362	m <sup>3</sup>	€10,-	per m <sup>3</sup>	€6.220.000,-
<b>Gates</b>	156	Gates	€250.000,-	per Gate	€39.000.000,-
<b>Construction Dock</b>	350	m <sup>1</sup>	€45.000,-	per m <sup>1</sup>	€16.250.000,-
	1	Gate	€500.000,-	per Gate	
<b>Sill</b>	84 942	m <sup>3</sup>	€35,-	per m <sup>2</sup>	€2.120.000,-
<b>Seepage Screen</b>	858	m <sup>1</sup>	€50.000	per m <sup>1</sup>	€42.900.000,-
<b>OTAO-Process</b>	26	Caissons	€1.750.000,-	per Caisson	€45.500.000,-
<b>Dredging Work</b>	9 136 000	m <sup>3</sup>	€10,-	per m <sup>3</sup>	€91.360.000,-
<b>Dune Construction</b>	10 451 000	m <sup>3</sup>	€10,-	per m <sup>3</sup>	€104.510.000,-
				Σ	<b>€474.320.000,-</b>

**Table L.3:** Cost of concept Caisson

# M

## Strength Verification of Concept Caisson

In this appendix, the strength verification can be found for the concept Caisson. It has been analysed if the external and internal walls and floors are able to withstand the loads acting upon them. Within this thesis, the following strength verification checks have been considered: bending moment, shear force and crack width. The resistance for each failure mechanisms is determined according to NEN-EN 1992-1-1 (2011b). For the loads acting upon the walls and floors, NEN 6720 (1995) is used. To obtain the characteristic bending moment and shear force, NEN 6720 is used. This code is a withdrawn Dutch code which provides formulas to obtain the bending moment and shear force in plates. In the current Eurocodes, these formulas have been removed and is referred to other literature. For the verification of the elements of the caisson, all the elements are assumed to act as concrete plates. The distribution of the bending moment and the shear forces are determined by the theory of elasticity.

### M.1. Theory of Elasticity

In the theory of elasticity, the walls and floors are assumed to be homogeneous and elastic slab material. The slabs can either be hinged or fixed supported or a combination of the two. In Figure M.1, the formulas can be seen that are used to obtain the bending moment in the plates according to the theory of elasticity for multiple situations. As mentioned before, this figure follows from the NEN 6720. Each situation shows a different way of supporting the slab.

In the caisson, the walls and floor will be somewhere between fully fixed and fully hinged. Therefore, situation I,II,IV-A and IV-B in Figure M.1 are relevant for the strength verification. In the first column of this figure, the formulas are given that need to be used to calculate the moments for each situation. With the length and width ratio of the slab, a value can be found by the use of interpolation, which needs to be multiplied with the formula in the first column.

		$l_y/l_x$	1.0	1.2	1.4	1.6	1.8	2.0	2.5	3.0
I		$m_{vx} = 0.001 p_d l_x^2$ $m_{vy} = 0.001 p_d l_x^2$	41	54	67	79	87	97	110	117
		$m_{vx} = 0.001 p_d l_x^2$ $m_{vy} = 0.001 p_d l_x^2$ $m_{vx} = -0.001 p_d l_x^2$ $m_{vy} = -0.001 p_d l_x^2$ $a_x/l_x =$ $a_y/l_y =$	41	35	31	28	26	25	24	23
II		$m_{vx} = 0.001 p_d l_x^2$ $m_{vy} = 0.001 p_d l_x^2$ $m_{vx} = -0.001 p_d l_x^2$ $m_{vy} = -0.001 p_d l_x^2$ $a_x/l_x =$ $a_y/l_y =$	18	26	32	36	39	41	42	43
		$m_{vx} = 0.001 p_d l_x^2$ $m_{vy} = 0.001 p_d l_x^2$ $m_{vx} = -0.001 p_d l_x^2$ $m_{vy} = -0.001 p_d l_x^2$ $a_x/l_x =$ $a_y/l_y =$	18	16	12	10	10	10	10	10
III		$m_{vx} = 0.001 p_d l_x^2$ $m_{vy} = 0.001 p_d l_x^2$ $m_{vx} = -0.001 p_d l_x^2$ $m_{vy} = -0.001 p_d l_x^2$ $a_x/l_x =$ $a_y/l_y =$	25	36	45	53	58	62	67	69
		$m_{vx} = 0.001 p_d l_x^2$ $m_{vy} = 0.001 p_d l_x^2$ $m_{vx} = -0.001 p_d l_x^2$ $m_{vy} = -0.001 p_d l_x^2$ $a_x/l_x =$ $a_y/l_y =$	25	23	20	19	18	17	17	17
IV A		$m_{vx} = 0.001 p_d l_x^2$ $m_{vy} = 0.001 p_d l_x^2$ $m_{vx} = -0.001 p_d l_x^2$ $m_{vy} = -0.001 p_d l_x^2$ $a_x/l_x =$ $a_y/l_y =$	16	28	42	56	69	80	100	112
		$m_{vx} = 0.001 p_d l_x^2$ $m_{vy} = 0.001 p_d l_x^2$ $m_{vx} = -0.001 p_d l_x^2$ $m_{vy} = -0.001 p_d l_x^2$ $a_x/l_x =$ $a_y/l_y =$	29	32	32	30	27	24	20	18
IV B		$m_{vx} = 0.001 p_d l_x^2$ $m_{vy} = 0.001 p_d l_x^2$ $m_{vx} = -0.001 p_d l_x^2$ $m_{vy} = -0.001 p_d l_x^2$ $a_x/l_x =$	29	34	38	40	42	42	42	42
		$m_{vx} = 0.001 p_d l_x^2$ $m_{vy} = 0.001 p_d l_x^2$ $m_{vx} = -0.001 p_d l_x^2$ $m_{vy} = -0.001 p_d l_x^2$ $a_x/l_x =$	16	14	13	13	13	13	13	13
V A		$m_{vx} = 0.001 p_d l_x^2$ $m_{vy} = 0.001 p_d l_x^2$ $m_{vx} = -0.001 p_d l_x^2$ $m_{vy} = -0.001 p_d l_x^2$ $a_x/l_x =$ $a_y/l_y =$	27	41	54	67	78	89	105	115
		$m_{vx} = 0.001 p_d l_x^2$ $m_{vy} = 0.001 p_d l_x^2$ $m_{vx} = -0.001 p_d l_x^2$ $m_{vy} = -0.001 p_d l_x^2$ $a_x/l_x =$ $a_y/l_y =$	38	37	34	30	27	25	24	23
V B		$m_{vx} = 0.001 p_d l_x^2$ $m_{vy} = 0.001 p_d l_x^2$ $m_{vx} = -0.001 p_d l_x^2$ $m_{vy} = -0.001 p_d l_x^2$ $a_x/l_x =$	27	21	19	18	17	17	17	17
		$m_{vx} = 0.001 p_d l_x^2$ $m_{vy} = 0.001 p_d l_x^2$ $m_{vx} = -0.001 p_d l_x^2$ $m_{vy} = -0.001 p_d l_x^2$ $a_x/l_x =$	91	98	107	113	118	120	124	124
VI A		$m_{vx} = 0.001 p_d l_x^2$ $m_{vy} = 0.001 p_d l_x^2$ $m_{vx} = -0.001 p_d l_x^2$ $m_{vy} = -0.001 p_d l_x^2$ $a_x/l_x =$ $a_y/l_y =$	18	29	39	47	54	59	66	69
		$m_{vx} = 0.001 p_d l_x^2$ $m_{vy} = 0.001 p_d l_x^2$ $m_{vx} = -0.001 p_d l_x^2$ $m_{vy} = -0.001 p_d l_x^2$ $a_x/l_x =$ $a_y/l_y =$	23	23	20	17	15	14	13	13
VI B		$m_{vx} = 0.001 p_d l_x^2$ $m_{vy} = 0.001 p_d l_x^2$ $m_{vx} = -0.001 p_d l_x^2$ $m_{vy} = -0.001 p_d l_x^2$ $a_x/l_x =$ $a_y/l_y =$	18	15	14	13	13	13	13	13
		$m_{vx} = 0.001 p_d l_x^2$ $m_{vy} = 0.001 p_d l_x^2$ $m_{vx} = -0.001 p_d l_x^2$ $m_{vy} = -0.001 p_d l_x^2$ $a_x/l_x =$ $a_y/l_y =$	60	70	76	80	82	83	83	83

Figure M.1: Table 18 of NEN 6720 (1995)

An important requirement to use this figure, is that the distributed loads acting on the slab are uniformly distributed. Some of the loads acting on the walls in the caisson are not uniformly but are triangular loads. These loads are substituted for uniformly distributed loads to full fill the requirement. if the triangular load,  $q_t$ , is changed to a uniform distributed load,  $q_u$ , the value of the load is reduced. The reduction that is required is retrieved from the moments that occur at a beam due to a distributed load. In Figure M.2, a fully fixed beam and a beam with two hinged supports can be seen. The moments corresponding to the triangular and uniform load can be seen as well.

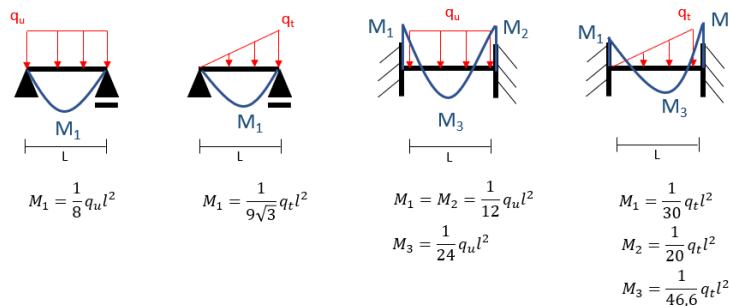


Figure M.2: Bending moment due to a distributed load

The moment with the uniform distributed loads must be equal to the moment with the triangular load. This requires that the uniform distributed load is 0.512 times the triangular distributed load for the hinged situation.

$$M_{1,u} = M_{1,t} \rightarrow \frac{1}{8} q_u l^2 = \frac{1}{9\sqrt{3}} q_t l^2 \rightarrow q_u = \frac{9\sqrt{3}}{8} q_t = 0.512 q_t$$

For the fully fixed situation, the uniform distributed load should be equal to 0.6 times the triangular distributed load.

$$M_{1,u} = M_{2,t} \rightarrow \frac{1}{12} q_u l^2 = \frac{1}{20} q_t l^2 \rightarrow q_u = \frac{20}{12} q_t = 0.6 q_t$$

The most unfavourable situation is the fixed situation and therefore a value of 0.6 will be used in the substitution of the loads. The shear force in the slab is either determined according to the theory of elasticity method of NEN 6720 or modelled as a beam on two supports. If the original distributed load is uniformly, for example internal floors, then the theory of elasticity is applied, see Figure M.3a. If the original distributed load is triangular, for example internal walls, then the slab is modelled as a beam on two supports, see Figure M.3b.

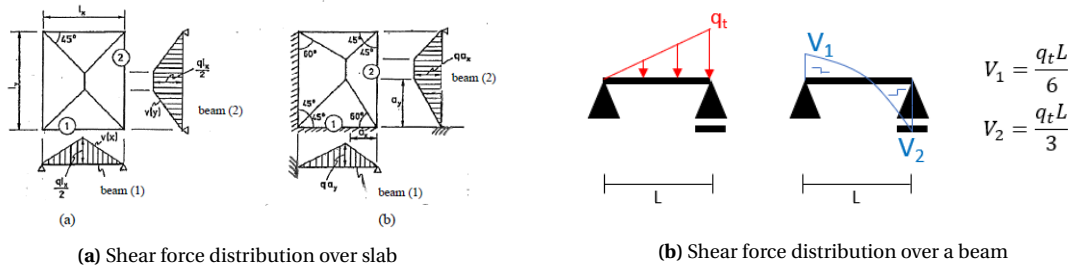
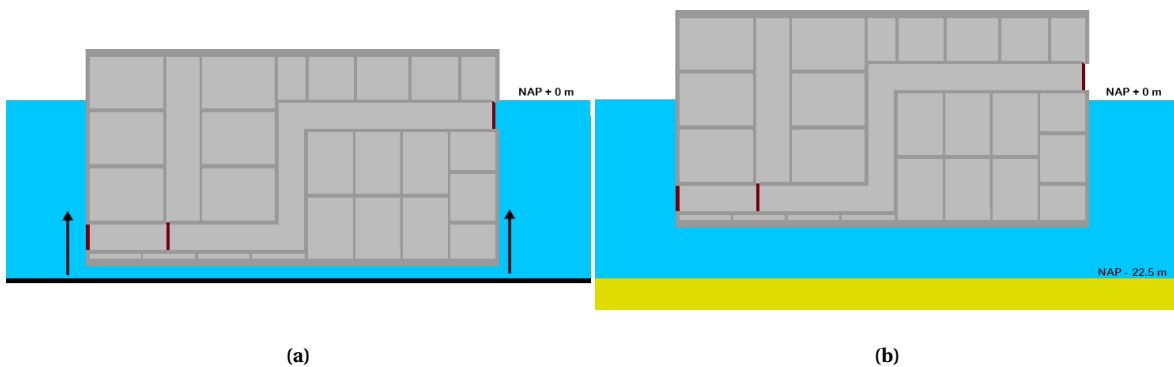
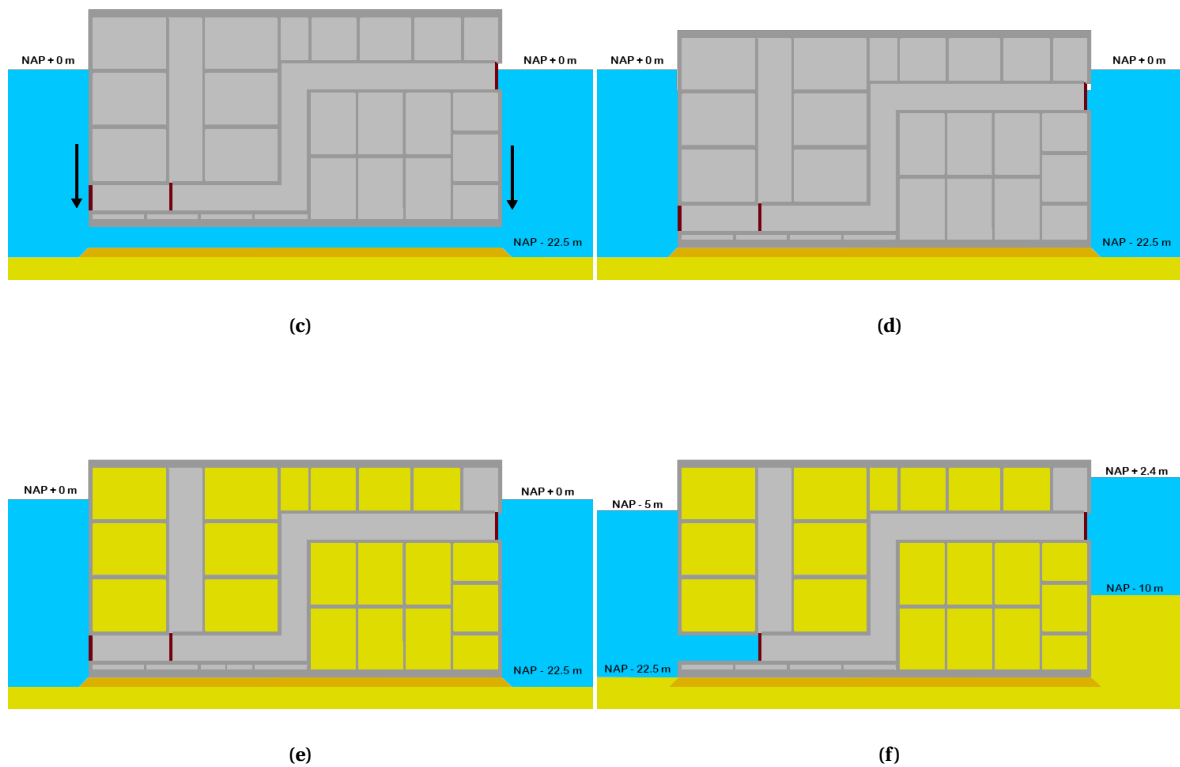


Figure M.3: Shear force distribution

## M.2. Stages after Prefabrication

After the construction of the caisson, multiple steps have to be taken before the spillway can be used. In Figure M.4, the different stages between the construction and the use of the spillway can be seen. In the figure, the improved lay-out is used. More about this lay-out can be seen in Section M.4. Each stage leads to different loads on the caisson. For the strength verification of each element, the governing stage is decided and for this situation the strength of the elements is checked.





**Figure M.4:** (a) Stage 1: Inundation (b) Stage 2: Transport (c) Stage 3: Immersion (d) Stage 4: Just after Immersion (e) Stage 5: Ballasting (f) Stage 6: Final Situation

In total, there are six relevant stages for the strength verification.

- **Stage 1: Inundation:** The construction pit is filled with water and the caisson starts to float.
- **Stage 2: Transport:** The caisson is transported to the final location.
- **Stage 3: Immersion:** At the final location, the caisson is immersed by filling tanks inside the caisson with water (Not shown in Figure).
- **Stage 4: Just after Immersion:** After immersion, the ballast material is still missing but the ballast water is keeping the caisson at the bottom of the energy storage lake.
- **Stage 5: Ballasting:** The ballast water is replaced by ballast sand.
- **Stage 6: Final Situation:** At the tidal lake side, sand is placed to reach the normal bed level in the tidal lake, NAP - 10 m.

### M.3. Initial Lay-out of the Caisson

The initial lay-out of the caisson is based on the functional and the stability requirements, see Section 6.5.3.9. In Figure M.5, the initial lay-out can be seen. The governing external and internal walls and floors are show in this figure. These walls are governing because the highest resulting load is acting upon these elements.

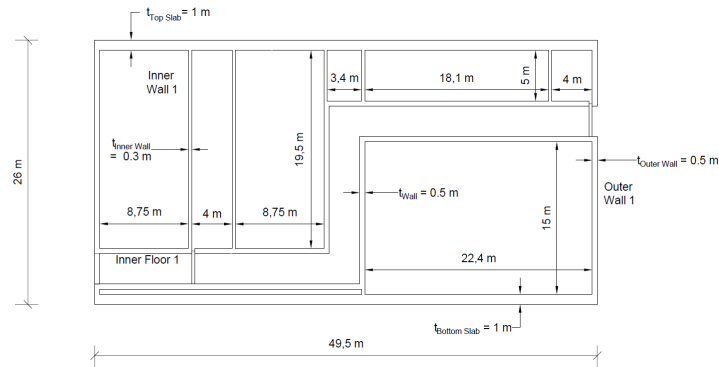


Figure M.5: The initial lay-out of the caisson

In Figure M.6, some of the distributed loads are shown. Only the relevant distributed loads are show, this to improve the clarity of the figure. The loads are determined by the same formulas as used in Appendix H.

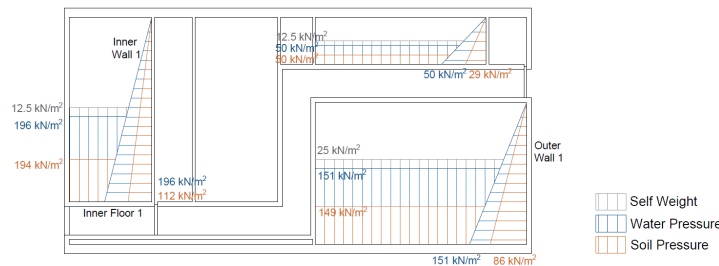


Figure M.6: The characteristic distributed loads

Below, the calculation for the distributed load for internal wall 1 can be seen. These loads are caused by the ballast material.

$$p_{water} = \gamma_w \cdot h = 10.06 \cdot 19.5 = 196 \text{ kN/m}^2$$

$$\sigma_{soil,v} = \gamma'_z \cdot h = (20 - 10.06) \cdot 19.5 = 194 \text{ kN/m}^2$$

$$\sigma_{soil,h} = k_n \cdot \sigma_{soil,v} = 0.577 \cdot (20 - 10.06) \cdot 19.5 = 112 \text{ kN/m}^2$$

#### M.3.1. Internal Wall 1

Internal wall 1 is the first element that is analysed. The reason for this is the relatively small thickness, 300 mm, and the large span, 19.5 m. If this large span is combined with a large load, a large bending moment and shear force occurs. The small thickness leads to a relatively low bending moment and shear capacity. Therefore this element can be seen as a critical element in the design. The maximum load on internal wall 1 occurs during the last two stages, ballasting and the final situation. In these situations, the internal wall is load by the ballast material. In the other stages, there is no load acting on the wall. The loads acting upon the wall in the last two stages can be seen in more detail in Figure M.6. The triangular loads are substituted to uniform distributed loads for the calculation of the bending moment, see Figure M.7.

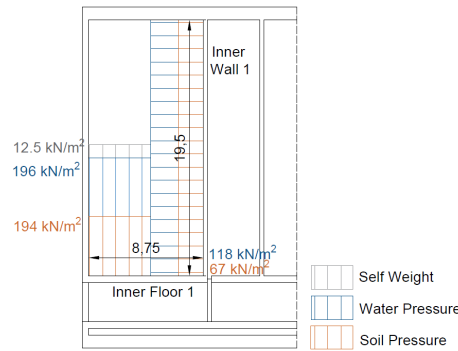


**Figure M.7:** The characteristic distributed loads on internal wall and floor 1

The height of internal wall 1 is 19.5 m and the length of the wall is 10 m. This results in a  $L_x$  of 10 m and  $L_y$  of 19.5 m. The ratio between the two is 1.95. The assessment of the bending moment is done in the ultimate limit state. This means that load factors have to be taken into account. According to EN-NEN 1992-1-1 (2011b), a load factor of 1.35 has to be used for permanent loads and 1.5 for variable loads. The loads due to the ballast material are permanent loads. The characteristic load on the internal wall is 184.8 kN/m<sup>2</sup> and the design distributed load is 249.5 kN/m<sup>2</sup>.

$$q_c = q_{\text{Soil}} + q_{\text{Water}} = 118 + 67 = 185 \text{ kN/m}^2$$

$$q_d = (q_{\text{Soil}} + q_{\text{Water}}) \cdot \gamma_s = (118 + 67) \cdot 1.35 = 249.75 \text{ kN/m}^2$$

With the design distributed load and the length to width ratio, the following bending moments for situations I,II,IV-A and IV-B can be found.

**Situation I:**

$$m_{vx} = 0.001 \cdot 94.5 \cdot p_d \cdot l_x^2 = 0.001 \cdot 94.5 \cdot 249.75 \cdot 10^2 = 2358 \text{ kNm/m}$$

$$m_{vy} = 0.001 \cdot 25.25 \cdot p_d \cdot l_x^2 = 0.001 \cdot 25.25 \cdot 249.75 \cdot 10^2 = 630 \text{ kNm/m}$$

**Situation II:**

$$m_{vx} = 0.001 \cdot 40.5 \cdot p_d \cdot l_x^2 = 0.001 \cdot 40.5 \cdot 249.75 \cdot 10^2 = 1010 \text{ kNm/m}$$

$$m_{vy} = 0.001 \cdot 10 \cdot p_d \cdot l_x^2 = 0.001 \cdot 10 \cdot 249.75 \cdot 10^2 = 249.5 \text{ kNm/m}$$

$$m_{sx} = -0.001 \cdot 81.75 \cdot p_d \cdot l_x^2 = -0.001 \cdot 81.75 \cdot 249.75 \cdot 10^2 = -2040 \text{ kNm/m}$$

$$m_{sy} = -0.001 \cdot 53.25 \cdot p_d \cdot l_x^2 = -0.001 \cdot 53.25 \cdot 249.75 \cdot 10^2 = -1329 \text{ kNm/m}$$

**Situation IV-A:**

$$m_{vx} = 0.001 \cdot 77.25 \cdot p_d \cdot l_x^2 = 0.001 \cdot 77.25 \cdot 249.75 \cdot 10^2 = 1927 \text{ kNm/m}$$

$$m_{vy} = 0.001 \cdot 24.75 \cdot p_d \cdot l_x^2 = 0.001 \cdot 24.75 \cdot 249.75 \cdot 10^2 = 618 \text{ kNm/m}$$

$$m_{sy} = -0.001 \cdot 111.5 \cdot p_d \cdot l_x^2 = -0.001 \cdot 111.5 \cdot 249.75 \cdot 10^2 = -2782 \text{ kNm/m}$$

**Situation IV-B:**

$$m_{vx} = 0.001 \cdot 42 \cdot p_d \cdot l_x^2 = 0.001 \cdot 42 \cdot 249.75 \cdot 10^2 = 1048 \text{ kNm/m}$$

$$m_{vy} = 0.001 \cdot 13 \cdot p_d \cdot l_x^2 = 0.001 \cdot 13 \cdot 249.75 \cdot 10^2 = 324 \text{ kNm/m}$$

$$m_{sx} = -0.001 \cdot 83 \cdot p_d \cdot l_x^2 = -0.001 \cdot 83 \cdot 249.75 \cdot 10^2 = -2071 \text{ kNm/m}$$

The maximum moments can be seen in situation I and IV-A, respectively 2358 kNm/m and -2782 kNm/m. A positive value is a moment at the bottom of the plate and a negative value at the top of the plate. Internal wall 1 has a thickness of 300 mm. The effective height is assumed to be 250 mm and the width is taken as 1000

mm. In Figure M.8, concrete class C50/60 is not present but it is assumed that the reinforcement ratios will be somewhere between the values for C445/55 and C53/65.

$$\frac{M_d}{bd^2 f_{cd}} = \frac{2782}{1 \cdot 0.25^2 \cdot 33.33} = 1337$$

The value of 1337 [-] can not be seen in Figure M.8 because this results in unrealistic large reinforcement ratios. Therefore it can be concluded that the internal wall can not withstand the loads.

$\frac{M_d}{bd^2 f_{cd}}$	$\psi$	$k_x$	$k_z$	$\rho$ [%]				
				C20/25	C28/35	C35/45	C45/55	C53/65
10	0,010	0,013	0,98	0,03	0,05	0,06	0,08	0,09
20	0,020	0,027	0,99	0,07	0,10	0,13	0,15	0,18
30	0,030	0,040	0,98	0,10	0,15	0,19	0,23	0,27
40	0,041	0,055	0,98	0,14	0,20	0,25	0,31	0,37
50	0,051	0,068	0,97	0,18	0,25	0,32	0,39	0,46
60	0,062	0,083	0,97	0,21	0,30	0,39	0,47	0,56
70	0,073	0,097	0,98	0,25	0,35	0,45	0,55	0,66
80	0,084	0,112	0,98	0,28	0,41	0,52	0,64	0,75
90	0,095	0,127	0,95	0,33	0,46	0,59	0,72	0,85
100	0,106	0,141	0,94	0,37	0,51	0,68	0,81	0,95
110	0,117	0,156	0,94	0,40	0,56	0,73	0,89	1,05
120	0,129	0,172	0,93	0,44	0,62	0,80	0,98	1,16
130	0,140	0,187	0,93	0,48	0,68	0,87	1,08	1,26
140	0,152	0,203	0,92	0,52	0,73	0,94	1,15	1,36
150	0,164	0,219	0,91	0,57	0,79	1,02	1,24	1,47
160	0,176	0,235	0,91	0,61	0,85	1,09	1,34	1,58
170	0,188	0,251	0,90	0,65	0,91	1,17	1,43	1,69
180	0,201	0,268	0,90	0,69	0,97	1,25	1,53	1,80
190	0,214	0,285	0,89	0,74	1,03	1,33	1,62	1,92
200	0,227	0,303	0,88	0,78	1,10	1,41	1,72	2,04
210	0,240	0,320	0,88	0,83	1,16	1,49	1,82	2,16
220	0,253	0,337	0,87	0,87	1,22	1,57	1,92	2,27
230	0,267	0,356	0,86	0,92	1,28	1,65	2,03	2,39
240	0,281	0,375	0,85	0,97	1,35	1,75	2,13	2,52
250	0,295	0,393	0,85	1,02	1,43	1,83	2,24	2,64
260	0,310	0,413	0,84	1,07	1,50	1,93	2,35	2,78
270	0,325	0,433	0,83	1,12	1,57	2,02	2,47	2,91
280	0,340	0,453	0,82	1,17	1,64	2,11	2,58	3,05
290	0,356	0,475	0,81	1,23	1,72	2,21	2,70	3,19
300	0,372	0,496	0,81	1,28	1,80	2,31	2,82	3,34
310	0,388	0,517	0,80	1,34	1,87	2,41	2,94	3,48
320	0,405	0,540	0,79	1,40	1,96	2,51	3,07	3,63

Figure M.8: Reinforcement ratios and bending moments capacities (Voorendt and Molenaar, 2020b)

### M.3.2. Internal Floor 1

Although the thickness of internal floor 1, 500 mm, is larger than internal wall 1 and the span width is lower, the floor is still critical due to the large load acting upon the floor in the last two stages, ballasting and the final situation. The loads acting upon internal floor 1 can be seen in Figure M.7. The same calculations have been performed as for internal wall 1. For internal floor 1, there is no reduction in soil pressure because the pressures are vertical. Therefore the load due to the ballast material is larger than for internal wall 1. An additional load for this calculation is the self weight of the element. The loads acting on the floor are permanent and therefore a load factor of 1.35 is used. The characteristic load on the floor is 402.5 kN/m<sup>2</sup> and the design load is equal to 543 kN/m<sup>2</sup>.

$$q_c = q_{\text{Soil}} + q_{\text{Water}} + q_{\text{Self Weight}} = 194 + 196 + 12.5 = 402.5 \text{ kN/m}^2$$

$$q_d = (q_{\text{Soil}} + q_{\text{Water}} + q_{\text{Self Weight}}) \cdot \gamma_S = (194 + 196 + 12.5) \cdot 1.35 = 543 \text{ kN/m}^2$$

The dimension of the floor are 8.75 m ( $L_x$ ) by 10 m ( $L_y$ ). The ratio between these two is 1.14. This leads to a maximum bending moment of respectively 2092 kNm/m and -3346 kNm/m. Using Figure M.8, the required reinforcement ratio for this floor can be found.

$$\frac{M_d}{bd^2 f_{cd}} = \frac{3346}{1 \cdot 0.45^2 \cdot 33.33} = 496$$



Just like the internal wall, the required reinforcement ratio can not be found in the figure because the ratio must be larger than the maximum allowable ratio. Therefore it can be concluded that the internal floor cannot withstand the loads and improvements are made.

### M.4. The Improved Lay-out

In Section M.3, it is shown that the initial lay-out is not sufficient to withstand the loads. To improve the lay-out, two different improvements are introduced. First, the thickness of certain elements is changed and secondly, the caisson is divided into different compartments. By increasing the thickness of an element, the capacity of this element increases and by dividing the caisson in multiple compartments, the loads acting on the elements are decreased. The new element thickness and compartment dimensions are found by an iterative process in which a trial and error method is used. The change in thickness of the elements differ per element and can be seen below:

- Internal wall thickness increased from 300 mm to 400 mm
- External wall thickness increased from 500 mm to 600 mm
- Internal floor thickness increased from 300 mm to 600 mm
- Culvert wall thickness increased locally from 500 mm to 600 mm (Only on the left side of the culvert)

The reason for the locally increased thickness of the culvert wall is that at that location a bigger load is present than on the other culvert walls. The new lay-out can be seen in Figure M.9.

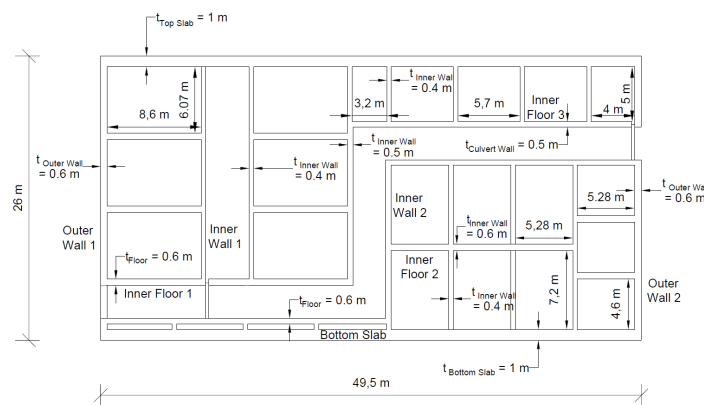


Figure M.9: The improved lay-out of the caisson

In the improved lay-out, the loads acting on the walls and floors are decreased due to the use of compartments. The new loads can be seen in Figure M.10.

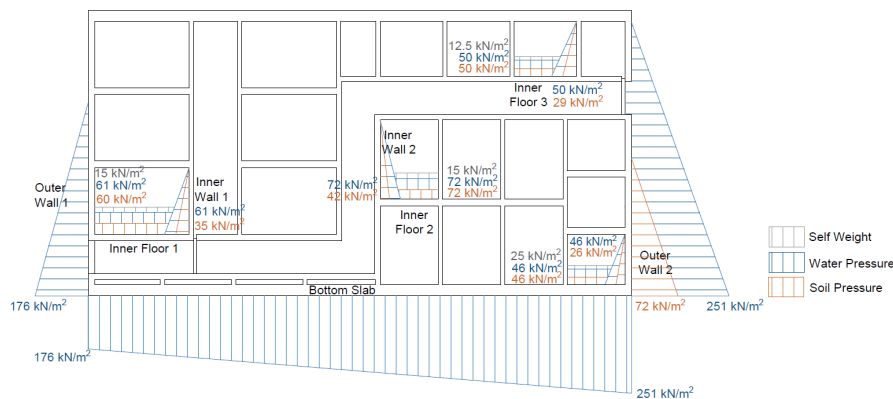


Figure M.10: The loads in the new lay-out of the caisson

### M.4.1. Concrete Cover

For the verification of the strength and the lay-out of the reinforcement, the required concrete cover is important. The required cover is depending on multiple factors. One of the reasons to ensure enough cover is to protect the steel reinforcement bars from corrosion. The concrete cover is based on a minimum cover,  $c_{min}$ , and an allowance of deviation,  $\Delta c_{dev}$ .

$$c_{nom} = c_{min} + \Delta c_{dev} \quad (M.1)$$

According to the National Annex of NEN-EN 1992-1-1, article 4.4.1.3, the allowance of deviation is 5 mm. The minimum cover is determined according to NEN-EN 1992-1-1, article 4.4.1.2.

$$c_{min} = \max\{c_{min,b}; c_{min,dur} + \Delta c_{dur,\gamma} - \Delta c_{dur,st} - \Delta c_{dur,add}; 10mm\} \quad (M.2)$$

The  $c_{min,b}$  value is based on the maximum reinforcement diameter. The maximum diameter that is used for the structure is 32 mm. The minimum required cover for durability reason,  $c_{min,dur}$ , is depending on the exposure class and structural class. With XS2 and S5, the minimum required cover is 45 mm. According to the National Annex of NEN-EN 1992-1-1, article 4.4.1.2, the values for  $\Delta c_{dur,\gamma}$ ,  $\Delta c_{dur,st}$  and  $\Delta c_{dur,add}$  can be taken as 0 mm. This results in a minimum cover of 45 mm.

$$c_{min} = \max\{c_{min,b}; c_{min,dur} + \Delta c_{dur,\gamma} - \Delta c_{dur,st} - \Delta c_{dur,add}; 10mm\} = \max\{32; 45; 10\} = 45mm$$

Including the allowance for deviation results in a minimum concrete cover of 50 mm.

### M.4.2. Internal Wall 1

#### M.4.2.1. The Reinforcement

The proposed longitudinal reinforcement for internal wall 1 can be seen in Figure M.11. The used reinforcement is  $\varnothing 25-110$ . This means that the reinforcement bars have a diameter of 25 mm and the centre to centre distance is 110 mm. This leads to 9 bars in 1 m of wall and a reinforcement area of 4418 mm<sup>2</sup>/m. The reinforcement is the same in both length as width direction.

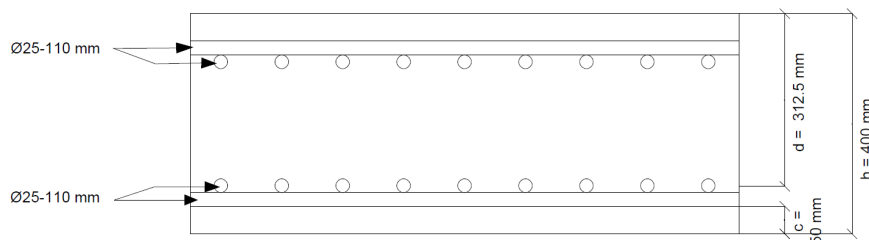


Figure M.11: Reinforcement in internal wall 1

#### M.4.2.2. Bending Moment

The bending moment capacity of the internal wall, obtained by the proposed reinforcement, must exceed the design value of the bending moment.

$$M_{Rd} \geq M_{Ed}$$

with:

$$M_{Rd} = A_s \cdot z \cdot f_{yd}$$

Firstly, the design moment,  $M_{Ed}$ , is determined by using Figure M.1. The governing stage for the internal elements are stages 5 and 6, ballasting and the final situation. In these situations, the elements are loaded by the ballast material and this causes the governing moments and shear forces. In Figure M.12a, the loads acting on internal wall 1, corresponding to these stages, can be seen. Again, the triangular distributed loads are substituted by uniform distributed loads, see Figure M.12b. The total characteristic load acting on the wall,  $q_c$ , is  $58 \text{ kN/m}^2$  and the design load is  $78 \text{ kN/m}^2$ . For the design load a load factor of 1.35 is used because the load due to the ballast material is permanent.

$$q_c = q_{soil} + q_{water} = 21 + 37 = 58 \text{ kN/m}^2$$

$$q_d = (q_{soil} + q_{water}) \cdot \gamma_s = (21 + 37) \cdot 1.35 = 78 \text{ kN/m}^2$$

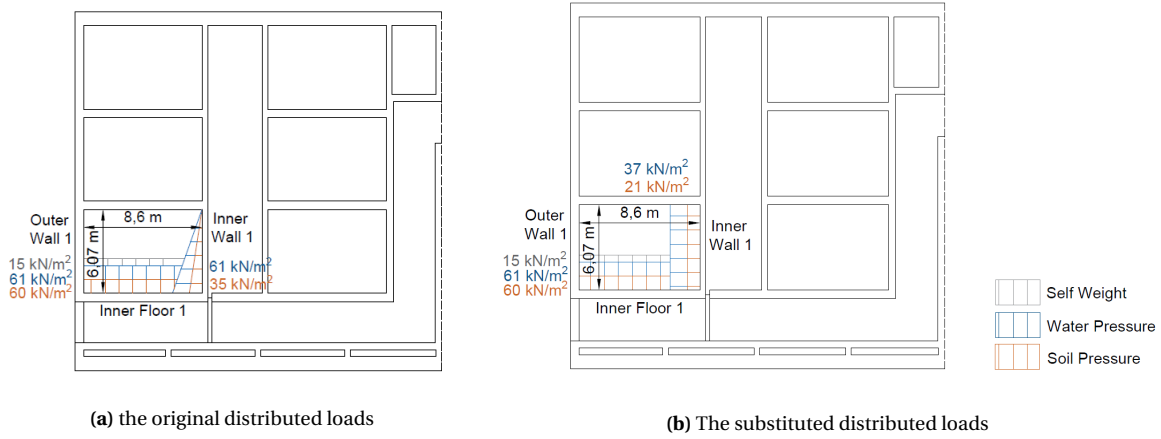


**Figure M.12:** The loads on Internal Wall 1, Internal Floor 1 and External Wall 1

The length,  $L_x$ , and the width,  $L_y$ , of the wall are respectively 6.07 m and 10 m. This leads to a ratio of 1.65 and the following values for  $M_{Ed}$ :

**Situation I:**

$$m_{vx} = 0.001 \cdot 80.9 \cdot p_d \cdot l_x^2 = 0.001 \cdot 80.9 \cdot 78.3 \cdot 6.07^2 = 233 \text{ kNm/m}$$

$$m_{vy} = 0.001 \cdot 27.5 \cdot p_d \cdot l_x^2 = 0.001 \cdot 27.5 \cdot 78.3 \cdot 6.07^2 = 79 \text{ kNm/m}$$

**Situation II:**

$$m_{vx} = 0.001 \cdot 36.7 \cdot p_d \cdot l_x^2 = 0.001 \cdot 36.7 \cdot 78.3 \cdot 6.07^2 = 106 \text{ kNm/m}$$

$$m_{vy} = 0.001 \cdot 10 \cdot p_d \cdot l_x^2 = 0.001 \cdot 10 \cdot 78.3 \cdot 6.07^2 = 29 \text{ kNm/m}$$

$$m_{sx} = -0.001 \cdot 78.7 \cdot p_d \cdot l_x^2 = -0.001 \cdot 78.7 \cdot 78.3 \cdot 6.07^2 = -227 \text{ kNm/m}$$

$$m_{sy} = -0.001 \cdot 54 \cdot p_d \cdot l_x^2 = -0.001 \cdot 54 \cdot 78.3 \cdot 6.07^2 = -156 \text{ kNm/m}$$

**Situation IV-A:**

$$m_{vx} = 0.001 \cdot 59.1 \cdot p_d \cdot l_x^2 = 0.001 \cdot 59.1 \cdot 78.3 \cdot 6.07^2 = 170 \text{ kNm/m}$$

$$m_{vy} = 0.001 \cdot 29.3 \cdot p_d \cdot l_x^2 = 0.001 \cdot 29.3 \cdot 78.3 \cdot 6.07^2 = 84 \text{ kNm/m}$$

$$m_{sy} = -0.001 \cdot 106.2 \cdot p_d \cdot l_x^2 = -0.001 \cdot 106.2 \cdot 78.3 \cdot 6.07^2 = -306 \text{ kNm/m}$$

**Situation IV-B:**

$$m_{vx} = 0.001 \cdot 40.5 \cdot p_d \cdot l_x^2 = 0.001 \cdot 40.5 \cdot 78.3 \cdot 6.07^2 = 117 \text{ kNm/m}$$

$$m_{vy} = 0.001 \cdot 13 \cdot p_d \cdot l_x^2 = 0.001 \cdot 13 \cdot 78.3 \cdot 6.07^2 = 38 \text{ kNm/m}$$

$$m_{sx} = -0.001 \cdot 82.2 \cdot p_d \cdot l_x^2 = -0.001 \cdot 82.2 \cdot 78.3 \cdot 6.07^2 = -237 \text{ kNm/m}$$

The maximum moments can be found in situation I and IV-A, respectively 233 kNm/m and -306 kNm/m. The moment of 233 kNm/m can be found at the bottom of the plate and the 306 kNm/m can be found at the top of the plate. Secondly, the bending moment capacity,  $M_{Rd}$ , is determined.

$$M_{Rd} = A_s \cdot z \cdot f_{yd}$$

where:  $M_{Rd}$  [Nmm] = bending moment capacity  
 $A_s$  [mm<sup>2</sup>] = the reinforcement area  
 $z$  [mm] = arm of internal leverage  
 $f_{yd}$  [N/mm<sup>2</sup>] = design yield stress of the reinforcement steel (=435 N/mm<sup>2</sup>)

The reinforcement area is 4418 mm<sup>2</sup>/m and the design yield stress of the reinforcement steel is 435 N/mm<sup>2</sup>. The arm of internal leverage,  $z$ , is determined by:

$$z = d - \beta \cdot x_u$$

where:  $d$  [mm] = effective height  
 $\beta$  [-] = parameter (=7/18 for C50/60)  
 $x_u$  [mm] = height of compression zone

The effective height is calculated by:

$$d = h - c - \varnothing_h - 0.5\varnothing_v$$

where:  $h$  [mm] = height of the slab  
 $c$  [mm] = concrete cover  
 $\varnothing_v$  [mm] = diameter of the reinforcement in vertical direction  
 $\varnothing_h$  [mm] = diameter of the reinforcement in horizontal direction

The horizontal and vertical reinforcement are the same and have a diameter of 25 mm. The concrete cover that is required for the design is 50 mm. This required cover is determined in Appendix M.4.1. The height of the slab is 400 mm.

$$d = h - c - \varnothing_h - 0.5\varnothing_v = 400 - 50 - 25 - 0.5 \cdot 25 = 312.5 \text{ mm}$$

With the effective height, the effective concrete area and the reinforcement ratio are determined. The reinforcement ratio is equal to 1.41%. According to Braam (2011), the minimum and maximum reinforcement ratio's for C50/60 are respectively 0.21% and 3.08%. The current lay-out results in a reinforcement ratio between these boundaries.

$$\rho = \frac{A_s}{A_c} = \frac{A_s}{b \cdot d} = \frac{4418}{1000 \cdot 312.5} = 1.41\%$$

The height of the compression zone is retrieved from the equality between the force of the steel and the compression force in the concrete,  $N_s = N_c$ .

$$\begin{aligned} N_s &= A_s \cdot f_{yd} \\ N_c &= 0.75 \cdot x_u \cdot b \cdot f_{cd} \\ N_s = N_c &\rightarrow x_u = \frac{A_s \cdot f_{yd}}{0.75 \cdot b \cdot f_{cd}} \end{aligned}$$

where:  $b$  [mm] = width of the slab  
 $f_{cd}$  [N/mm<sup>2</sup>] = design compressive strength (=33.3 N/mm<sup>2</sup> for C50/60)

For the width a value of 1000 mm is taken. The reason for this is that the given loads are also given per meter. The height of the compression zone is:

$$x_u = \frac{A_s \cdot f_{yd}}{0.75 \cdot b \cdot f_{cd}} = \frac{4418 \cdot 435}{0.75 \cdot 1000 \cdot 33.3} = 76.95 \text{ mm}$$

This results in a arm of internal leverage of 282.6 mm.

$$z = d - \beta \cdot x_u = 320 - \frac{7}{18} \cdot 76.95 = 282.6 \text{ mm}$$

The bending moment capacity becomes:

$$M_{Rd} = A_s \cdot z \cdot f_{yd} = 4418 \cdot 282.6 \cdot 435 = 5.43 \cdot 10^8 \text{ Nmm/m}$$

The bending moment capacity,  $M_{Rd}$ , of internal wall 1 is equal to 543 kNm/m. With a design moment equal to 306 kNm/m, the unity check for the bending moment becomes 0.56.

$$UC = \frac{M_{Ed}}{M_{Rd}} = \frac{306}{543} = 0.56$$

### M.4.2.3. Shear Force

In the ultimate limit state, the shear force capacity must exceed the design shear force. This can be achieved with or without the use of shear reinforcement.

$$V_{Rd,c} \geq V_{Ed} \quad \text{or} \quad V_{Rd,s} \geq V_{Ed}$$

First the design shear force is determined and afterwards it is checked if shear reinforcement is required. In the case that it is required, it is checked if the proposed shear force reinforcement is sufficient. The design shear force in the wall is determined by the modelled beam method due to the triangular forces. The design load on the wall is 129.6 kN/m which results in a  $V_{Ed}$  of:

$$V_{Ed} = \frac{q_d \cdot L_x}{2} = \frac{129.6 \cdot 6.07}{3} = 262 \text{ kN/m}$$

The shear force resistance of the slab without reinforcement is determined by:

$$V_{Rd,c} = (C_{Rd,c} \cdot k \cdot (100 \cdot \rho_1 \cdot f_{ck})^{\frac{1}{3}} + k_1 \cdot \sigma_{cp}) \cdot b_w \cdot d$$

with a minimum of:

$$V_{Rd,c,min} = (v_{min} + k_1 \cdot \sigma_{cp}) \cdot b_w \cdot d$$

where:	$V_{Rd,c}$	[kN]	=	shear force resistance
	$V_{Rd,min}$	[kN]	=	minimum shear force resistance
	$C_{Rd,c}$	[-]	=	a coefficient ( $= \frac{0.18}{\gamma_m} = \frac{0.18}{1.5} = 0.12$ )
	$\gamma_m$	[-]	=	material factor (= 1.5)
	$k$	[-]	=	$1 + \sqrt{\frac{200}{d}} \leq 2.0$ with d in mm
	$\rho_1$	[-]	=	reinforcement ratio
	$f_{ck}$	[N/mm <sup>2</sup> ]	=	characteristic compressive cylinder strength of concrete
	$k_1$	[-]	=	a coefficient (= 0.15)
	$\sigma_{cp}$	[N/mm <sup>2</sup> ]	=	compressive stress in the concrete from axial load ( $\sigma_{cp} = \frac{N_{Ed}}{A_c} < 0,2 \cdot f_{cd}$ )
	$N_{Ed}$	[N]	=	the axial force in the cross-section
	$b_w$	[mm]	=	the smallest width of the cross-section
	$d$	[mm]	=	the effective height of the cross-section
	$v_{min}$	[-]	=	$0.035 \cdot k^{\frac{3}{2}} \cdot \sqrt{f_{ck}}$

Firstly the parameters  $k$ ,  $\rho_1$  and  $v_{min}$  are determined and afterwards the shear resistance is calculated. For the calculation of the shear force resistance, the normal force,  $N_{Ed}$ , is neglected. The normal force has a positive effect on the shear force resistance and therefore neglecting it results in a conservative design.

$$k = 1 + \sqrt{\frac{200}{d}} = 1 + \sqrt{\frac{200}{312.5}} = 1.8 \leq 2.0$$

$$\rho_1 = \frac{A_s}{b \cdot d} = \frac{4418}{1000 \cdot 312.5} = 1.41\%$$

$$v_{min} = 0.035 \cdot k^{\frac{3}{2}} \cdot \sqrt{f_{ck}} = 0.035 \cdot 1.8^{\frac{3}{2}} \cdot \sqrt{50} = 0.59$$

The shear resistance without reinforcement is equal to:

$$V_{Rd,c} = (C_{Rd,c} \cdot k \cdot (100 \cdot \rho_1 \cdot f_{ck})^{\frac{1}{3}} + k_1 \cdot \sigma_{cp}) \cdot b_w \cdot d$$

$$= 0.12 \cdot 1.8 \cdot (100 \cdot 0.0141 \cdot 50)^{\frac{1}{3}} + 0.15 \cdot 0 \cdot 1000 \cdot 312.5$$

$$= 396 \text{ kN/m}$$

The minimum value is equal to:

$$V_{Rd,c,min} = (v_{min} + k_1 \cdot \sigma_{cp}) \cdot b_w \cdot d$$

$$= (0.59 + 0.15 \cdot 0) \cdot 1000 \cdot 312.5$$

$$= 304 \text{ kN/m}$$

Without the use of shear reinforcement, the shear force acting on the wall does not exceed the shear force resistance of the concrete,  $262 \text{ kN/m} < 396 \text{ kN/m}$ . The unity check for the shear force is equal to 0.66. Therefore it can be concluded that the wall full fills the requirements for shear resistance.

#### M.4.2.4. Crack Width

According to the National Annex of NEN-EN 1992 (2011b), article 7.3.1, the maximum allowable crack width is 0.2 mm. The theoretical determined value of the crack width may not exceed this maximum value.

$$w_k \leq w_{max}$$

The theoretical crack width is determined with Formula M.3.

$$w_k = s_{r,max} \cdot \frac{\sigma_s - k_t \cdot \frac{f_{ct,eff}}{\rho_{p,eff}} \cdot (1 + \alpha_e \cdot \rho_{p,eff})}{E_s} \quad (\text{M.3})$$

where:	$w_k$	[mm]	=	theoretical crack width
	$s_{r,max}$	[mm]	=	maximum crack spacing
	$\sigma_s$	[N/mm <sup>2</sup> ]	=	tensile stress in the steel bar
	$k_t$	[-]	=	load duration coefficient
	$f_{ct,eff}$	[N/mm <sup>2</sup> ]	=	mean value of the concrete tensile strength (= $f_{ctm}$ )
	$\rho_{p,eff}$	[-]	=	reinforcement ratio
	$E_s$	[N/mm <sup>2</sup> ]	=	Youngs' modulus of steel (= $200 \cdot 10^3 \text{ N/mm}^2$ )
	$E_c$	[N/mm <sup>2</sup> ]	=	Youngs' modulus of concrete
	$\alpha_e$	[-]	=	ratio between Youngs' moduli of steel and concrete (= $\frac{E_s}{E_c}$ )

The load duration factor,  $k_t$ , is respectively 0.4 for long-term loading and 0.6 for short-term loading. The long-term loading is governing because most of the loads acting on the caisson are permanent and present during the lifetime of the spillway. Therefore the  $k_t$  value is set to 0.4. The maximum crack spacing is defined as:

$$s_{r,max} = k_3 c + k_1 k_2 k_4 \frac{\varnothing}{\rho_{p,eff}} \leq \text{MAX}\{(50 - 0.8 \cdot f_{ck}) \cdot \varnothing; 15 \cdot \varnothing\} \quad (\text{M.4})$$

where:  $k_1$  [-] = bond stress coefficient (= 0.8)  
 $k_2$  [-] = coefficient for the distribution of the strain over the height of the concrete area (= 0.5)  
 $k_3$  [-] = coefficient (= 3.4)  
 $k_4$  [-] = coefficient (= 0.425)  
 $c$  [mm] = concrete cover  
 $\varnothing$  [mm] = diameter of the reinforcement

The k factors are depending on the country in which the structure is constructed. In the Netherlands, the values for these factors can be found in the National Annex of NEN-EN 1992. The first step in calculating the crack width is the determination of the maximum crack spacing. For this spacing, the effective reinforcement ratio is required.

$$\rho_{p,eff} = \frac{A_s}{h_{eff} \cdot b}$$

in which:

$$h_{eff} = \text{MIN}\{2.5 \cdot (h - d); \frac{(h - x_u)}{3}; \frac{h}{2}\}$$

The effective height,  $d$ , is equal to 312.5 mm,  $x_u$  is 76.95 mm and  $h$  is 400 mm. This results in a  $h_{eff}$  of:

$$\begin{aligned} h_{eff} &= \text{MIN}\{2.5 \cdot (h - d); \frac{(h - x_u)}{3}; \frac{h}{2}\} \\ &= \text{MIN}\{2.5 \cdot (400 - 312.5); \frac{(400 - 76.95)}{3}; \frac{400}{2}\} \\ &= \text{MIN}\{218.75; 108; 200\} \\ &= 108 \text{ mm} \end{aligned}$$

Again, the width,  $b$ , is set to 1000 mm and this results in a effective reinforcement ratio of:

$$\rho_{p,eff} = \frac{A_s}{h_{eff} \cdot b} = \frac{4418}{108 \cdot 1000} = 4.1\%$$

The maximum crack space becomes:

$$s_{r,max} = k_3 c + k_1 k_2 k_4 \frac{\varnothing}{\rho_{p,eff}} = 3.4 \cdot 50 + 0.8 \cdot .5 \cdot 0.425 \frac{25}{0.041} = 274 \text{ mm}$$

The maximum value for the maximum crack space is equal to 375 mm. The calculated value of 274 does not exceed this maximum value.

$$\text{MAX}\{(50 - 0.8 \cdot f_{ck}) \cdot \varnothing; 15 \cdot \varnothing\} = \text{MAX}\{(50 - 0.8 \cdot 50) \cdot 25; 15 \cdot 25\} = \text{MAX}\{250; 375\} = 375 \text{ mm}.$$

Next, the tensile stress in the steel bar is calculated.

$$\sigma_s = \frac{M_{freq}}{M_{Ed}} \frac{A_{s,req}}{A_{s,provided}} \cdot f_{yd}$$

The value of  $M_{Ed}$  is the design moment in the ULS state which is equal to 306 kNm/m and the  $M_{freq}$  is the moment in the SLS state, which is equal to 227 kNm/m. Because the loads acting on the wall are all permanent

loads, the ratio between ULS and SLS moment is equal to the load factor 1.35. The provided reinforcement area is equal to 4418 mm<sup>2</sup> and the minimum required reinforcement is determined by:

$$A_{s,req} = \frac{M_{Ed}}{f_{yd} \cdot z}$$

With the design yield stress equal to 435 N/mm<sup>2</sup> and the value of z equal to 282.6 mm, the required reinforcement area is 2489 mm<sup>2</sup>/m.

$$A_{s,req} = \frac{M}{f_{yd} \cdot z} = \frac{306 \cdot 10^6}{435 \cdot 282.6} = 2489 \text{ mm}^2/\text{m}$$

This results in a tensile stress in the bar of 182 N/mm<sup>2</sup>.

$$\begin{aligned} \sigma_s &= \frac{M_{freq}}{M_{Ed}} \frac{A_{s,req}}{A_{s,provided}} \cdot f_{yd} \\ &= \frac{227}{306} \frac{2489}{4418} \cdot 435 \\ &= 182 \text{ N/mm}^2 \end{aligned}$$

The mean value of the concrete tensile strength,  $f_{ct,eff}$ , is equal to  $f_{ctm}$ , which is 4.07 N/mm<sup>2</sup> for C50/60. The Young's modulus of concrete with a concrete class C50/60 equals 37000 N/mm<sup>2</sup>. The maximum occurring crack is therefore equal to:

$$\begin{aligned} w_k &= s_{r,max} \cdot \frac{\sigma_s - k_t \cdot \frac{f_{ct,eff}}{\rho_{p,eff}} \cdot (1 + \alpha_e \cdot \rho_{p,eff})}{E_s} \\ &= 274 \cdot \frac{182 - 0.4 \cdot \frac{4.07}{0.041} \cdot (1 + \frac{200000}{37000} \cdot 0.041)}{200000} \\ &= 0.182 \text{ mm} \end{aligned}$$

The theoretical crack width does not exceed the maximum allowable crack width and therefore the wall full fills the crack width requirement. The proposed amount of reinforcement is sufficient. The unity check is equal to 0.91.

$$UC = \frac{w_k}{w_{allowable}} = \frac{0.182}{0.2} = 0.91$$

### M.4.3. Internal Floor 1

#### M.4.3.1. Reinforcement

The proposed longitudinal reinforcement for internal floor 1 can be seen in Figure M.13. The longitudinal reinforcement consists of 2 rows of reinforcement in both directions. The first row is  $\varnothing 32-100$  and the second row is  $\varnothing 25-100$ . This results in a reinforcement area of 12951 mm<sup>2</sup>/m. For the shear reinforcement, 2 legged stirrups of  $\varnothing 20-100$  are used which means a diameter of 20 mm and a centre to centre distance of 100 mm.



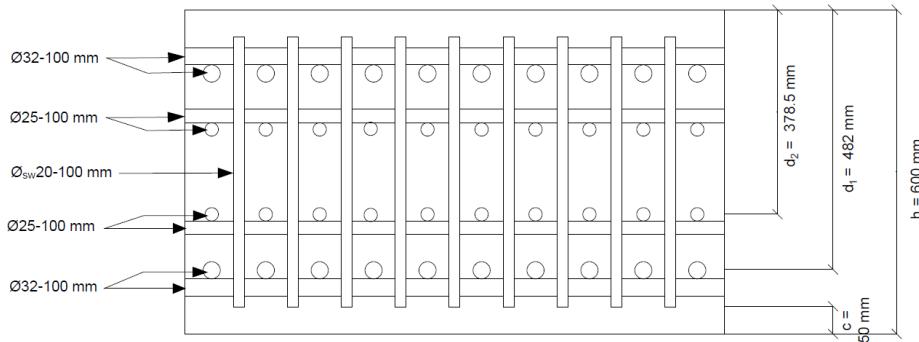


Figure M.13: Reinforcement in internal floor 1

### M.4.3.2. Bending Moment

Again, the proposed longitudinal reinforcement is sufficient if the bending moment capacity,  $M_{Rd}$ , is exceeding the design bending moment,  $M_{Ed}$ .

$$M_{Rd} \geq M_{Ed}$$

First, the design bending moment is determined. As mentioned in Section M.4.2.2, the governing stage for the internal elements are stage 5 and 6. The loads corresponding to these stages can be seen in Figure M.12b. The characteristic load acting on the floor,  $q_c$ , is  $136 \text{ kN/m}^2$ . All the loads are permanent and therefore a load factor of 1.35 is used for the calculation of the design load,  $d$ . The design load for internal floor 1 is  $183.6 \text{ kN/m}^2$ .

$$q_c = q_{soil} + q_{water} + q_{selfweight} = 60 + 61 + 15 = 136 \text{ kN/m}^2$$

$$q_d = (q_{soil} + q_{water} + q_{selfweight}) \cdot \gamma_s = (60 + 61 + 15) \cdot 1.35 = 183.6 \text{ kN/m}^2$$

The length,  $L_x$ , and the width,  $L_y$ , are respectively 8.6 m and 10 m. This leads to a ratio of 1.16 and a governing moment at the top of the plate of  $700 \text{ kNm/m}$  and at the bottom of  $1114 \text{ kNm/m}$ . The values are determined with Figure M.1.

Secondly, the bending moment capacity is calculated by the same steps as for the internal wall 1. Only difference is the second row of reinforcement. Both rows are calculated separately and added up to retrieve the bending moment capacity. For the first row the bending moment capacity is  $1496 \text{ kNm/m}$  and for the second row  $737 \text{ kNm/m}$ . The total bending moment capacity becomes  $2233 \text{ kNm/m}$ . The unity check for the bending resistances becomes:

$$UC = \frac{M_{Ed}}{M_{Rd}} = \frac{1114}{2233} = 0.50$$

### M.4.3.3. Shear Force

In the ultimate limit state, the shear force capacity must exceed the design shear force. This can be achieved with or without the use of shear reinforcement.

$$V_{Rd,c} \geq V_{Ed} \quad \text{or} \quad V_{Rd,s} \geq V_{Ed}$$

The same steps are followed as for the internal wall 1. First the design shear force in the slab is calculated with Figure M.3a. This results in a  $V_{Ed}$  of  $789 \text{ kN/m}$ . Next, the shear resistance without shear reinforcement

is determined. This leads to a  $V_{Rd,c}$  of 456 kN/m and a minimum  $V_{Rd,c}$  of 259 kN/m. It can be concluded that shear reinforcement is required because the  $V_{Ed}$  is exceeding the  $V_{Rd,c}$ .

The shear resistance with shear reinforcement is given by the minimum value of Formula M.5 and M.6.

$$V_{Rd,s} = \frac{A_{sw}}{s} \cdot z \cdot f_{ywd} \cdot \cot(\theta) \quad (M.5)$$

$$V_{Rd} = \frac{\alpha_{cw} \cdot b_w \cdot z \cdot v_1 \cdot f_{cd}}{\cot\theta + \tan(\theta)} \quad (M.6)$$

where: $V_{Rd,s}$	[N]	= shear resistance with stirrups governing
$V_{Rd}$	[N]	= shear resistance with concrete compressive struts governing
$A_{sw}$	[mm <sup>2</sup> ]	= the cross-sectional area of the reinforcement
$s$	[mm]	= the spacing of the stirrups
$f_{ywd}$	[N/mm <sup>2</sup> ]	= the design yield strength of the shear reinforcement
$\theta$	[deg]	= angle between the concrete compression strut and the beam axis
$\alpha_{cw}$	[-]	= coefficient taking account of the state of the stress in the compression chord (= 1.0)
$v_1$	[-]	= strength reduction factor (=0.6)

For the shear reinforcement there is chosen for stirrups  $\varnothing 20$ -100. This leads to a shear reinforcement area of 628 mm<sup>2</sup> and 6280 mm<sup>2</sup>/m. The angle between the concrete compression strut and the beam axis is taken as 45°. Normally, this angle is between 21.8° and 45° in which 45° is the most unfavourable angle. The internal leverage arm of the floor is depending on the effective height,  $d$ , and the height of the compression zone.

$$d_1 = h - c - \varnothing_{sw} - \varnothing_{v,1} - 0.5 \cdot \varnothing_{h,1}$$

$$= 600 - 50 - 20 - 32 - 0.5 \cdot 32 = 482 \text{ mm}$$

$$d_2 = h - c - \varnothing_{sw} - \varnothing_{v,1} - \varnothing_{h,1} - s_{spacing} - \varnothing_{v,2} - 0.5 \cdot \varnothing_{2,1}$$

$$= 600 - 50 - 20 - 32 - 32 - 50 - 25 - 0.5 \cdot 25 = 378.5 \text{ mm}$$

$$d = \frac{d_1 + d_2}{2} = \frac{482 + 378.5}{2} = 430 \text{ mm}$$

$$x_u = \frac{A_s \cdot f_{yd}}{0.75 \cdot f_{cd} \cdot b}$$

$$= \frac{12951 \cdot 435}{0.75 \cdot 33.3 \cdot 1000} = 226 \text{ mm}$$

$$z = d - \beta \cdot x_u = 430 - \frac{7}{18} \cdot 226 = 343 \text{ mm}$$

The shear resistance for this situation is the minimum value of:

$$\begin{aligned}
 V_{Rd,s} &= \frac{A_{sw}}{s} \cdot z \cdot f_{ywd} \cdot \cot(\theta) \\
 &= \frac{628}{100} \cdot 343 \cdot 435 \cdot \cot(45) \\
 &= 936 \text{ kN/m} \\
 V_{Rd} &= \frac{\alpha_{cw} \cdot b_w \cdot z \cdot v_1 \cdot f_{cd}}{\cot\theta + \tan(\theta)} \\
 &= \frac{1.0 \cdot 1000 \cdot 343 \cdot 0.6 \cdot 33.3}{\cot 45 + \tan(45)} \\
 &= 3422 \text{ kN/m}
 \end{aligned}$$

The shear force resistance with shear reinforcement is 936 kN/m and is able to withstand the shear force in the element. The unity check for the shear force is equal to 0.84 [-].

$$UC = \frac{V_{Ed}}{V_{Rd,s}} = \frac{789}{936} = 0.84$$

#### M.4.3.4. Crack Width

In the service limit state, the crack width may not exceed the maximum crack width (= 0.2 mm).

$$w_k \leq w_{max}$$

The theoretical crack width,  $w_k$ , in the internal floor is determined with the same method as for internal wall 1. A difference between the two is the used diameter in the formula for the spacing. Due to the double row of reinforcement, the averaged diameter has to be taken:

$$\varnothing_{gem} = \frac{\varnothing_1^2 \cdot N_1 + \varnothing_2^2 \cdot N_2}{\varnothing_1 \cdot N_1 + \varnothing_2 \cdot N_2} = \frac{32^2 \cdot 10 + 25^2 \cdot 10}{32 \cdot 10 + 25 \cdot 10} = 28.9 \text{ mm.}$$

The effective reinforcement ratio is equal to 8.11 %. The maximum crack spacing for the floor is 231 mm. The required reinforcement area 7477 mm<sup>2</sup> and the provided area is 12951 mm<sup>2</sup>. The ULS moment is equal to 1114 kNm/m and the SLS moment is 825 kNm/m. This results in a tensile stress in the steel bar of 186 N/mm<sup>2</sup>. The maximum occurring crack width is 0.181 mm. This means that the maximum occurring crack width will not exceed the maximum allowable crack width of 0.2 mm.

$$UC = \frac{w_{occurring}}{w_{allowable}} = \frac{0.181}{0.2} = 0.91$$

### M.4.4. Internal Wall 2

#### M.4.4.1. Reinforcement

The proposed longitudinal reinforcement for Internal Wall 2 is  $\varnothing 32-110$ . These bars will be placed at the top and the bottom of the plate. This leads to a reinforcement area of 7238 mm<sup>2</sup>/m. The reinforcement can be seen in Figure M.14.

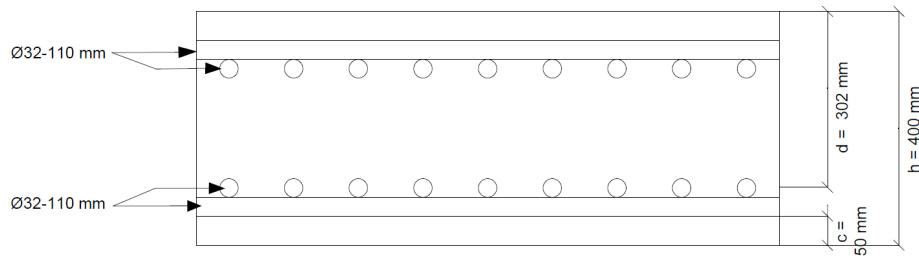
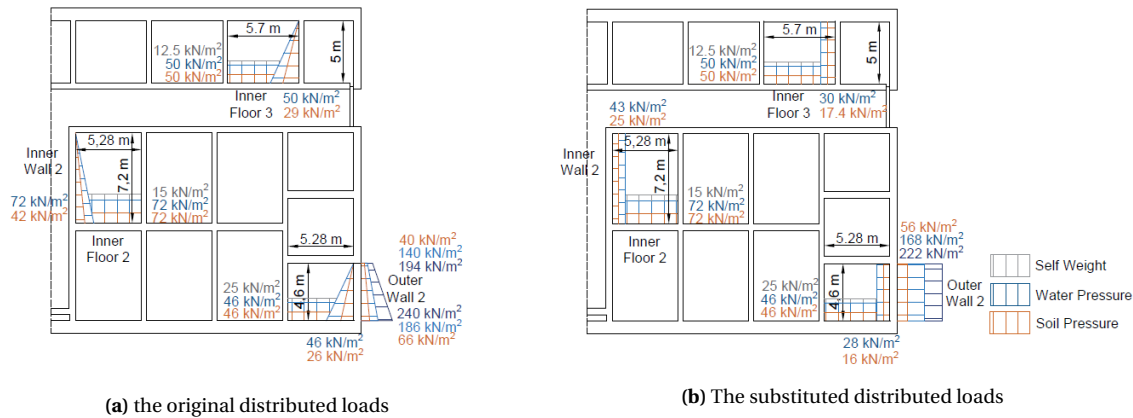


Figure M.14: Reinforcement in internal wall 2

M.4.4.2. Bending Moment



(a) the original distributed loads

(b) The substituted distributed loads

Figure M.15: The loads on Internal Wall 2, Internal Floor 2 and External Wall 2

In Figure M.15, the loads acting on internal wall 2 can be seen. These loads correspond to stages 5 and 6, ballasting and the final situation. The characteristic load is equal to 68 kN/m<sup>2</sup> and the design load equal to 91.8 kN/m<sup>2</sup>.

$$q_c = q_{soil} + q_{water} = 25 + 43 = 68 \text{ kN/m}^2$$

$$q_d = (q_{soil} + q_{water}) \cdot \gamma_S = (25 + 43) \cdot 1.35 = 91.8 \text{ kN/m}^2$$

The wall has a length, L<sub>x</sub>, of 7.2 m and a width, L<sub>y</sub>, of 10 m. This results in a ratio of 1.39. The design load results in a maximum bending moment in the top of the plate of 458 kNm/m (Situation IV-A) and in the bottom of 315 kNm/m (Situation I).

The reinforcement area is equal to 7238 mm<sup>2</sup>/m. With the minimum cover of 50 mm this results in a bending moment capacity of 797 kNm/m. The unity check for the bending moment results in:

$$UC = \frac{M_{Ed}}{M_{Rd}} = \frac{458}{797} = 0.58$$

M.4.4.3. Shear Force

The shear force in the slab, V<sub>Ed</sub>, is equal to  $\frac{7.2 \cdot 153.9}{2} = 369 \text{ kN/m}$ . This shear force is determined by the formula in Figure M.3a. The shear resistance without reinforcement, V<sub>Rd,c</sub>, is equal to 418 kN/m. The unity check for the shear force without reinforcement is:

$$UC = \frac{V_{Ed}}{V_{Rd,c}} = \frac{369}{418} = 0.88$$

Therefore no shear reinforcement is necessary to withstand the shear force.

#### M.4.4.4. Crack Width

The maximum allowable crack width is 0.2 mm. The maximum crack spacing in the wall is 239 mm. The effective reinforcement area is 7.93 %. The bending moment in SLS is equal to 339 kNm/m and in ULS 458 kNm/m. The provided reinforcement area is 7238 mm<sup>2</sup>/m and the required reinforcement area is 4171 mm<sup>2</sup>/m. This results in a tensile stress in the steel bar of 186 N/mm<sup>2</sup>. The maximum occurring crack width belonging to internal wall is therefore 0.187mm. The unity check for crack width is:

$$UC = \frac{w_{occurring}}{w_{max}} = \frac{0.187}{0.2} = 0.94$$

### M.4.5. Internal Floor 2

#### M.4.5.1. Reinforcement

The proposed longitudinal reinforcement for internal floor 2 is  $\varnothing 32$ -125 mm. These bars will be placed on the top and bottom of the slab. This leads to a reinforcement area of 6434 mm<sup>2</sup>/m. For the shear reinforcement, stirrups  $\varnothing 16$ -125 are placed in the slab. The reinforcement can be seen in Figure M.16.

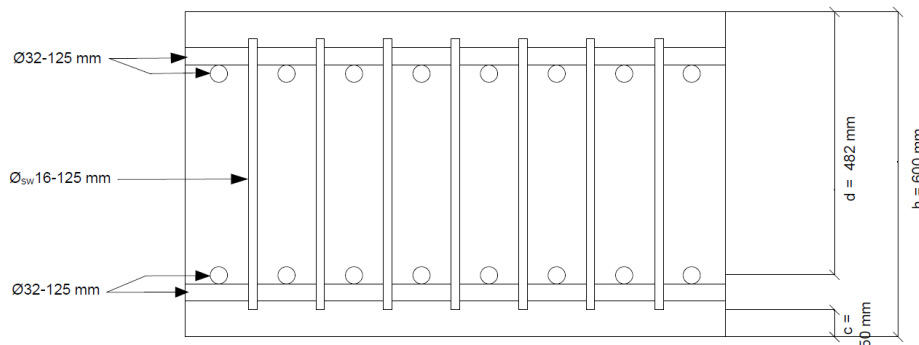


Figure M.16: Reinforcement in internal floor 2

#### M.4.5.2. Bending Moment

In Figure M.15b, the loads acting on internal floor 2 in stages 5 and 6 can be seen. The characteristic load is equal to 159 kN/m<sup>2</sup> and the design load equal to 215 kN/m<sup>2</sup>.

$$q_c = q_{soil} + q_{water} + q_{selfweight} = 72 + 72 + 15 = 159 \text{ kN/m}^2$$

$$q_d = (q_{soil} + q_{water} + q_{selfweight}) \cdot \gamma_S = (72 + 72 + 15) \cdot 1.35 = 215 \text{ kN/m}^2$$

The wall has a length,  $L_x$ , of 5.28 m and a width,  $L_y$ , of 10 m. This results in a ratio of 1.89. The design load results in a maximum bending moment in the top of the plate of 665 kNm/m (Situation IV-A) and in the bottom of 550 kNm/m (Situation I).

The reinforcement area is equal to 6434 mm<sup>2</sup>/m. With the minimum cover of 50 mm this results in a bending moment capacity of 1238 kNm/m. The unity check for the bending moment results in:

$$UC = \frac{M_{Ed}}{M_{Rd}} = \frac{665}{1238} = 0.54$$

### M.4.5.3. Shear Force

The shear force in the slab,  $V_{Ed}$ , is equal to  $\frac{5 \cdot 28 \cdot 215}{2} = 568$  kN/m. This shear force is determined by the formula in Figure M.3a. The shear resistance without reinforcement,  $V_{Rd,c}$ , is equal to 509 kN/m. It can be concluded that shear reinforcement is necessary.

For the shear reinforcement there is chosen for stirrups  $\varnothing 16-125$ . This results in a shear reinforcement area of  $3216 \text{ mm}^2/\text{m}$ . The angle between the concrete compression strut and the beam axis is taken as  $45^\circ$ . This results in a shear resistance of 619 kN/m.

$$UC = \frac{V_{Ed}}{V_{Rd,s}} = \frac{568}{619} = 0.92$$

### M.4.5.4. Crack Width

The maximum allowable crack width is 0.2 mm. The maximum crack spacing in the wall is 308 mm. The effective reinforcement area is 3.96 %. The bending moment in SLS is equal to 493 kNm/m and in ULS 664 kNm/m. The provided reinforcement area is  $6434 \text{ mm}^2/\text{m}$  and the required reinforcement area is  $3445 \text{ mm}^2/\text{m}$ . This results in a tensile stress in the steel bar of  $172 \text{ N/mm}^2$ . The maximum occurring crack width belonging to internal wall is therefore 0.188 mm. The unity check for crack width is:

$$UC = \frac{w_{occurring}}{w_{max}} = \frac{0.188}{0.2} = 0.94$$

## M.4.6. Internal Floor 3

### M.4.6.1. Reinforcement

The proposed longitudinal reinforcement for internal floor 3 is  $\varnothing 32-110$ . These bars will be placed on the top and bottom of the slab. This leads to a reinforcement area of  $7238 \text{ mm}^2/\text{m}$ . The reinforcement can be seen in Figure M.17.

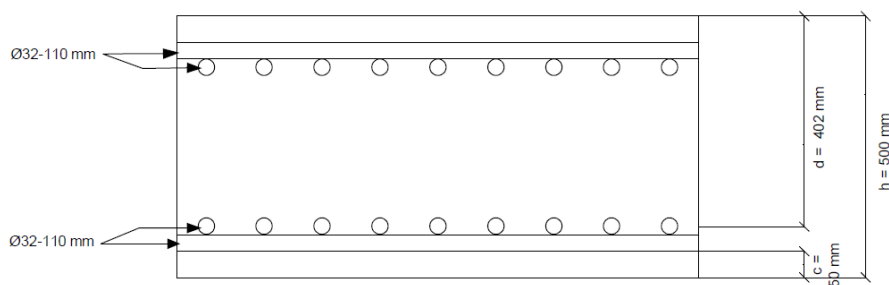


Figure M.17: Reinforcement in internal floor 3

### M.4.6.2. Bending Moment

In Figure M.15, the loads acting on internal floor 3 can be seen. Again, the governing stages are stages 5 and 6. The characteristic load is equal to  $112.5 \text{ kN/m}^2$  and the design load equal to  $152 \text{ kN/m}^2$ .

$$q_c = q_{soil} + q_{water} + q_{self\ weight} = 50 + 50 + 12.5 = 112.5 \text{ kN/m}^2$$

$$q_d = (q_{soil} + q_{water} + q_{self\ weight}) \cdot \gamma_{S,Permanent} = (50 + 50 + 12.5) \cdot 1.35 = 152 \text{ kN/m}^2$$

The wall has a length,  $L_x$ , of 5.7 m and a width,  $L_y$ , of 10 m. This results in a ratio of 1.75. The design load results in a maximum bending moment in the top of the plate of 537 kNm/m (Situation IV-A) and in the bottom of 420 kNm/m (Situation I).

The reinforcement area is equal to 7238 mm<sup>2</sup>/m. With the minimum cover of 50 mm this results in a bending moment capacity of 1111 kNm/m. The unity check for the bending moment results in:

$$UC = \frac{M_{Ed}}{M_{Rd}} = \frac{537}{1111} = 0.52$$

#### M.4.6.3. Shear Force

The shear force in the slab,  $V_{Ed}$ , is equal to  $\frac{5.7 \cdot 152}{2} = 433$  kN/m. This shear force is determined by the formula in Figure M.3a. The shear resistance without reinforcement,  $V_{Rd,c}$ , is equal to 489 kN/m. It can be concluded that shear reinforcement is not necessary.

$$UC = \frac{V_{Ed}}{V_{Rd,c}} = \frac{433}{489} = 0.89$$

#### M.4.6.4. Crack Width

The maximum allowable crack width is 0.2 mm. The maximum crack spacing in the wall is 264 mm. The effective reinforcement area is 5.81 %. The bending moment in SLS is equal to 398 kNm/m and in ULS 537 kNm/m. The provided reinforcement area is 7238 mm<sup>2</sup>/m and the required reinforcement area is 3497 mm<sup>2</sup>/m. This results in a tensile stress in the steel bar of 156 N/mm<sup>2</sup>. The maximum occurring crack width belonging to internal wall is therefore 0.157 mm. The unity check for crack width is:

$$UC = \frac{w_{occurring}}{w_{max}} = \frac{0.157}{0.2} = 0.78$$

### M.4.7. Culvert Wall 1

#### M.4.7.1. Reinforcement

The proposed longitudinal reinforcement for culvert wall 1 is  $\varnothing 32-100$  in the first row and  $\varnothing 20-100$  in the second row. These bars will be placed on the top and bottom of the slab. This leads to a reinforcement area of 11184 mm<sup>2</sup>/m. The shear reinforcement is  $\varnothing 20-100$ . The reinforcement can be seen in Figure M.18.

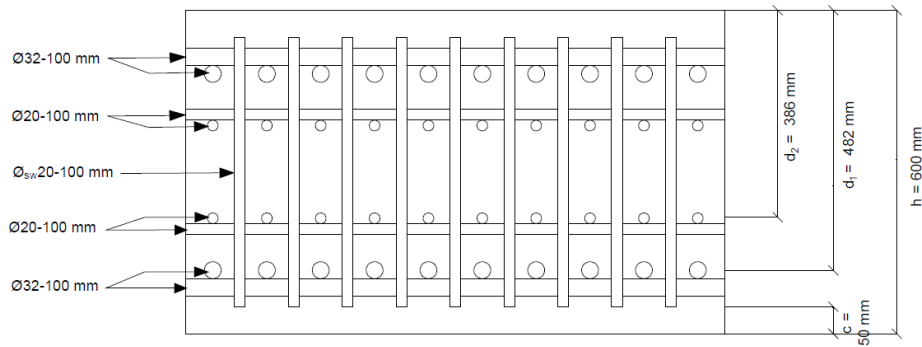
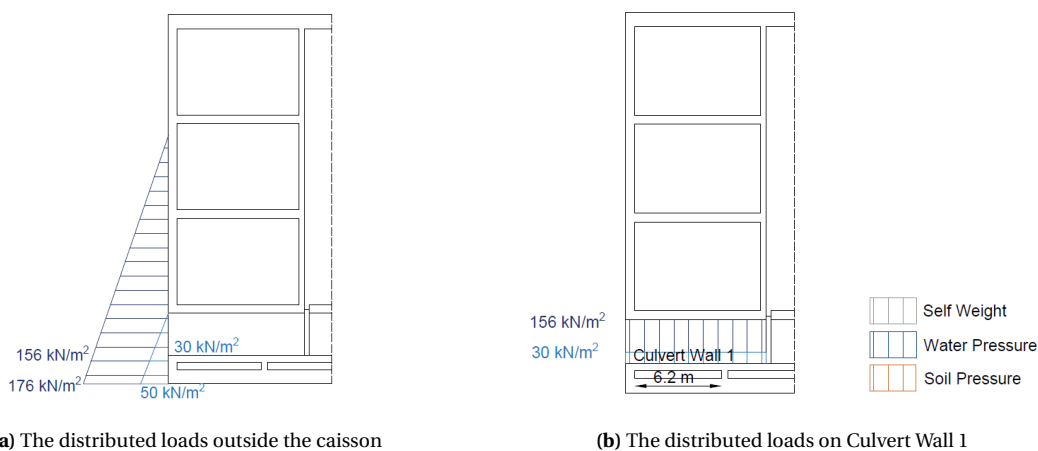


Figure M.18: Reinforcement in culvert wall 1

### M.4.7.2. Bending Moment



(a) The distributed loads outside the caisson

(b) The distributed loads on Culvert Wall 1

Figure M.19: The loads on Culvert Wall 1

In Figure M.19, the loads acting on culvert wall 1 can be seen. The governing stage is stage 6, in which water can enter the spillway during high water level, NAP - 5 m, in the energy storage lake. The characteristic load is equal to 171 kN/m<sup>2</sup> and the design load equal to 295 kN/m<sup>2</sup>.

$$q_c = q_{water} + q_{selfweight} = 156 + 15 = 711 \text{ kN/m}^2$$

$$q_d = (q_{Water,Permanent} + q_{SelfWeight}) \cdot \gamma_{S,Permanent} + q_{water,Variable} \cdot \gamma_{S,Variable}$$

$$= (30 + 15) \cdot 1.35 + (156 - 30) \cdot 1.5 = 295 \text{ kN/m}^2$$

The wall has a length,  $L_x$ , of 6.2 m and a width,  $L_y$ , of 10 m. This results in a ratio of 1.75. The design load results in a maximum bending moment in the top of the plate of 1194 kNm/m (Situation IV-A) and in the bottom of 902 kNm/m (Situation I).

The reinforcement area is equal to 11656 mm<sup>2</sup>/m. With the minimum cover of 50 mm this results in a bending moment capacity of 1994 kNm/m. The first row contributes for 75 % with a bending moment capacity of 1495 kNm/m and the second row for 25% with 498 kNm/m. The unity check for the bending moment results in:

$$UC = \frac{M_{Ed}}{M_{Rd}} = \frac{1194}{2033} = 0.59$$



### M.4.7.3. Shear Force

The shear force in the slab,  $V_{Ed}$ , is equal to  $\frac{6.2 \cdot 295}{2} = 915$  kN/m. This shear force is determined by the formula in Figure M.3a. The shear resistance without reinforcement,  $V_{Rd,c}$ , is equal to 514 kN/m. It can be concluded that shear reinforcement is necessary.

For the shear reinforcement there is chosen for  $\varnothing 20-100$ . The angle between the concrete compression strut and the beam axis is taken as  $45^\circ$ . This results in a shear resistance of 979 kN/m.

$$UC = \frac{V_{Ed}}{V_{Rd,s}} = \frac{915}{979} = 0.93$$

### M.4.7.4. Crack Width

The maximum allowable crack width is 0.2 mm. The maximum crack spacing in the wall is 237 mm. The effective reinforcement area is 6.97 %. The bending moment in SLS is equal to 692 kNm/m and in ULS 1194 kNm/m. The provided reinforcement area is 11184 mm<sup>2</sup>/m and the required reinforcement area is 7662 mm<sup>2</sup>/m. This results in a tensile stress in the steel bar of 173 N/mm<sup>2</sup>. The maximum occurring crack width belonging to internal wall is therefore 0.166 mm. The unity check for crack width is:

$$UC = \frac{w_{occurring}}{w_{max}} = \frac{0.166}{0.2} = 0.83$$

## M.4.8. External Wall 1

### M.4.8.1. Reinforcement

The proposed reinforcement for external wall 1 is  $\varnothing 32-100$ . These bars will be placed at the top and bottom of the slab. This leads to a reinforcement area of 8042 mm<sup>2</sup>/m. The shear reinforcement consists of two sided stirrups  $\varnothing 16-100$ . The reinforcement can be seen in Figure M.20.

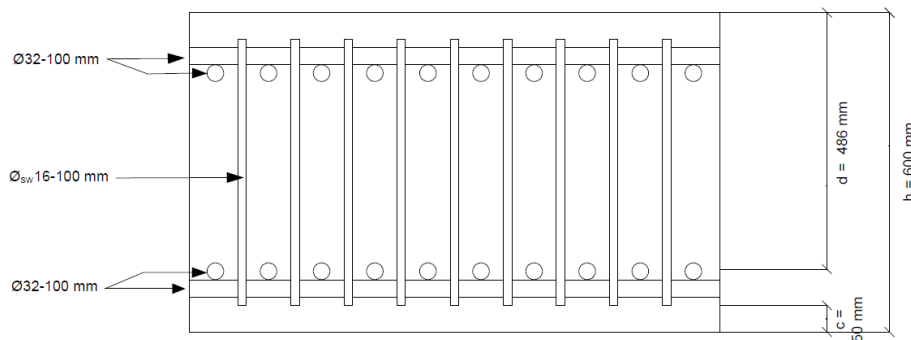
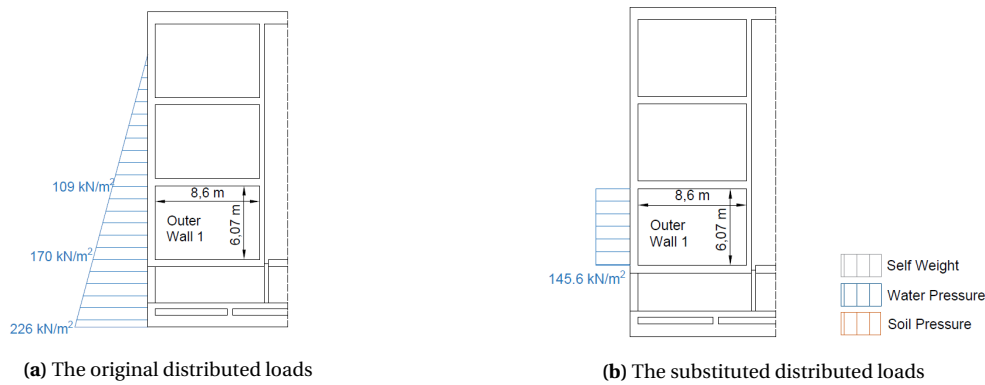


Figure M.20: Reinforcement in external wall 1

### M.4.8.2. Bending Moment

For external wall 1, the governing situation differs from the earlier mentioned elements. For the other elements, stages 5 and 6 are governing but for external wall 1, higher loads occur during stage 4. In this stage the caisson is at the final location but not yet filled with ballast material. The load at external wall 1 is fully caused by the outside water pressure. The water level during this stage is NAP + 0 m, which leads to a water depth of 22.5 m. The forces in this stage can be seen in Figure M.21.



**Figure M.21:** The loads on External Wall 1

The characteristic load is equal to  $145.6 \text{ kN/m}^2$  and the design load equal to  $197 \text{ kN/m}^2$ . For the design load a load factor of 1.35 is used because the water level will be permanent during this stage. The wall has a length,  $L_x$ , of 6.07 m and a width,  $L_y$ , of 10 m. This results in a ratio of 1.65. The design load results in a maximum bending moment in the top of the plate of  $771 \text{ kNm/m}$  (Situation IV-A) and in the bottom of  $587 \text{ kNm/m}$  (Situation I).

The reinforcement area is equal to  $8042 \text{ mm}^2/\text{m}$ . With the minimum cover of 50 mm this results in a bending moment capacity of  $1510 \text{ kNm/m}$ . The unity check for the bending moment results in:

$$UC = \frac{M_{Ed}}{M_{Rd}} = \frac{771}{1510} = 0.51$$

### M.4.8.3. Shear Force

The shear force in external wall 1,  $V_{Ed}$ , is equal to  $\frac{6.07 \cdot 109 \cdot 1.35}{2} + \frac{6.07 \cdot (170 - 109) \cdot 1.35}{3} = 613 \text{ kN/m}$ . This shear force is determined by the formula in Figure M.3a. The shear resistance without reinforcement,  $V_{Rd,c}$ , is equal to  $539 \text{ kN/m}$ . It can be concluded that shear reinforcement is necessary.

For the shear reinforcement there is chosen for stirrups  $\varnothing 16-100$ . This results in a shear reinforcement area of  $4020 \text{ mm}^2/\text{m}$ . The angle between the concrete compression strut and the beam axis is taken as  $45^\circ$ . This results in a shear resistance of  $755 \text{ kN/m}$ .

$$UC = \frac{V_{Ed}}{V_{Rd,s}} = \frac{613}{755} = 0.81$$

### M.4.8.4. Crack Width

The maximum allowable crack width is 0.2 mm. The maximum crack spacing in the wall is 274 mm. The effective reinforcement area is 5.25%. The bending moment in SLS is equal to  $570 \text{ kNm/m}$  and in ULS  $771 \text{ kNm/m}$ . The provided reinforcement area is  $8042 \text{ mm}^2/\text{m}$  and the required reinforcement area is  $4107 \text{ mm}^2/\text{m}$ . This results in a tensile stress in the steel bar of  $164 \text{ N/mm}^2$ . The maximum occurring crack width belonging to internal wall is therefore 0.170 mm. The unity check for crack width is:

$$UC = \frac{w_{occurring}}{w_{max}} = \frac{0.170}{0.2} = 0.85$$

## M.4.9. External Wall 2

### M.4.9.1. Reinforcement

The proposed reinforcement for external wall 2 is  $\varnothing 32-100$ . These bars will be placed at the top and bottom of the slab. This leads to a reinforcement area of  $8042 \text{ mm}^2/\text{m}$ . For the shear reinforcement, stirrups  $\varnothing 20-100$  are used. The reinforcement can be seen in Figure M.22.

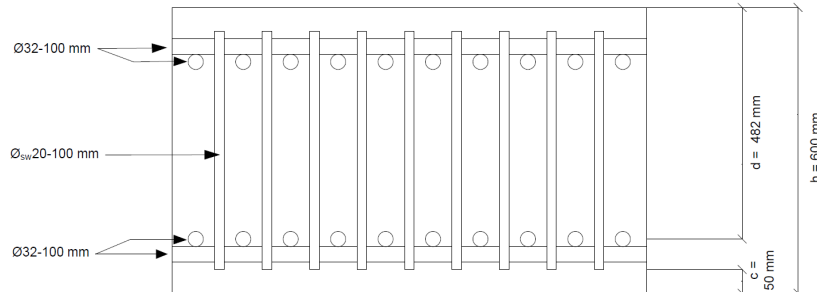


Figure M.22: Reinforcement in external wall 2

### M.4.9.2. Bending Moment

In Figure M.15b, the loads acting on external wall 2 can be seen. The governing load stage is stage 6 in which high water at the tidal lake can occur. The wave forces are neglected because compared to the water pressure, the wave pressure are very low. The outside water pressure is divided into two pressures because one is a permanent pressure and the other is a variable load. The loads due to the ballast material is favourable loads and a load factor of 0.9 is used. For the unfavourable outside water pressure, 1.35 is used for the permanent water pressure and 1.5 is used for the variable water pressure. The characteristic load is equal to  $234 \text{ kN/m}^2$  and the design load equal to  $344 \text{ kN/m}^2$ .

$$q_c = q_{water,out} + q_{soil,out} - q_{soil,ballast} - q_{water,ballast} = 222 + 56 - 28 - 16 = 234 \text{ kN/m}^2$$

$$q_d = (q_{water,out} + q_{soil,out}) \cdot \gamma_{S,permanent} + q_{water,out} \cdot \gamma_{S,variable} - (q_{soil,ballast} + q_{water,ballast}) \cdot \gamma_{S,favourable}$$

$$= (168 + 56) \cdot 1.35 + (222 - 168) \cdot 1.5 - (28 + 16) \cdot 1.35 = 344 \text{ kN/m}^2$$

The wall has a length,  $L_x$ , of 4.6 m and a width,  $L_y$ , of 10 m. This results in a ratio of 2.17. The design load results in a maximum bending moment in the top of the plate of  $815 \text{ kNm/m}$  (Situation IV-A) and in the bottom of  $739 \text{ kNm/m}$  (Situation I).

The longitudinal reinforcement, with a reinforcement area of  $8042 \text{ mm}^2/\text{m}$ , leads to a bending moment capacity of  $1496 \text{ kNm/m}$ . The unity check for the bending resistances becomes:

$$UC = \frac{M_{Ed}}{M_{Rd}} = \frac{815}{1495} = 0.55$$

### M.4.9.3. Shear Force

The shear force in external wall 2 is determined by modelling the wall as a beam due to the triangular loads. Because part of the loads are permanent and some are variable, the distributed load is split in two parts. All the distributed loads can be seen in Figure M.15a. The permanent part leads to a distributed load with an upper value of  $(140 + 40) \cdot 1.35 = 243 \text{ kN/m}^2$  and a lower value of  $(186+66) \cdot 1.35 - (46+26) \cdot 0.9 = 275.4 \text{ kN/m}^2$ . The variable load is a uniformly distributed load of  $(240-186) \cdot 1.5 = 81 \text{ kN/m}^2$ . This results in a shear force,  $V_{Ed}$ , of  $795 \text{ kNm/m}$ .

$$V_{Ed} = \frac{243 \cdot 4.6}{2} + \frac{(275.4 - 243) \cdot 4.6}{3} + \frac{81 \cdot 4.6}{2} = 795 \text{ kNm/m}$$

The shear resistance without reinforcement,  $V_{Rd,c}$ , is equal to 536 kN/m. It can be concluded that shear reinforcement is necessary.

For the shear reinforcement stirrups  $\varnothing 20-100$  are added to the slab. This results in a total shear reinforcement area of  $6280 \text{ mm}^2/\text{m}$ . The angle between the concrete compression strut and the beam axis is taken as  $45^\circ$ . This results in a shear resistance of 1168 kN/m.

$$UC = \frac{V_{Ed}}{V_{Rd,s}} = \frac{795}{1168} = 0.68$$

#### M.4.9.4. Crack Width

The maximum allowable crack width is 0.2 mm. The maximum crack spacing in the wall is 273 mm. The effective reinforcement area is 5.25%. The bending moment in SLS is equal to 555 kNm/m and in ULS 815 kNm/m. The provided reinforcement area is  $8042 \text{ mm}^2/\text{m}$  and the required reinforcement area is  $4382 \text{ mm}^2/\text{m}$ . This results in a tensile stress in the steel bar of  $161 \text{ N/mm}^2$ . The maximum occurring crack width belonging to internal wall is therefore 0.166 mm. The unity check for crack width is:

$$UC = \frac{w_{occurring}}{w_{max}} = \frac{0.166}{0.2} = 0.83$$

#### M.4.10. Bottom Slab

##### M.4.10.1. Reinforcement

The proposed reinforcement for bottom slab is  $\varnothing 32-125$ . These bars will be placed at the top and bottom of the slab. This leads to a reinforcement area of  $6434 \text{ mm}^2/\text{m}$ . The reinforcement can be seen in Figure M.23.

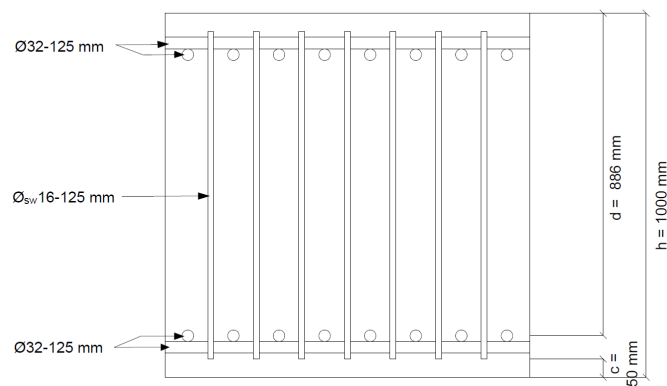


Figure M.23: Reinforcement in the bottom slab

### M.4.10.2. Bending Moment

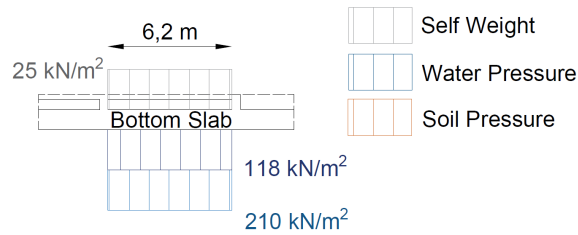


Figure M.24: The loads on the bottom slab

In Figure M.24, the loads acting on the bottom slab can be seen. These loads occur in stage 6, during high water at both the tidal lake as the energy storage lake. The outside water pressure is divided into two pressures because one is a permanent pressure and the other is a variable pressure. The load due to the self weight is favourable loads and a load factor of 0.9 is used. For the unfavourable outside water pressure, 1.35 is used for the permanent water pressure and 1.5 is used for the variable water pressure. The characteristic load is equal to 187 kN/m<sup>2</sup> and the design load equal to 277 kN/m<sup>2</sup>.

$$q_c = q_{Water} - q_{SelfWeight} = 187 \text{ kN/m}^2$$

$$\begin{aligned} q_d &= q_{Water,Permanent} \cdot \gamma_{S,Permanent} + q_{Water,Variable} \cdot \gamma_{S,Variable} - q_{SelfWeight} \cdot \gamma_{S,Favourable} \\ &= 121 \cdot 1.35 + (212 - 121) \cdot 1.5 - 25 \cdot 0.9 = 277 \text{ kN/m}^2 \end{aligned}$$

The wall has a length,  $L_x$ , of 6.2 m and a width,  $L_y$ , of 10 m. This results in a ratio of 1.39. The design load results in a maximum bending moment in the top of the plate of 1122 kNm/m (Situation IV-A) and in the bottom of 847 kNm/m (Situation I).

The reinforcement area is equal to 6434 mm<sup>2</sup>/m. With the minimum cover of 50 mm this results in a bending moment capacity of 2358 kNm/m. The unity check for the bending moment results in:

$$UC = \frac{M_{Ed}}{M_{Rd}} = \frac{1122}{2358} = 0.48$$

### M.4.10.3. Shear Force

The shear force in the slab,  $V_{Ed}$ , is equal to 863 kN/m. In the determination of the shear force a combination of the two methods is used.

$$V_{Ed} = \frac{110 \cdot 1.35 \cdot 6.2}{2} + \frac{(121 - 110) \cdot 1.35 \cdot 6.2}{3} + \frac{(216 - 128.5) \cdot 1.5 \cdot 6.2}{2} + \frac{(216 - 206) \cdot 1.5 \cdot 6.2}{6} - \frac{25 \cdot 0.9 \cdot 6.2}{2} = 863 \text{ kN/m}$$

This shear force is determined by the formula in Figure M.3a. The shear resistance without reinforcement,  $V_{Rd,c}$ , is equal to 652 kN/m. It can be concluded that shear reinforcement is necessary.

For the shear reinforcement there is chosen for  $\varnothing 16-125$ . The angle between the concrete compression strut and the beam axis is taken as 45°. This results in a shear resistance of 1179 kN/m.

$$UC = \frac{V_{Ed}}{V_{Rd,s}} = \frac{863}{1179} = 0.73$$

### M.4.10.4. Crack Width

The maximum allowable crack width is 0.2 mm. The maximum crack spacing in the wall is 411 mm. The effective reinforcement area is 2.26 %. The bending moment in SLS is equal to 757 kNm/m and in ULS 1121 kNm/m. The provided reinforcement area is 6434 mm<sup>2</sup>/m and the required reinforcement area is 3059 mm<sup>2</sup>/m. This results in a tensile stress in the steel bar of 140 N/mm<sup>2</sup>. The maximum occurring crack width belonging to the bottom slab is therefore 0.172 mm. The unity check for crack width is:

$$UC = \frac{w_{occurring}}{w_{max}} = \frac{0.172}{0.2} = 0.86$$

## M.5. Overview

In Table M.1, an overview of the used reinforcement for each element and the corresponding unity checks for the three failure mechanisms are shown.

Element	Reinforcement		Load			Resistance			Unity Check		
	Diameter $\varnothing$ [mm]	Number of Bars per m [-]	MEd [kNm/m]	VEd [kN/m]	w [mm]	MRd [kNm/m]	VRd [kN/m]	wmax [mm]	Bending Moment [-]	Shear Force [-]	Crack Width [-]
Internal Wall 1	25	9	306	238	0.182	543	396	0.2	0.56	0.60	0.91
Internal Floor 1	32 (Row 1) 25 (Row 2)	10	1114	789	0.181	2233	936	0.2	0.50	0.84	0.91
Internal Wall 2	32	9	458	369	0.188	797	418	0.2	0.58	0.92	0.94
Internal Floor 2	32	8	665	568	0.18	1283	619	0.2	0.52	0.86	0.90
Internal Floor 3	32	9	537	433	0.157	1111	489	0.2	0.52	0.89	0.78
Culvert Wall 1	32 (Row 1) 20 (Row 2)	10	1194	915	0.166	2033	979	0.2	0.59	0.93	0.83
External Wall 1	32	10	771	613	0.170	1510	755	0.2	0.51	0.81	0.85
External Wall 2	32	10	815	795	0.166	1495	1168	0.2	0.55	0.68	0.83
Bottom Slab	32	8	1122	863	0.172	2358	1179	0.2	0.48	0.73	0.86

Table M.1: Overview of the reinforcement

## M.6. Stability of the Caisson

With the improved lay-out of the caisson, the stability of the caisson has changed as well. Therefore the stability requirements have been performed again to see if the change in lay-out still results in a caisson that meets the stability requirements. The stability is determined by the same method as used in Chapter 6 and Appendix H. The only part that changes in the calculations is the self weight of the caisson. In the improved lay-out, part of the ballast sand is replaced by concrete elements, which leads to an increase in weight. However, the spaces in the lower left corner of the improved caisson, will not be filled with ballast sand. This leads to an overall reduction of the total weight of the caisson compared to the initial lay-out.

### M.6.1. Sliding Resistance

The governing situation for the sliding resistance is still situation 3, in which the water level at the tidal lake is high, NAP +2.4m and the water level in the energy storage is at NAP - 11.25 m. The horizontal loads and the uplift pressure acting on the caisson do not change compared to the initial calculations. The self-weight of the caisson decreased from 19 880 kN/m to 19 732 kN/m. The values in the calculations below, already contain the load factors.

$$\begin{aligned}
 V_{\text{uplift}} &= 9721 \text{ kN/m} \\
 V_{\text{Self-weight}} &= 19732 \text{ kN/m} \\
 \sum V &= V_{\text{Self-weight}} - V_{\text{Uplift}} = 10011 \text{ kN/m} \\
 \sum H &= 3657 \text{ kN/m}
 \end{aligned}$$

Since the change in self weight is only 142 kN/m, the change in sliding resistance and in the unity check are also very small. The unity check increases from 0.91 [-] to 0.92 [-].

$$R_d = \sum V \cdot \tan(\delta(d)) = 10011 \cdot \tan 21.67 = 3977 \text{ kN/m}$$

$$UC = \frac{\sum H}{R_d} = \frac{3657}{3977} = 0.92$$

### M.6.2. Rotational Stability

The governing situation for the rotation stability is the situation with the highest water level difference. This leads to a water level in the tidal lake and energy storage lake of respectively NAP +2.4 m and NAP -17.5 m. Due to the decrease of self-weight, the moment due to the vertical forces changes. The moments and sum of vertical forces then becomes:

$$M_H = 35812 \text{ kNm/m}$$

$$M_V = 48444 \text{ kNm/m}$$

$$\sum M = 84256 \text{ kNm/m}$$

$$\sum V = 11955 \text{ kN/m}$$

The eccentricity corresponding to this situation is 7.05 m. The core of the caisson is defined by the area 8.25 m away from the centre of the caisson. The eccentricity of the resulting load is within the core of the caisson. The unity check corresponding to this failure mechanism is 0.85 [-]. The initial unity check was 0.83 [-].

$$e = \frac{\sum M}{\sum V} = \frac{84256}{11955} = 7.05 \text{ m}$$

$$UC = \frac{e}{\frac{1}{6}B} = \frac{7.05}{8.25} = 0.85 \text{ [-]}$$

### M.6.3. Bearing Capacity

The governing layer for the bearing capacity is the sand layer below the sill. The governing situation for the bearing capacity is the situation with the highest eccentricity, the situation with the highest water level difference. Due to the decrease in self-weight, the bearing capacity of the sand layer becomes 1016 kN/m<sup>2</sup> and the stress due to the weight of the caisson becomes 501 kN/m<sup>2</sup>. This results in a unity check of 0.49 [-].

### M.6.4. Draught

The self-weight of the caisson without ballast increases due to the addition of more concrete elements. This leads to an increase from 7 582 kN/m to 9 050 kN/m. The draught of the caisson during transport is increased to 18 m. This means that the caisson has sufficient clearance. The caisson has a height of 26 m, so with a draught of 18 m, the caisson will stand out of the water.

$$d = \frac{F_G}{B \cdot L \cdot \gamma_w} = \frac{9050}{49.5 \cdot 1 \cdot 10.06} = 18 \text{ m}$$

### M.6.5. Floating Stability

Due to the addition of extra concrete elements, the gravity centre of the caisson changes slightly. The floating stability during transports has increased due to the improved lay-out. The metacentric height of the caisson during transport is equal to 6.39 m. Only 0.5 m is required for a stable transport. The reason for the improvement of the stability is the decrease of the centre of gravity of the caisson. Due to the addition of multiple walls inside of the caisson, the gravity centre is lowered.

## Verification of the Scour Protection

The calculation for the scour protection are shown in this appendix. First the different flow situations are described, next the flow velocities are discussed and lastly, the design of the scour protection is calculated and shown.

### N.1. The Flow Situations

For the design of the scour protection in up- and downstream of the spillway, two configurations are relevant. In the first one, the pumping station is not functioning and the spillway is at maximum capacity,  $20.200 \text{ m}^3/\text{s}$ . This situation can be seen in Figure N.1a. In the second one, the pumping station is at maximum capacity as well,  $10.000 \text{ m}^3/\text{s}$ . This can be seen in Figure N.1b.

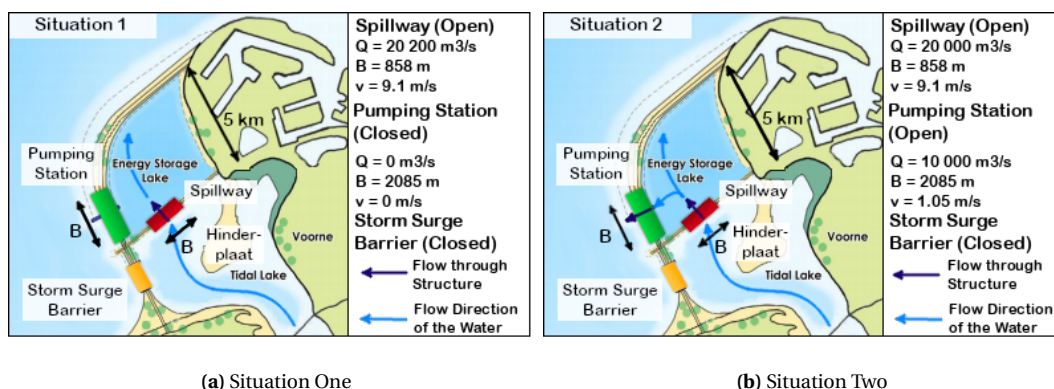


Figure N.1: The Different flow Situations

In both situations the storm surge barrier is closed. When the barrier is open, the discharge of the spillway is either far below the maximum discharge or zero. The reason for this is that in case of an open barrier, the need for a large discharge of the spillway is low. Apart from that, if the barrier is open, the water level in the Tidal Lake is below NAP + 1.5 m and consequently, the maximum discharge can not be achieved.

The flow patterns in Figure N.1 are assumed because for a precise indication of the flow pattern in the Energy Storage Lake, more research has to be done. It can also be possible that in situation one, the flow will be circular in the lake, just like situation two. For the design of the scour protection, only the local scour is taken into consideration. Erosion of the dunes or due to the pumping station is not taken into account.



## N.2. The Flow Velocities

The design of the scour protection depends on the flow velocity due to the discharge of the spillway. First, the velocities in the Energy Storage Lake are discussed and afterwards the flow velocities in the Tidal Lake. The reason behind this is that the Energy Storage Lake side is governing side due to the development of the velocities at that side.

### N.2.1. Energy Storage Lake

During the use of the spillway at maximum discharge,  $20\,200\text{ m}^3/\text{s}$ , the corresponding water level in the Energy Storage Lake in this situation is NAP - 17.5 m. The water depth in this situation is 5 m. The flow velocity in the spillway during the maximum capacity is 9.1 m/s. The flow enters the Energy Storage Lake as a jet flow. The situation can be seen in Figure N.2.

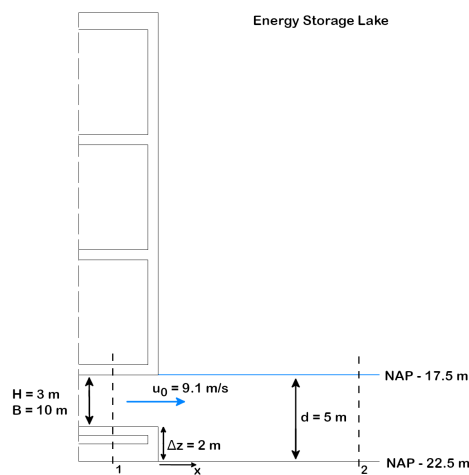


Figure N.2: Outflow conditions of the Spillway at the Energy Storage Lake

For the scour protection behind the spillway, the development of the flow velocity is important. When the flow enters the Energy Storage Lake, the flow has a velocity of 9.1 m/s. This velocity is not directly present near the bed. The reason for this is the two meter height difference between the bed and the outlet of the spillway. More downstream of the spillway, the flow depth will increase to the depth of the Energy Storage Lake, 5 m. This leads to a decrease in maximum flow velocity. The rate of decay of the maximum flow velocity is difficult to determine. Normally this is done by doing experimental test. This is outside the scope of the thesis and therefore assumptions are made based on relevant research reports.

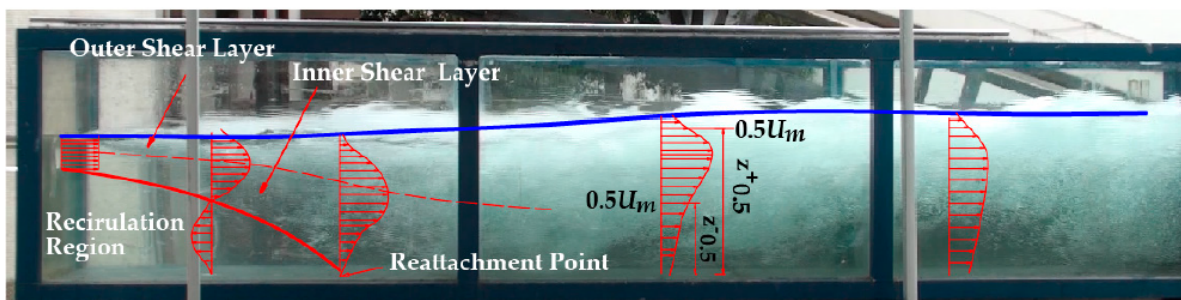


Figure N.3: Development of the flow velocity profile in deep water case (Li et al., 2019)

In Figure N.3, a deep water case of a jet flow is shown. After the flow enters the Energy Storage Lake, the flow will go through different regions. The first region is the recirculation region in which a reversed flow occurs below the jet flow. The second region is the reattachment region in which the flow is attached to the

bottom of the lake. Next, the flow will go through the wall jet region and last, it will go to the recovering region. In a shallow water jet flow, the same region can be found but the flow can stick to the bed instead of the free surface in the wall jet region. In each region, the change in velocity is different. In the last region, the recovering region, the flow can be considered as uniform flow. In the recirculation, reattachment and the wall jet region, the decay in velocity is mainly depending on the offset height, the difference between the bottom of the outlet and the bed of the lake. According to Li et al. (2019), the decay in maximum velocity for a offset jet can be described as in Figure N.4.

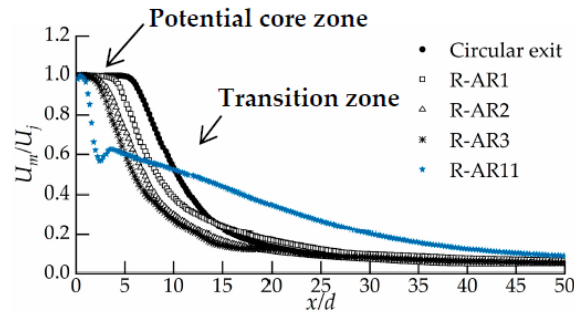


Figure N.4: Velocity decay of jet flow according to Li et al. (2019)

In Figure N.4, the decay for four different types of rectangular outlets can be seen. Li et al. (2019), modelled four different rectangular outlets which differ on offset ratio ( $OR = \frac{H}{z}$ ), expansion ratio and length/width ratio ( $= \frac{W}{H}$ ). For the outlet of the concept Caisson, the offset ratio is  $\frac{2}{3}$  and the length/width ratio is  $\frac{10}{3}$ . Comparing this to the research of Li et al. (2019), the most comparable outlet is R-AR1 and R-AR3. R-AR1 is more comparable for the offset ratio ( $OR = 1$ ) and R-AR2 is more comparable for the length/width ratio ( $AR = 3$ ). Due to the importance of the offset ratio, it is assumed that the decay will correspond mostly to the R-AR1.

In other research the same change in velocity profile and the same maximum velocity decay shape can be found. Ead and Rajaratnam (2000) analysed the velocity decay for different values of the Froude number and offset ratios. In Figure N.5, the expected decay in velocity can be seen. A big difference between the earlier shown decay is that the decay is slower. Another difference is that the offset ratio for this research has a minimum of 5 which exceeds the offset ratio of the outlet of the spillway.

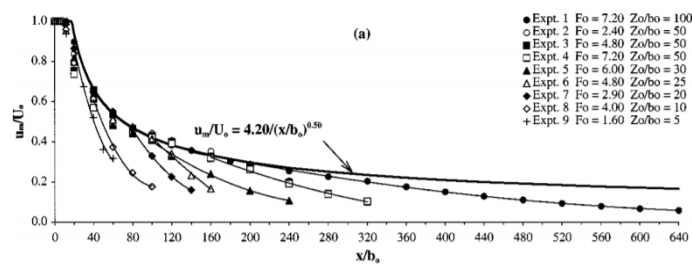


Figure N.5: Velocity decay of jet flow according to Ead and Rajaratnam (2000)

Gao and Ewing (2007), analysed the velocity decay for low offset ratios. According to this research the velocity decay is even slower, see Figure N.6. If the results of this research are extrapolated it would take approximate 48 times the height of the jet to decrease the velocity with 50%.

It can be concluded that to predict the decay of maximum velocity behind the outlet of the spillway, more research is required. Therefore the depth averaged velocity is used in this report. The depth-averaged velocity is taken equal to the uniform flow velocity. In Figure N.7, the assumed change in velocity profile can be seen. At point 1, the velocity is equal to the outflow velocity of the spillway, 9.1 m/s. The recirculation region is between point 1 and 3. At point 2, within the recirculation region, the direction of the flow near the bed is the opposite of the direction of the jet flow. The value of the flow velocity near the bed is approximate 27 % of the jet flow velocity. At point 3, the recirculation region changes into the wall jet region. Exactly at point 3, the

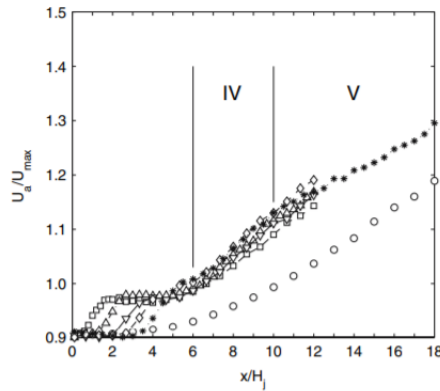


Figure N.6: Velocity decay of jet flow according to Gao and Ewing (2007)

reattachment point can be found at which the maximum turbulence can be found but the velocity near the bed is almost zero. In the wall jet region, the maximum velocity is moving downwards towards the bed. At a certain distance from the spillway, the wall jet region changes to the recovering region in which the velocity is uniform.

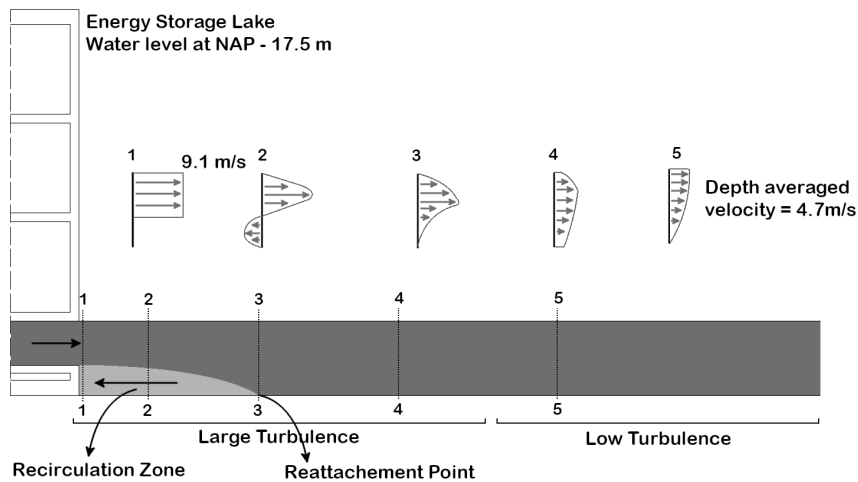


Figure N.7: Approximate change in velocity profile

The uniform flow velocity is determined by using the momentum equation and the conservation of mass between point 1 and point 2, N.2. According to the momentum equation and the conservation of mass, the discharge at point 1 is equal to the discharge at point 2. The velocity at point two is therefore determined by:

$$\begin{aligned}
 Q_1 &= Q_2 \\
 A_1 \cdot v_1 &= A_2 \cdot v_2 \\
 B_1 \cdot h_1 \cdot v_1 &= B_2 \cdot h_2 \cdot v_2 \\
 \rightarrow v_2 &= \frac{B_1 \cdot h_1 \cdot v_1}{B_2 \cdot h_2} \\
 &= \frac{Q_1}{B_2 \cdot h_2}
 \end{aligned}$$

The discharge is equal to the maximum discharge capacity of the spillway, 20 200 m<sup>3</sup>/s. The depth at point two is 5 m and the width at point two is the total width of the spillway, 858 m. This results in an uniform flow

velocity at point 2 of 4.75 m/s. Between the outflow of the spillway and the point at which open channel flow occurs, the flow velocity decreases from 9.1 m/s at the outlet to a uniform flow velocity of 4.75 m/s.

### N.2.2. Tidal Lake

The Tidal Lake side of the spillway has a different development in flow pattern and flow velocity. One of the reasons is that the water flows into the spillway at this side. This leads to accelerating flow instead of decelerating and therefore a different change in velocity. In Figure N.8, the assumed velocity profiles at different distances from the spillway can be found. At point 1, the velocity in front of the inlet is 9.1 m/s. At point two, the flow is reattached to both boundaries and it is assumed that the depth-averaged flow velocity is equal to the uniform flow velocity. At a certain distance from the spillway, point 3, the uniform flow conditions can be found. The governing situation for the flow velocity is a large discharge and a low water level. The largest discharge occurs when the water level in the Energy Storage Lake is at NAP -17.5 m and in the Tidal Lake at NAP +1.5 m. In this case the water level in Tidal Lake is high which results in a lower depth-averaged velocity. Therefore the situation in which the Tidal Lake is at NAP + 0 m is and the Energy Storage Lake at NAP -17.5 m is taken as governing. With the Bernoulli equation, the discharge in this situation is calculated at 19 300 m<sup>3</sup>/s. The choice for NAP + 0 m as governing water level is because below this value, a large discharge is not required because the water level is already low.

$$\Delta H = f \frac{L}{D} \frac{v_s^2}{2g} + \sum \zeta \frac{v_s^2}{2g} \rightarrow v = \sqrt{\frac{\Delta H}{f \frac{L}{2 \cdot g \cdot D} + \frac{\zeta}{2 \cdot g}}}$$

$$D = \frac{4A}{P} = \frac{2h \cdot w}{h + w} = \frac{2 \cdot 3 \cdot 10}{10 + 3} = 4.61 \text{ m}$$

$$v = \sqrt{\frac{17.5}{f \frac{65}{2 \cdot 9.81 \cdot 4.61} + \frac{4.3}{2 \cdot 9.81}}} \rightarrow f = 0.0152 \text{ [-]}, v = 8.72 \text{ m/s (Iterative process)}$$

$$Q = N \cdot A \cdot v = 74 \cdot 30 \cdot 8.72 = 19\,300 \text{ m}^3/\text{s}$$

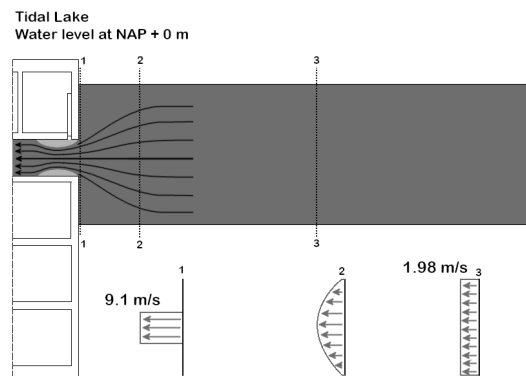


Figure N.8: Approximate change in velocity profile

Upstream of the spillway, at the point of uniform flow conditions, the uniform flow velocity is calculated by the conservation of mass ( $Q$  remains constant). The uniform flow velocity is equal to 2.27 m/s.

$$v = \frac{Q}{A} = \frac{Q}{B \cdot h} = \frac{19300}{858 \cdot 10} = 2.27 \text{ m/s}$$

It is assumed that the flow velocity of 2.27 m/s is the governing uniform flow velocity for the design of the scour protection. The difference between accelerating flow and decelerating flow is the amount of turbulence. In accelerating flow, the relative turbulence decreases. The turbulence for accelerating flow is zero (Schierreck, 2012).

## N.3. The Required Scour Protection

### N.3.1. Energy Storage Lake

#### N.3.1.1. Type of Protection

In Section N.2.1, the occurring velocities in the Energy Storage Lake are discussed. Without the use of a proper scour protection, a scour hole close to the caisson will occur due to the high flow velocities. This will lead to stability issues for the caisson. To overcome these issues, a scour protection is required. The scour protection at the Energy Like side consists of a granular geometrically closed filter made out of rocks and gravel.

#### N.3.1.2. Dimensions of the Scour Protection

The dimension on the required rock for the armour layer, the top layer, of the scour protection depends on the depth averaged flow velocity. The used rock diameter should be greater than the minimum required rock diameter obtained from the Shields Equation, Formula N.1.

$$d \geq \frac{K_v^2 \cdot u_c^2}{K_s \cdot \psi_c \cdot C^2} \quad (\text{N.1})$$

where:	$d$	[m]	=	nominal diameter of the grain
	$K_v$	[-]	=	velocity/turbulence factor ( $= \frac{1+3r_{cs}}{1+3r_{cu}}$ )
	$r_{cs}$	[-]	=	vertically averaged turbulence intensity
	$r_{cu}$	[-]	=	relative turbulence intensity in uniform flow (=0.075)
	$u_c$	[m/s]	=	critical, depth-averaged, velocity in uniform flow for incipient motion
	$K_s$	[-]	=	slope factor
	$\psi_c$	[-]	=	the threshold of motion parameter
	$C$	[m <sup>0.5</sup> /s]	=	Chezy Coefficient ( $=18 \log(12 \frac{h}{k_r})$ )

The critical, depth-averaged, flow velocity in uniform flow in the Energy Storage Lake is decreasing downstream of the spillway. Just downstream of the spillway, the flow velocity is equal to 4.75 m/s. Further downstream this velocity decreases due to the increase in flow area (width B is increasing). This increase is caused by the horizontal spreading of the flow. The spreading angle is equal to 1:7. The development of the uniform velocity can be seen in Figure N.9 (Schierck, 2012).

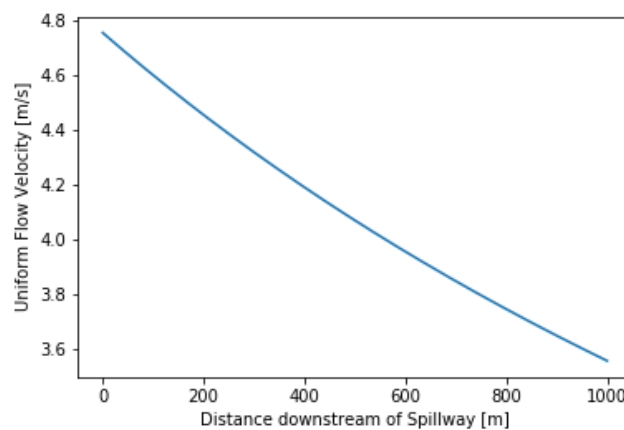


**Figure N.9:** Development of the uniform flow velocity

Just downstream of the spillway, the flow is decelerating which goes together with large turbulence. Therefore a turbulence factor is taken into account. The vertically averaged turbulence intensity is assumed to be 0.3 [-]. This is corresponding to the relative turbulence intensity of a free jet. This results in a  $K_v$  factor of 1.55 [-]. For

preliminary designs, the threshold of motion,  $\psi_c$ , is set at 0.03 [-]. The Chezy Coefficient is depending on the depth of the Energy Storage Lake, 5 m, and the  $k_r$ , the roughness of the bed. This roughness can be assumed to be equal to twice the nominal diameter ( $2 \cdot d_{n50}$ ) (Schiereck, 2012). Since there is no slope, the slope factor is equal to 1. The determination of the required nominal diameter is an iterative process because the diameter is present at both sides of the formula. Immediately after the spillway, the required nominal diameter of the rock is 0.97 m. For the armour layer, a standard grading is used and for a nominal diameter of 0.97, this results in HM<sub>A</sub> 3-6t. More about the characteristics of the standard grading HM<sub>A</sub> 3-6t can be found in Section N.3.4. However, the maximum flow velocity of 4.75 m/s is derived by using the depth-averaged flow velocity. Since the velocity at the outlet is 9.1 m/s, it is likely that the depth just downstream of the caisson is exceeding the 4.75 m/s. Therefore, colloidal concrete will be used at the first section of the scour protection. The layers of the scour protection will be cast in colloidal concrete, which improves the resistance against high velocities.

As mentioned before, further downstream of the spillway the flow velocity is decreasing due to the horizontal expansion. Therefore the required nominal diameter is also decreasing further downstream of the spillway. Besides the velocity, the turbulence is also decreasing further downstream. The latter is not taken into account because more research has to be done to verify the exact decrease in turbulence. As mentioned before, for the horizontal expansion a slope of 1:7 is assumed. At 150 m distance from the spillway, this results in a new width of:

$$B_{x=150} = B_{x=0} + 2 \cdot \frac{x}{7} = 858 + 2 \cdot \frac{150}{7} = 901 \text{ m}$$

With the increase in width, the velocity decreases:

$$v_{x=150} = \frac{Q}{B_{x=150} \cdot h} = \frac{20200}{901 \cdot 5} = 4.5 \text{ m/s}$$

Using Formula N.1, in combination with a  $K_v$  factor of 1.55 [-], leads to a required diameter of 0.8 m. This leads to a standard grading of HM<sub>A</sub> 1-3t.

At a certain distance downstream of the spillway, the flow becomes fully uniform in which the  $K_v$  value becomes 1. This point is assumed to be around 250 m downstream of the spillway. The width at this point is 930 m and the velocity 4.3 m/s.

$$B_{x=250} = B_{x=0} + 2 \cdot \frac{x}{7} = 858 + 2 \cdot \frac{250}{7} = 930 \text{ m}$$

$$v_{x=250} = \frac{Q}{B_{x=250} \cdot h} = \frac{20200}{930 \cdot 5} = 4.3 \text{ m/s}$$

With Formula N.1 and a  $K_v$  factor of 1, the required nominal diameter is 0.28 m. The standard grading that is used is LM<sub>A</sub> 40-200 with a nominal diameter of 0.34 m.

A geometrically closed filter is only functioning correctly if one or multiple filter layers are placed below the top layers. These filter layers consists of smaller rocks than the top layer. For the determination of the layers below the top layer, the following requirements are used:

$$\text{Stability: } \frac{d_{15,F}}{d_{85,B}} < 5, \quad \text{Internal Stability: } \frac{d_{85}}{d_{15}} < 12 - 15, \quad \text{Permeability: } \frac{d_{15,F}}{d_{15,B}} > 5$$

In the requirements, the F stands for the filter layer and the B for the base layer, which is the layer below the filter layer. In Table N.1, information about the used material in the layers for the scour protection can be found. All these layers full fill the requirements for the geometrically closed filters. In Figure N.13, the design of the scour protection can be seen.

Scour Protection $x < 150$ m						
Layer	Type	Standard Grading	d15 [mm]	dn50 [mm]	d85 [mm]	Thickness Layer [m]
1	Rock	HMa 3-6t	1120	1180	1300	2.4
2	Rock	LMA 10-60	220	240	330	0.5
3	Rock	CP 45/125	42	64	120	0.2
4	Gravel	-	2	4	10	0.2
5	Sand	-	0.3	0.35	0.6	-

Scour Protection between $x = 150$ m and $x = 250$ m						
Layer	Type	Standard Grading	d15 [mm]	dn50 [mm]	d85 [mm]	Thickness Layer [m]
1	Rock	HMA 1-6t	880	900	1170	1.4
2	Rock	LMA 10-60	220	240	330	0.2
3	Rock	CP 45/125	42	64	120	0.2
4	Gravel	-	2	4	10	0.2
5	Sand	-	0.3	0.35	0.6	-

Scour Protection from $x > 250$ m						
Layer	Type	Standard Grading	d15 [mm]	dn50 [mm]	d85 [mm]	Thickness Layer [m]
1	Rock	LMA 40-200	320	340	460	0.7
2	Rock	CP 45/125	42	64	120	0.2
3	Gravel	-	2	4	10	0.2
4	Sand	-	0.3	0.35	0.6	-

Table N.1: Scour Protection of the Energy Storage Lake

### N.3.1.3. Length of the Scour Protection

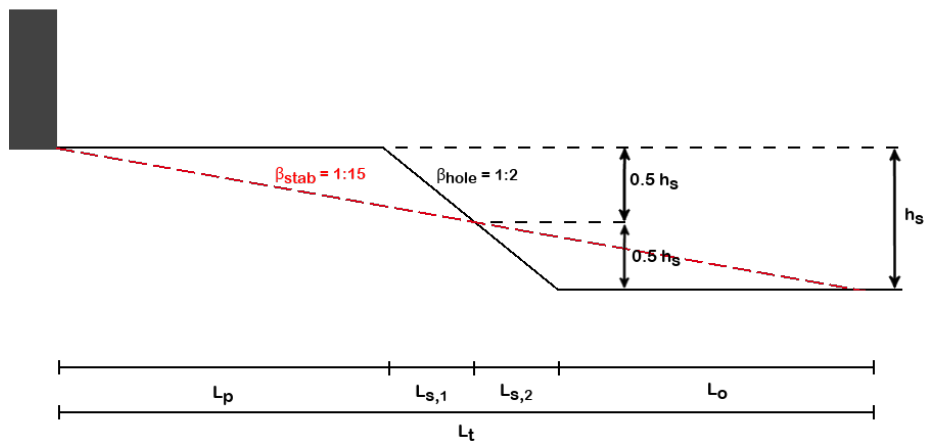


Figure N.10: The protection length variables

The length of the scour protection depends on the depth of the scour hole behind the scour protection, the consistency of the soil and the slope of the scour hole. To calculate the length of the protection Formula N.2 is used. In this formula the slope of the scour hole is assumed to be 1:2 m and it is assumed that the soil has a loose consistency. Consequently, the loose consistency leads to a slope of the soil after lost of stability of 1:15 m. These slopes can be seen in Figure N.10. To take into account the uncertainties a safety factor of 1.1 is applied.

$$L_p = \gamma_s \cdot h_s \cdot \frac{\beta_{stab} - \beta_{hole}}{2} \tag{N.2}$$

where:  $L_p$  [m] = protection length  
 $\gamma_s$  [-] = safety factor (= 1.1)  
 $h_s$  [m] = scour hole depth  
 $\beta_{stab}$  [-] = slope angle value a (1:a) of slope after stability is lost  
 $\beta_{hole}$  [-] = slope angle value a (1:a) of the scour hole

For the scour hole depth, the equilibrium depth is used. This equilibrium depth is determined according to Formula N.3.

$$h_{se} = \frac{0.5\alpha\bar{u} - \bar{u}_c}{\bar{u}_c} \cdot h_0 \quad (N.3)$$

where:  $h_{se}$  [m] = the scour depth  
 $\alpha$  [-] = amplification factor for the velocity  
 $\bar{u}$  [m/s] = the flow velocity  
 $\bar{u}_c$  [m/s] = the critical flow velocity of the bed material  
 $h_0$  [m] = the water depth

The amplification factor is approximate 2.5 for a turbulence intensity of 0.3. Therefore this value is taken for the determination of the scour depth. The flow velocity at the end of the scour protection is depending on the length of the protection. The critical flow velocity of sand is approximately 0.4 m/s and the water depth at the end of the protection is 5 m during the maximum discharge. The maximum occurring velocity is depending on the discharge and the distance from the spillway. Further downstream of the spillway, the velocity decreases because the flow width increases. An important factor in the development of the scour hole is time. The maximum velocity should be present for a long time to lead to a scour hole with the equilibrium depth. Because the flow velocity depends on the discharge, the velocity decreases over time because the discharge is decreases when the water level in the Energy Storage Lake increases.

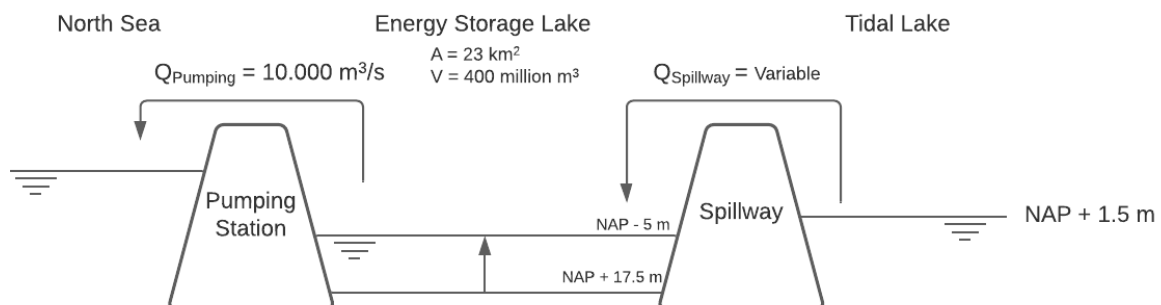


Figure N.11: Simplification of the Model

To take the change in velocity and water level into account, a mean value for the velocity and depth is taken. With the use of Python, a small model is built to analyse the change in water level in the Energy Storage Lake, the change in discharge and velocity of the spillway when functioning. In this model, the water level of the Tidal Lake is kept constant at NAP + 1.5 m. The discharge of the pumping station is set at 10 000 m<sup>3</sup>/s and the volume of the Energy Storage Lake is 400 million m<sup>3</sup>. With a maximum water depth of 17.5 m, the area of the lake is approximately 23 km<sup>2</sup>. A simplification of model can be seen in Figure N.11. The water level in the Energy Storage Lake is determined by:

$$h_{ESL} = \frac{Q_{in} - Q_{out}}{A_{ESL}} = \frac{Q_{in} - 10000}{23000000}$$

With the use of the Bernoulli equation, also done in Appendix E, the discharge of the spillway,  $Q_{in}$ , is determined. The discharge of the spillway can be seen in Figure N.12a and the water level of the Energy Storage Lake in Figure N.12b.



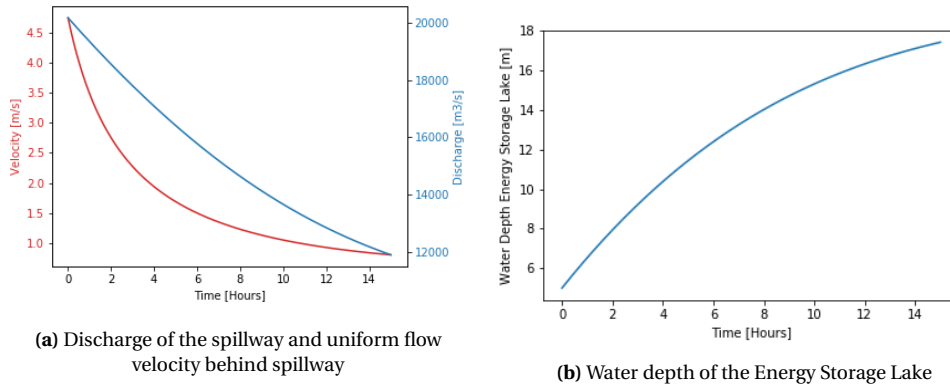


**Figure N.12:** Variation in Discharge, Velocity and Water level during the use of the spillway

With the calculated discharge and water level, the uniform flow velocity is determined ( $v = \frac{Q}{B \cdot h}$ ). This flow velocity is the flow velocity just downstream of the spillway and can be seen in Figure N.12a. For the determination of the scour depth, the velocity at the end of the protection is needed. For the first estimation of the scour depth, the velocity just downstream the spillway is taken as governing velocity. This means that the horizontal spreading is not taken into account. Therefore the determined depth is a conservative value. For the mean values of the water level and the velocity, the area below the graph is calculated and divided by the total time steps.

$$\bar{u} = \int_0^T u dt$$

$$\bar{h} = \int_0^T h dt$$

This results in a mean velocity of 1.65 m/s and a mean depth of 12.8 m. Using these values in Formula N.3, results in a equilibrium depth of 53 m. The length of the protection is now determined with Formula N.2. This leads to a required protection length of 380 m.

$$L_p = \gamma_s \cdot h_s \cdot \frac{\beta_{stab} - \beta_{hole}}{2} = 1.1 \cdot 53 \cdot \frac{15 - 2}{2} = 380 \text{ m}$$

### N.3.2. Tidal Lake

#### N.3.2.1. Type of Scour Protection

For the upstream side of the spillway, the Tidal Lake side, the design of the scour protection will be a geometrically closed filter made out of rocks.

#### N.3.2.2. Dimensions of the Scour Protection

For the scour protection at the upstream side, the Shields equation is used, Formula N.1. The maximum occurring velocity is 2.27 m/s. The required diameter to withstand the flow velocity of 2.27 m/s is 0.03 m. This leads to a standard grading of the top layer of CP 45/125 with a  $d_{n50}$  of 0.064 m. For the layers below the top layer, the same requirements need to be full filled:

$$\text{Stability: } \frac{d_{15,F}}{d_{85,B}} < 5, \quad \text{Internal Stability: } \frac{d_{85}}{d_{15}} < 12 - 15, \quad \text{Permeability: } \frac{d_{15,F}}{d_{15,B}} > 5$$

Taking the requirements into account leads a geometrically closed filters with the following layers, see Table N.2 and Figure N.13.

scour protection Tidal Lake						
Layer	Type	Standard Grading	d15 [mm]	dn50 [mm]	d85 [mm]	Thickness Layer [m]
1	Rock	CP 45/125	42	64	120	0.2
2	Gravel	-	2	7	15	0.2
3	Sand	-	0.3	0.35	0.6	

Table N.2: Scour Protection of the Tidal Lake

### N.3.2.3. Length of the Protection

For the determination of the length of the protection Formula N.2 is used. In the calculation of the scour depth at the Tidal Lake side, the maximum velocity is used instead of a mean value. The reason for this is that the mean velocity is difficult to determine because the change in water level in the Tidal Lake is hard to model. The inflow discharge from the Rhine and Meuse are not easy to implement in a simplified model. Therefore the length of the protection is determined using the water depth of 10 m and a flow velocity of 2.27 m/s (the extreme case). This is a conservative method but acceptable for a preliminary design. This results in an equilibrium depth of 61 m.

$$h_{se} = \frac{0.5\alpha\bar{u} - \bar{u}_c}{\bar{u}_c} \cdot h_0 = \frac{0.5 \cdot 2.5 \cdot 2.27 - 0.4}{0.4} \cdot 10 = 61 \text{ m}$$

A scour depth of 61 m results in a required length of 436 m. For the determination of the length of the protection, the same assumptions are used as for the Energy Storage Lake side.

$$L = \gamma_s \cdot h_s \cdot \frac{\beta_{stab} - \beta_{hole}}{2} = 1.1 \cdot 61 \cdot \frac{15 - 2}{2} = 436 \text{ m} \approx 440 \text{ m}$$

### N.3.3. Design of the Scour Protection

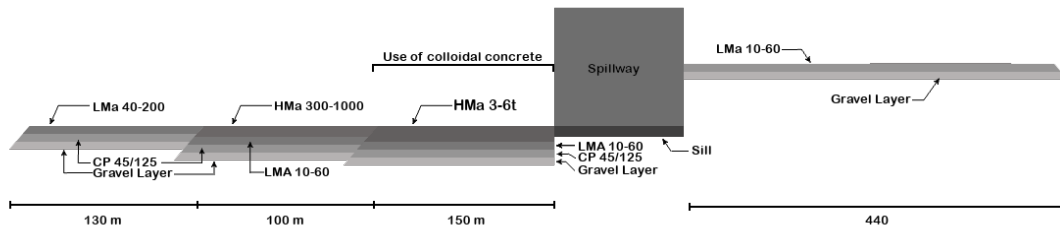


Figure N.13: scour protection design (NTS)

### N.3.4. The Standard Gradings

In this thesis, the standard gradings are used in the design of the scour protection. In Table N.14, the characteristics of these standard gradings can be found.

Class name	described in EN13383		$d_{50}$ (cm)	$d_{85}/d_{15}$	$d_{n50}$ (cm)	(2)	(3)
	range	(1)					
CP45/125		0.4-1.2					
CP63/180		1.2-3.1					
CP90/250	45/125 mm	1.2-3.1	6.3-9.0	2.8	6.4	20	300
CP45/180	63/180 mm	3.1-9.3	9.0-12.5	2.8	9	20	300
CP90/180	90/250 mm	0.4-1.2	12.5-18	2.8	12.8	20	300
LM <sub>A</sub> 5-40	45/200 mm	2.1-2.8	6.3-9.0	4.0	6.4	20	300
LM <sub>A</sub> 10-60	90/180 mm	10-20	11-12	2.0	9.7	20	300
LM <sub>A</sub> 40-200	5-40 kg	20-35	18-23	1.7	17	25	500
LM <sub>A</sub> 60-300	10-60 kg	80-120	23-28	1.5	21	32	550
LM <sub>A</sub> 15-300	40-200 kg	120-190	37-42	1.5	34	52	850
HM <sub>A</sub> 300-1000	60-300 kg	45-135	42-49	1.5	38	57	950
	15-300 kg	450-690	30-44	2.7	31	46	700
HM <sub>A</sub> 1000-3000	300-1000 kg	1700-2100	65-75	1.4	59	88	1325
	1-3 ton	4200-	103-110	1.4	90	135	2050
HM <sub>A</sub> 3000-6000	3-6 ton	4800	138-144	1.2	118	177	2700
HM <sub>A</sub> 6000-10000	6-10 ton	7500-8500	167-174	1.2	144	216	3250

CP - Course gradings (1): range of  $W_{50}$  for category "A" (kg)  
 LM - Light gradings (2): Layer thickness 1.5  $d_{n50}$  (cm)  
 HM - Heavy gradings (3): Minimal dumping quantity with layer of 1.5  $d_{n50}$  (kg/m<sup>2</sup>)

**Figure N.14:** The standard gradings (Schierreck, 2012)

# References

- Army Engineer Waterways Experiment Station (1977). Corps of engineers hydraulic design criteria. volume i. Technical report, Army Engineer Waterways Experiment Station.
- Attema, J., Bakker, A., Beersma, J., Bessembinder, J., Boers, R., Brandsma, T., van den Brink, H., Drijfhout, S., Eskes, H., Haarsma, R., et al. (2014). Knmi'14: Climate change scenarios for the 21st century—a netherlands perspective. Technical report, KNMI: De Bilt, The Netherlands.
- Benson, M. A. and World Meteorological Organization (1968). *Measurement of peak discharge by indirect methods*. Secretariat of the World Meteorological Organization.
- Bosboom, J. (2015). *Coastal dynamics I*. Delft Academic Press, Delft.
- Braam, C. (2011). *Constructie leer gewapend beton : studieboek voor het HBO, de opleidingen Bouwkunde en Civiele Techniek*. neas Cement&BetonCentrum, Boxtel 's-Hertogenbosch.
- Buis, A. (2020). Milankovitch (orbital) cycles and their role in earth's climate. Internet site <https://climate.nasa.gov/news/2948/milankovitch-orbital-cycles-and-their-role-in-earths-climate/>.
- Buishand, T. and Lenderink, G. (2004). Estimation of future discharges of the river rhine in the swurve project. Technical report, KNMI.
- CETMEF, C. C. (2007). *The Rock Manual. The use of rock in hydraulic engineering (2nd edition)*, 2nd edition edition.
- Christy, J. R. (2016). Testimony of John R. Christy. During meeting of U.S. House Committee on Science, Space & Technology.
- Core Writing Team, Pachauri, R., and Meyer, L. (2014). Climate change 2014: Synthesis report. Technical report, IPCC. Contribution of Working Groups I, II and III to the Fifth Assessment Report of the Intergovernmental Panel on Climate Change.
- de Winter, R. C., Sterl, A., de Vries, J. W., Weber, S. L., and Ruessink, G. (2012). The effect of climate change on extreme waves in front of the Dutch coast. *Ocean Dynamics*, 62(8):1139–1152.
- Deltares (2018). Mogelijke gevolgen van versnelde zeespiegelstijging voor het deltaprogramma. Technical report, Deltares.
- Demon, A. (2005). *De langetermijnvisie PKB Ruimte voor de Rivier*. RIZA, S.I.
- Dillingh, D. (2013). Kenmerkende waarden kustwateren en grote rivieren. Technical report, Deltares.
- Döll, P. and Schmied, H. M. (2012). How is the impact of climate change on river flow regimes related to the impact on mean annual runoff? a global-scale analysis. *Environmental Research Letters*, 7(1):014037.
- Ead, S. A. and Rajaratnam, N. (2000). Plane turbulent surface jets in shallow tailwater. *Journal of Fluids Engineering*, 123(1):121–127.
- EduRev (2020). Structures for water storage. Retrieved from the internet, site: [https://edurev.in/studytube/Structures-for-Water-Storage-%E2%80%93-Investigation--Plan/23eddb58-27cf-41ee-b20e-8ff4d3c09c3f\\_t](https://edurev.in/studytube/Structures-for-Water-Storage-%E2%80%93-Investigation--Plan/23eddb58-27cf-41ee-b20e-8ff4d3c09c3f_t).
- Ferguson, H., Blokland, P., and H. Kuiper (1970). The haringvliet sluices. Technical report, Rijkswaterstaat.
- Fugro (2020). Sondeeronderzoek. Downloaded at 16-11-2020, from Dinoloket <https://www.dinoloket.nl/ondergrondgegevens>.

- Gao, N. and Ewing, D. (2007). Experimental investigation of planar offset attaching jets with small offset distances. *Experiments in Fluids*, 42(6):941–954.
- Government of The Netherlands (2020a). Ministry of economic affairs and climate policy. Retrieved 20-10-20, Website Government of The Netherlands <https://www.government.nl/ministries/ministry-of-economic-affairs-and-climate-policy>.
- Government of The Netherlands (2020b). Ministry of infrastructure and water management. Retrieved 20-10-20, Website Government of The Netherlands <https://www.government.nl/ministries/ministry-of-infrastructure-and-water-management>.
- Government of The Netherlands (2020c). Natura2000. Retrieved 20-10-20, Website Government of The Netherlands <https://www.government.nl/topics/nature-and-biodiversity/natura-2000>.
- Hertogh, M., Bosch-Rekvelde, M., and Houwing, E. (2019). *Dictaat CTB1220 Integraal Ontwerp en Beheer*. Faculteit Civiele Techniek en Geowetenschappen, TU Delft.
- Het Hoogwaterbeschermingsprogramma (2019). Programmaplan hoogwaterbeschermingsprogramma 2019-2023. Technical report, Het Hoogwaterbeschermingsprogramma.
- Itaipu Binacional (2020). Technical features. Internet, retrieved from <https://www.itaipu.gov.br/en/energy/technical-features>.
- Johnson, J. (1952). Chapter 2 generalized wave diffraction diagrams. In *Coastal Engineering*.
- Jongejan, R. and Steenbergen, R. (2015). Beoordeling van de constructieve veiligheid van waterbouwkundige kunstwerken volgens het bouwbesluit en de waterwet. Technical report, InfraQuest.
- Jonkman, S., Jorissen, R., Schweckendiek, T., and van den Bos, J. (2018). *Flood defences Lecture notes CIE5314*. Department of Hydraulic Engineering, Faculty of Civil Engineering and Geosciences, Delft University of Technology, 3rd edition edition.
- Klijn, F., Hegnauer, M., Beersma, J., and Sperna-Weiland, F. (2015a). The plausibility of extreme high discharges in the river Rhine. Technical report, Deltares.
- Klijn, F., Hegnauer, M., Beersma, J., and Weiland, F. S. (2015b). Wat betekenen de nieuwklimaatscenario's voor derivierafvoeren van Rijn en Maas? Technical report, KNMI and Deltares.
- KNMI (2020). Potential wind speed of the netherlands. Internet, site [http://projects.knmi.nl/klimatologie/onderzoeksgegevens/potentiele\\_wind/index.cgi?language=eng](http://projects.knmi.nl/klimatologie/onderzoeksgegevens/potentiele_wind/index.cgi?language=eng). 4 data sets used.
- KNMI (2020). Superstorm. Internet, site: <https://www.knmi.nl/kennis-en-datacentrum/uitleg/superstormen>.
- Kuipers, B. (2018). Het Rotterdam effect, de impact van mainport Rotterdam op de Nederlandse economie. Technical report, Erasmus Centre for Urban, Port and Transport Economics.
- Kwadijk, J. (2004). Continie operationele afvoer en waterstandvoorspelling. Technical report, Rijkswaterstaat.
- Kweku, D., Bismark, O., Maxwell, A., Desmond, K., Danso, K., Oti-Mensah, E., Quachie, A., and Adormaa, B. (2018). Greenhouse effect: Greenhouse gases and their impact on global warming. *Journal of Scientific Research and Reports*, 17(6):1–9.
- Lavooij, H. and Berke, L. (2018a). Delta21 en energie. Technical report, Delta21.
- Lavooij, H. and Berke, L. (2018b). Delta21 en natuurherstel. Technical report, Delta21.
- Lavooij, H. and Berke, L. (2018c). Delta21 en waterveiligheid. Technical report, Delta21.
- Lavooij, H. and Berke, L. (2019). Update 2019: Delta21, een actualisering van het plan. resreport, Delta21.
- Lavooij, H. and Berke, L. (2020). Kennisprogramma zeespiegelstijging(zss) – delta21. Internet <https://www.delta21.nl/kennisprogramma-zeespiegelstijging/>.

- Li, X., Zhou, M., Zhang, J., and Xu, W. (2019). Numerical study of the velocity decay of offset jet in a narrow and deep pool. *Water*, 11(1):59.
- Ministerie van Infrastructuur en Milieu (2015). Natura 2000 ontwerpbeheerplan deltawateren 2015-2021. resreport, Ministerie van Infrastructuur en Milieu. Bijlage Haringvliet.
- Mori, N., Yasuda, T., Mase, H., Tom, T., and Oku, Y. (2010). Projection of extreme wave climate change under global warming. *Hydrological Research Letters*, 4(0):15–19.
- Munson, B. R., Young, D. F., and Okiishi, T. H. (2009). *Fundamentals of Fluid Mechanics [With Web Registration Card]*. JOHN WILEY & SONS INC.
- NASA (2020). Is it too late to prevent climate change? Internet from NASA <https://climate.nasa.gov/faq/16/is-it-too-late-to-prevent-climate-change/>.
- Normcommissie 351 001 "Technische Grondslagen voor Bouwconstructies" (1995). *NEN 6720*. Nederlands Normalisatie-instituut, Postbus 5059, 2600 GB Delft, TGB 1990 - Voorschriften Beton - Constructievereisen en rekenmethoden (VBC 1995) edition.
- Normcommissie 351 001 "Technische Grondslagen voor Bouwconstructies" (2006). *NEN-EN 1992-3*. Nederlands Normalisatie-instituut, Postbus 5059, 2600 GB Delft, Eurocode 2: Design of concrete structures - Part3: Liquid retaining and containment structures edition.
- Normcommissie 351 001 "Technische Grondslagen voor Bouwconstructies" (2011a). *NEN-EN 1991-1-4+A1+C2*. Koninklijk Nederlands Normalisatie-instituut, Eurocode 1: Actions on structures - Part 1-4: General actions - Wind actions edition.
- Normcommissie 351 001 "Technische Grondslagen voor Bouwconstructies" (2011b). *NEN-EN 1992-1-1+C2*. Nederlands Normalisatie-instituut, Postbus 5059, 2600 GB Delft, Eurocode 2: Design of concrete structures –Part 1-1: General rules and rules for buildings edition.
- Normcommissie 351 006 "Geotechniek" (2016). *NEN-EN 1997-1+C1+A1*. Postbus 5059, 2600 GB Delft, Eurocode 7: Geotechnical design - Part 1: General rules edition.
- Normcommissie 351 006 "Geotechniek" (2019). *NEN-EN 1997-1+C1+A1/NB*. Koninklijk Nederlands Normalisatie-instituut, Postbus 5059, 2600 GB Delft, National Annex to NEN-EN 1997-1 Eurocode 7: Geotechnical design –Part 1: General rules edition.
- Nuccitelli, D. (2016). Republicans' favorite climate chart has some serious problems. Internet site <https://www.theguardian.com/environment/climate-consensus-97-per-cent/2016/feb/19/republicans-favorite-climate-chart-has-some-serious-problems>.
- Paasman, Y. (2020). Design for the in- and outlet structure of the Energy Storage Lake within the Delta21 plan. Technical report, Technische Universiteit Delft.
- Rijksoverheid (2019). Klimaatakkoord.
- Rijkswaterstaat (1961). Verslag over de stormvloed van 1953. Technical report, Rijkswaterstaat.
- Rijkswaterstaat (2017). *Handreiking ontwerpen met overstromingskansen*. Rijkswaterstaat Water, Verkeer en Leefomgeving, oi2014v4 edition.
- Rijkswaterstaat (2019). Water management in the Netherlands. Internet site: <http://www.helpdeskwater.nl/watermanagement>. Update of 2009 Edition.
- Rijkswaterstaat (2020a). De deltawerken. Retrieved 23-10-20, Rijkswaterstaat site: <https://www.rijkswaterstaat.nl/water/waterbeheer/bescherming-tegen-het-water/waterkeringen/deltawerken/>.
- Rijkswaterstaat (2020b). Our mission. Retrieved 20-10-2020, Rijkswaterstaat website: <https://www.rijkswaterstaat.nl/over-ons/onze-organisatie/onze-missie/index.aspx>.
- Rijkswaterstaat (2021). Hoe de bodem voor zeesluis ijmuiden wordt beschermd. Internet, website: <https://www.rijkswaterstaat.nl/nieuws/archief/2021/04/hoe-de-bodem-voor-zeesluis-ijmuiden-wordt-beschermd>.

- Rodgers, L. (2018). Climate change: The massive CO2 emitter you may not know about. *BBC News*, 17(12).
- Roozenburg, N. and Eekels, J. (1995). *Product design : fundamentals and methods*. Wiley, Chichester New York.
- Schierck, G. (2012). *Introduction to bed, bank and shore protection : [engineering the interface of soil and water]*. VSSD, Delft.
- Slootjes, N. and van der Most, H. (2016). Achtergronden bij de normering van de primaire waterkeringen in Nederland. Techreport, Ministerie van Infrastructuur en Milieu.
- Staf Deltacommissaris (2015). Het deltaprogramma 2015. Technical report, Het ministerie van Infrastructuur en Milieu.
- Stichting Deltawerken Online (2004). Retrieved 05-10-2020, from Deltawerken Online website: <http://www.deltawerken.com/16>.
- TAW, Technische Adviescommissie voor de Waterkeringen (2003). *Leidraad kunstwerken*. TAW, Technische Adviescommissie voor de Waterkeringen, Delft.
- U.S. Army Corps of Engineers (1990). *Engineering and Design: Hydraulic Design of Spillways*. U.S. Army Corps of Engineers.
- US Army Corps of Engineers (2012). Garrison project statistics. Internet, retrieved from: <https://www.nwo.usace.army.mil/Media/Fact-Sheets/Fact-Sheet-Article-View/Article/487634/garrison-project-statistics/>.
- Van den Hurk, B., Tank, A. K., Lenderink, G., van Ulden, A., van Oldenborgh, G. J., Katsman, C., van den Brink, H., Keller, F., Bessembinder, J., Burgers, G., Komen, G., Hazeleger, W., and Drijfhout, S. (2006). KNMI climate change scenarios 2006 for the Netherlands. Technical report, KNMI.
- Van der Meer, J., Allsop, N., Bruce, T., De Rouck, J., Kortenhaus, A., Pullen, T., Schüttrumpf, H., Troch, P., and Zanuttigh, B. (2018). *EurOtop: Manual on wave overtopping of sea defences and related structures : an overtopping manual largely based on European research, but for worldwide application*.
- van Heel, L. (2019). Is dit kunstmatige eiland (dat schone stroom opwekt) het deltawerk van de toekomst? Site AD <https://www.ad.nl/rotterdam/is-dit-kunstmatige-eiland-dat-schone-stroom-opwekt-het-deltawerk-van-de-toekomst-a0c82fd3/>.
- van Waveren, H. (2018). Help, de zeespiegel stijgt. Internet site: <https://www.rijkswaterstaat.nl/water/waterbeheer/blogs-waterexperts/help-de-zeespiegel-stijgt.aspx>.
- Voorendt, M. and Molenaar, W. (2020a). *Hydraulic Structures General Lecture Notes*. TU Delft, 2020 edition.
- Voorendt, M. and Molenaar, W. (2020b). *Manual Hydraulic Structures*. TU Delft, february 2020 edition.
- Walski, T. M., Sharp, W. W., and Douglas (Shields Jr.), F. (1988). Predicting internal roughness in water mains. *Journal-American Water Works Association*, 80(11):34–40.
- Waterschap Hollandse Delta (2020). Wat doet het waterschap. Internet, site <https://www.wshd.nl/wat-doet-het-waterschap>.
- Wijsman, J., Escaravage, V., Huismans, Y., Nolte, A., van der Wijk, R., Wang, Z. B., and and, T. Y. (2018). Potenties voor herstel getijdenatuur in het Haringvliet, Hollands Diep en de Biesbosch. Technical report, Wageningen Marine Research AND Deltares.